HIF-2α in oxygen chemosensitivity and paraganglioma development

Holly Jones

Green Templeton College

Ludwig Institute for Cancer Research

Nuffield Department of Medicine

University of Oxford



Supervised by

Professor Tammie Bishop, Dr Thomas P. Keeley and

Professor Sir Peter J. Ratcliffe

A thesis submitted for the degree of

Doctor of Philosophy

Trinity Term 2026

ABSTRACT

HIF-2α is highly expressed in specialised neuroendocrine tissues, including carotid body glomus cells and developing chromaffin cells. HIF-2 is necessary for the normal development and function of these cells, both of which are ablated through HIF-2 inactivation. Aberrant activation of HIF-2 also prevents normal development and predisposes to tumour formation. Together, this suggests that levels of HIF-2 must be precisely balanced for normal development and function of these cells. How HIF-2α activity contributes to normal sympathoadrenal development, establishes oxygen chemosensitivity, and predisposes to the development of tumours remains incompletely understood and is the central aim of this thesis.

Stabilisation of HIF-2α during development was sufficient to confer a hypoxia-responsive phenotype on adult adrenal medullary chromaffin cells, demonstrating that HIF-2α can confer oxygen chemosensitivity in cells that would otherwise be insensitive to acute hypoxia (Chapter 2). This required both the transcriptional activity of HIF-2α and its activation during development (Chapter 3). HIF-2α also altered the developmental fate of extra-adrenal chromaffin tissue. Direct developmental stabilisation of HIF-2α (Chapter 2), and indirect activation of HIF signalling through inactivation of *Phd2* (previously published work) or *Sdhb* (Chapter 4), resulted in persistence of the foetal organ of Zuckerkandl into adulthood. Examination of aged pseudohypoxic mice revealed paragangliomas at this site, identifying the persistent chromaffin cell population as a potential substrate for tumour development (Chapter 5).

Together, these findings identify HIF-2α as an important regulator of both the functional maturation and persistence of immature chromaffin cells that are predisposed to tumour development. They suggest that HIF-2α-driven persistence of an immature, oxygen-responsive

chromaffin state may provide a link between physiological oxygen sensing and susceptibility to pseudohypoxic paraganglioma.

Table of Contents

LIST OF FIGURES 8

LIST OF TABLES 12

ACKNOWLEDGEMENTS 13

Chapter 1 - INTRODUCTION 15

1.1 **Hypoxia inducible factors** 16

1.1.1 *The HIF/PHD pathway* 16

1.1.2 *Discovery of HIF* 18

1.1.3 *Structure of HIFs* 19

1.1.4 *Structure and functional diversity of HIFs and PHD enzymes* 20

1.1.5 *Metabolic regulation of the HIF pathway* 23

1.2 **The acute response to hypoxia - the carotid body** 24

1.2.1 *The carotid body response to sustained hypoxia* 26

1.2.2 *Structure and morphology* 27

1.2.3 *Oxygen chemosensitivity* 31

1.3 **Other oxygen sensitive tissues - chromaffin cells** 36

1.3.1 *Oxygen chemosensitivity in chromaffin cells* 37

1.3.2 *The organ of Zuckerkandl* 38

1.4 **HIF-2α in carotid body and chromaffin cell chemosensitivity** 41

1.5 **Pheochromocytomas and paragangliomas** 43

1.5.1 *Mouse models of pheochromocytomas and paragangliomas* 48

1.6 **Summary** 51

1.7 **Research aims** 52

Chapter 2 - STABILISATION OF HIF-2A, BUT NOT HIF-1A, CONFERS OXYGEN CHEMOSENSITIVITY IN CHROMAFFIN CELLS ..... --- 53

2.1 **Introduction** 53

2.2 **Results** 57

2.2.1 *TH-restricted, developmental Hif-1αdPA and Hif-2αdPA mouse models* 57

2.2.2 *Confirmation of Hif-1αdPA and Hif-2αdPA expression in neuroendocrine tissues* 60

2.2.3 *The carotid body is enlarged in Hif-2αdPA, but not Hif-1αdPA, mice* 61

2.2.4 *Developmental stabilisation of HIF-2α, but not HIF-1α, causes an enhanced hypoxic ventilatory response* 64

2.2.5 *Developmental stabilisation of HIF-2α, but not HIF-1α, results in the retention of immature, noradrenergic chromaffin cells in the adult adrenal medulla* 67

2.2.6 *Developmental stabilisation of HIF-2α, but not HIF-1α, confers acute oxygen chemosensitivity in the adult adrenal medulla* 70

2.2.7 *Developmental stabilisation of HIF-2α, but not HIF-1α, causes retention of the foetal organ of Zuckerkandl in adulthood* 75

2.2.8 *The Hif-2αdPA organ of Zuckerkandl is oxygen chemosensitive* 78

2.3 **Discussion** 79

Chapter 3 **-** INVESTIGATION INTO THE MECHANISMS BY WHICH HIF-2A CONFERS FOETAL-LIKE, PARAGANGLIOMA-LIKE GLOMUS AND CHROMAFFIN CELL PHENOTYPES 86

3.1 **Introduction** 86

3.2 **Results** 89

3.2.1 *Adult-onset Hif-2αdPA mouse model* 89

3.2.2 *Confirmation of adult-onset Hif-2αdPA expression* 91

3.2.3 *Adult-onset Hif-2αdPA stabilisation does not cause an increase in carotid body volume or hypoxic ventilatory response* 93

3.2.4 *Adult-onset Hif-2αdPA does not confer an immature gene expression profile or acute oxygen chemosensitivity in chromaffin cells of the adrenal medulla* 98

3.2.5 *Adult-onset Hif-2αdPA does not induce re-establishment of the organ of Zuckerkandl* 102

3.2.6 *Hif-2αdPA DNA binding mutant mouse model* 103

3.2.7 *Confirmation of Hif-2αdPA DNA binding mutant construct expression in the adrenal medulla* 107

3.2.8 *Reversion of carotid body hyperplasia and the enhanced hypoxic ventilatory response in Hif-2αdPA DNA binding mutant mice* 111

3.2.9 *Reversion of the switch towards immature gene expression and retention of oxygen chemosensitivity in Hif-2αdPA DNA binding mutant mice* 114

3.2.10 *Hif-2αdPA DNA binding mutant mice do not retain the organ of Zuckerkandl into adulthood* 118

3.3 **Discussion** 120

Chapter 4 - TH-RESTRICTED MUTATIONS IN BOTH ALLELES OF SDHB CONFER IMMATURE CHROMAFFIN CELL PHENOTYPES IN MICE 127

4.1 **Introduction** 127

4.2 **Results** 133

4.2.1 *Mouse models with mutations in Sdhb* 133

4.2.2 *Mice with mutations in both alleles of Sdhb are runted* 135

4.2.3 *Confirmation of SDHB loss in the mouse models with mutations in Sdhb* 136

4.2.4 *Carotid body morphology is altered in mice with mutations in both alleles of Sdhb* 138

4.2.5 *Mice with mutations in both alleles of Sdhb are unable to tolerate acute hypoxia* 140

4.2.6 *Reduction in Chromogranin A expression in the adrenal medulla of mice with mutations in both alleles of Sdhb* 141

4.2.7 *Mutations in both alleles of Sdhb results in an immature gene expression profile in the adrenal medulla* 144

4.2.8 *The adrenal medulla from mice with mutations in both alleles of Sdhb is unresponsive to acute hypoxia* 147

4.2.9 *Mutation of both alleles of Sdhb causes retention of the organ of Zuckerkandl in adult mice* 151

4.2.10 *The retained organ of Zuckerkandl in mice with mutations in both alleles of Sdhb mice expresses carotid body marker genes and responds to acute hypoxia* 153

4.3 **Discussion** 157

Chapter 5 - DEVELOPMENTAL STABILISATION OF HIF-2A CONFERS RETENTION OF A PRE-NEOPLASTIC ORGAN OF ZUCKERKANDL 163

5.1 **Introduction** 163

5.2 **Results** 166

5.2.1 *Reduced HIF target gene expression in the wildtype organ of Zuckerkandl over the postnatal period* 166

5.2.2 *The neonatal wild-type organ of Zuckerkandl is responsive to acute hypoxia* 169

5.2.3 *Comparison of the retained organ of Zuckerkandl in adult mice with developmental pseudohypoxic mutations* 172

5.2.4 *Environmental hypoxia during the early postnatal period is sufficient to cause retention of the organ of Zuckerkandl* 175

5.2.5 *Interaction between environmental hypoxia and pseudohypoxia* 177

5.2.6 *A proportion of aged Phd2ko mice develop proliferating organ of Zuckerkandl paragangliomas* 180

5.2.7 *HIF-2α and HIF target gene expression in the frank organ of Zuckerkandl paragangliomas* 184

5.2.8 *Increased proliferation markers in the frank organ of Zuckerkandl paragangliomas* 187

5.2.9 *The non-tumour organ of Zuckerkandl from aged Phd2ko mice contains clusters of cyclin D1-expressing cells* 190

5.3 **Discussion** 192

Chapter 6 – FINAL DISCUSSION 200

Chapter 7 208

7.1 **Materials and chemicals** 208

7.2 **Ethical approval** 208

7.3 **Animals** 208

7.4 **Genotyping** 208

7.5 **Tamoxifen administration** 210

7.6 **Plethysmography** 210

7.7 **Postnatal hypoxia** 211

7.8 **Immunohistochemistry** 211

7.9 ***In situ* hybridisation** 213

7.10 **Tissue preparation for calcium imaging** 214

7.11 **Fluorescent calcium imaging** 214

7.12 **Hemagglutinin immunoblotting** 216

7.13 **Statistical analysis** 217

BIBLIOGRAPHY 218

LIST OF FIGURES

Figure 1.1. The Hypoxia inducible factor (HIF) pathway

Figure 1.2. Structure of HIF-α and HIF-β

Figure 1.3. Metabolic interaction with the HIF pathway

Figure 1.4. Structure of the carotid body

Figure 1.5. Catecholamine synthesis pathway

Figure 1.6. Oxygen sensing pathway in carotid body glomus cells

Figure 1.7. Sites of pheochromocytomas and paragangliomas

Figure 1.8. Pheochromocytoma and paraganglioma susceptibility genes

Figure 2.1. Schematic illustrating the neuroendocrine phenotype of wild-type and *Phd2ko* mice

Figure 2.2. Schematic illustrating the *Hif-1αdPA* and *Hif-2αdPA* mouse models

Figure 2.3. Confirmation of construct expression in the adrenal medulla of *Hif-1αdPA* and *Hif-2αdPA* mice

Figure 2.4. The carotid body is enlarged in *Hif-2αdPA*, but not *Hif-1αdPA*, mice

Figure 2.5. Developmental stabilisation of HIF-2α, but not HIF-1α, confers an enhanced hypoxic ventilatory response to 10% O_2/3% CO_2

Figure 2.6. Developmental stabilisation of HIF-2α, but not HIF-1α, causes a switch in gene expression in the adrenal medulla

Figure 2.7. The genetically encoded Ca^{2+} indicator GCaMP6f enables measurement of intracellular Ca^{2+} responses through changes in GFP florescence

Figure 2.8. Developmental stabilisation of HIF-2α, but not HIF-1α, confers acute oxygen chemosensitivity in the adult adrenal medulla

Figure 2.9. The organ of Zuckerkandl is present in adult *Hif-2αdPA* mice, but not in adult wild-type or *Hif-1αdPA* mice

Figure 2.10. Expression of carotid body-enriched genes in the *Hif-2αdPA* organ of Zuckerkandl

Figure 2.11. The adult *Hif-2αdPA* organ of Zuckerkandl is oxygen chemosensitive

Figure 3.1. Schematic illustrating the adult-onset *Hif-2αdPA* mouse model and experimental timeline

Figure 3.2. HIF-2α protein stabilisation in adrenal medullae of control versus adult-onset *Hif-2αdPA* mice

Figure 3.3. Adult-onset stabilisation of HIF-2α does not alter carotid body volume

Figure 3.4. Adult-onset *Hif-2αdPA* mice do not have an enhanced hypoxic ventilatory response to 10% O_2/3% CO_2

Figure 3.5. Adult-onset HIF-2α stabilisation does alter gene expression in the adrenal medulla

Figure 3.6. Adult-onset HIF-2α stabilisation does not confer oxygen chemosensitivity on the adrenal medulla

Figure 3.7. Adult-onset HIF-2α stabilisation does not induce re-establishment of the organ of Zuckerkandl

Figure 3.8. *Hif-2αdPA* DNA binding mutant construct

Figure 3.9. *Hif-2αdPA* DNA binding mutant mice

Figure 3.10. HIF-2α protein stabilisation in chromaffin tissues of wild-type versus *Hif-2αdPA versus Hif-2αdPA* DNA binding mutant mice

Figure 3.11. HIF-2α DNA binding is necessary for the enlarged carotid bodies seen in *Hif-2αdPA* mice

Figure 3.12. *Hif-2αdPA* DNA binding mutant mice do not have an enhanced hypoxic ventilatory response to 10% O_2/3% CO_2

Figure 3.13. The transcriptional activity of HIF-2α is necessary for the gene expression switch seen in the *Hif-2αdPA* adrenal medulla

Figure 3.14. HIF-2α DNA binding is necessary for acute oxygen chemosensitivity in the *Hif-2αdPA* adult adrenal medulla

Figure 3.15. HIF-2α DNA binding is necessary for retention of the organ of Zuckerkandl in adult *Hif-2αdPA* mice

Figure 4.1. Schematic representation of succinate dehydrogenase

Figure 4.2. Schematic summarising the mouse models with mutations in *Sdhb*

Figure 4.3. Mice with mutations in both alleles of *Sdhb* were runted compared to wild-type and heterozygous littermates

Figure 4.4. TH-restricted loss of SDHB protein expression in the carotid body and adrenal medulla from mice with mutations in *Sdhb*

Figure 4.5. SDHB inactivation causes altered glomus cell morphology and reduced chromogranin A expression the carotid body

Figure 4.6. The hypoxic ventilatory response in wild-type and $Sdhb^{f/+}$*;THCre* mice

Figure 4.7. Normal tyrosine hydroxylase but reduced chromogranin A expression in the adrenal medulla of mice with mutations in both alleles of *Sdhb*

Figure 4.8. A shift towards immature gene expression in adrenal medullae from mice with mutations in both alleles of *Sdhb*

Figure 4.9. Example traces of the fluorescent response of GCaMP6f-expressing carotid bodies exposed to hypoxia using the previous and current methodologies

Figure 4.10. Mutation of both alleles of *Sdhb* does not confer acute oxygen chemosensitivity in the adult adrenal medulla

Figure 4.11. The organ of Zuckerkandl is retained in adult mice with mutations in both alleles of *Sdhb*

Figure 4.12. Expression of carotid body-enriched genes in the organ of Zuckerkandl from adult mice with mutations in both alleles of *Sdhb*

Figure 4.13. The retained organ of Zuckerkandl in mice with mutations in both alleles of *Sdhb* is oxygen chemosensitive

Figure 5.1. Organ of Zuckerkandl volume and gene expression over the perinatal period

Figure 5.2. Oxygen chemosensitivity in the neonatal organ of Zuckerkandl decreases after birth

Figure 5.3. Comparison of the retained organ of Zuckerkandl across pseudohypoxic genotypes

Figure 5.4. Exposure to 10% oxygen during the postnatal period is sufficient to confer retention of the organ of Zuckerkandl

Figure 5.5. Exposure to 10% oxygen during the postnatal period causes a smaller organ of Zuckerkandl in *Phd2ko* mice

Figure 5.6. Development of organ of Zuckerkandl paragangliomas in aged *Phd2ko* mice

Figure 5.7. HIF-2α and HIF-2α target gene expression in the non-neoplastic organ of Zuckerkandl versus an organ of Zuckerkandl paraganglioma

Figure 5.8. Increased expression of proliferation markers in the frank organ of Zuckerkandl paragangliomas versus the non-neoplastic organ of Zuckerkandl from age-matched *Phd2ko* mice

Figure 5.9. 'Rests' of cyclin D1-expressing cells in the retained organ of Zuckerkandl from aged, but not young adult, *Phd2ko* mice

LIST OF TABLES

Table 5.1 Incidence of organ of Zuckerkandl paragangliomas in aged pseudohypoxic mice by genotype and sex

Table 7.1 PCR primers used for genotyping

Table 7.2 Gas mixtures used for Ca^{2+} imaging of fresh tissues

ACKNOWLEDGEMENTS

I would like to start by saying a massive thank you to my supervisors, Tammie, Peter and Tom. Tom, I am so grateful for all your support over the past four years, and for putting up with far too many silly microscope questions! I am truly inspired by you as a scientist, and I like to think that I have learnt a great deal from you about how to become a better one myself. Peter, I am so inspired by the way you think. Over the course of my DPhil, I have come to appreciate just how much of science involves looking at things from every possible angle, questioning assumptions and thinking things through again and again. This is something you do brilliantly, and it is a lesson I will carry with me throughout my career and beyond. And last, but very much not least, Tammie - I cannot fully express my gratitude for everything you have done for me over the past four years. I am endlessly grateful for your support, guidance and encouragement. You have truly gone above and beyond what anyone could expect of a supervisor, and I feel incredibly lucky to have had you guiding me through my DPhil.

I also could not have made it through the past four years without the support of so many people in the lab group. Gloria, you have supported me from day one, and I owe so much to you for all you have done for me and for your endless kindness. Debs, you have been a lifesaver with the animals, and a quick chat (or rant!) with you never fails to lift my mood. Claire and Jeremy, I can't thank you enough for your support with my experiments, particularly in these final few weeks. I'm not sure I could've made it to the finish line without you! Thank you also to David, Chris, Norah, Han, Ariege and the many undergraduates who have passed through the lab over the years. You have all helped me along the way, and I am so grateful for your contributions.

To the others in the group who, although we may not have worked directly together, have become such good friends: thank you for making everyday life that little bit brighter. Lunches with you all have been a highlight, and I feel very lucky to have found such wonderful friends

in the group. And to Catherine, thank you for solving so many of my minor inconveniences over the years – I owe a lot to you! I also want to thank former members of the lab, especially Joanna, Samvid and Olivia, who taught me so much in the lab and became great friends along the way. I miss you all a lot! I have always felt incredibly lucky to be part of a lab where everyone is so kind and supportive. I could not have asked for better colleagues, and you have all made my time in the lab so much more enjoyable.

Beyond the lab group, I would also like to thank the members of the Ludwig Institute for all the technical support they have given me throughout my DPhil. Indi, I have lost count of how many blocks you have sectioned for me, and I am so grateful for all your help. Robbie, I am sorry for the many times I have nearly broken the slide scanner, and thank you for your patience and for never making me feel bad about it!

Finally, I would not have made it through the past four years without the love and moral support of my amazing family and friends. Thank you for always being there for me, for listening when I needed to vent, and for putting up with me through all the stresses and ups and downs of a PhD. I love you all so much, and I am so grateful to have you all in my life.

Chapter 1

INTRODUCTION

Oxygen is essential for survival and normal cellular function. As the terminal electron acceptor in the electron transport chain, oxygen enables oxidative phosphorylation and thereby supports the production of adenosine triphosphate (ATP), which provides the majority of cellular energy under aerobic conditions. Therefore, oxygen homeostasis must be tightly regulated at both the cellular and systemic levels. However, oxygen supply and demand are constantly changing, and reductions in oxygen availability can occur under physiological conditions, including during development and exposure to high altitude, as well as in pathological states such as anaemia, vascular disease and tumour growth. When oxygen availability is insufficient to meet tissue demand, cells experience hypoxia, which can alter mitochondrial metabolism, redox balance, ion channel activity and gene expression. Severe or prolonged hypoxia can ultimately impair cellular function and result in cell death.

Consequently, mammals have evolved mechanisms to sense and respond to changes in oxygen availability over multiple timescales (Michiels, 2004). Rapid systemic responses to hypoxia include an increase in ventilation, heart rate and cardiac output, as well as redistribution of blood flow to vital organs (Kane et al., 2020; Siebenmann & Lundby, 2015; Zoccal et al., 2024). Longer-term cellular responses involve changes in gene expression that promote oxygen delivery to cells and adaptation to reduced oxygen availability (P. Lee et al., 2020; Semenza, 2020; Wenger, 2002). These include increased erythropoiesis and angiogenesis, together with metabolic reprogramming that shifts cellular ATP production to glycolysis, thereby reducing cellular dependence on oxidative phosphorylation. These rapid and longer-term responses are complementary: acute physiological responses increase oxygen availability, whilst

transcriptional and metabolic responses enable cellular adaptation to sustained hypoxia. Therefore, together these mechanisms help to maintain oxygen homeostasis despite fluctuations in oxygen availability.

1.1 **Hypoxia inducible factors**

The transcriptional response to hypoxia is mediated by the hypoxia inducible factor (HIF) family of transcription factors (Greer et al., 2012; P. Lee et al., 2020; Schofield & Ratcliffe, 2004). HIFs regulate the expression of a broad range of genes involved in oxygen delivery, metabolism, cell survival and adaptation to hypoxia. They consist of two subunits, HIF-α and HIF-β, which heterodimerise to form a functional transcription factor. HIF-β, also known as aryl hydrocarbon receptor nuclear translocator (ARNT), is constitutively expressed, whereas HIF-α subunits are regulated in an oxygen-dependent manner. Reduced oxygen availability leads to stabilisation of HIF-α, allowing HIF-α-ARNT complexes to form and regulate transcription of hypoxia-responsive genes (Lisy & Peet, 2008).

1.1.1 *The HIF/PHD pathway*

The oxygen-dependent regulation of HIF-α is principally mediated by prolyl hydroxylase domain (PHD)-containing enzymes (Fong & Takeda, 2008; Kaelin & Ratcliffe, 2008; Schofield & Ratcliffe, 2004). These enzymes belong to the Fe^{2+}- and 2-oxoglutarate (2-OG)-dependent dioxygenase superfamily and require oxygen as a co-substrate. Under normoxic conditions, PHD enzymes hydroxylate conserved proline residues within the oxygen-dependent degradation domain (ODD) of HIF-α. Hydroxylated HIF-α is recognised by the von Hippel-Lindau protein (pVHL), which forms part of an E3 ubiquitin ligase complex. HIF-α is subsequently polyubiquitinated and targeted for proteasomal degradation. Therefore, HIF-α is continuously broken down in the presence of sufficient oxygen.

A second oxygen-dependent regulatory mechanism is mediated by factor inhibiting HIF (FIH), another 2-OG-dependent dioxygenase (Lando et al., 2002). FIH hydroxylates an asparagine residue within the C-terminal activation domain of HIF-α, inhibiting recruitment of transcriptional coactivators including p300/CBP. Consequently, oxygen suppresses HIF activity at both the level of protein stability, through PHD-dependent prolyl hydroxylation, and transcriptional activity, through FIH-dependent asparaginyl hydroxylation. However, during hypoxia, reduced oxygen availability limits the activity of these enzymes, allowing HIF-α to escape pVHL-mediated proteasomal degradation, recruit transcriptional coactivators and activate hypoxia-responsive gene expression. The HIF pathway is illustrated in **Figure 1.1**.

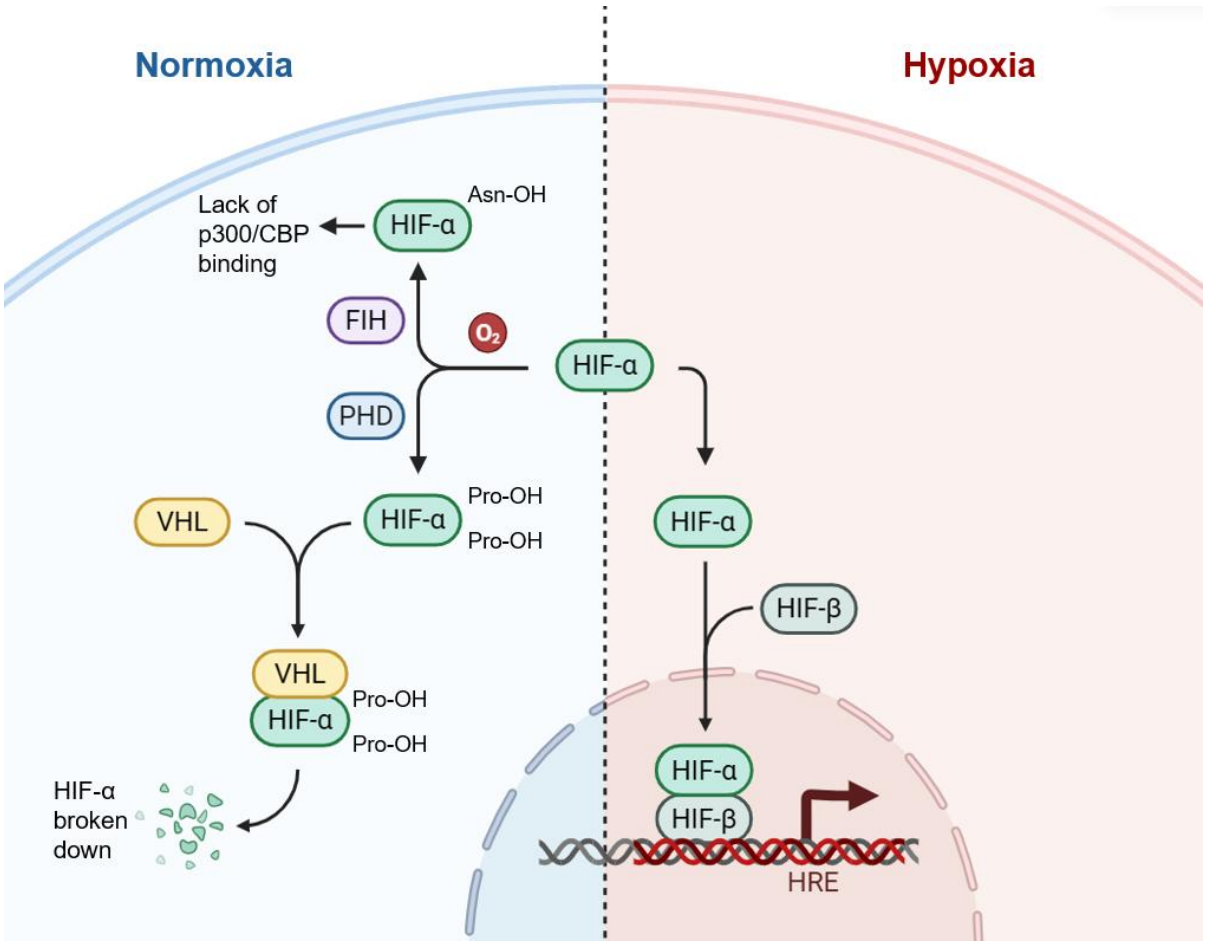

Figure 1.1. The hypoxia inducible factor (HIF) pathway. Under normoxic conditions, HIF-α is hydroxylated at two conserved proline residues by prolyl hydroxylase domain (PHD) enzymes. This hydroxylation enables the von Hippel-Lindau (VHL) protein to target HIF-α for ubiquitination and

subsequent proteasomal degradation. HIF-α is also hydroxylated at a conserved asparagine residue by factor inhibiting HIF (FIH), which prevents the recruitment of transcriptional coactivators, including p300/CBP. Under hypoxic conditions, PHD- and FIH-mediated hydroxylation cannot occur, allowing HIF-α to accumulate, form heterodimers with HIF-β and bind to hypoxia response elements (HRE) within target gene promoters or regulatory regions. This promotes transcription of hypoxia-responsive genes. Figure made in biorender.com, adapted from doi:10.1002/ame2.12192.

1.1.2 *Discovery of HIF*

HIFs were first identified through studies investigating the regulation of erythropoietin (EPO), a hormone produced predominantly by the foetal liver and adult kidneys that stimulates red blood cell production in response to hypoxia and anaemia (Suresh et al., 2020). Seminal work by Semenza and colleagues identified a hypoxia-responsive enhancer in the 3' flanking sequence of the human *EPO* gene and subsequently identified a hypoxia-inducible nuclear factor, termed HIF-1, that bound to a specific sequence within this enhancer, known as the hypoxia response element (HRE) (Semenza et al., 1991; Semenza & Wang, 1992). In parallel, Ratcliffe and colleagues identified a functionally similar hypoxia-responsive enhancer 3' of the mouse *Epo* gene (Pugh et al., 1991). Subsequent studies demonstrated that HIF activity was not restricted to EPO-producing cells but occurs across a wide range of mammalian cell types, establishing HIF as a general mechanism by which mammalian cells respond to hypoxia (Maxwell et al., 1993; G. L. Wang & Semenza, 1993). HIF-1 was subsequently purified and shown to be a heterodimeric complex composed of HIF-1α and HIF-1β/ARNT, with HIF-1α identified as the oxygen-dependent subunit (G. L. Wang et al., 1995; G. L. Wang & Semenza, 1995).

Subsequent studies established the mechanisms underlying the oxygen-dependent regulation of HIF-1α. Several groups demonstrated that hypoxia causes an increase in HIF-α protein levels without a corresponding increase in mRNA, suggesting that its regulation occurs post-

translationally at the level of protein synthesis or degradation (L. E. Huang et al., 1996; Jiang et al., 1996; Kallio et al., 1997). Work from the Ratcliffe and Kaelin laboratories then demonstrated that HIF-α is targeted for degradation by an E3 ubiquitin ligase complex containing pVHL, and that oxygen-dependent hydroxylation of HIF-α mediates pVHL binding and subsequent proteasomal degradation (Ivan et al., 2001; Jaakkola et al., 2001; Maxwell et al., 1999). The following identification of the PHD enzymes as the oxygen-dependent HIF prolyl hydroxylases completed the core HIF oxygen sensing pathway (Bruick & McKnight, 2001; Epstein et al., 2001; Ivan et al., 2002). FIH was also identified as an oxygen-dependent hydroxylase that can suppress the transcriptional activity of HIF (Mahon et al., 2001). Together, these discoveries established a direct biochemical link between oxygen availability, HIF stability and transcriptional regulation, and were recognised by the 2019 Nobel Prize in Physiology and Medicine awarded to Gregg Semenza, Sir Peter Ratcliffe and William Kaelin (C.-C. Lee et al., 2020).

1.1.3 *Structure of HIFs*

HIF-α and HIF-β are members of the basic helix-loop-helix (bHLH) and Per-ARNT-AHR-Sim (PAS) domain-containing family of transcription factors (Semenza, 2012; Wilkins et al., 2016). Their structures are illustrated in **Figure 1.2**. The N-terminal bHLH domains mediate DNA binding, while the adjacent PAS domain contributes to heterodimerisation and transcriptional complex formation. HIF-α subunits additionally contain an oxygen-dependent degradation domain (ODD), containing two conserved proline residues that are targeted for hydroxylation by PHD enzymes, and N-terminal and C-terminal transactivation domains that regulate interactions with transcriptional coactivators including p300/CBP. FIH-dependent hydroxylation of an asparagine residue in the C-terminal transactivation domain inhibits recruitment of p300/CBP and consequently supresses HIF transcriptional activity (Lando et al., 2002) .

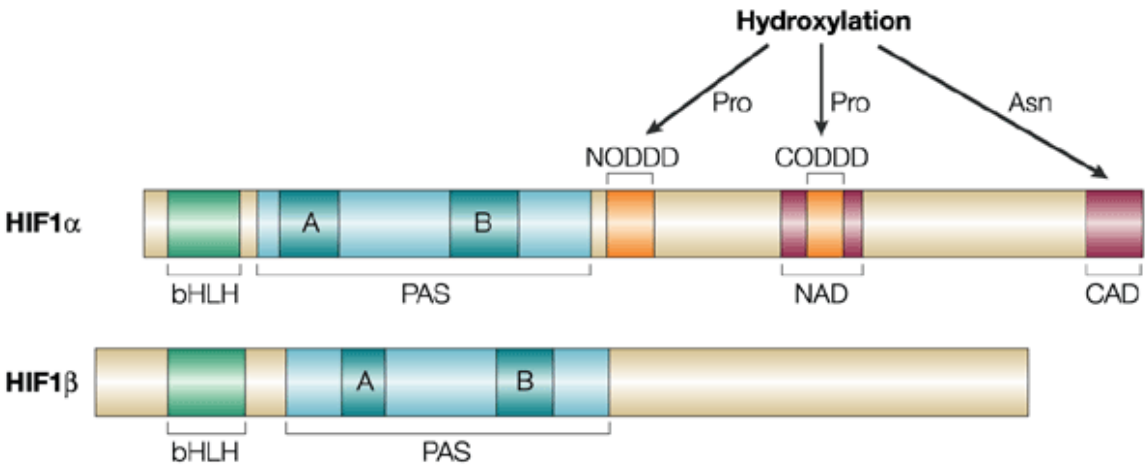

Figure 1.2. Structure of HIF-α and HIF-β. Structure of the HIF-α and HIF-β subunits, including the basic helix-loop-helix (bHLH) domains; PAS (PER (period circadian protein), AHR (aryl-hydrocarbon receptor), ARNT (aryl-hydrocarbon-receptor nuclear translocator), SIM (single-minded protein)) domains; the amino-terminal oxygen-dependent degradation domain (NODDD); the carboxy-terminal oxygen-dependent degradation domain (CODDD); the amino-terminal activation domain (NAD); and the carboxy-terminal activation domain (CAD). Figure taken from Schofield and Ratcliffe (2004) (License number: 6363020081569).

1.1.4 *Structure and functional diversity of HIFs and PHD enzymes*

Following the discovery of HIF-1α, a second isoform of HIF-α, HIF-2α, was identified (Tian et al., 1997). HIF-2α is encoded by the *EPAS1* gene, originally identified from its prominent expression in endothelial cells, and shares substantial sequence homology with HIF-1α, particularly within the conserved bHLH and PAS domains (Ema et al., 1997; Flamme et al., 1997; O'Rourke et al., 1999; Tian et al., 1997). Although HIF-1α and HIF-2α recognise the same HRE sequence, differences in their transactivation domains and interactions with transcriptional coregulators allow them to regulate overlapping but distinct transcriptional programmes (Hu et al., 2007).

HIF-1α and HIF-2α therefore have both shared and isoform-specific functions. They both regulate some common target genes, including *VEGFA*, but the relative contribution of each

isoform is strongly dependent on cell type, developmental stage and the nature and duration of the stimulus (Hu et al., 2003; Raval et al., 2005; Sowter et al., 2003). HIF-1α is often associated with acute metabolic adaptation and induction of glycolytic pathways, whereas HIF-2α has prominent roles in EPO production, vascular remodelling, cellular proliferation and maintenance of differentiated cell states (Covello et al., 2006; Hu et al., 2003; Skuli et al., 2012; Sowter et al., 2003). This functional divergence is also reflected in their genomic binding profiles, with HIF-1 preferentially occupying hypoxia-responsive enhancers located closer to gene promoters, whereas HIF-2 binds more distal regulatory elements, suggesting that differences in genomic occupancy contribute to isoform-specific transcriptional programmes (Smythies et al., 2019).

The differences between HIF-1α and HIF-2α are reflected in genetic knockout models. Loss of *Hif-1α* in mice has been reported to cause mid-gestational embryonic lethality associated with severe cardiovascular and developmental abnormalities (Iyer et al., 1998). Similarly, several studies have reported embryonic lethality in *Epas1*-null mice, with reported abnormalities including cardiovascular and pulmonary defects and impaired catecholamine homeostasis (J. Peng et al., 2000; Scortegagna et al., 2003; Tian et al., 1998). These non-overlapping phenotypes indicate that, despite having substantial biochemical similarity, the HIF-α isoforms are not completely functionally redundant.

HIF-1α and HIF-2α also differ markedly in their expression patterns. HIF-1α is broadly expressed across mammalian tissues, whereas HIF-2α expression is more restricted and is particularly prominent in specialised populations including vascular endothelial cells, certain epithelial populations and cells of the sympathoadrenal lineage, as well as in tissues such as the lungs, heart and placenta (Rajakumar & Conrad, 2000; Talks et al., 2000; Tian et al., 1998; Wiesener et al., 2003). This restricted expression pattern suggests that HIF-2α may have

specialised functions in particular cellular and developmental contexts. Within the sympathoadrenal system, HIF-2α is highly expressed in the carotid body and in developing chromaffin cell populations (Gao, Bonilla-Henao, et al., 2017; Tian et al., 1998; Zhou et al., 2016), highlighting its potential importance in tissues in which oxygen sensing is coupled to specialised neuroendocrine functions.

A third HIF-α isoform, HIF-3α, has also been identified (Gu et al., 1998). Unlike HIF-1α and HIF-2α, HIF-3α generates multiple splice variants with distinct C-terminal domains and transcriptional properties (Ravenna et al., 2016). Some HIF-3α isoforms have been proposed to act as transcriptional regulators of HIF signalling rather than functioning solely as conventional transcriptional activators (Heikkilä et al., 2011). However, the physiological functions of HIF-3α are less well characterised than those of HIF-1α and HIF-2α.

Three mammalian isoforms of PHD have been identified: PHD1, PHD2 and PHD3, encoded by *EGLN2*, *EGLN1* and *EGLN3,* respectively (Epstein et al., 2001) . Although these isoforms share a conserved catalytic domain, they differ in their expression, subcellular localisation, regulation and relative contributions to HIF hydroxylation (Appelhoff et al., 2004; J. Huang et al., 2002; Metzen et al., 2003). PHD2 is generally considered the principal HIF prolyl hydroxylase controlling HIF-α stability under normoxic conditions in most cell types due to its abundant expression (Appelhoff et al., 2004; Berra et al., 2003), although the relative importance of each PHD isoform is context dependent. PHD3 is itself strongly induced by HIF-dependent transcription during hypoxia and can therefore contribute to negative feedback within the HIF pathway (Pescador et al., 2005).

Mouse knockout studies support distinct functional roles for the individual PHD isoforms, with PHD2 appearing particularly important for embryonic development. Whereas global loss of *Phd2* causes embryonic lethality between embryonic days 12.5 and 14.5, accompanied by

severe cardiac and placental abnormalities, mice lacking *Phd1* or *Phd3* are viable and do not exhibit comparable developmental defects (Takeda et al., 2006). Adult PHD1-deficient mice show altered basal metabolism, including reduced oxygen consumption and a shift towards more anaerobic ATP production, which confers increased tolerance to ischaemia (Aragonés et al., 2008), whereas PHD3-deficient mice exhibit abnormalities in sympathoadrenal development, including increased numbers of sympathetic neurons, adrenal chromaffin cells and carotid body glomus cells, but reduced sympathoadrenal function (Bishop et al., 2008). These distinct phenotypes associated with loss of individual PHD isoforms indicate that they are not functionally redundant.

1.1.5 *Metabolic regulation of the HIF pathway*

The HIF pathway is closely integrated with cellular metabolism. Changes in the activity of metabolic enzymes can alter the intracellular concentration of metabolic intermediates that regulate 2-OG-dependent dioxygenases and consequently influence HIF stability and transcriptional activity (**Figure 1.3**) (Fletcher & Coleman, 2020; Losman et al., 2020). For example, succinate dehydrogenase (SDH) is both a component of the Krebs cycle, where it catalyses the conversion of succinate to fumarate, and complex II of the mitochondrial electron transport chain, where it transfers electrons from $FADH_2$ through iron-sulfur clusters to reduce ubiquinone to ubiquinol. A reduction in SDH activity causes intracellular accumulation of succinate, which can inhibit 2-OG-dependent dioxygenases, including PHD enzymes that hydroxylate HIF-α (MacKenzie et al., 2007). Consequently, succinate accumulation can lead to stabilisation of HIF in the absence of hypoxia, a phenomenon termed ‘pseudohypoxia’.

Accumulation of succinate and other oncometabolites can also inhibit other 2-OG-dependent enzymes, including TET DNA demethylases and Jumonji C-domain histone demethylases, resulting in widespread changes in DNA and histone methylation (Xiao et al., 2012). Therefore,

metabolic disruption can influence cellular phenotype through both HIF-dependent and HIF-independent mechanisms.

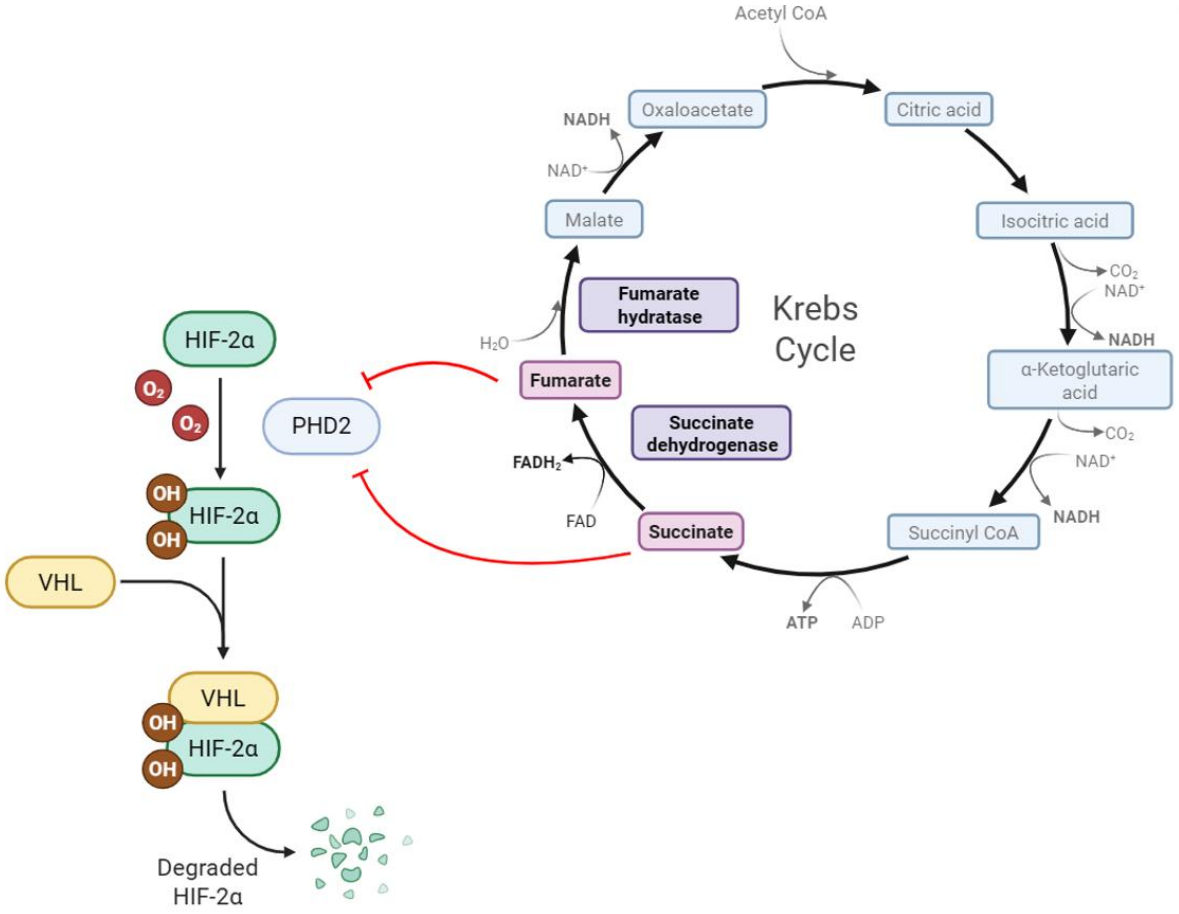

Figure 1.3. Metabolic interaction with the HIF pathway. Loss-of-function mutations in the Krebs cycle enzymes succinate dehydrogenase (SDH) and fumarate hydratase (FH) can cause accumulation of their substrates succinate and fumarate, respectively. These competitively inhibit 2-oxoglutarate-dependent dioxygenases including prolyl hydroxylase domain (PHD) enzymes, preventing PHD-mediated hydroxylation of HIF-α, leading to stable expression of HIF-α under normoxic conditions, termed pseudohypoxia. Figure made in biorender.com.

1.2 **The acute response to hypoxia - the carotid body**

The HIF/PHD transcriptional pathway enables cells and tissues to adapt to sustained changes in oxygen availability over timescales ranging from hours to days. However, maintenance of

arterial oxygenation requires much more rapid physiological responses, initiated within seconds of a fall in arterial oxygen tension. Therefore, mammals possess specialised cell types that sense hypoxaemia and initiate these rapid responses (Weir et al., 2005). The carotid body is the principal peripheral chemoreceptor responsible for detecting changes in arterial oxygen tension (Gonzalez et al., 1994; Iturriaga et al., 2021; P. Kumar & Prabhakar, 2012). It is a small, highly vascularised organ located bilaterally at the bifurcation of the common carotid artery, allowing it to monitor changes in the composition of arterial blood (Baashar & Alsahafi, 2026; López-Barneo et al., 2008). Hypoxia-induced activation of the carotid body increases afferent activity in the carotid sinus nerve, which projects to respiratory and autonomic centres in the brainstem. This produces a rapid increase in ventilation and contributes to sympathetic activation. In contrast to the relatively slow transcriptional responses mediated by the HIF pathway, carotid body activation occurs within seconds of a reduction in oxygen availability (Black et al., 1971).

Detailed histological studies by Fernando de Castro in the 1920s described the dense sensory innervation of the carotid body and led him to propose that it contained specialised receptors capable of detecting changes in the composition of the blood (de Castro, 1926, 1928; De Castro, 2009; Gonzalez et al., 2014). This hypothesis was subsequently supported by the physiological experiments of Corneille Heymans and colleagues, who used cross-circulation in anesthetised dogs to investigate the roles of the carotid and aortic regions in the regulation of respiration (C. Heymans, 1930; J. F. Heymans & Heymans, 1927). In these experiments, blood from one dog was used to perfuse the head of another dog while its neural connections to the brain remained intact. Exposure of the donor animal to hypoxia or hypercapnia elicited increased ventilation in the recipient animal, demonstrating that changes in arterial blood composition could evoke a reflex respiratory response. Subsequent sectioning of the carotid sinus and cardio-aortic afferent nerves established the importance of these pathways in mediating ventilatory responses

to changes in arterial blood composition (C. Heymans, 1930, 1938). This work resulted in Heymans being awarded the 1938 Nobel Prize in Physiology or Medicine. Later electrophysiological studies using isolated carotid body-carotid sinus nerve preparations demonstrated that hypoxia produces a rapid increase in carotid sinus nerve activity (BISCOE et al., 1967), whilst electron microscopy identified numerous dense core secretory vesicles within carotid body glomus cells, supporting their role as secretory cells involved in chemosensory transduction (Gronblad & Eranko, 1978). Together, these observations established the carotid body as a specialised arterial chemoreceptor that detects changes in blood composition and rapidly converts these stimuli into neuronal signals that drive respiratory and autonomic responses.

1.2.1 *The carotid body response to sustained hypoxia*

As well as mediating the rapid response to acute hypoxia, the carotid body undergoes substantial functional and structural plasticity during sustained hypoxia. Following the initial rapid increase in ventilation produced by acute hypoxia, ventilation typically falls from its peak as hypercapnia develops then progressively rises again over the following hours to days (Douglas et al., 1913; Howard & Robbins, 1995b, 1995a). This secondary increase in ventilation is termed ventilatory acclimatisation to hypoxia (VAH). It is accompanied by enhanced sensitivity to subsequent hypoxic challenges and contributes to the maintenance of arterial oxygenation during prolonged exposure to reduced oxygen availability (Vizek et al., 1987).

VAH is associated with both structural and functional remodelling of the carotid body. Sustained hypoxia increases carotid body chemosensory activity and enhances carotid sinus nerve responses to hypoxia (Nielsen et al., 1988), accompanied by changes in glomus cell ion channels and neurotransmitter signalling. Several neuromodulatory pathways have been

implicated, including endothelin and dopamine signalling. Chronic hypoxia increases endothelin-1 and ET_A receptor expression in the carotid body (Y. Chen et al., 2002), while pharmacological inhibition of ET_A receptors reduces carotid body proliferation and carotid sinus nerve activity in hypoxia-acclimatised rats (J. Chen et al., 2007). Dopaminergic signalling has also been implicated, with D2 receptor blockade mimicking aspects of VAH (Bisgard, 2000; Tatsumi et al., 1995). However, increased dopamine synthesis during chronic hypoxia suggests that altered dopaminergic signalling is unlikely to fully account for the acclimatory response (Czyzyk-Krzeska et al., 1992).

Sustained hypoxia also causes marked enlargement of the carotid body (Bishop et al., 2013; Dhillon et al., 1984; Pardal et al., 2007; Pequignot & Hellstrom, 1983) and increased vascularisation driven by vascular endothelial growth factor (VEGF) (Fielding et al., 2018; Laidler & Kay, 1975). The importance of the carotid body to VAH is demonstrated by denervation studies which markedly attenuate or abolish VAH (Forster et al., 1981; Smith et al., 1986). Therefore, prolonged hypoxia induces functional and structural changes within the carotid body that enhance peripheral chemosensitivity and contribute to the progressive increase in ventilatory drive during VAH.

1.2.2 *Structure and morphology*

The carotid body is composed of two principal cell population arranged into highly vascularised clusters, known as glomeruli (illustrated in **Figure 1.4**) (McDonald & Mitchell, 1975). These are the oxygen-sensitive type I, or glomus, cells, and the glia-like type II, or sustentacular, cells. Glomus cells are relatively small, neural crest-derived neuroendocrine cells arising from the sympathoadrenal lineage (Kameda, 2020). They contain numerous dense core vesicles containing neurotransmitters and neuromodulators, including ATP, dopamine, acetylcholine and serotonin (Iturriaga & Alcayaga, 2004; McDonald & Mitchell, 1975).

Glomus cells express tyrosine hydroxylase (TH), the rate-limiting enzyme in catecholamine synthesis **(Figure 1.5)** (Kameda et al., 1990; Z.-Z. Wang et al., 1991), enabling their immunohistochemical detection using antibodies against TH. They form close contacts with capillaries and afferent sensory fibres, which are important for their ability to rapidly sense hypoxia and transmit signals to the nervous system.

In contrast, carotid body sustentacular cells are glia-like cells that surround glomus cells and have traditionally been considered to provide structural and metabolic support (Kameda, 1996). They are characterised by their expression of markers including glial fibrillary acidic protein (GFAP) and lack the dense core vesicles characteristic of glomus cells (De Kock, 1951). Sustentacular cells have also been implicated in carotid body regeneration, with early lineage-tracing studies suggesting that $GFAP^+$ type II cells can function as multipotent neural crest-derived progenitors capable of generating new glomus cells during sustained hypoxia (Pardal et al., 2007). However, subsequent studies identified an immature TH^+/HNK-1^+ population that proliferates during chronic hypoxia (Sobrino et al., 2018), suggesting that carotid body growth may involve expansion and maturation of a pre-existing immature glomus cell population rather than direct conversion of sustentacular cells into glomus cells. Consistent with this, more recent lineage-tracing studies indicate that sustained hypoxia primarily drives rapid expansion of the existing TH^+ type I cell lineage, with little evidence of transdifferentiation between type I and type II populations (Fielding et al., 2018). Therefore, while sustentacular cells may contribute to carotid body maintenance and regeneration, hypoxia-induced expansion of the type I cell population cannot be explained solely by conversion of sustentacular cells into glomus cells. Together, these findings highlight the carotid body as a multicellular sensory organ in which neuroendocrine, glial, vascular and neuronal cells interact to mediate both acute oxygen sensing and longer-term structural plasticity.

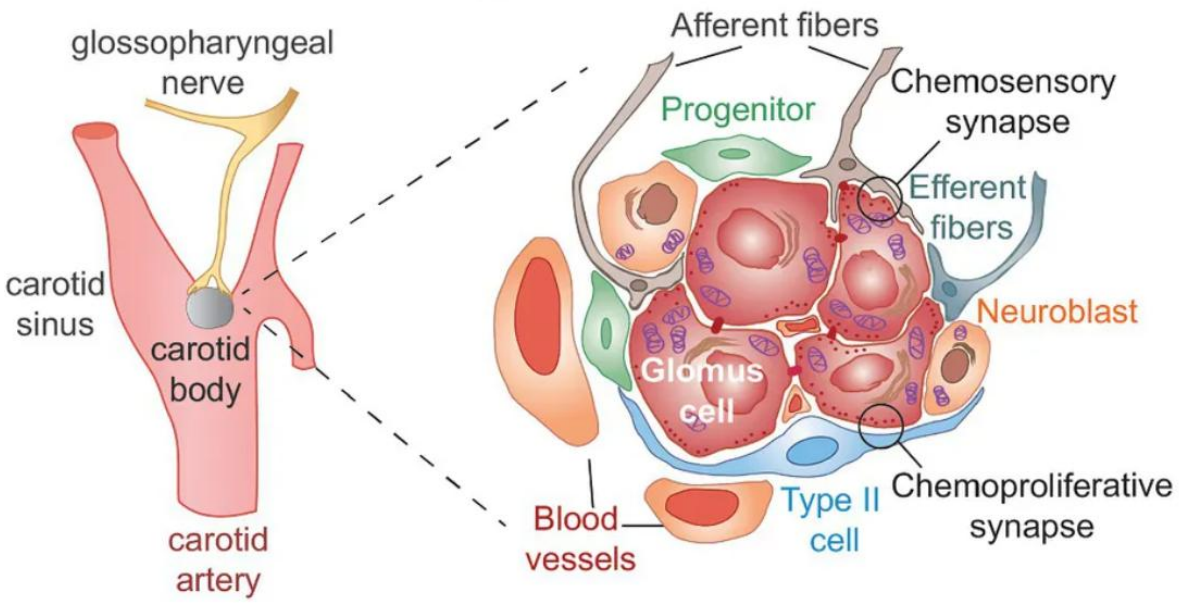

Figure 1.4. Structure of the carotid body. Anatomical location of the carotid body within the carotid bifurcation (left) and diagram of the diverse cell types within the carotid body (right). Figure taken from Ortega-Sáenz et al. (2020).

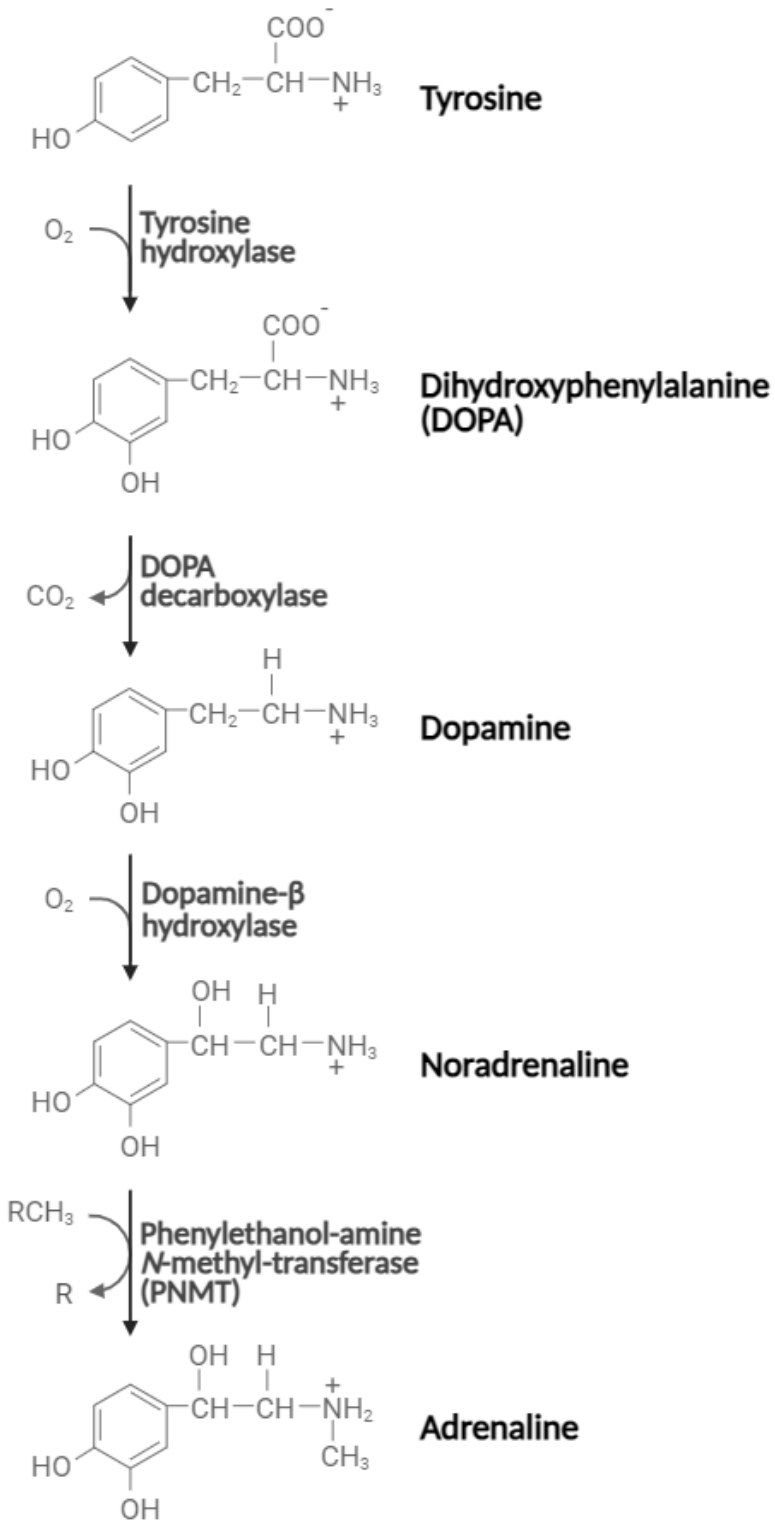

Figure 1.5. Catecholamine synthesis pathway. Tyrosine is converted to dihydroxyphenylalanine (DOPA) by tyrosine hydroxylase. This is the rate-limiting step within the catecholamine synthesis pathway. DOPA is then converted to dopamine by DOPA decarboxylase, dopamine is converted to noradrenaline by dopamine-β-hydroxylase, and noradrenaline is converted to adrenaline by phenylethanolamine-N-methyltransferase (PNMT). Figure generated in biorender.com.

1.2.3 *Oxygen chemosensitivity*

Acute hypoxia rapidly activates carotid body glomus cells (Ortega-Sáenz & López-Barneo, 2020; Semenza & Prabhakar, 2018). A reduction in arterial oxygen tension inhibits oxygen-sensitive potassium (K^+) conductances, causing membrane depolarisation and opening of voltage-gated calcium (Ca^{2+}) channels (Buckler, 1997; Fieber & McCleskey, 1993; López-Barneo et al., 1988). The resulting Ca^{2+} influx triggers exocytosis of secretory vesicles and release of neurotransmitters into the synaptic cleft (Hansen, 1981; Ureña et al., 1994). These activate receptors on afferent fibres of the carotid sinus nerve, increasing signalling to the respiratory and autonomic centres within the brainstem. Although this sequence of events (illustrated in **Figure 1.6**) is well established, how reduced oxygen availability is detected and coupled to inhibition of K^+ conductances remains incompletely understood. In particular, the identity of the oxygen sensor and the molecular intermediates linking oxygen sensing to channel inhibition remain an area of ongoing investigation.

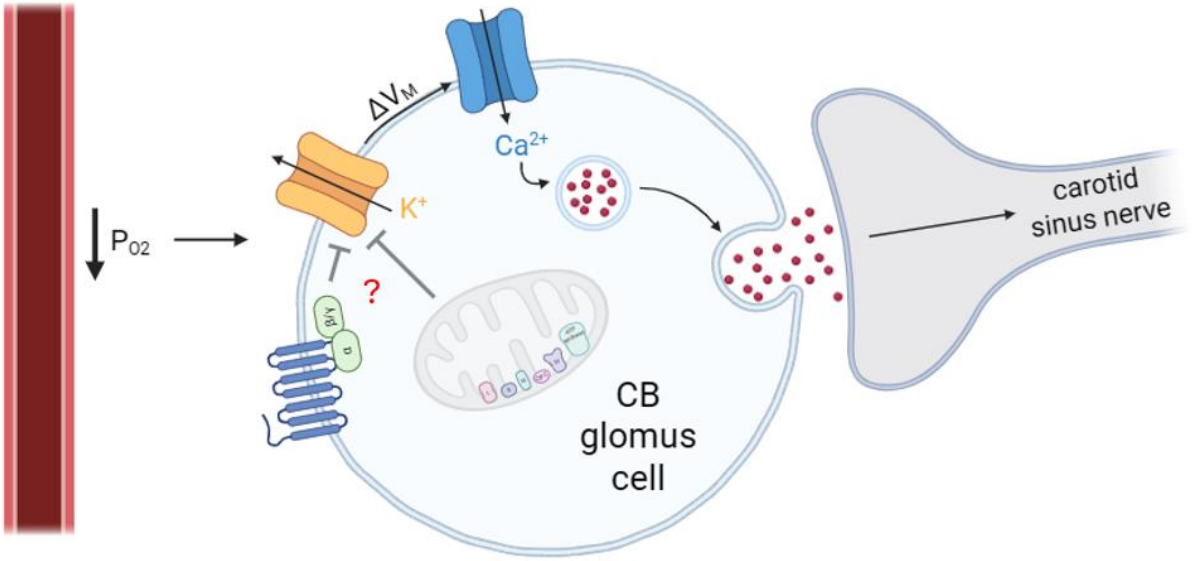

Figure 1.6. Oxygen sensing pathway in carotid body glomus cells. Carotid body glomus cells detect a reduction in arterial oxygen tension, resulting in the inhibition of membrane K^+ channels. This inhibition causes membrane depolarisation and subsequent opening of voltage-gated Ca^{2+} channels. the resulting influx of Ca^{2+} triggers regulated exocytosis of dense core vesicles, leading to the release of neurotransmitters into the synaptic cleft. These can activate afferent fibres of the carotid sinus nerve, initiating signalling to the central nervous system. The precise molecular signal that transmits the reduction in oxygen to K^+ channel inhibition is unknown, but may involve mitochondrial or G protein-coupled receptor (GPCR) signalling Figure created in biorender.com.

A number of K^+ channel families have been implicated in the carotid body response to hypoxia (Buckler, 2015; López-López & Pérez-García, 2007; Ortega-Sáenz & López-Barneo, 2020; Rocher & Aaronson, 2024). Glomus cells express voltage-gated K^+ channels, large conductance Ca^{2+}-activated K^+ (BK) channels and two-pore-domain K^+ (K2P) channels, including members of the Twik-related acid-sensitive K^+ (TASK) channel family. TASK channels are sensitive to extracellular pH and volatile anaesthetics and contribute to the regulation of glomus cell membrane potential and excitability (Buckler et al., 2000). In isolated glomus cells, hypoxia was shown to inhibit TASK-like background K^+ currents, leading to the proposal that inhibition of these channels could provide the molecular link between reduced oxygen availability and membrane depolarisation (Buckler, 1997; López-Barneo et al., 1988). Subsequent studies identified TASK-1/TASK-3 heterodimers as a major contributor to the oxygen-sensitive background K^+ current in rat glomus cells (D. Kim et al., 2009). However, genetic studies provided evidence that TASK-1/TASK-3 channels are not the sole mediators of hypoxic signalling. Although deletion of TASK-1 and/or TASK-3 altered glomus cell electrical properties and attenuated some carotid body and ventilatory responses to hypoxia, hypoxia-induced catecholamine secretion was retained in double knockout TASK-1/TASK-3 glomus cells (Ortega-Sáenz et al., 2010; Trapp et al., 2008). This suggests that other K^+ channels may contribute to hypoxic transduction, either through parallel pathways or

compensatory/redundant mechanisms. Furthermore, early patch-clamp experiments indicated that hypoxic inhibition of K^+ channels can depend on the intracellular environment; hypoxia reduced BK channel activity in perforated-patch recordings, in which the intracellular environment is preserved, but not in excised outside-out patches, in which diffusible intracellular components are largely lost (Wyatt & Peers, 1995). Similarly, hypoxia caused inhibition of TASK-like K^+ channels in cell-attached patches but had no effect on channel activity in inside-out patches (Buckler et al., 2000). Together, these findings suggest that K^+ channels may function as downstream effectors of an upstream oxygen-sensing mechanism rather than serving as the primary oxygen sensors themselves (Buckler, 1997; Wyatt & Peers, 1995). This led to increasing interest in mitochondria as a potential site of oxygen sensing, providing a possible link between reduced oxygen availability and changes in glomus cell membrane excitability.

The carotid body is highly sensitive to mitochondrial dysfunction, and pharmacological inhibition of the mitochondrial electron transport chain can mimic several features of hypoxic glomus cell activation, including membrane depolarisation, Ca^{2+} influx and neurotransmitter secretion (Ortega-Saenz et al., 2003; Wyatt & Buckler, 2004). These observations contributed to the development of the mitochondria-to-membrane model of oxygen sensing, which proposes that hypoxia-induced changes in mitochondrial function generate intracellular signals that modulate ion channel activity at the plasma membrane (López-Barneo et al., 2016; López-Barneo & Ortega-Sáenz, 2022; Ortega-Sáenz & López-Barneo, 2020). However, a major challenge for this model is that mitochondrial respiration is generally considered to be relatively insensitive to reductions in oxygen within the range that activates the carotid body, because cytochrome c oxidase (complex IV), the terminal oxygen-consuming component of the electron transport chain, has a very low K_m for oxygen (López-Barneo et al., 2016). Nevertheless, studies have shown that reductions in oxygen can alter mitochondrial function in

rat carotid body glomus cells at substantially higher PO_2 levels than those required to affect superior cervical ganglion neurons, suggesting that carotid body mitochondria possess specialised properties that enable them to respond to physiologically relevant changes in oxygen availability (Buckler & Turner, 2013). Proposed mitochondrial signals include changes in reactive oxygen species (ROS), mitochondrial redox state, NADH, the ADP/ATP ratio and other metabolic intermediates (Arias-Mayenco et al., 2018; Fernández-Agüera et al., 2015; Gao, González-Rodríguez, et al., 2017; Holmes et al., 2022; López-Barneo et al., 2016). However, the relative contribution of these signals remains unresolved, and current evidence favours a model in which multiple mitochondrial, metabolic and membrane-associated processes interact to generate the acute hypoxic response, rather than a singular molecular oxygen sensor.

The advent of transcriptomic approaches has provided a complementary route to understanding the molecular specialisation of carotid body cells. Early bulk transcriptomic and expression-profiling studies established that the carotid body has a distinct molecular phenotype compared with non-chemosensory tissues (Chang et al., 2015; Ganfornina et al., 2005; Mkrtchian et al., 2012). However, its cellular heterogeneity, including glomus cells, sustentacular cells, endothelial cells, vascular smooth muscle cells and fibroblasts, limits the ability of bulk approaches to resolve cell type-specific gene expression. Single-cell RNA sequencing subsequently enabled the transcriptional profile of individual glomus cells to be examined directly, providing greater resolution of their molecular specialisation (Gao, Bonilla-Henao, et al., 2017; Zhou et al., 2016).

Single-cell analysis of mouse carotid body glomus cells identified high expression of genes associated with HIF signalling, G protein-coupled receptor (GPCR) signalling and ion channel function, highlighting the diverse molecular pathways involved in glomus cell signalling (Gao,

Bonilla-Henao, et al., 2017). Among the most highly enriched genes were the atypical mitochondrial electron transport chain components *Ndufa4l2* and *Cox4i2*. Comparative transcriptomic analysis of the carotid body with developmentally related, but relatively hypoxia-insensitive sympathoadrenal tissues further demonstrated enrichment of these genes, implicating them in oxygen sensing (Zhou et al., 2016). A subsequent comparison of carotid body and adrenal medulla transcriptomes identified *Higd1c* as an additional highly enriched mitochondrial gene (Timón-Gómez et al., 2022). COX4I2 and HIGD1C are atypical complex IV-associated proteins that, when co-expressed, increase the sensitivity of mitochondrial respiration to oxygen availability. Genetic deletion of *Cox4i2* or *Higd1c* impairs carotid body oxygen sensing in mice, providing functional evidence that these mitochondrial components contribute to the specialised oxygen-sensing phenotype of glomus cells. *Cox4i2* deletion reduces hypoxia-evoked Ca^{2+} responses in glomus cells and the hypoxic ventilatory response (Moreno-Domínguez et al., 2020), while *Higd1c* deletion similarly reduces the hypoxic ventilatory response and attenuates hypoxia-induced carotid sinus nerve activity (Timón-Gómez et al., 2022). Together, these transcriptomic and functional studies support a role for specialised mitochondrial metabolism in carotid body oxygen sensing.

As well as atypical mitochondrial components, single-cell transcriptomic analyses also identified enrichment of components of G protein-coupled receptor (GPCR) signalling in the carotid body. This includes the GPCRs *Olfr78* and *Adora2a*, together with downstream signalling components such as *Gnas* and the regulators of G protein signalling *Rgs4* and *Rgs5* (Zhou et al., 2016). Consistent with this, comparative transcriptomic analysis demonstrated enrichment of genes associated with GPCR signalling in the carotid body relative to hypoxia-insensitive sympathoadrenal tissues, in particular *Rgs5* (Gao, Bonilla-Henao, et al., 2017). RGS4 and RGS5 are substrates of the oxygen dependent enzyme 2-aminoethanethiol dioxygenase (ADO), which promotes their N-terminal cysteine oxidation and subsequent

degradation through the N-degron pathway (Masson et al., 2019). In hypoxia, inhibition of ADO leads to stabilisation of RGS4 and RGS5, raising the possibility that this pathway links oxygen availability to GPCR signalling in carotid body glomus cells. Together, these findings suggest that GPCR-mediated signalling forms part of the specialised molecular phenotype of carotid body glomus cells, although whether these pathways directly contribute to acute oxygen sensing or instead modulate the downstream response to hypoxia is incompletely understood. Importantly, these transcriptomic studies shifted the field beyond individual candidate channels and signalling proteins towards defining the broader transcriptional programme that distinguishes oxygen-sensitive glomus cells.

1.3 **Other oxygen sensitive tissues - chromaffin cells**

As well as carotid body glomus cells, rapid responses to acute hypoxia have been described in several other cell types, including pulmonary artery smooth muscle cells (Cornfield et al., 1994; Murray et al., 1990), neuroepithelial cell bodies in the airway epithelium (Lauweryns & Cokelaere, 1973) and neonatal chromaffin cells (Cornfield et al., 1994; Mojet et al., 1997; Seidler & Slotkin, 1985). Neonatal chromaffin cells are of particular interest as they share a neural crest origin and close developmental relationship with the carotid body (Hockman et al., 2018). Both cell populations subsequently undergo distinct differentiation programmes and acquire different physiological functions.

Chromaffin cells are specialised neuroendocrine cells that produce, store and secrete catecholamines as part of the sympathetic fight-or-flight response (Carbone et al., 2019). The principal chromaffin cell population is located within the adrenal medulla, where preganglionic sympathetic stimulation induces rapid, Ca^{2+}-dependent secretion of adrenaline and noradrenaline into the circulation. During foetal and early postnatal development, chromaffin

cells are also found at extra-adrenal sites, including the organ of Zuckerkandl (Coupland, 1965).

1.3.1 *Oxygen chemosensitivity in chromaffin cells*

Neonatal chromaffin cells are directly responsive to acute hypoxia. Experiments using isolated newborn rat adrenal chromaffin cells demonstrated that hypoxia increases intracellular Ca^{2+} and stimulates catecholamine secretion, showing this response is intrinsic to chromaffin cells rather than dependent on intact sympathetic innervation (Mojet et al., 1997). Electrophysiological studies further showed that hypoxia inhibits voltage-dependent K^+ currents in neonatal chromaffin cells, resulting in membrane depolarisation, activation of voltage-gated Ca^{2+} channels and subsequent catecholamine secretion (Thompson et al., 1997). Inhibition of mitochondrial respiration was also found to mimic several effects of hypoxia, suggesting that mitochondrial metabolism contributes to the oxygen-sensing pathway in chromaffin cells (Mojet et al., 1997). Consistent with these findings, studies in foetal sheep demonstrated that hypoxia stimulates adrenal secretion of noradrenaline and adrenaline thorough inhibition of K^+ currents, and that this response requires Ca^{2+} entry through voltage-gated L-type Ca^{2+} channels; blockade with nifedipine markedly reduces hypoxia-induced catecholamine secretion (Adams, 1996; Rychkov et al., 1998). Collectively, these findings demonstrate that developing chromaffin cells possess an intrinsic oxygen-sensing mechanism capable of detecting reduced oxygen availability and signalling to cause Ca^{2+}-dependent catecholamine secretion.

The oxygen-sensing properties of developing chromaffin cells share several fundamental features with those of carotid body glomus cells. Both are neuroendocrine cells that contain dense core vesicles and respond to hypoxia through inhibition of K^+ conductance, membrane depolarisation, Ca^{2+} entry and regulated secretion. However, their developmental trajectories

are markedly different. Carotid body glomus cells have relatively limited oxygen sensitivity at birth which increases throughout postnatal maturation (Carroll & Kim, 2005). In contrast, the direct hypoxia sensitivity of chromaffin cells is progressively lost after birth, with both the proportion of responsive adrenal chromaffin cells and the magnitude of the secretory response significantly reduced in adulthood compared with foetal and neonatal stages (García-Fernández et al., 2007). Importantly, this reduction in hypoxia sensitivity is not simply a consequence of loss of cellular excitability, as adult adrenal medullary chromaffin cells retain robust secretory activity (Carbone et al., 2019). Rather, maturation appears to alter the mechanisms coupling reduced oxygen availability to cellular excitation. This contrasting developmental pattern may reflect the distinct physiological roles of these oxygen-sensing systems. The carotid body is primarily coupled to afferent respiratory and autonomic reflexes which become particularly important at birth, whereas developing chromaffin cells can respond directly to hypoxia and secrete catecholamines independently of sympathetic innervation (Bournaud et al., 2007; Levitsky & López-Barneo, 2009). This cell-autonomous mechanism therefore provides a means of initiating an endocrine response to hypoxia early in development, before functional splanchnic innervation of the adrenal medulla is established. This has led to the hypothesis that developing chromaffin cells may contribute to oxygen-sensitive autonomic responses during early life, when carotid body oxygen sensing is not yet functionally mature.

1.3.2 *The organ of Zuckerkandl*

The organ of Zuckerkandl is a prominent extra-adrenal chromaffin cell structure located along the abdominal aorta, typically near to the origin of the inferior mesenteric artery (Coupland, 1965). It is present during late embryonic development and the early postnatal period before undergoing substantial postnatal involution (Schober et al., 2013). In rodents, there is marked expansion of the organ of Zuckerkandl before and immediately after birth, followed by a rapid reduction in chromaffin cell number during the postnatal period, with only small residual cell

populations remaining by postnatal day 10 (Schober et al., 2013). In humans, extra-adrenal chromaffin tissue in the region of the organ of Zuckerkandl persists into early childhood and peaks in size at around 2-3 years of age before regressing (Coupland, 1965). The postnatal regression of the organ of Zuckerkandl is associated with loss of chromaffin cells through programmed cell death and autophagy, processes that are influenced by glucocorticoid signalling (Schober et al., 2013).

The organ of Zuckerkandl is composed predominantly of chromaffin cells derived from the neural crest lineage, with recent linage-tracing studies indicating that most arise from nerve-associated Schwann cell precursors (Kastriti et al., 2019). Like adrenal chromaffin cells, these cells synthesise, secrete and store catecholamines, but unlike the majority of mature adrenal chromaffin cells, they lack expression of phenylethanolamine N-methyltransferase (PNMT) and therefore predominantly produce noradrenaline rather than adrenaline (Otlyga et al., 2025). During foetal development, the organ of Zuckerkandl represents an important source of circulating noradrenaline and is thought to contribute to cardiovascular homeostasis during physiological stress, including hypoxia (West et al., 1953). This predominantly noradrenergic output is well suited to the foetal response to hypoxia, in which increased catecholamine signalling contributes to peripheral vasoconstriction and maintenance of arterial pressure, while hypoxia-induced bradycardia prolongs ventricular filling and helps preserve stroke volume despite increased cardiac afterload (Giussani, 2016; Giussani et al., 1993). Experimental studies have demonstrated catecholamine stores and secretion from extra-adrenal chromaffin tissue during foetal and neonatal development (Bondarenko et al., 2016; Hervonen & Korkala, 1972; West et al., 1953), supporting a role for these tissues in the perinatal sympathoadrenal response.

The potential relationship between the organ of Zuckerkandl and oxygen sensing is particularly relevant during development, when the foetus is exposed to relatively low oxygen availability and fluctuations in oxygen supply. Unlike the postnatal circulation, in which the lungs provide oxygen directly to the blood, foetal oxygenation depends on transfer across the placenta, resulting in substantially lower foetal arterial oxygen tensions than after birth (Nye et al., 2018). Foetal oxygen demand can also increase with metabolic activity, while oxygen delivery may be transiently reduced by changes in placental or umbilical blood flow. Importantly, the transition to birth is preceded by labour, during which uterine contractions repeatedly reduce uteroplacental perfusion and cause transient episodes of foetal hypoxaemia (Turner et al., 2020). The foetus must therefore maintain oxygen delivery despite comparatively low baseline oxygen availability, changing metabolic demands and fluctuations in oxygen supply. Catecholamines are an important component of this response, promoting vasoconstriction and redistribution of blood flow to vital organs (Giussani, 2016). Whether the organ of Zuckerkandl directly senses changes in oxygen availability or instead contributes to the catecholamine response through indirect systemic or neural signals, remains less well established. Nevertheless, the developmental timing and physiological role of this extra-adrenal chromaffin tissue are consistent with a contribution to hypoxia-responsive catecholamine regulation during the perinatal period.

This possibility is further supported by the expression of *EPAS1*, encoding HIF-2α, within the developing organ of Zuckerkandl (Tian et al., 1998). In the original identification of the mouse *Epas1* gene, *in situ* hybridisation revealed strikingly high expression of *Epas1* in the organ of Zuckerkandl, and the authors proposed that *Epas1* could contribute to hypoxia-responsive regulation of catecholamine production (Tian et al., 1998). In *Epas1*-deficient embryos, catecholamine levels were substantially reduced and the embryos developed marked bradycardia. Administration of the noradrenaline precursor DOPS partially rescued the

cardiovascular phenotype, providing functional evidence that *Epas1* is required for normal catecholamine homeostasis during embryonic development. These findings provide an important link between the developmental function of the organ of Zuckerkandl and HIF-2α and raise the possibility that HIF-2α contributes to the specialised oxygen-responsive phenotype of developing extra-adrenal chromaffin cells.

1.4 **HIF-2α in carotid body and chromaffin cell chemosensitivity**

The expression and functional importance of HIF-2α in both carotid body glomus cells and developing chromaffin populations provides a potential molecular link between these oxygen-sensitive cell types. *EPAS1*, encoding HIF-2α, is among the most highly expressed transcripts in carotid body glomus cells, with single-cell transcriptomic studies identifying *Epas1* alongside components of the oxygen sensing pathway (Gao, Bonilla-Henao, et al., 2017; Tian et al., 1998; Zhou et al., 2016). HIF-2α is also expressed in developing chromaffin cell populations, including the organ of Zuckerkandl and subpopulations within the neonatal adrenal medulla (Gao, Bonilla-Henao, et al., 2017; Tian et al., 1998; Zhou et al., 2016). Together, these observations support a potential role for HIF-2α in establishing or maintaining the specialised oxygen-sensitive phenotype of these cells.

Genetic and pharmacological studies have provided direct evidence for an essential role of HIF-2α in carotid body development and function. Developmental deletion of *Epas1* in catecholaminergic (TH^+) cells results in a profound reduction in mature carotid body glomus cells in adult mice (Macias et al., 2018). Further, conditional inactivation of HIF-2α in adult mice markedly impairs carotid body responses to acute hypoxia, evidenced by a reduced hypoxic ventilatory response and diminished hypoxia-induced Ca^{2+} influx into glomus cells (Moreno-Domínguez et al., 2020). Importantly, this reduction in hypoxic ventilatory response is not reproduced by equivalent loss of *Hif-1α* (Macias et al., 2018), indicating that the HIF-2α

isoform specifically is important in both carotid body development and function. HIF-2α also contributes to carotid body adaptation during sustained hypoxia. In adult mice, conditional HIF-2α inactivation markedly attenuates ventilatory acclimatisation and supresses the hypoxia-induced proliferation of carotid body cells (Hodson et al., 2016), while pharmacological inhibition of HIF-2α with PT2385 similarly attenuates both ventilatory acclimatisation and carotid body proliferative responses during sustained hypoxia (Cheng et al., 2020).

The role of HIF-2α in acute oxygen sensing is linked, at least in part, to its regulation of specialised mitochondrial components. Inactivation of *Epas1* reduces the expression of atypical mitochondrial electron transport subunits that are highly enriched in carotid body glomus cells, including *Cox4i2* and *Ndufa4l2* (Moreno-Domínguez et al., 2020). Importantly, *Cox4i2* and *Ndufa4l2* have been shown to be HIF-2α-dependent genes in carotid body glomus cells, linking HIF-2α transcriptional activity directly to the specialised mitochondrial phenotype of these cells. Furthermore, genetic deletion of *Cox4i2* impairs glomus cell responses to hypoxia and the hypoxic ventilatory response, mimicking the phenotype of *Epas1*-null mice (Moreno-Domínguez et al., 2020). Similarly, loss of *Higd1c* also impairs carotid body oxygen sensing (Timón-Gómez et al., 2022). These findings suggest that HIF-2α-dependent transcription establishes aspects of the specialised mitochondrial phenotype required for acute oxygen sensing, rather than directly mediating the rapid response itself. This distinction is important because the acute hypoxic response occurs within seconds, whereas changes in gene expression would be expected to occur over a substantially longer timescale. Nevertheless, pharmacological inhibition of HIF-2α has been shown to impair hypoxic ventilatory responses within one hour (Cheng et al., 2020), raising the possibility that HIF-2α may also have more rapid, potentially non-transcriptional effects on carotid body function.

Transcriptomic evidence demonstrates that immature chromaffin cell populations also express HIF-2α, together with components of the mitochondrial programme associated with acute oxygen sensitivity. Single-cell analysis of developing adrenal chromaffin cells identified populations expressing *Epas1* and *Cox4i2* (Akkuratova et al., 2022). The adrenal medulla is most sensitive to hypoxia during this period, suggesting that HIF-2α and its associated mitochondrial programme may also contribute to the oxygen sensitivity of neonatal chromaffin cells.

1.5 **Pheochromocytomas and paragangliomas**

The relevance of HIF-2α to oxygen sensitive sympathoadrenal tissues extends to their associated tumours. Pheochromocytomas and paragangliomas are rare neuroendocrine tumours arising from chromaffin cells of the adrenal medulla and from extra-adrenal paraganglia, respectively (Mete et al., 2022). Paragangliomas can occur at multiple anatomical locations, from the head and neck down to the abdomen, including in the carotid body and organ of Zuckerkandl (illustrated in **Figure 1.7**). They have two important links with HIF-2α: first, their occurrence in tissues derived from the sympathoadrenal lineage that are associated with oxygen chemosensitivity, and second, the frequent presence of mutations that directly or indirectly activate HIF signalling.

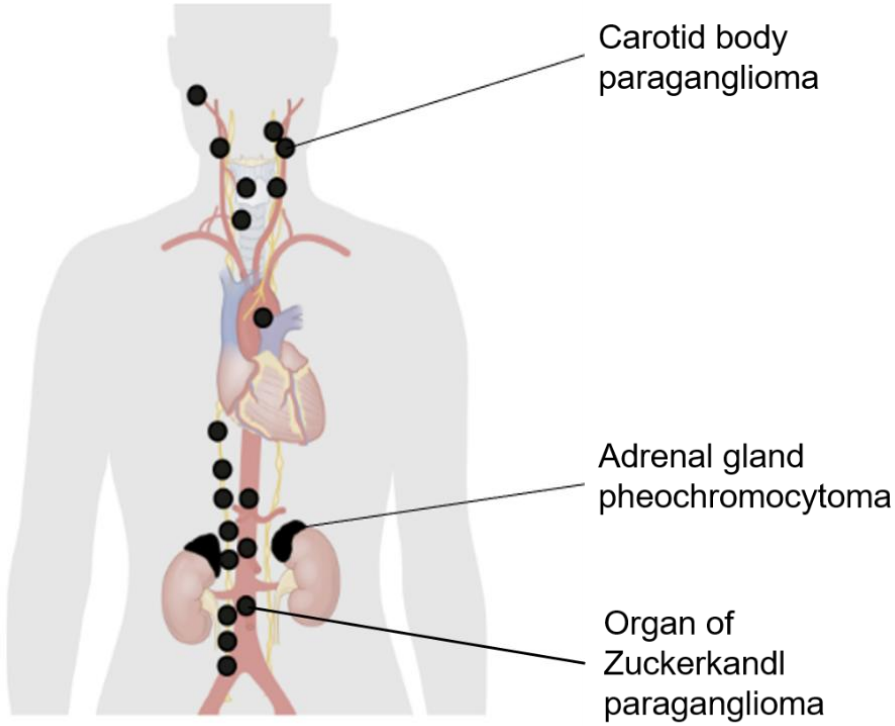

Figure 1.7. Sites of pheochromocytomas and paragangliomas. Diagram illustrating the multiple anatomical sites of pheochromocytomas and paragangliomas along the autonomic nervous system, shown by black dots. This includes carotid body paragangliomas, adrenal gland pheochromocytomas and organ of Zuckerkandl paragangliomas. Figure taken and adapted from Crona et al. (2017) (License number: 6363020969306).

Pheochromocytomas and paragangliomas have an exceptionally high genetic burden and are among the most highly heritable human tumour types. Approximately 40% of patients carry a germline pathogenic variant in a recognised susceptibility gene, whilst additional tumours contain somatic mutations in these susceptibility genes (Dahia, 2014; Favier et al., 2015). More than 20 pheochromocytoma and paraganglioma susceptibility genes have been identified, and these can be broadly grouped according to the cellular signalling pathways they disrupt (**Figure 1.8**) (Fishbein et al., 2017). These include mutations affecting kinase signalling, Wnt-related signalling and hypoxia/pseudohypoxia pathways. The pseudohypoxic cluster of susceptibility genes includes direct components of the HIF pathway, such as *VHL, EPAS1*, and, more rarely,

EGLN1, as well as genes encoding metabolic enzymes, including subunits of SDH (*SDHA, SDHB, SDHC* and *SDHD*) and fumarate hydratase (*FH*) (Buffet et al., 2020; Favier et al., 2015).

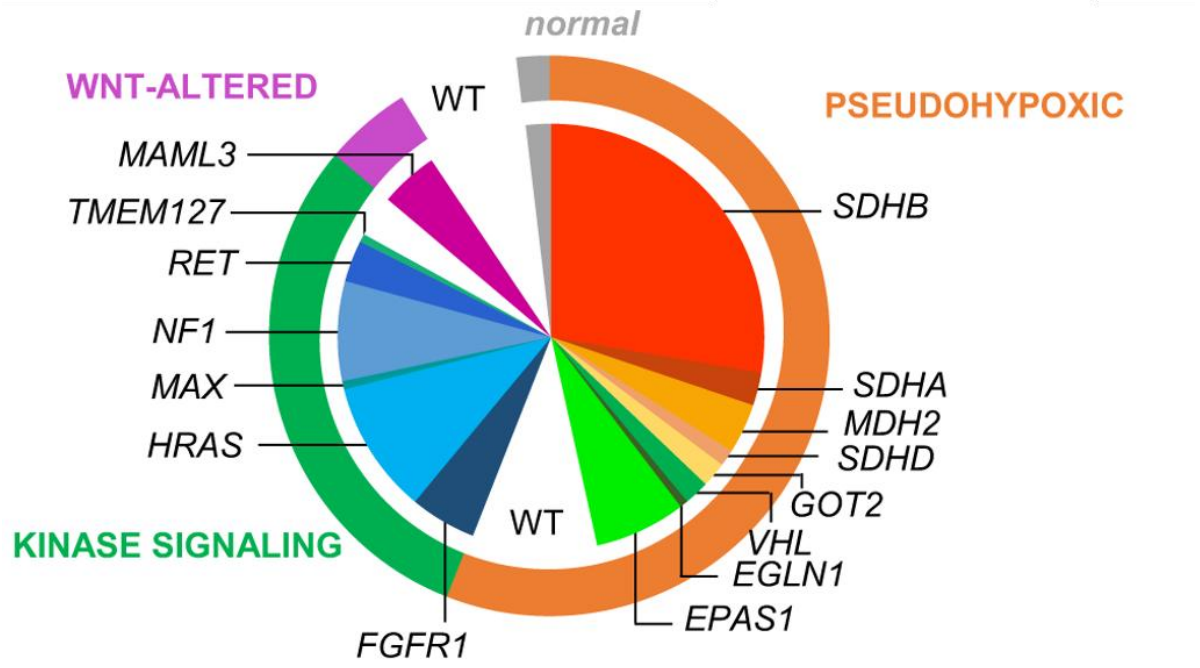

Figure 1.8. Pheochromocytoma and paraganglioma susceptibility genes. Pie chart showing genes mutated in a cohort of 156 pheochromocytomas and paragangliomas, separated based on genomic clusters. Figure taken from Calsina et al. (2023).

Somatic gain-of-function mutations in *EPAS1* have been identified in pheochromocytomas and paragangliomas, demonstrating that constitutive HIF-2α activation can function directly as a tumour-driving event (Comino-Méndez et al., 2013; Toledo et al., 2013; Welander, Andreasson, Brauckhoff, et al., 2014). These mutations are often located in the oxygen-dependent degradation domain of HIF-2α and impair its hydroxylation and subsequent recognition by pVHL, resulting in HIF-2α stabilisation and therefore persistent activation of hypoxia-responsive transcriptional programmes. Activating *EPAS1* mutations are also associated with a

distinctive syndrome characterised by combinations of pheochromocytomas and paragangliomas, polycythaemia and somatostatinomas, known as Pacak-Zhuang syndrome (Z. Zhuang et al., 2012).

The pathogenic relevance of this mechanism is particularly evident in patients with cyanotic congenital heart disease (CCHD), who have an increased risk of developing pheochromocytomas and paragangliomas, and in whom somatic *EPAS1* mutations occur at a markedly high frequency (Ogasawara et al., 2022; Opotowsky et al., 2015; Vaidya et al., 2018). Furthermore, in a cohort of patients with *EPAS1*-mutated paragangliomas, 59% had a haemoglobin disorder such as sickle cell disease, sickle cell train or heterozygous haemoglobin C disease (Mancini et al., 2024). These associations are consistent with chronic hypoxia providing a positive selection pressure for cells harbouring *EPAS1* mutations. Recent work suggests that this effect depends on both the timing of hypoxic exposure and the developmental lineage of the affected tissue (Arenillas et al., 2025). In patients with CCHD, in whom systemic hypoxia is present from birth, *EPAS1* mutations were identified in 24/27 sympathetic pheochromocytomas and paragangliomas, but were absent from seven parasympathetic carotid body paragangliomas examined. CCHD-associated pheochromocytomas and paragangliomas were also diagnosed at a younger age and were more frequently multiple and metastatic, suggesting early life systemic hypoxia preferentially selects for *EPAS1*-mutant tumours within the sympathoadrenal lineage. In contrast, hypoxia developing in later life was more strongly associated with parasympathetic, particularly carotid body, paragangliomas. Together, these findings indicate that chronic hypoxia influences pheochromocytoma and paraganglioma development in a temporally and anatomically specific manner, potentially reflecting differences in the susceptibility of sympathoadrenal populations at distinct developmental stages.

Importantly, however, altered *EPAS1* signalling is not exclusively associated with pathological phenotypes. Naturally occurring variation in this gene has also been implicated in physiological adaptation to chronic hypoxia at high altitude. In Tibetan populations, several *EPAS1* variants occur at high frequency and are associated with reduced haemoglobin concentrations and a blunted erythropoietic response to hypoxia compared to lowland populations (Y. Peng et al., 2017). Functional studies suggest that the Tibetan-enriched *EPAS1* haplotype can reduce *EPAS1* expression (Gray et al., 2022), providing a potential mechanism for limiting excessive erythrocytosis while maintaining adequate oxygen delivery. Similar associations between *EPAS1* variation and high altitude adaptation have been reported in other high altitude populations. In particular, a naturally selected H194R variant identified in Andean populations has been shown to impair HIF-2α interaction with HIF-1β and to function as a hypomorphic allele, providing direct evidence that partial reduction of HIF-2α activity can contribute to high altitude adaptation (Jorgensen et al., 2023). However, the specific variants and associated phenotypes differ between populations, reflecting distinct evolutionary histories and adaptive mechanisms. Together, these findings demonstrate that genetic modulation of HIF-2α signalling can produce either pathological or beneficial phenotypes in the context of chronic hypoxia, highlighting the importance of the magnitude and cellular context of pathway activation.

More broadly, the magnitude of HIF signalling appears to influence its biological consequences, particularly in relation to tumour development. Rather than acting simply as an on/off switch, the relationship between HIF stabilisation and tumorigenesis is complex and may depend on the level of pathway activation. This is particularly evident in VHL disease, in which patients inherit one pathogenic copy of *VHL* and acquire a somatic inactivating mutation in the remaining copy later in life (Vortmeyer et al., 2002). The nature of the germline mutation influences the spectrum of tumours to which they are predisposed. Type 1 mutations, which

generally result in severe disruption of pVHL structure or function, are associated with a low risk of pheochromocytoma, whereas type 2 mutations, which are thought to cause only partial inactivation of pVHL, are associated with an increased risk of pheochromocytoma (Clifford, 2001; S.-J. Liu et al., 2018). This suggests a dose-dependent role of HIF-α in tumorigenesis. The cellular consequences of HIF activation are therefore likely to depend on both the magnitude of signalling and the relative contribution of individual HIF isoforms.

As well as mutations that directly activate HIF, the pseudohypoxic cluster of susceptibility genes also includes mutations which indirectly activate HIF, including those in the metabolic enzymes SDH and FH. A reduction in the activity of SDH and FH results in accumulation of their substrates, succinate and fumarate, respectively, which can competitively inhibit 2-OG dependent dioxygenases. This includes the PHD enzymes, leading to HIF stabilisation and hence a transcriptional state resembling cellular hypoxia despite normal oxygen availability. However, accumulation of these metabolites also alters epigenetic regulation through inhibition of TET and Jumonji domain demethylases. Therefore, the tumour phenotype associated with these metabolic mutations likely reflects a combination of HIF-dependent and HIF-independent mechanisms (Morin et al., 2020a).

1.5.1 *Mouse models of pheochromocytomas and paragangliomas*

Despite the strong genetic evidence linking pseudohypoxic signalling to human pheochromocytomas and paragangliomas, modelling these tumours in mice has proved challenging. Several genetically engineered models have demonstrated that disruption of the HIF pathway can alter sympathoadrenal development, carotid body structure and chromaffin cell phenotype, but fail to develop frank pheochromocytomas or paragangliomas (Armstrong et al., 2022; Eckardt et al., 2021; Fielding et al., 2018; Lepoutre-Lussey et al., 2016; Macias et al., 2014; Prange-Barczynska et al., 2024).

Mouse models of VHL disruption include mice carrying the Chuvash polycythaemia-associated *Vhl* mutation (R200W). This mutation reduces the binding affinity of VHL for HIF-2α, leading to HIF-2α stabilisation. Like Chuvash patients, these mice do not develop tumours, but display carotid body hyperplasia and increased ventilatory sensitivity to hypoxia (Slingo et al., 2014). Global inactivation of *Vhl* causes embryonic lethality, whereas inactivation of Vhl in catecholaminergic (TH^+) cells causes atrophy of these tissues, including the carotid body and adrenal medulla. Therefore, in contrast to promoting tumour formation in neuroendocrine tissues of mice, *Vhl* deletion rather impairs their development (Macías et al., 2014).

Mouse models affecting mitochondrial metabolism similarly do not show tumour formation driven solely by pseudohypoxia. Like global *Vhl* deletion, global *Sdhb* loss causes embryonic lethality (Armstrong et al., 2022; Lepoutre-Lussey et al., 2016). *Sdhb* disruption restricted to neuroendocrine (TH^+) tissues causes succinate accumulation and associated metabolic abnormalities, but these mice do not develop frank pheochromocytomas or paragangliomas (Armstrong et al., 2022; Lepoutre-Lussey et al., 2016; Morin et al., 2020a). Pheochromocytomas have been identified in mice with mutations in both *Sdhb* and *Nf1*, however this combination of mutations does not reflect a recognised human genotype underlying tumorigenesis (Lepoutre-Lussey et al., 2016). Furthermore, *Nf1* loss itself can drive pheochromocytoma formation in mice. These observations suggest that disruption of mitochondrial metabolism alone may be insufficient to drive tumorigenesis in mice, and that additional species-, tissue- or developmental-specific factors, or other gene mutations, may be required.

Another pseudohypoxic mouse model conditionally inactivated *Phd2* in TH^+ neuroendocrine cells (*Phd2$^{f/f}$;THCre*) (Eckardt et al., 2021; Fielding et al., 2018; Prange-Barczynska et al., 2024). PHD2 is the predominant HIF prolyl hydroxylase regulating HIF stability under

normoxic conditions (Berra et al., 2003). Consequently, loss of *Phd2* in TH^+ cells produces constitutive activation of HIF signalling without altering environmental oxygen availability. In these mice, *Phd2* inactivation causes marked enlargement of the carotid bodies, by approximately 10-fold in volume compared to wild-type controls, as well as ultrastructural abnormalities of glomus cell dense core vesicles (Fielding et al., 2018). Furthermore, the adrenal medulla of these mice retains features of an immature chromaffin cell phenotype, including reduced expression of the enzyme PNMT, which catalyses conversion of noradrenaline to adrenaline in mature chromaffin cells, the presence of ectopic chromaffin cells within the adrenal cortex and external to the adrenal gland, and retention of acute oxygen chemosensitivity in the adult adrenal medulla (Eckardt et al., 2021; Prange-Barczynska et al., 2024). These mice also retain the foetal organ of Zuckerkandl in adulthood, which is also oxygen chemosensitive (Prange-Barczynska et al., 2024). These findings suggest that constitutive activation of the PHD-HIF pathway can promote proliferation and halt differentiation within the sympathoadrenal lineage.

Notably, the carotid body and adrenal medullary phenotypes caused by *Phd2* inactivation are dependent on HIF-2α, but not HIF-1α (Fielding et al., 2018). Furthermore, the abnormalities cannot be reproduced by equivalent *Phd2* inactivation during adult life, suggesting that dysregulation of the PHD2-HIF-2α pathway during development is particularly important in generating these phenotypes (Eckardt et al., 2021). These findings provide a potential developmental link between HIF-2α signalling, sympathoadrenal cell differentiation and pseudohypoxic pathology. However, like the *Sdhb* mouse models, frank pheochromocytomas and paragangliomas were also not detected in these mice.

1.6 **Summary**

Taken together, the evidence links the physiological function of HIF-2α in establishing specialised oxygen-sensitive cell states with its pathological activation in tumours of the sympathoadrenal and paraganglionic systems. The carotid body and developing chromaffin populations provide specialised examples of neural crest-derived cells that respond to oxygen through rapid changes in electrical activity and secretion. HIF-2α is highly expressed in these cell populations and is required for normal carotid body development, aspects of acute oxygen sensing, and the proliferative and ventilatory responses to sustained hypoxia. Transcriptomic and functional studies further indicate that HIF-2α helps establish a specialised mitochondrial programme associated with oxygen chemosensitivity in carotid body glomus cells.

The same pathway is also implicated in pheochromocytoma and paraganglioma pathogenesis. Direct activation of HIF-2α through *EPAS1* mutation can drive tumorigenesis, while disruption of VHL, PHD or mitochondrial metabolism can activate HIF signalling indirectly. However, the phenotypic consequences of these perturbations are not uniform. Metabolic mutations can have HIF-independent effects, HIF-2α activation can cause hyperplasia without frank tumour formation, and the outcome of pathway activation depends on developmental timing and cellular context. These observations argue against a simple model in which HIF activation alone is sufficient to explain pheochromocytoma and paraganglioma development. Instead, they suggest that understanding how HIF-2α establishes and modifies the phenotype of specialised sympathoadrenal cells is essential for determining why some cells adapt to hypoxia while others undergo pathological hyperplasia or progress to tumorigenesis.

The organ of Zuckerkandl provides an incompletely characterised context in which these relationships can be examined. Its transient developmental nature, high *EPAS1* expression and close relationship to other oxygen-responsive sympathoadrenal tissues make it relevant to

understanding how oxygen signalling regulates chromaffin cell fate and function. Whether organ of Zuckerkandl chromaffin cells possess intrinsic oxygen chemosensitivity, whether this property is established by HIF-2α-dependent transcriptional programmes, and how activation of the oxygen signalling pathway affects their persistence and tumour susceptibility remains unsolved. Addressing these questions provides greater insight into the relationship between developmental oxygen sensing, HIF-2α signalling and pseudohypoxic tumour susceptibility.

1.7 **Research aims**

The first aim of this thesis was to determine whether HIF-1α and/or HIF-2α is sufficient to drive the foetal-like, paraganglioma-like neuroendocrine cell phenotypes previously observed with developmental inactivation of *Phd2* (Chapter 2).

Given the observation that HIF-2α, but not HIF-1α, is sufficient to drive these neuroendocrine phenotypes, the mechanisms underlying the role of HIF-2α in this phenotype were then investigated. In particular, whether HIF-2α must be active during development, and whether the transcriptional activity of HIF-2α is necessary for these phenotypes, were tested (Chapter 3).

Mice carrying developmental TH-restricted mutations in *Sdhb* were then developed with the aim of establishing a mouse model of pheochromocytoma and paraganglioma in which genetic mutation indirectly induces pseudohypoxia (Chapter 4). These mice did not develop frank tumours but, like mice with developmental inactivation of *Phd2* or stabilisation of HIF-2α, retained their organ of Zuckerkandl into adulthood.

Given that all three pseudohypoxic mouse models retained an organ of Zuckerkandl, and this is a common site of extra-adrenal paragangliomas, this tissue and its relationship with HIF signalling, oxygen sensing, and tumorigenesis were then explored in greater detail (Chapter 5).

Chapter 2

STABILISATION OF HIF-2A, BUT NOT HIF-1A, CONFERS OXYGEN CHEMOSENSITIVITY IN CHROMAFFIN CELLS.

2.1 **Introduction**

Hypoxia inducible factors (HIF) mediate the transcriptional response to low oxygen. They are commonly activated in tumours by the hypoxic microenvironment, and antagonists of HIF target genes are used as anti-oncogenic agents (Cardones & Banez, 2006; Muz et al., 2015; Petrova et al., 2018). However, genetic mutations in the HIF pathway are rare in most types of cancer, despite ubiquitous operation of the HIF pathway across all cell types. An exception to this is in tumours of the autonomic paraganglia, known as pheochromocytomas and paragangliomas. Pheochromocytomas occur in the adrenal medulla, whilst paragangliomas occur at extra-adrenal locations from the skull down to the pelvis, including in the carotid body and along the abdominal aorta (Neumann et al., 2019). Although these tumours are rare, with an incidence of 0.04-0.94 cases per 100,000 individuals per year (Al Subhi et al., 2022), they have two distinctive features of interest. First, they are highly heritable, with up to 40% of pheochromocytomas and paragangliomas possessing germline or early somatic mutations (Buffet et al., 2020). Second, they commonly have mutations in components of the HIF pathway or which affect HIF signalling (S. Peng et al., 2020).

HIFs are heterodimeric transcription factors comprising an oxygen-sensitive HIF-α subunit and a constitutively expressed HIF-β subunit (Kaelin & Ratcliffe, 2008; Semenza, 2012). In normoxic conditions, two proline residues in HIF-α are hydroxylated by prolyl hydroxylase domain (PHD) containing enzymes, causing the E3 ubiquitin ligase von Hippel-Lindau (VHL) to target it for proteasomal degradation. Conversely, during hypoxia, HIF-α is not hydroxylated

so remains stably expressed and dimerises with HIF-β to form a functional transcription factor. This binds to hypoxia response elements (HRE) in the genome, allowing transcription of a wide range of genes that either enhance oxygen delivery to cells or help cells to adapt and survive in low oxygen conditions. The two principal mammalian HIF-α isoforms are HIF-1α and HIF-2α. There are also three mammalian isoforms of PHD: PHD1, PHD2 and PHD3.

Mutations in HIF pathway components have been reported in pheochromocytomas and paragangliomas, including gain-of-function mutations in *EPAS1*, which encodes HIF-2α, and loss-of-function mutations in genes encoding negative regulators of HIF-α, including *EGLN2* and *EGLN1*, which encode PHD1 and PHD2, respectively, as well as *VHL*. In addition to mutations in direct HIF pathway components, mutations are observed in other pathways that can indirectly alter HIF levels, such as in the tricarboxylic acid (TCA) cycle enzymes succinate dehydrogenase (SDH) and fumarate hydratase (FH) (Dahia et al., 2005; Favier & Gimenez-Roqueplo, 2010; Ladroue et al., 2008; Redlich et al., 2021; Yang et al., 2015; Z. Zhuang et al., 2012). Inactivation of *SDH* and *FH* leads to accumulation of the oncometabolites succinate and fumarate which competitively inhibit 2-oxoglutarate-dependent dioxygenases, including the PHD enzymes and ten-eleven translocation (TET) dioxygenases **(Figure 1.3)** (Kantorovich et al., 2010). Inhibition of PHDs/activation of HIF-2α and inhibition of TET enzymes has been shown to synergistically induce epithelial-to-mesenchymal transition (EMT)-like phenotypes seen in SDHB-deficient tumours (Morin et al., 2020a). All of the above mutations cause activation of HIF, in particular HIF-2α, in the absence of environmental hypoxia, hence these tumours are termed ‘pseudohypoxic’.

To study the pathogenesis of pseudohypoxic pheochromocytomas and paragangliomas, previous work in this laboratory used mice in which the dominant regulator of HIF-α, *Phd2*, was inactivated (Bishop et al., 2013; Eckardt et al., 2021; Fielding et al., 2018; Hodson et al., 2016; Prange-Barczynska et al., 2024). PHD2 is the most abundant PHD isoform in most cell

types, and global inactivation of *Phd2* (*Phd2*$^{-/-}$) in mice leads to embryonic lethality between embryonic day 12.5 (E12.5) and E14.5, whereas *Phd1*$^{-/-}$ and *Phd3*$^{-/-}$ mice survive and appear normal (Takeda et al., 2006). *Phd2* was therefore inactivated specifically in catecholaminergic cells of the sympathoadrenal system, the site of these tumours (Eckardt et al., 2021; Fielding et al., 2018; Prange-Barczynska et al., 2024). This was achieved by crossing mice carrying loxP flanked exon 2 of *Phd2* (*Phd2*$^{f/f}$) (Mazzone et al., 2009) with mice expressing Cre recombinase driven by the promoter of tyrosine hydroxylase (TH) (THCre), generating *Phd2*$^{f/f}$*;THCre* mice (referred to hereafter as *Phd2ko*). TH is expressed in catecholaminergic cells, including carotid body glomus cells and chromaffin cells, from approximately E11.5, resulting in *Phd2* inactivation during development in these cell populations (Katz & Erb, 1990).

Although *Phd2ko* mice did not develop frank tumours, *Phd2* inactivation induced paraganglioma-like phenotypes, including carotid body hyperplasia, retention of immature chromaffin cell features in the adrenal medulla, and retention of the foetal organ of Zuckerkandl, which normally atrophies postnatally (Eckardt et al., 2021; Prange-Barczynska et al., 2024). These changes were associated with acute oxygen chemosensitivity in the normally insensitive adult adrenal medulla and in the retained organ of Zuckerkandl (summarised in the schematic in **Figure 2.1**) (Prange-Barczynska et al., 2024).

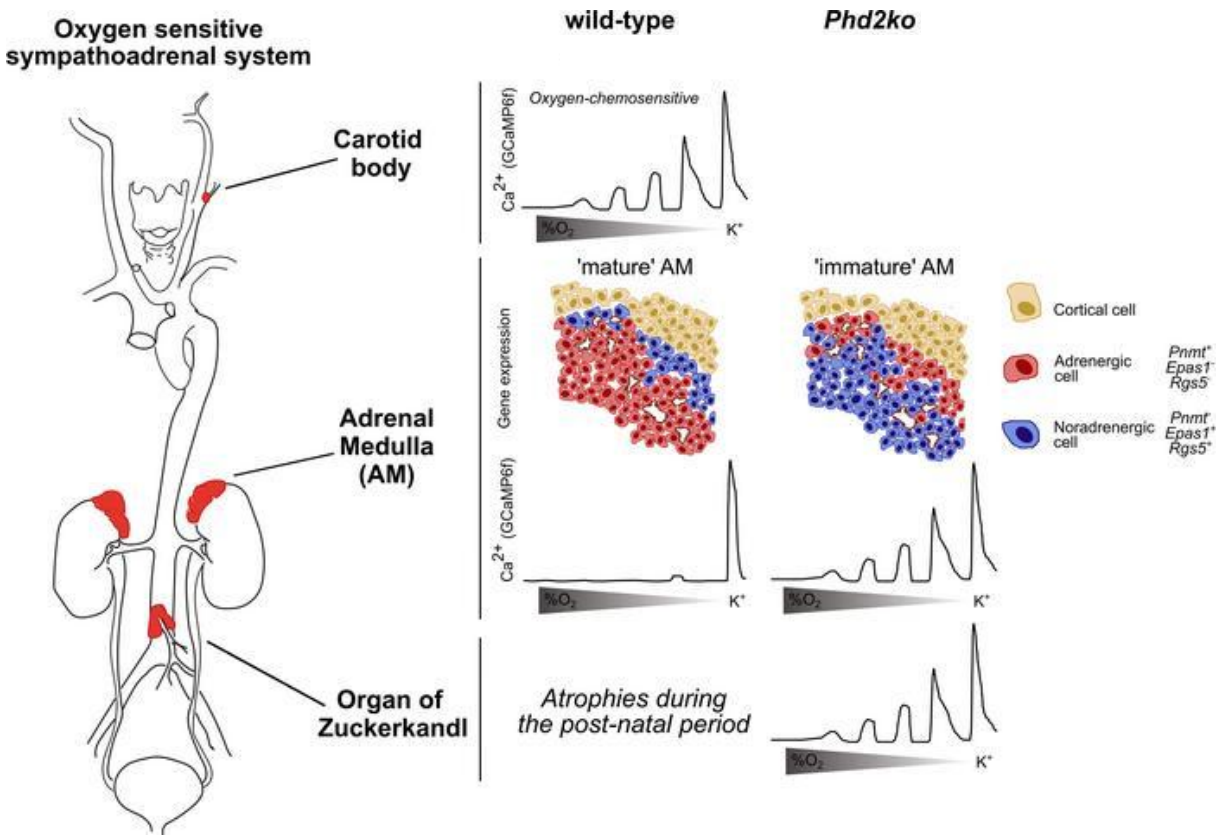

Figure 2.1. Schematic illustrating the neuroendocrine phenotype of wild-type and *Phd2ko* mice. The sympathoadrenal system is illustrated on the left, with the carotid body, adrenal medulla and organ of Zuckerkandl annotated. The phenotype of these tissues in adult wild-type and *Phd2ko* mice is illustrated on the right. This includes a switch towards an immature gene expression profile in the *Phd2ko* adrenal medulla, associated with retention of oxygen chemosensitivity, as well as retention of an oxygen chemosensitive organ of Zuckerkandl.

Inactivation of *Phd2* causes stabilisation of both HIF-1α and HIF-2α isoforms. Concurrent inactivation of *Phd2* and either *Hif-1α* or *Hif-2α* demonstrated that HIF-2α, but not HIF-1α, is necessary for both carotid body hyperplasia and the gene expression changes in the adrenal medulla (Eckardt et al., 2021; Fielding et al., 2018). This raised the question of whether HIF-2α, but not HIF-1α, might not only be necessary, but also sufficient to induce the morphological, gene expression and chemosensitivity changes observed in *Phd2ko* mice. To address this, this chapter examined mice expressing stable forms of either HIF-1α or HIF-2α,

HIF-1αdPA and *HIF-2αdPA* respectively (W. Y. Kim et al., 2006). These constructs are modified forms of the human *HIF-1α* and *HIF-2α* transcripts, in which the two proline residues that are normally targeted for PHD-dependent hydroxylation are substituted for alanine, preventing degradation and allowing stable expression during normoxia. Mice expressing these constructs at the Rosa26 locus preceded by a lox-STOP-lox sequence were crossed with THCre mice (Lindeberg et al., 2004) to generate *Hif-1αdPA$^{f/+}$;THCre* and *Hif-2αdPA$^{f/+}$;THCre* mice (hereafter known as *Hif-1αdPA* and *Hif-2αdPA*). Cre-mediated excision of the stop sequence results in constitutive expression of HIF-1α or HIF-2α in TH^+ cells from the onset of TH expression during development (**Figure 2.2**).

This chapter demonstrates that developmental, TH-restricted expression of HIF-2α, but not HIF-1α, is sufficient to recapitulate the paraganglioma-like, immature neuroendocrine phenotype caused by developmental inactivation of *Phd2*. The *Hif-2αdPA* model provides greater mechanistic specificity for HIF-2α signalling and therefore an improved animal model for studying the pathogenesis of pseudohypoxic pheochromocytomas and paragangliomas and the mechanism underlying acute oxygen sensing.

2.2 **Results**

2.2.1 *TH-restricted, developmental Hif-1αdPA and Hif-2αdPA mouse models*

To address whether stabilisation of HIF-1α or HIF-2α is sufficient to confer the phenotypes observed with developmental, TH-restricted *Phd2* inactivation (*Phd2$^{f/f}$;THCre*, referred to hereafter as *Phd2ko*), mice expressing a stable form of either HIF-1α or HIF-2α, *Hif-1αdPA* or *Hif-2αdPA*, were examined (W. Y. Kim et al., 2006). These are modified forms of the human *HIF-1α* and *HIF-2α* transcripts, in which the two proline residues which are normally targeted for hydroxylation by PHD enzymes (Pro402 and Pro564 in HIF-1α and Pro-405 and Pro-531

in HIF-2α) are substituted for alanine **(Figure 2.2A)**. This prevents PHD-mediated hydroxylation of HIF-1α and HIF-2α, thereby inhibiting their proteasomal degradation during normoxia and resulting in stable protein expression. The *HIF-1αdPA* and *HiF-2αdPA* constructs also contain an N-terminal hemagglutinin (HA) tag, allowing their expression to be detected.

The *HIF-1αdPA* or *HIF-2αdPA* allele was expressed at the Rosa26 (R26) locus, preceded by a lox-STOP-lox (LSL) sequence. Rosa26 is a safe-harbour locus that allows ubiquitous transgene expression across all tissues and developmental stages without gene-silencing or causing any known abnormalities in mice (Friedrich & Soriano, 1991). The lox-STOP-lox sequence prevents the inserted transgene from being expressed unless Cre recombinase is also present in the cell to excise the stop sequence; this enables tissue-restriction of HIF-α overexpression. R26-LSL-*HIF-1αdPA* or *HIF-2αdPA mice* were bred with mice expressing Cre recombinase under the tyrosine hydroxylase (TH) promoter (THCre) (Lindeberg et al., 2004) **(Figure 2.2B)**. TH is the rate-limiting enzyme in dopamine biosynthesis and is therefore present in catecholaminergic cells.

These breedings generated *Hif-1αdPA$^{f/+}$;THCre or Hif-2αdPA$^{f/+}$;THCre* mice, referred to hereafter as *Hif-1αdPA* and *Hif-2αdPA*. These mice express stable HIF-1α or HIF-2α from the point of TH expression during development (approximately E11.5) in their catecholaminergic cells, including carotid body glomus cells and chromaffin cells (**Figure 2.2**), common sites of pheochromocytomas and paragangliomas. Therefore, these mice provide a model to investigate the effects of TH-restricted, developmental stabilisation of either HIF-1α or HIF-2α.

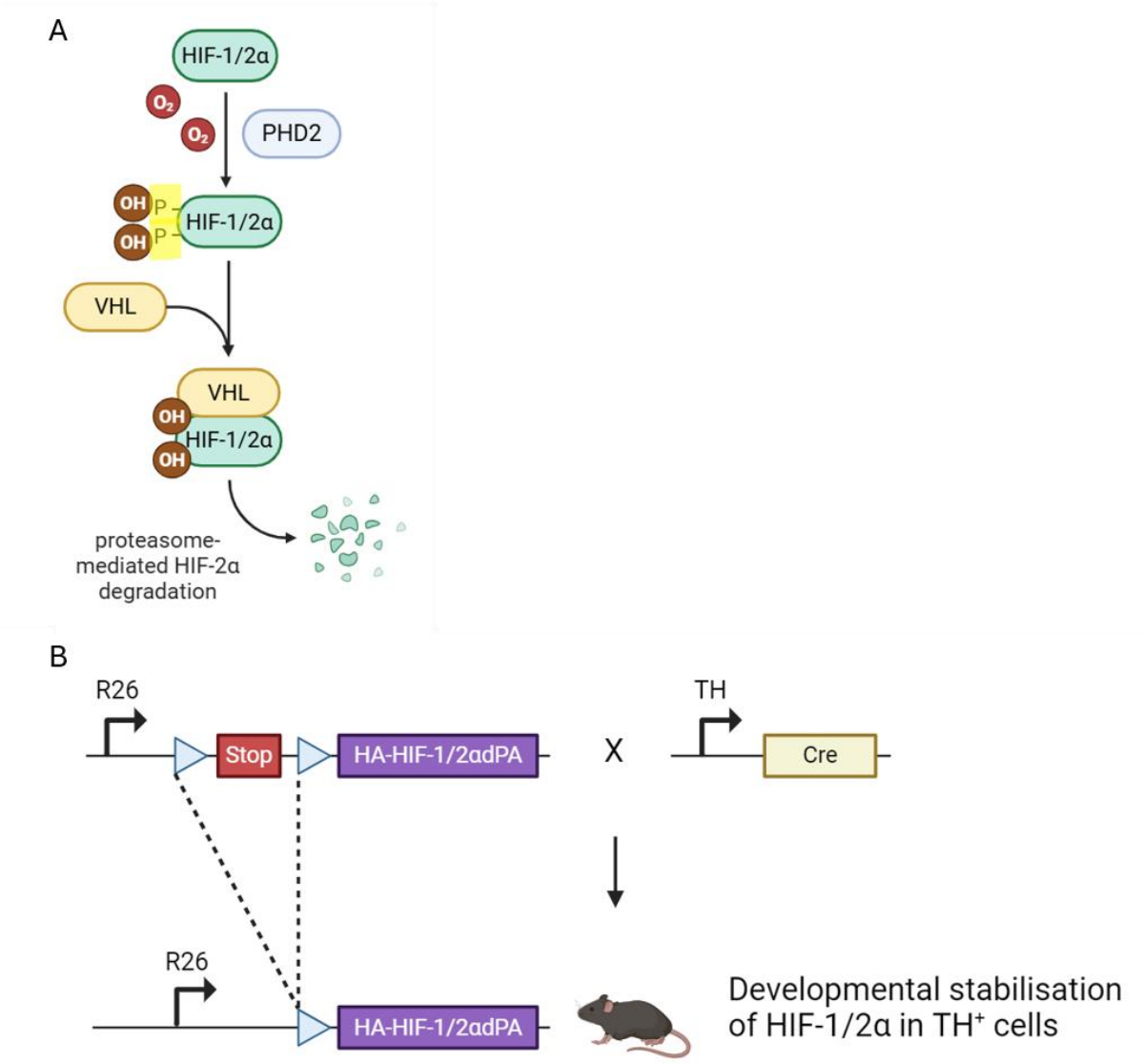

Figure 2.2. Schematic illustrating the *Hif-1/2αdPA* mouse models. (A) The HIF pathway, with the proline residues which are substituted with alanine in the *Hif-1/2αdPA* constructs highlighted (P402A and P564A in *Hif-1αdPA* and P405A and P531A in *Hif-2αdPA*). **(B)** Mice expressing the *Hif-1/2αdPA* construct at the Rosa26 (R26) locus preceded by a lox-stop-lox sequence, with loxP sites represented by arrowheads, were crossed with mice expressing Cre recombinase under the tyrosine hydroxylase (TH) promoter. Cre-mediated excision of the stop sequence in TH^+ cells of offspring expressing both alleles results in developmental stabilisation of HIF-1/2α in these cells. The *Hif-1/2dPA* constructs contain a hemagglutinin (HA) tag at the N terminus. Figure generated with biorender.com.

2.2.2 *Confirmation of Hif-1αdPA and Hif-2αdPA expression in neuroendocrine tissues*

To confirm expression of the *HIF-1αdPA* and *HIF-2αdPA* constructs in TH-expressing tissues of *Hif-1αdPA* and *Hif-2αdPA* mice, immunoblotting using an antibody for the HA tag on the N-terminus of these constructs was performed. The adrenal medulla was used because the small size of the carotid body gives insufficient tissue for immunoblotting. In three mice of each genotype, the immunoblot demonstrated successful expression of the HA tag in adrenal medullae from *Hif-1αdPA* and *Hif-2αdPA*, but not wild-type, mice (**Figure 2.3A**, each lane represents two pooled adrenal medullae from one mouse). The bands appear at approximately 100-120 kDa, consistent with the reported molecular masses of human HIF-1α and HIF-2α observed by western blotting (W. Y. Kim et al., 2006; Klinger et al., 2011). Although these proteins have lower theoretical molecular masses, they exhibit slower electrophoretic migration due to post-translational modifications (Bilton & Booker, 2003). Differences in post-translational modifications may therefore account for the difference in band migration between *Hif-1αdPA* and *Hif-2αdPA.* The immunoblot also revealed weaker expression of *Hif-1αdPA* than *Hif-2αdPA,* consistent with published work which showed weaker bands on an HA immunoblot of mouse embryonic fibroblasts from *Hif-1αdPA* mice compared with *Hif-2αdPA* mice (W. Y. Kim et al., 2006).

To confirm correct intracellular localisation of HIF and enable further comparison of construct expression levels across genotypes, immunohistochemistry was attempted using multiple antibodies targeting the HA tag. However, none of the HA antibodies tested produced a detectable signal by immunohistochemistry. Instead, antibodies against HIF-1α or HIF-2α were used (**Figure 2.3B**). The HIF-1α antibody used here also proved unsuccessful for immunohistochemistry. Nevertheless, HIF-2α expression was not detected in adrenal medullae from wild-type or *Hif-1αdPA* mice, but was detected in the nucleus of cells within the adrenal medulla of *Hif-2αdPA* mice (evident by the nuclear brown staining). Taken together, the HA

immunoblot and HIF-2α immunohistochemistry confirm expression of the *Hif-1αdPA* or *Hif-2αdPA* constructs in the adrenal medulla of *Hif-1αdPA* and *Hif-2αdPA* mice.

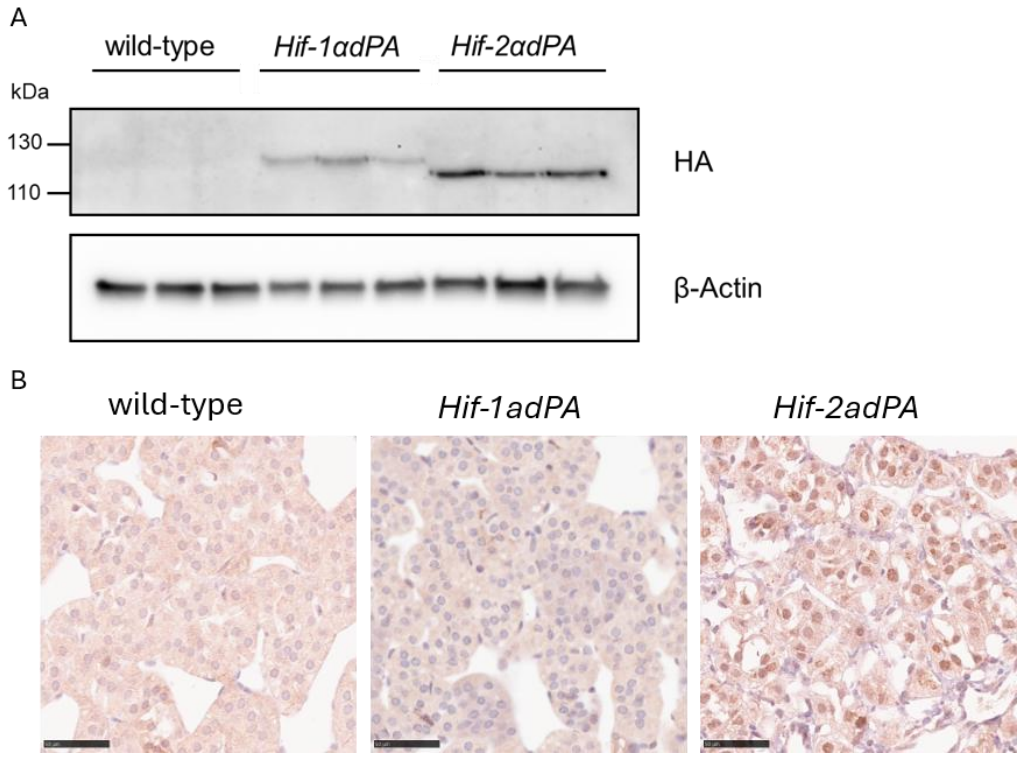

Figure 2.3. Confirmation of construct expression in the adrenal medulla of *Hif-1αdPA* and *Hif-2αdPA* mice. (A) Immunoblot for hemagglutinin (HA) or β-actin confirming HA-tagged *Hif-1αdPA or Hif-2αdPA* transgene expression in the adrenal medulla from *Hif-1αdPA or Hif-2αdPA*, but not wild-type, mice (n = 3 mice per genotype, with one mouse per lane). **(B)** HIF-2α immunohistochemistry showing nuclear HIF-2α protein (brown) stabilisation in chromaffin cells from the adrenal medulla of *Hif-2αdPA,* but not wild-type or *Hif-1αdPA*, adult mice. Scale bars represent 0.05 mm.

2.2.3 *The carotid body is enlarged in Hif-2αdPA, but not Hif-1αdPA, mice*

To test whether stabilisation of HIF-1α and/or HIF-2α is sufficient to induce the carotid body hyperplasia observed in *Phd2ko* mice(Fielding et al., 2018), the volumes of carotid bodies from adult wild-type, *Hif-1αdPA* and *Hif-2αdPA* mice were compared. Immunohistochemistry for TH was performed on serial sections throughout the carotid bifurcation. Although TH is a marker of type I cells, it is also expressed in surrounding sympathetic ganglia. Therefore, to

differentiate between these and the carotid body, immunostaining for chromogranin A (CgA) was performed on adjacent sections; this is a protein secreted by neuroendocrine cells and is present in carotid body type I cells but not in surrounding ganglia (**Figure 2.4A**). Therefore, the area of CgA-positive tissue was used to estimate carotid body volume (**Figure 2.4B**).

The mean carotid body volume in wild-type mice was 0.0012 (± 0.0003) mm^3, consistent with previously published data[23]. In comparison, *Hif-1αdPA* carotid bodies had a mean volume of 0.0018 (± 0.0004) mm^3, which was not significantly greater than that of wild-type controls. In contrast, *Hif-2αdPA* carotid bodies had a mean volume of 0.0052 (± 0.0015) mm^3, a 4.3-fold increase in volume compared with wild-type mice. These findings indicate that stabilisation of HIF-2α, but not HIF-1α, is sufficient to induce carotid body growth. No apparent differences in the morphology of carotid body glomus cells were observed in either *Hif-1αdPA* or *Hif-2αdPA* mice compared with wild-type controls. Notably, both *Hif-1αdPA* and *Hif-2αdPA* carotid bodies were smaller than the reported *Phd2ko* carotid body volume of 0.01 mm^3.

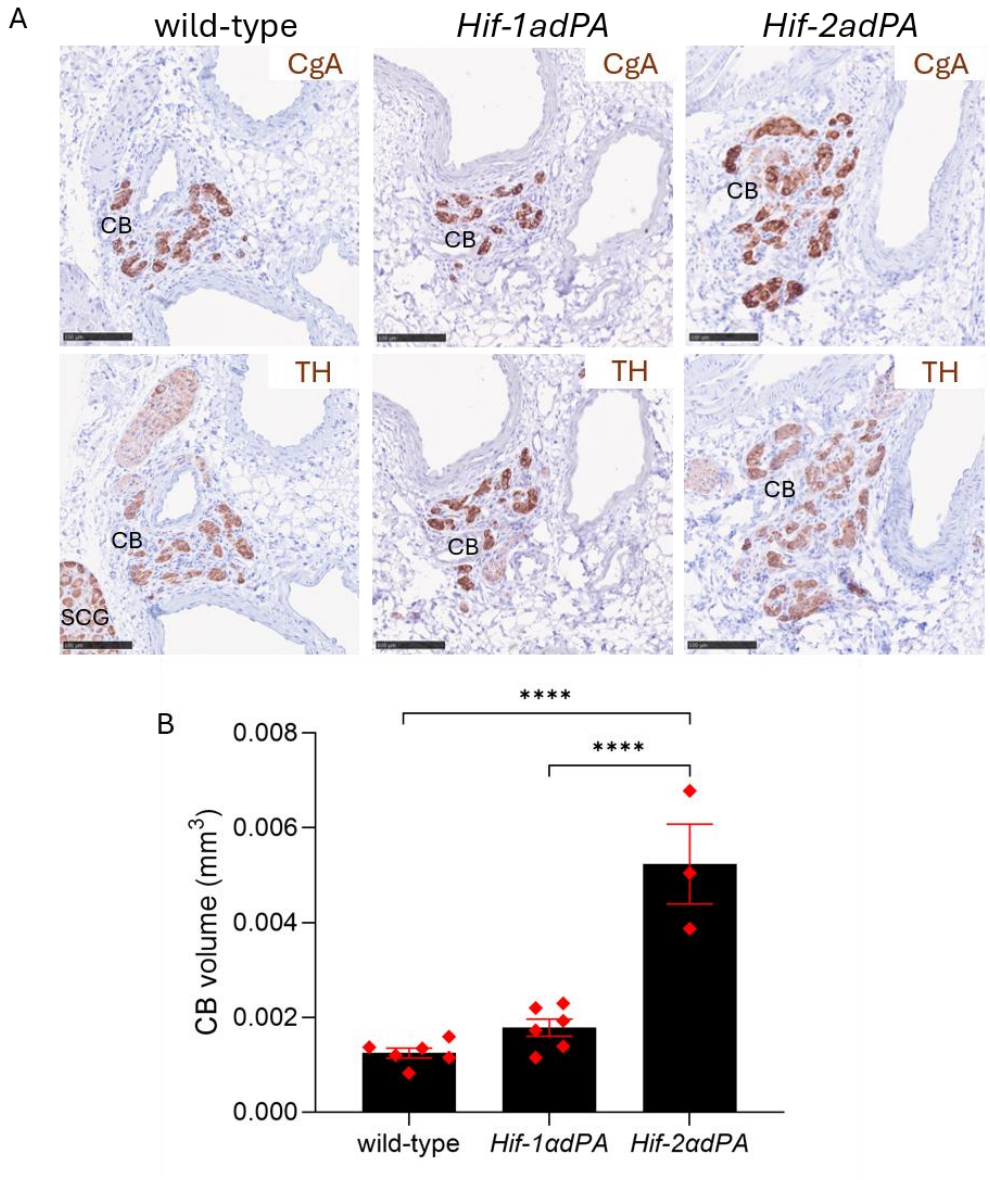

Figure 2.4. The carotid body is enlarged in *Hif-2αdPA*, but not *Hif-1αdPA*, mice. (A) Representative images of chromogranin A (CgA) and tyrosine hydroxylase (TH) immunohistochemistry in carotid body sections from wild-type, *Hif-1αdPA* and *Hif-2αdPA* mice. Scale bars = 0.01 mm. CB = carotid body, SCG = superior cervical ganglion. **(B)** Volume quantification of carotid bodies (CB) from wild-type, *Hif-1αdPA* and *Hif-2αdPA* mice. Data are presented as mean ± SEM and were analysed by one-way ANOVA with Tukey's multiple comparisons test, **** $p < 0.0001$.

2.2.4 *Developmental stabilisation of HIF-2α, but not HIF-1α, causes an enhanced hypoxic ventilatory response*

As the carotid body mediates ventilatory changes in response to hypoxia (Ortega-Sáenz & López-Barneo, 2020; Weir et al., 2005), and *Hif-2αdPA* mice have enlarged carotid bodies, the hypoxic ventilatory response (HVR) was assessed in *Hif-1αdPA* and *Hif-2αdPA* mice and matched wild-type controls to determine the effect of developmental HIF-1α or HIF-2α stabilisation on carotid body function. This was achieved using whole-body plethysmography, a technique that measures the respiratory pattern of conscious, unrestrained animals in an airtight container by detecting pressure fluctuations associated with breathing during exposure to hypoxic stimuli (Prada-Dacasa et al., 2020). During inspiration, air entering the lungs is warmed and humidified, resulting in a change in air volume and pressure within the chamber. During expiration, the reverse occurs, generating an opposite pressure change. These pressure changes were recorded by a transducer connected to the container which converts them into respiratory metrics including tidal volume and respiratory rate. To assess the effect of direct HIF-1α or HIF-2α stabilisation on the HVR, minute ventilation (tidal volume multiplied by respiratory rate) was recorded in mice exposed to normal air, followed by a five-minute hypoxic stimulus, then back into normal air.

In response to 10% oxygen, male and female wild-type mice exhibited a small increase in ventilation which was not sustained across the hypoxic stimulus. This was also the case in *Hif-1αdPA* and *Hif-2αdPA* mice, with no significant difference in the acute ventilatory response (AVR – calculated as the difference in minute ventilation between the first minute of stable hypoxic exposure minus the last minute of normal air exposure) between genotypes (**Figure 2.5B and D**). Attenuation of the HVR prior to stimulus offset is likely due to hypocapnia induced by hyperventilation (Krapf, 1991). In humans, this is partially overcome by end-tidal clamping of CO_2 levels (Howard & Robbins, 1995b). However, this is not possible in mice;

instead, 3% carbon dioxide was added to the hypoxic gas mixture, based on previous literature showing this prevents a significant fall in P_{CO2} or arterial pH upon hypoxic exposure (Ishiguro et al., 2006).

When exposed to 10% O_2/3% CO_2, wild-type mice showed a sustained increase in minute ventilation which returned to baseline upon stimulus offset (**Figure 2.5A and C**). The AVR to 10% O_2/3% CO_2 was significantly enhanced in female (and a non-significant trend towards an increase in male) *Hif-2αdPA* compared to wild-type mice (**Figure 2.5D**), but not in female or male *Hif-1αdPA* compared to wild-type mice (**Figure 2.5B**).

Last, exposure to 3% carbon dioxide alone was tested to assess the hypercapnic responses of each genotype. This caused an AVR of similar magnitude in wild-type, *Hif-1αdPA* and *Hif-2αdPA* mice (**Figure 2.5B and D**), suggesting that there is no difference in the response to hypercapnia between genotypes, and the differences in response to 10% O_2/3% CO_2 are specific to hypoxia.

In summary, developmental stabilisation of HIF-2α, but not HIF-1α, resulted in an enhanced HVR in female mice and a smaller, non-significant increase in male mice, suggesting that the increased carotid volume observed in *Hif-2αdPA* mice is associated with an increased HVR.

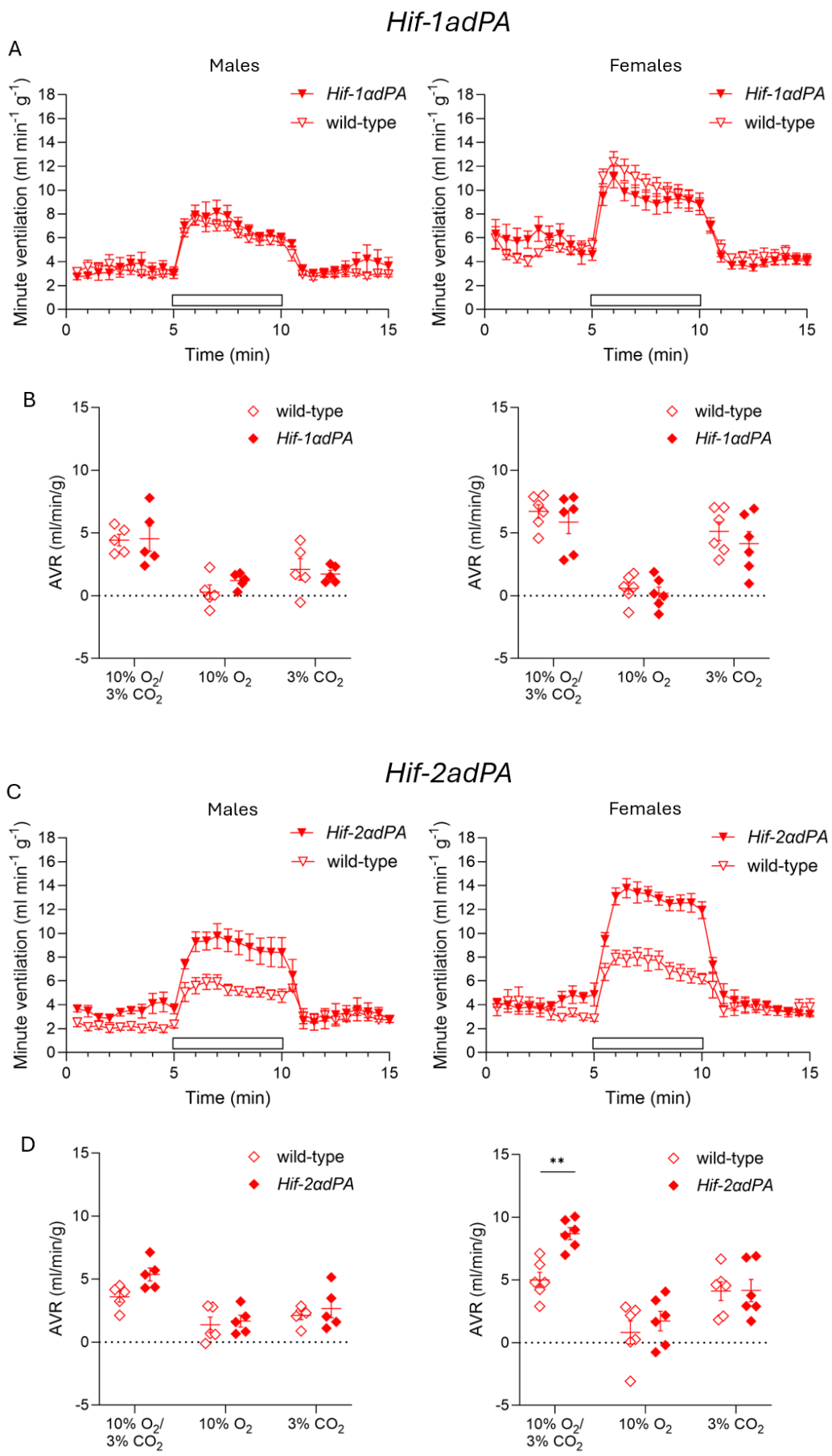
Hif-1adPA
A
Males
Females
Hif-1adPA
wild-type
Minute ventilation (ml min-1 g-1)
Time (min)
B
wild-type
Hif-1adPA
AVR (ml/min/g)
10% O2/ 3% CO2
10% O2
3% CO2
Hif-2adPA
C
Males
Females
Hif-2adPA
wild-type
Minute ventilation (ml min-1 g-1)
Time (min)
D
wild-type
Hif-2adPA
AVR (ml/min/g)
**
10% O2/ 3% CO2
10% O2
3% CO2

Figure 2.5. Developmental stabilisation of HIF-2α, but not HIF-1α, confers an enhanced hypoxic ventilatory response to 10% O_2/3% CO_2. (A) and **(C)** Ventilatory responses to five minutes of 10% O_2/3% CO_2 (white bars) in male and female mice, n = 6 females and 5 males of each genotype. **(B)** and **(D)** The acute ventilatory response (AVR) to each hypoxic stimuli. Data were compared between genotypes for each hypoxic stimuli by Holm-Sidak's multiple comparisons tests, with significance shown in the graph, ** $p < 0.001$

2.2.5 *Developmental stabilisation of HIF-2α, but not HIF-1α, results in the retention of immature, noradrenergic chromaffin cells in the adult adrenal medulla*

The effects of developmental HIF-1α and HIF-2α stabilisation on the adrenal medulla, the site of pheochromocytomas, were then characterised. *Phenylethanolamine N-methyltransferase* (*Pnmt*), the enzyme that converts noradrenaline to adrenaline, is typically acquired by adrenal medullary chromaffin cells during development, so that the majority of cells in the adult wild-type adrenal medulla are $Pnmt^+$ (Eckardt et al., 2021). This expression is binary and inversely correlates with expression of *Epas1*, the gene encoding HIF-2α, and *Regulator of G-Protein Signalling 5* (*Rgs5*), which encodes a negative regulator of G protein-coupled receptor signalling (Eckardt et al., 2021). Developmental *Phd2* inactivation has previously been shown to induce a switch in the expression of these genes towards a majority immature $Pnmt^-/Epas1^+/Rgs5^+$ cell population in the adult adrenal medulla (demonstrated in the schematic in **Figure 2.6B**) (Eckardt et al., 2021).

To investigate whether developmental stabilisation of HIF-1α and/or HIF-2α is sufficient to induce this gene expression population switch, *in situ* hybridisation for *Pnmt*, *Epas1* and *Rgs5* was performed on adjacent sections of adrenal glands from wild-type, *Hif-1αdPA* and *Hif-2αdPA* mice (**Figure 2.6A**). As expected, the majority of cells in the adult wild-type adrenal medulla expressed *Pnmt*. Expression of *Pnmt* inversely correlated with expression of *Epas1* and the HIF-2α target gene *Rgs5*, with a majority of cells being $Pnmt^+/Epas1^-/Rgs5^-$ and only

a minority population of *Pnmt*$^{-}$*/Epas1*$^{+}$*/Rgs5*$^{+}$ cells, mostly around the edges of the medulla. This was also the case in the adult *Hif-1αdPA* adrenal medulla, suggesting that developmental stabilisation of HIF-1α does not affect the expression of these genes. In contrast, in the *Hif-2αdPA* adrenal medulla, the majority of chromaffin cells did not express *Pnmt* but did express *Rgs5* (and, to a lesser extent, *Epas1*) and only a minority of cells were *Pnmt*$^{+}$*/Epas1*$^{-}$*/Rgs5*$^{-}$. The *Pnmt*$^{-}$*/Epas1*$^{+}$*/Rgs5*$^{+}$ cells populated the centre of the medulla, whereas the *Pnmt*$^{+}$*/Epas1*$^{-}$*/Rgs5*$^{-}$ cells appeared in clusters, typically around the edges of the adrenal medulla adjacent to the cortex. Therefore, developmental stabilisation of HIF-2α, but not HIF-1α, is sufficient to result in the retention of a majority of immature chromaffin cells in the adult adrenal medulla, similar to that previously observed with *Phd2* inactivation.

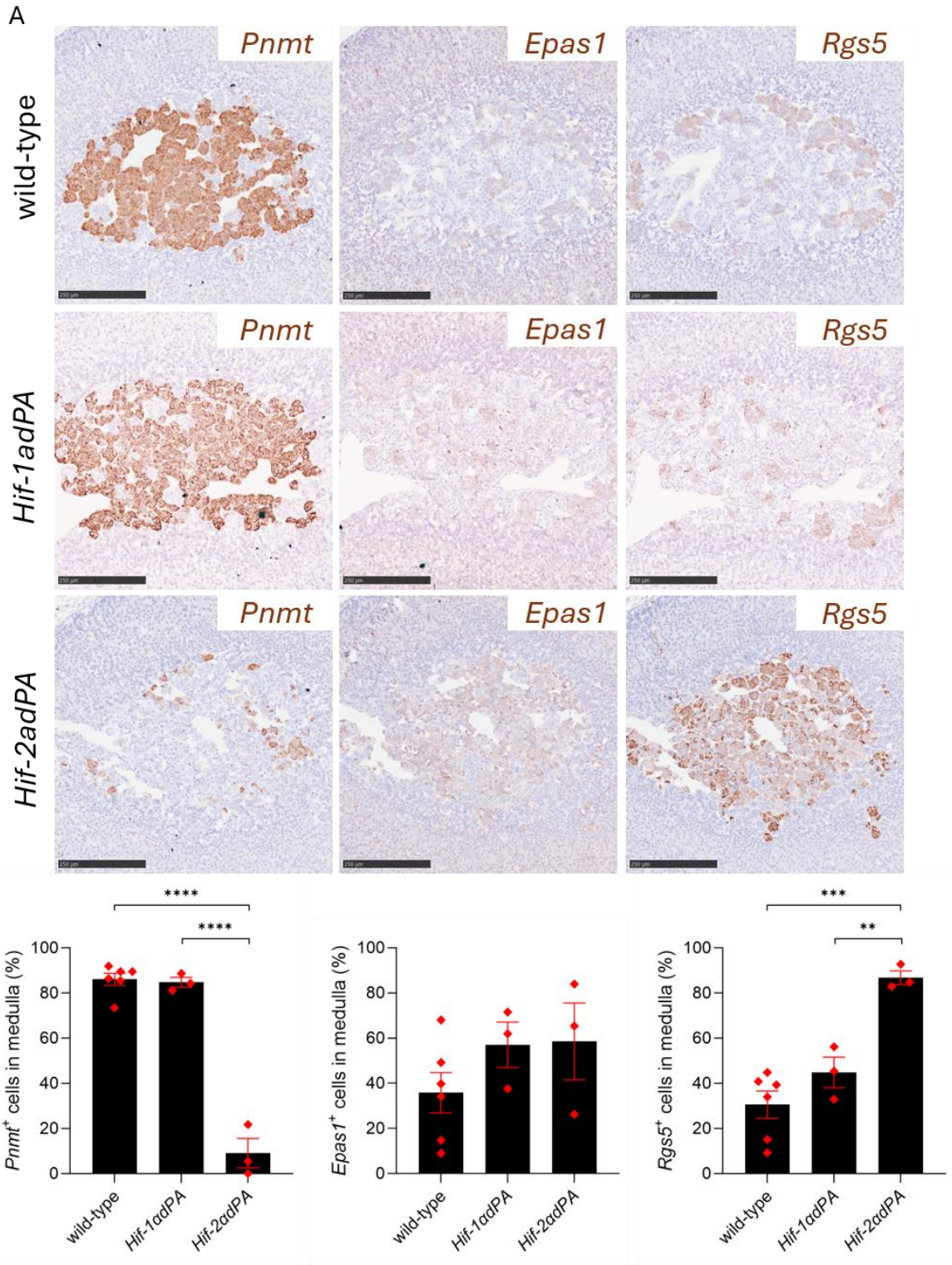
A
wild-type
Hif-1adPA
Hif-2adPA
Pnmt
Epas1
Rgs5
Pnmt+ cells in medulla (%)
Epas1+ cells in medulla (%)
Rgs5+ cells in medulla (%)
wild-type
Hif-1αdPA
Hif-2αdPA
****
****
***
**
B
wild-type
Hif-1αdPA
Phd2ko
Hif-2αdPA
adrenaline
noradrenaline
Pnmt+
Rgs5low
Epas1low
Rgs5+
Epas1+
Pnmt-

Figure 2.6. Developmental stabilisation of HIF-2α, but not HIF-1α, causes a switch in gene expression in the adrenal medulla. (A) *Pnmt*, *Epas1* and *Rgs5* mRNA signal (brown) in the adrenal medulla from adjacent sections of adult wild-type, *Hif-1αdPA* and *Hif-2αdPA* adrenal glands. Scale bars = 0.25 mm, n = 3 mice of each genotype. Graphs show the percentage of cells within the medulla expressing *Pnmt*, *Epas1* and *Rgs5*. Data are presented as mean ± SEM and were analysed by one-way ANOVA with Tukey's multiple comparisons test, ** $p < 0.01$, *** $p < 0.001$, **** $p < 0.0001$. **(B)** Schematic illustrating the switch in gene expression from a majority $Pnmt^{+}/Epas1^{-}/Rgs5^{-}$ cell population in the wild-type and *Hif-1αdPA* adrenal medulla, towards a majority $Pnmt^{-}/Epas1^{+}/Rgs5^{+}$ cell population in the *Phd2ko* and *Hif-2αdPA* adrenal medulla. Schematic made in biorender.com.

2.2.6 *Developmental stabilisation of HIF-2α, but not HIF-1α, confers acute oxygen chemosensitivity in the adult adrenal medulla*

It was previously demonstrated that the immature gene expression profile in the *Phd2ko* adrenal medulla was associated with retention of oxygen chemosensitivity in adulthood, a feature which is lost in the adrenal medulla of wild-type mice shortly after birth (Prange-Barczynska et al., 2024). As the carotid body-enriched genes *Epas1* and *Rgs5* were upregulated in the *Hif-2αdPA* adrenal medulla, it was next investigated whether developmental stabilisation of HIF-2α (or HIF-1α) was sufficient to induce oxygen chemosensitivity in the adult adrenal medulla.

The cellular response to hypoxia in carotid body glomus cells involves an influx of Ca^{2+} following membrane depolarisation **(Figure 1.6)** (Buckler & Vaughan-Jones, 1994; Pietruschka, 1985). Therefore, to assess hypoxia-induced cellular responses in the carotid body and other oxygen chemosensitive cell types, changes in intracellular Ca^{2+} concentration upon hypoxic stimulation were measured. This was achieved using the genetically encoded calcium indicator GCaMP6f, a synthetic fusion protein composed of calmodulin, M13, a myosin light-chain kinase peptide sequence, and green fluorescent protein (GFP). Binding of Ca^{2+} to the calmodulin domain triggers a conformational change that enhances GFP fluorescence (T.-W. Chen et al., 2013) **(Figure 2.7A)**.

To achieve tissue-specific signal, THCre-expressing mice were crossed with mice carrying the GCaMP6f allele at the Rosa26 locus, under the control of a lox-STOP-lox sequence (known as *Ai95*$^{f/+}$) **(Figure 2.7B)**. In TH-expressing tissues, Cre recombinase excises the stop sequence, allowing expression of GCaMP6f. Whole-mount carotid bodies isolated and subdissected from GCaMP6f-expressing mice exhibit rapid and reversible increases in fluorescence within seconds of superfusion with either a high K^+ or hypoxic solution, which were graded according to the severity of hypoxia, thus acting as a positive control (Prange-Barczynska et al., 2024) **(Figure 2.7C)**.

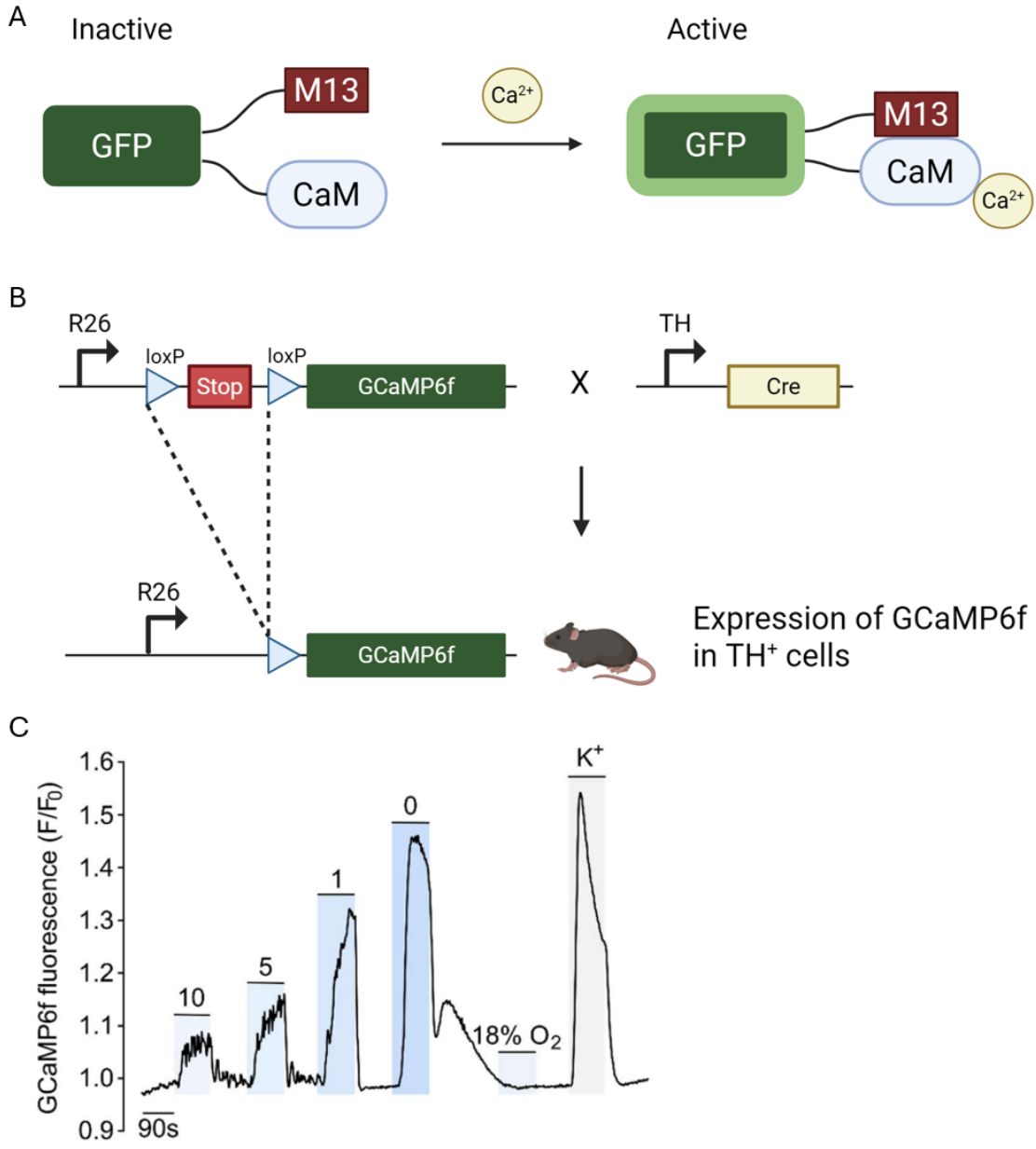

Figure 2.7. The genetically encoded Ca^{2+} indicator GCaMP6f enables measurement of intracellular Ca^{2+} responses through changes in GFP florescence. (A) Schematic demonstrating GCaMP6f in its inactive and active (Ca^{2+} bound) state. The light green border represents GFP fluorescence. **(B)** Mice expressing the GCaMP6f construct at the Rosa26 (R26) locus preceded by a lox-stop-lox sequence, with loxP sites represented by arrowheads, were crossed with mice expressing Cre recombinase under the tyrosine hydroxylase (TH) promoter. Cre-mediated excision of the stop sequence in TH^+ cells of offspring expressing both alleles results in expression of GCaMP6f. Schematics generated with biorender.com. **(C)** A representative trace showing F/F_0 fluorescence in the K^+-responsive cells of an *Ai95*$^{f/+}$*;THCre* carotid body exposed to graded hypoxia (numbers represent % O_2) and 45mM K^+, including 18% O_2 as a sham control.

While it is possible to image the whole carotid body, the adrenal gland is larger and the medulla is encircled by the adrenal cortex. Therefore, adrenal glands were sectioned into 150 μm slices for calcium imaging. Adrenal medullae from wild-type (*Ai95$^{f/+}$;THCre*) mice exhibited increases in florescence in response to 45mM K^+ (**Figure 2.8A and B**) as this induced membrane depolarisation, but showed little-to-no responses to perfusion with solutions of 10, 5, 1 and 0% oxygen (and 18% as a line switch control) (**Figure 2.8B and C**). This is consistent with previous reports that the adult wild-type adrenal medulla is insensitive to acute hypoxia (Prange-Barczynska et al., 2024; Thompson et al., 1997). The *Hif-1αdPA* adrenal medulla was similarly unresponsive to acute hypoxia (**Figure 2.8B and C**). In contrast, the *Hif-2αdPA* adrenal medulla showed rapid increases in fluorescence in response to both K^+ and hypoxia. These fluorescent peaks were reversed upon re-exposure to normoxia and showed graded increases in size with decreasing oxygen tension. Therefore, like *Phd2* inactivation, developmental stabilisation of HIF-2α, but not HIF-1α, is sufficient to induce immature gene expression in the adult adrenal medulla, and retention of oxygen chemosensitivity, similar to that in carotid body glomus cells.

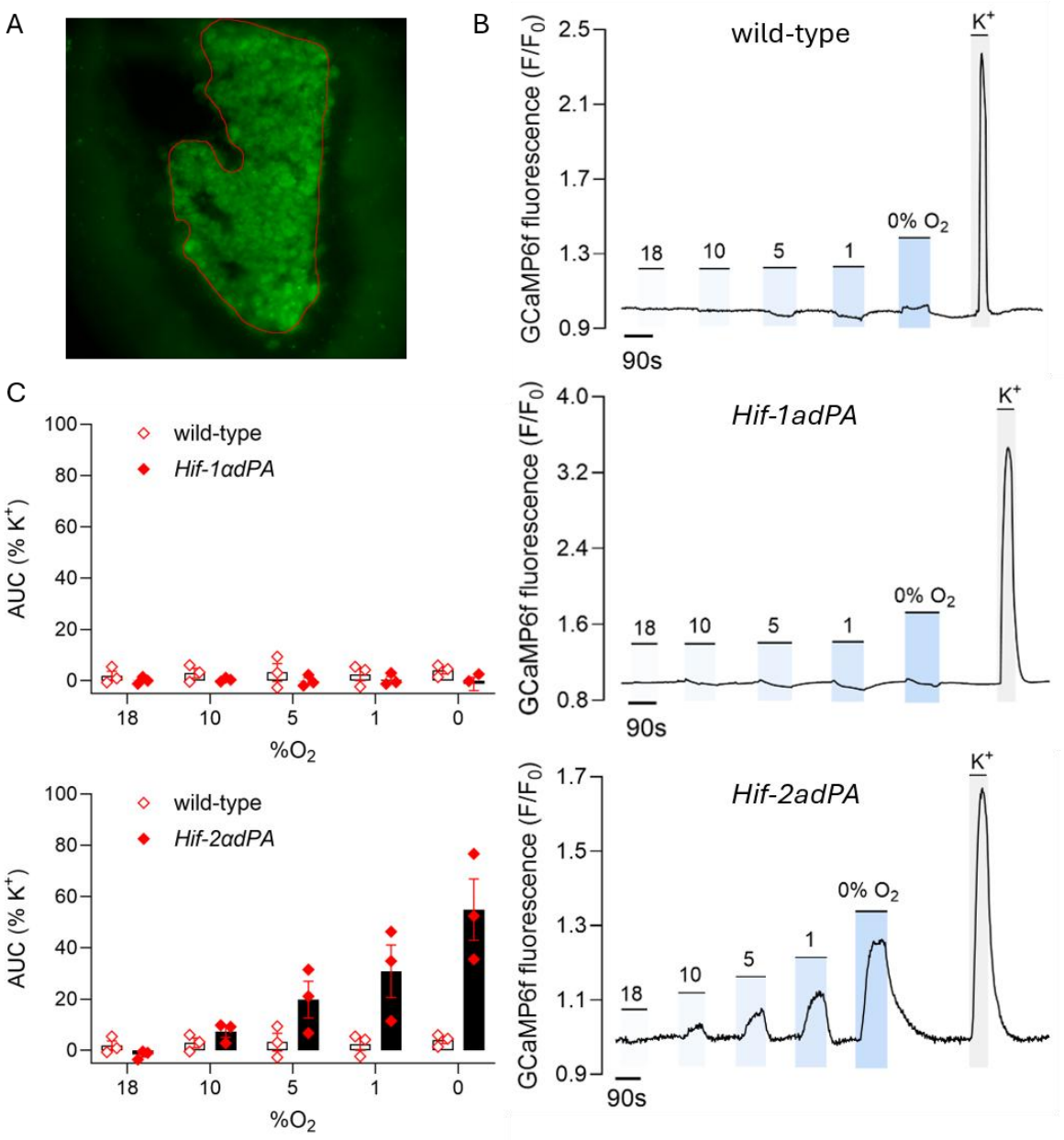

Figure 2.8. Developmental stabilisation of HIF-2α, but not HIF-1α, confers acute oxygen chemosensitivity in the adult adrenal medulla. (A) Representative image showing GFP fluorescence in the adrenal medulla of an adrenal gland slice exposed to 45mM K^+ from a mouse expressing GCaMP6f (*Ai95$^{f/+}$;THCre*). The red outline shows the K^+-responsive region where fluorescence was quantified. **(B)** Representative traces showing F/F_0 fluorescence in the K^+-responsive region of wild-type (*Ai95$^{f/+}$;THCre*), *Hif-1αdPA* (*Hif-1αdPA$^{f/+}$;Ai95$^{f/+}$;THCre*) and *Hif-2αdPA* (*Hif-2αdPA$^{f/+}$;Ai95$^{f/+}$;THCre*) adrenal gland slices exposed to graded hypoxia (numbers represent % O_2) and 45mM K^+, including 18% O_2 as a sham control. **(C)** Area under curve (AUC) graphs of each hypoxic or sham stimulus shown in (B) as a % of the AUC for K^+, n = 3 mice of each genotype.

2.2.7 *Developmental stabilisation of HIF-2α, but not HIF-1α, causes retention of the foetal organ of Zuckerkandl in adulthood*

Previous work showed that *Phd2* inactivation results in the retention of a foetal-like state in adult chromaffin cells, including morphological and gene expression changes in the adrenal medulla as well as the retention of ectopic chromaffin cells at the location of the foetal organ of Zuckerkandl (Eckardt et al., 2021; Prange-Barczynska et al., 2024). To test whether developmental stabilisation of HIF-1α or HIF-2α is sufficient to cause retention of the organ of Zuckerkandl, the abdominal region from adult *Hif-1αdPA* and *Hif-2αdPA* mice, as well as wild-type controls, was dissected between their superior and inferior mesenteric arteries, then sectioned transversely. Immunohistochemistry for TH and CgA was performed on adjacent sections to detect chromaffin cells. As expected, sections from wild-type mice contained some TH^+ cells, owing to the presence of sympathetic ganglia, but did not contain cells which co-expressed TH and CgA, confirming the absence of chromaffin cells in this region (**Figure 2.9A**). This was also the case in the abdominal sections from *Hif-1αdPA* mice (**Figure 2.9A**). On the other hand, TH and CgA immunohistochemistry revealed a large cluster of chromaffin cells along the abdominal aorta, in the region of the foetal organ of Zuckerkandl, in adult *Hif-2αdPA* mice (**Figure 2.9A**). The approximate volume of this structure was 0.0536 ($\pm$ 0.0129) mm^3 (**Figure 2.9B**).

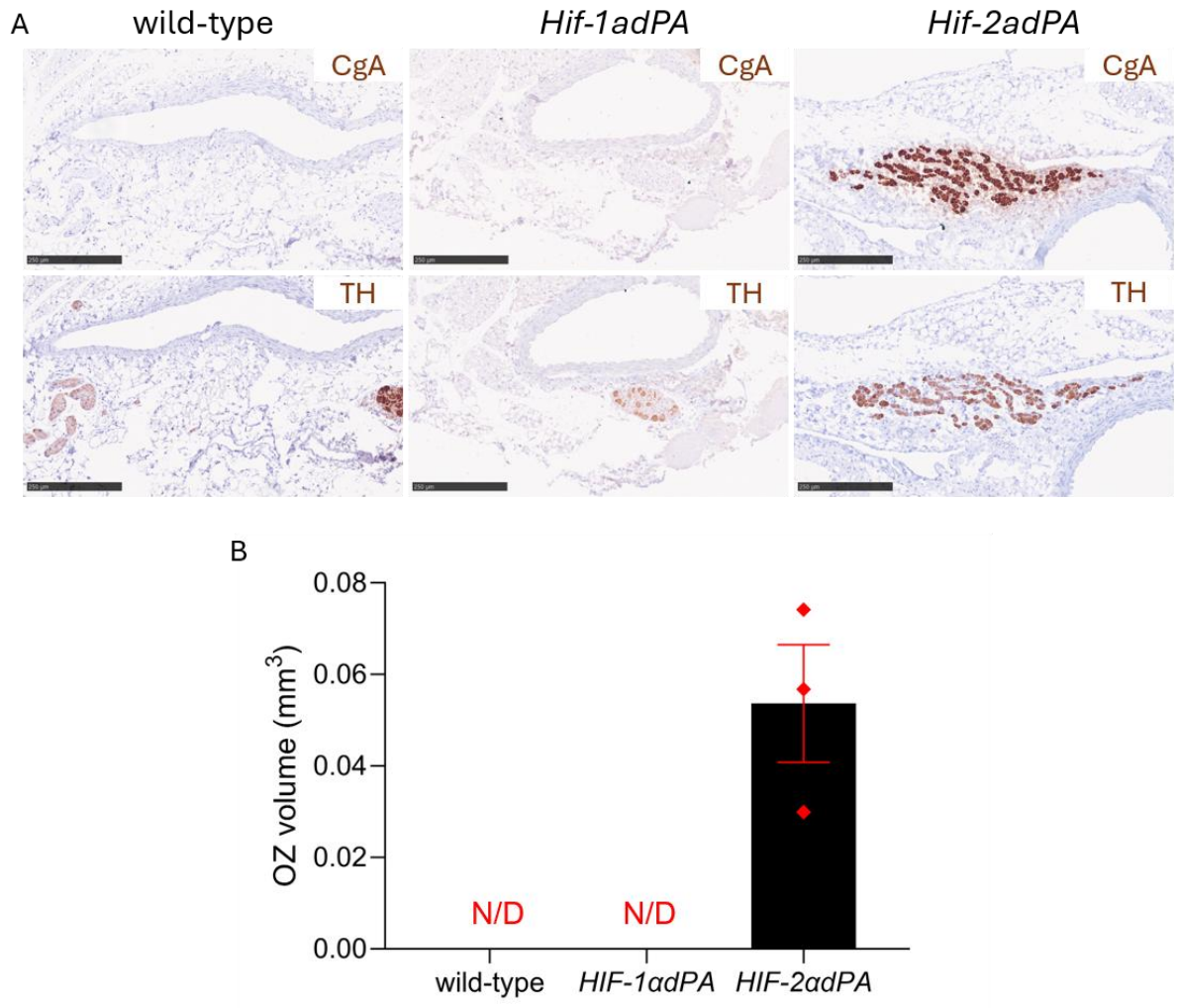

Figure 2.9. The organ of Zuckerkandl is present in adult *Hif-2αdPA* mice, but not in adult wild-type or *Hif-1αdPA* mice. (A) Representative images of chromogranin A (CgA) and tyrosine hydroxylase (TH) immunohistochemistry in transverse sections from the abdominal aorta region of adult wild-type, *Hif-1αdPA* and *Hif-2αdPA* mice. The organ of Zuckerkandl is present in *Hif-2αdPA* mice but was not detected (N/D) in wild-type and *Hif-1αdPA* mice. **(B)** Volume quantification of the organ of Zuckerkandl (OZ) in n = 3 adult *Hif-2αdPA* mice.

In situ hybridisation was performed to investigate gene expression in the *Hif-2αdPA* organ of Zuckerkandl. Genes which are expressed in the *Phd2ko* organ of Zuckerkandl and are associated with acute oxygen chemosensitivity were tested, including *Epas1*, which encodes Hif-2α; *Rgs5 and Vegfa*, which are HIF target genes; and *Cox4i2, Higd1c and Ndufa4l2,* which encode atypical isoforms of mitochondrial subunits (Gao, Bonilla-Henao, et al., 2017; Prange-

Barczynska et al., 2024; Zhou et al., 2016). All of these transcripts were expressed in the *Hif-2αdPA* organ of Zuckerkandl (**Figure 2.10**). Therefore, developmental stabilisation of HIF-2α, but not HIF-1α, is sufficient to cause retention of an organ of Zuckerkandl which expresses carotid body-enriched genes.

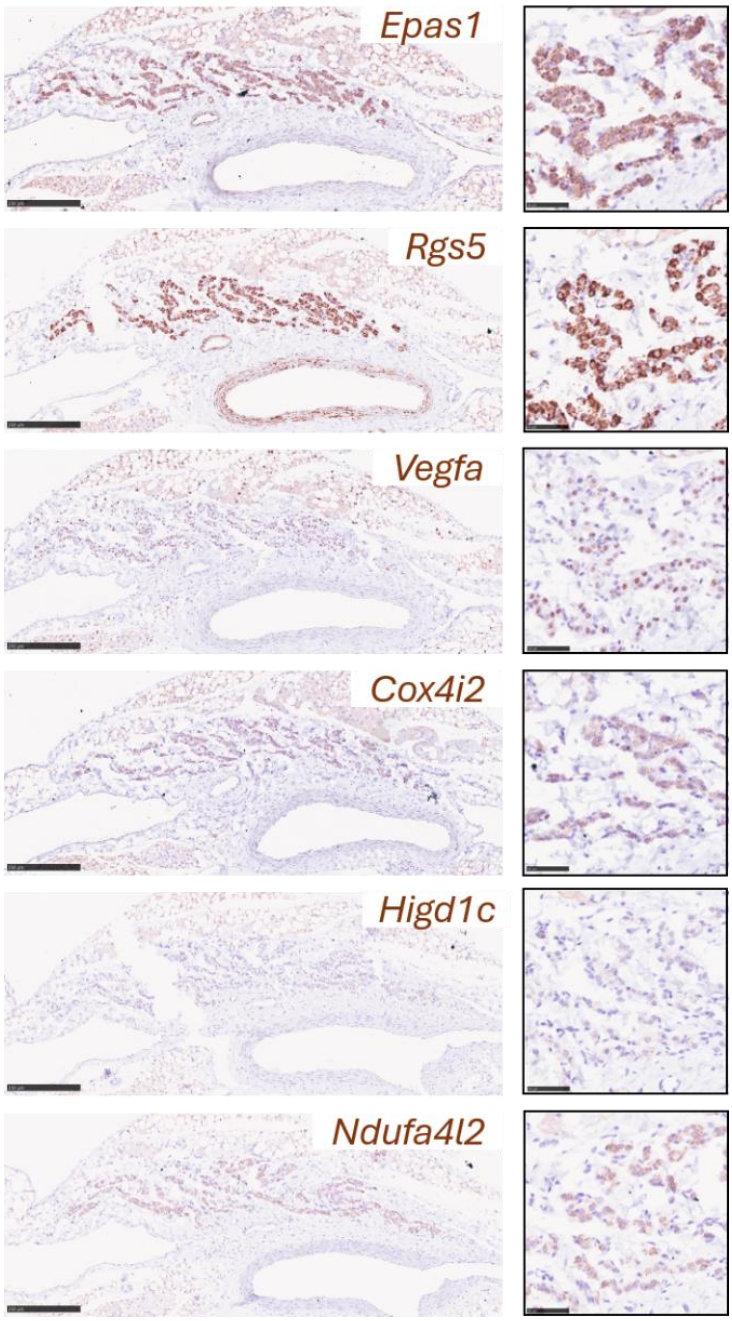

Figure 2.10. Expression of carotid body-enriched genes in the *Hif-2αdPA* organ of Zuckerkandl. Representative images of *in situ* hybridisation for *Epas1*, *Rgs5, Vegfa, Cox4i2, Higd1c* and *Ndufa4l2* mRNA in the organ of Zuckerkandl from an adult *Hif-2αdPA* mouse. Scale bars represent 0.25 mm on

lower magnification images (left) and 0.05 mm on high magnification inserts outlined in black boxes (right).

2.2.8 *The Hif-2αdPA organ of Zuckerkandl is oxygen chemosensitive*

Consistent with its expression of oxygen chemosensitivity-associated genes, the *Phd2ko* (*Phd2$^{f/f}$;Ai95$^{f/+}$;THCre*) organ of Zuckerkandl is responsive to acute hypoxia (Prange-Barczynska et al., 2024). To test whether this is also the case in the *Hif-2αdPA* organ of Zuckerkandl, this was dissected from *Hif-2αdPA* mice expressing GCaMP6f (*Hif-2αdPA$^{f/+}$;Ai95$^{f/+}$;THCre*) and tested in the perfusion setup described earlier. Unlike adrenal glands which require sectioning, whole-mount organ of Zuckerkandl tissue was used as it is smaller and not encased by cortex. 45mM K^+ was used as a positive control to determine the area of excitable tissue (**Figure 2.11A**). Similar to the adrenal medulla from these mice, the *Hif-2αdPA* organ of Zuckerkandl exhibited graded increases in fluorescence in response to acute hypoxic stimuli of decreasing oxygen tensions (**Figure 2.11B and C**). These responses were rapid (within seconds) and reversible. In summary, developmental stabilisation of HIF-2α, but not HIF-1α, is sufficient to induce retention of an immature adrenal medulla and of an organ of Zuckerkandl, both of which respond to acute hypoxia.

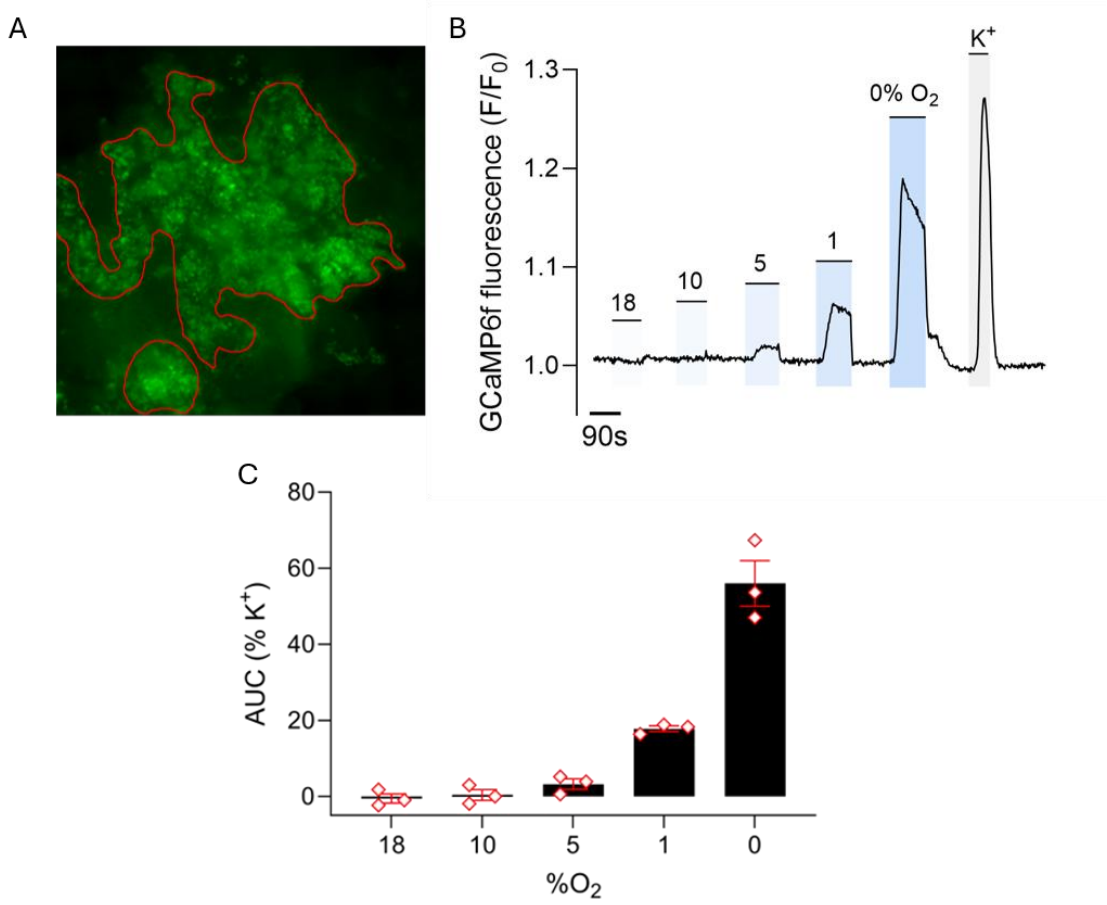

Figure 2.11. The adult *Hif-2αdPA* organ of Zuckerkandl is oxygen chemosensitive (A) Representative image showing GFP fluorescence in a *Hif-2αdPA* organ of Zuckerkandl from a mouse expressing GCaMP6f (*Hif-2αdPA$^{f/+}$;Ai95$^{f/+}$;THCre*) exposed to 45mM K^+. The red outline shows the K^+-responsive region where fluorescence was quantified. **(B)** A representative trace of F/F_0 fluorescence in the K^+-responsive cells during exposure to graded hypoxia (numbers represent % O_2) and 45mM K^+, including 18% O_2 as a sham control. **(C)** Area under curve (AUC) of each hypoxic or sham stimulus shown in (B) as a % of the AUC for K^+, n = 3 mice.

2.3 **Discussion**

This work demonstrates that developmental stabilisation of HIF-2α, but not HIF-1α, in the sympathoadrenal tissue of mice is sufficient to cause foetal-like, paraganglioma-like phenotypes, including carotid body hyperplasia, morphological and gene expression changes in the adrenal medulla, and retention of the organ of Zuckerkandl into adulthood. Importantly, the adrenal medulla and organ of Zuckerkandl from adult *Hif-2αdPA* mice displayed acute

oxygen chemosensitivity, whereas the adrenal medulla from adult *Hif-1αdPA* mice did not, indicating that stabilisation of HIF-2α, but not HIF-1α, is sufficient to confer acute oxygen sensitivity in tissues which are not sensitive, or not present, in adult wild-type mice. These glomus and chromaffin cell phenotypes are similar to those observed previously in mice with inactivation of *Phd2*.

Earlier work used mice with TH-restricted inactivation of *Phd2* (*Phd2ko*) as a model for investigating the effects of developmental HIF stabilisation in neuroendocrine cells. Therefore, the phenotypes observed in these mice may be mediated by HIF-1α and/or HIF-2α stabilisation, or other non-HIF substrates. The *Hif-1αdPA* and *Hif-2αdPA* mice used here were advantageous as they allowed dissection of the role of the individual HIF-α isoforms in the *Phd2ko* phenotypes observed, without influence from other proteins modulated by PHD2. It was possible to demonstrate sufficiency of HIF-2α alone, but not HIF-1α, to drive all of the *Phd2ko* phenotypes.

Although HIF-2α stabilisation was sufficient to mimic the phenotypes observed with *Phd2* inactivation, there were differences in some phenotypes between these mouse models, including a larger carotid body and organ of Zuckerkandl in *Phd2ko* mice than in *Hif-2αdPA* mice. These may reflect either qualitative differences in the pathways activated following these mutations, or quantitative differences in HIF-2α activity. The absence of neuroendocrine phenotypes in *Hif-1αdPA* mice suggests that additional HIF-1α stabilisation in *Phd2ko* mice is unlikely to explain these differences. However, other PHD2-regulated pathways, independent of HIF-1α, may contribute to the enhanced neuroendocrine growth phenotype following *Phd2* loss. Alternatively, these differences may reflect quantitative variation in HIF-2α activity between the two models. *Hif-2αdPA* mice express a stabilised human HIF-2α transgene, whereas *Phd2ko* mice retain endogenous mouse HIF-2α, whose activity may still be regulated by other PHD isoforms. Therefore, differences in the magnitude or regulation of HIF-2α

activity could contribute to the different degrees of carotid body and organ of Zuckerkandl growth observed between the models. Determining whether these phenotypes are dose-dependent would require experimental manipulation of HIF-2α activity, for example through increased *Hif-2αdPA* expression using mice with homozygous expression of this construct, or through pharmacological inhibition with a HIF-2α antagonist such as belzutifan. Overall, this work demonstrates that HIF-2α stabilisation is sufficient to reproduce the neuroendocrine phenotypes observed following *Phd2* loss, while the greater extent of carotid body and organ of Zuckerkandl growth may reflect additional PHD2-dependent pathways and/or differences in the magnitude of HIF-2α activity.

An important caveat to the conclusions made in this chapter is that immunoblotting for the hemagglutinin (HA) tag on the *Hif-1αdPA* and *Hif-2αdPA* constructs revealed weaker expression of *Hif-1αdPA* than *Hif-2αdPA* in adrenal medullae of the relevant mice. This finding is consistent with previously published data in mouse embryonic fibroblasts (MEFs) expressing these constructs (W. Y. Kim et al., 2006). The authors of this work proposed that this may be due to the action of VHL-independent ubiquitin ligases that specifically target HIF-1α, but not HIF-2α, for proteasomal degradation. In support of this, addition of a proteasome inhibitor, MG132, caused an increase in expression of *Hif-1αdPA*, but not *Hif-2αdPA*, in their HA immunoblot. Therefore, it is important to consider that the absence of the glomus and chromaffin cell phenotypes seen in *Phd2ko* and *Hif-2αdPA* mice in the *Hif-1αdPA* mice may be due to lower levels of HIF-1α stabilisation.

Despite this, the isoform-specificity of these phenotypes to HIF-2α is not unexpected. *EPAS1*, the gene encoding HIF-2α, is exceptionally highly expressed in the carotid body (Tian et al., 1998). It is the second most abundant transcript in carotid body glomus cells and is expressed at 102-fold higher levels here than in the developmentally related superior cervical ganglion (Gao, Bonilla-Henao, et al., 2017; Zhou et al., 2016). Previous work demonstrated that

inactivation of HIF-2α, but not HIF-1α, in cells of the sympathoadrenal system prevents development of the carotid body, while inducible inactivation of HIF-2α, but not HIF-1α, attenuates the ventilatory and proliferative responses of the wild-type carotid body to hypoxia (Hodson et al., 2016; Macias et al., 2018). With respect to the ventilatory response, HIF-2α inactivation results in a reduction in both the baseline HVR and in ventilatory acclimatisation to hypoxia (Hodson et al., 2016). The impairment of HVR following HIF-2α inactivation is also evident at the cellular level, with Ca^{2+}-responses to hypoxia also attenuated in carotid body glomus cells from inducible *Epas1* knockout mice (Macias et al., 2018). Similarly, concurrent *Phd2* and *Hif-α* knockout mouse models showed that HIF-2α, but not HIF-1α, is necessary for both carotid body hyperplasia and the shift in adrenal medullary gene expression towards a predominantly noradrenergic *Pnmt*$^{-}$ population in *Phd2ko* mice (Fielding et al., 2018). Evidence from human disease also supports the isoform-specificity of HIF-2α in these neuroendocrine cell phenotypes; gain-of-function mutations in *EPAS1* are established in paragangliomas, whereas there are currently no reports of mutations in *HIF-1α* in these tumours, although *HIF-1α* mutations may not be tolerated (Arenillas et al., 2025; Comino-Méndez et al., 2013; Welander, Andreasson, Brauckhoff, et al., 2014). Finally, atypical mitochondrial subunits such as COX4I2, HIGD1C and NDUFA4lL2, and G protein signalling components such as RGS5, which are all hypothesised to play a role in oxygen sensing, are uniquely regulated by HIF-2α, and not HIF-1α (Colinas et al., 2023). Taken together, these observations support the finding of this chapter that foetal-like, paraganglioma-like neuroendocrine cell phenotypes are induced by stabilisation of HIF-2α, but not HIF-1α.

A key finding of this work is that HIF-2α is sufficient to confer the ability to sense and respond to acute hypoxia on specialised cell types. However, the precise molecular mechanisms underlying rapid oxygen sensing and the role HIF-2α plays in this are incompletely understood. A proposed mechanism linking HIF-2α to acute oxygen sensing is through its transcriptional

regulation of mitochondrial proteins that are highly enriched in the carotid body, including COX4I2, HIGD1C and NDUFA4L2 (Gao, Bonilla-Henao, et al., 2017; Moreno-Domínguez et al., 2020; Timón-Gómez et al., 2022; Zhou et al., 2016). In most cell types, the affinity of the mitochondria for oxygen is considered too high to detect physiological reductions in oxygen tension (Buckler & Turner, 2013), whereas expression of these atypical mitochondrial components is proposed to increase mitochondrial sensitivity to changes in oxygen availability (Moreno-Domínguez et al., 2020; Timón-Gómez et al., 2022). Consequently, hypoxia may induce changes in redox state and metabolism, including altered production of NADH and reactive oxygen species, succinate accumulation and reduced ATP availability (Buckler & Turner, 2013; Swiderska et al., 2021; Yamamoto et al., 2006). These are potential signals that may trigger inhibition of membrane potassium channels, leading to membrane depolarisation, calcium influx and neurotransmitter release onto the afferent nerve. HIF-2α promotes expression of these atypical mitochondrial subunits, providing a potential mechanistic link between HIF-2α activity and the ability of specialised cell types to sense and respond to acute hypoxia (Moreno-Domínguez et al., 2020). Consistent with this model, mice lacking *Cox4i2* exhibited attenuated glomus cell Ca^{2+} responses to acute hypoxia and a reduced HVR (Moreno-Domínguez et al., 2020), while loss of *Higd1c* similarly reduces hypoxia-evoked glomus cell and carotid sinus nerve activity, as well as the HVR (Timón-Gómez et al., 2022).

As two tissues which are also able to rapidly sense and respond to acute hypoxia, the adult *Hif-2αdPA* adrenal medulla and organ of Zuckerkandl provide new models for further investigation into the mechanism underlying cellular oxygen chemosensitivity. The atypical mitochondrial subunits COX4I2, HIGD1C and NDUFA4L2, which are enriched in the carotid body, are also highly expressed in these tissues, supporting their proposed role in oxygen sensing. More detailed comparison of gene expression in these cells to other responsive cells, such as carotid body glomus cells, and to similar, but non-chemosensitive tissue such as the adult wild-type

adrenal medulla, may highlight novel genes which are also important in acute oxygen sensing. This relies on the assumption that acute oxygen sensing occurs via analogous mechanisms in chromaffin tissues and carotid body glomus cells. Their shared developmental origin from the neural crest and morphological and functional similarities suggest this may be true.

Transcriptomic approaches can only capture the transcriptional effects of HIF-2α on oxygen sensing. However, there is some evidence that HIF-2α may play a non-transcriptional role. Firstly, *Epas1* is exceptionally highly expressed in the carotid body, and is much more abundant than other transcription factors and its binding partners, ARNT and ARNT2 (Gao, Bonilla-Henao, et al., 2017; Zhou et al., 2016). Additionally, pharmacological inhibition of HIF-2α with PT2385 reduces the HVR in mice after an hour, which is faster than the transcriptional pathway would typically occur (Cheng et al., 2020). Furthermore, mice carrying a mutation in HIF-2α which alters the binding pocket of PT2385 but does not affect dimerisation with ARNT/ARNT2 have reduced ventilatory sensitivity to sustained hypoxia compared to wild-type mice, further suggesting a role for HIF-2α beyond its canonical transcriptional activity (Cheng et al., 2020). Therefore, while transcriptomic studies may be useful in helping to uncover the oxygen-sensing signal, it is important to determine whether the transcriptional activity of HIF-2α is required for acute oxygen sensing, or whether HIF-2α also has non-transcriptional functions.

Beyond its potential non-transcriptional effects, HIF-2α stabilisation may also influence the underlying developmental state of neuroendocrine cells. A number of the chromaffin cell phenotypes induced by direct and indirect stabilisation of HIF-2α reflect a foetal-like state. Firstly, the majority of adrenal medullary chromaffin cells in adult mice lack expression of *Pnmt*, a marker of mature adrenal medullary cells. Next, the organ of Zuckerkandl is a foetal structure which is typically lost postnatally but is retained in adulthood in these mice. Finally, the oxygen chemosensitivity observed in the adult *Hif-2αdPA* adrenal medulla and organ of Zuckerkandl is a feature which is reported in these chromaffin tissues in the wild-type foetus,

but not in the adult. This implies that stabilisation of HIF-2α may impair chromaffin cell development. Clinically, this link between developmental HIF-2α stabilisation and chromaffin cell phenotypes is interesting as a very high proportion of pheochromocytomas and paragangliomas carry germline or very early somatic mutations (Buffet et al., 2020; Crona et al. 2017), suggesting these mutations may alter cell development and render cells in a state where they are prone to tumorigenesis. To examine whether the time at which HIF-2α stabilisation occurs is important in conferring these phenotypes, further work should use inducible Cre models to allow temporal control over when activation of HIF-2α is induced.

To conclude, this chapter demonstrated that HIF-2α is sufficient to cause paraganglioma-like, foetal-like changes in carotid body glomus and chromaffin cells, including oxygen chemosensitivity in tissues which are either not sensitive, or present, in the adult wild-type animal. This provides a new model to help further the understanding of both the mechanism underlying acute oxygen sensing, and the pathogenesis of tumours associated with HIF-activating mutations.

Chapter 3

INVESTIGATION INTO THE MECHANISMS BY WHICH HIF-2A CONFERS FOETAL-LIKE, PARAGANGLIOMA-LIKE GLOMUS AND CHROMAFFIN CELL PHENOTYPES.

3.1 **Introduction**

Work presented in the previous chapter established HIF-2α as a key regulator of neuroendocrine cell identity. Developmental stabilisation of HIF-2α, but not HIF-1α, was sufficient to induce a foetal-like, paraganglioma-like phenotype in glomus and chromaffin cells of mice, recapitulating features previously observed following developmental inactivation of *Phd2* (Eckardt et al., 2021; Fielding et al., 2018; Prange-Barczynska et al., 2024). Importantly, this included retention of acute oxygen chemosensitivity in adrenal medullary and organ of Zuckerkandl chromaffin cells, a property that is typically lost during maturation. However, the mechanisms by which HIF-2α establishes these phenotypes remains unclear. In particular, it is important to determine whether HIF-2α activation is specifically required during development and whether its canonical transcriptional activity is necessary for the establishment of this phenotype.

The timing of HIF-2α activation may be important for the establishment of the foetal-like, paraganglioma-like neuroendocrine phenotype. Germline mutations in components of the oxygen sensing pathway such as *VHL* and *SDHB* are established causes of hereditary pheochromocytoma and paraganglioma syndromes (Fishbein et al., 2017). Furthermore, while activating mutations in *EPAS1* occur post-fertilisation, evidence from sympathetic paragangliomas arising in patients with cyanotic congenital heart disease suggests that chronic hypoxia promotes selection of *EPAS1*-mutant clones during early life (Arenillas et al., 2025).

Together, these observations raise the possibility that the consequences of HIF-2α pathway activation depend on the developmental context in which it occurs (Buffet et al., 2020; Dahia, 2014). Consistent with this, developmental inactivation of *Phd2* in mice results in reduced *Pnmt* expression in the adrenal medulla, whereas equivalent inactivation of *Phd2* in adulthood does not (Eckardt et al., 2021). However, adult-onset *Phd2* inactivation can still induce expression of HIF-2α target genes such as *Rgs5* and *Vegfa* in *Hif-2α*$^{+}$ populations, suggesting that HIF-2α may function in two distinct ways: during development, as a regulator of chromaffin cell maturation, and in adulthood, through dynamic regulation of its target genes. Therefore, comparing developmental versus adult-onset HIF-2α stabilisation may help distinguish phenotypes arising from altered chromaffin cell development from those resulting from dynamic HIF-2α activity.

A second question is whether the ability of HIF-2α to establish this neuroendocrine state depends on its canonical role as a transcription factor. HIF-2α classically regulates gene expression by heterodimerising with the aryl hydrocarbon receptor nuclear translocator proteins ARNT or ARNT2 and subsequently binding to hypoxia response elements (HRE) to activate gene expression (Keith & Simon, 2007; Ratcliffe, 2013). HIF-2α-dependent transcription has been implicated in the regulation of genes associated with oxygen sensing in the carotid body, including *Cox4i2*, *Higd1c* and *Ndufa4l2*, providing a potential mechanism through which HIF-2α could influence neuroendocrine cell phenotype and function (Moreno-Domínguez et al., 2020; Ortega-Sáenz et al., 2020). However, whether HIF-2α-dependent transcription is required for the broader foetal-like, paraganglioma-like neuroendocrine phenotype following developmental HIF-2α stabilisation remains unknown.

Several observations raise the possibility that HIF-2α may influence neuroendocrine cell phenotypes through mechanisms that extend beyond its canonical transcriptional activity. First, *Epas1*, which encodes HIF-2α, is expressed at exceptionally high levels in the carotid body,

despite comparatively lower expression of ARNT and ARNT2 (Gao, Bonilla-Henao, et al., 2017; Zhou et al., 2016). If HIF-2α activity is mediated exclusively through the formation of heterodimers with ARNT/ARNT2, the relative abundance of HIF-2α would be expected to be more closely matched with these binding partners. Second, combined inactivation of *Arnt* and *Arnt2* in mice produces milder reductions in the ventilatory, carotid body proliferative and hematopoietic adaptations to hypoxia than inactivation of HIF-2α itself, suggesting that HIF-2α may retain important biological activity that are not dependent on ARNT/ARNT2 (MPB, PJR and TB, unpublished observations). Third, the identification of a unique binding pocket within the PAS-B domain of HIF-2α raises the possibility that endogenous ligands could modulate HIF-2α activity independently of its established transcriptional interactions (Scheuermann et al., 2009). Supporting this theory, mice carrying a mutation in this PAS B domain that does not affect the ability of HIF-2α to bind to ARNT/ARNT2, S305M, have a hypomorphic ventilatory response to acute hypoxia, demonstrating that altering the PAS B domain impairs HIF-2α function, despite not altering its ability to function as a transcription factor (Cheng et al., 2020; Diao et al., 2022; J. Zhuang et al., 2024; Scheuermann et al., 2009). Taken together, these findings raise the possibility that HIF-2α may integrate transcriptional and non-transcriptional mechanisms to regulate neuroendocrine cell function.

This chapter therefore investigates the temporal and transcriptional requirements for HIF-2α-dependent establishment of the foetal-like, paraganglioma-like neuroendocrine cell state. First, a tamoxifen-inducible *Hif-2αdPA* model was used to stabilise HIF-2α selectively in TH-expressing cells during adulthood, allowing the consequences of adult-onset HIF-2α stabilisation to be compared with those of developmental HIF-2α stabilisation described in the previous chapter. Adult-onset stabilisation of HIF-2α did not reproduce the neuroendocrine phenotypes observed following developmental stabilisation of HIF-2α, supporting a specific role for HIF-2α during development in establishing the foetal-like, paraganglioma-like

phenotype. Second, the requirement for HIF-2α transcriptional activity was examined using a modified *Hif-2αdPA* construct carrying a deletion of a basic helix-loop-helix in the DNA binding domain that prevents HIF-2α binding to HREs. These mice also did not recapitulate the glomus and chromaffin cell phenotypes observed in *Hif-2αdPA* mice, indicating that the transcriptional activity of HIF-2α is essential for their development. Together, these experiments define the temporal and transcriptional requirements through which HIF-2α establishes the neuroendocrine phenotypes observed following developmental HIF-2α stabilisation.

3.2 **Results**

3.2.1 *Adult-onset Hif-2αdPA mouse model*

Given that pseudohypoxic mutations associated with pheochromocytomas and paragangliomas are frequently inherited in the germline or occur as early tumour-initiating somatic events, the developmental timing of HIF-2α activation may be important in establishing neuroendocrine cell phenotypes (Fishbein et al., 2017; Lenders et al., 2014). Therefore, to determine whether HIF-2α stabilisation must occur during development to produce the foetal-like, paraganglioma-like glomus and chromaffin cell phenotypes observed in the *Hif-2αdPA* mice or whether adult-onset HIF-2α stabilisation is sufficient, mice carrying the *Hif-2αdPA*$^{f/+}$ allele were crossed with *THCreER* mice (illustrated in the schematic in **Figure 3.1A**). THCreER is a tamoxifen-inducible Cre recombinase in which the TH-IRES-Cre construct used in the *Hif-2αdPA* model is fused to a modified estrogen receptor (ER) ligand binding domain. In the absence of tamoxifen, THCreER is sequestered in the cytoplasm. Following tamoxifen binding, it translocates to the nucleus where it can catalyse recombination (Feil et al., 1996). Therefore, offspring carrying both the *Hif-2αdPA*$^{f/+}$ and *THCreER* alleles (*Hif-2αdPA*$^{f/+}$*;THCreER* mice,

also referred to as adult-onset *Hif-2αdPA*) remain functionally wild-type for HIF-2α until tamoxifen administration, at which point Cre-mediated excision of the stop sequence preceding *Hif-2αdPA*$^{f/+}$ induces HIF-2α stabilisation. In these experiments, mice were treated with 2 mg tamoxifen once daily for five consecutive days, as described previously (Arsenault et al., 2013; Eckardt et al., 2021; Fielding et al., 2018), from approximately six weeks of age. Mice were subsequently analysed at two time points; an early time point approximately six weeks after tamoxifen administration, corresponding to the duration of HIF-2α overexpression in the developmental *Hif-2αdPA* model, and a late time point ≥ 5 months after tamoxifen administration to assess the longer-term effects of adult-onset HIF-2α stabilisation (summarised in **Figure 3.1B**). Mice carrying the THCreER allele alone were similarly treated with tamoxifen and used as controls.

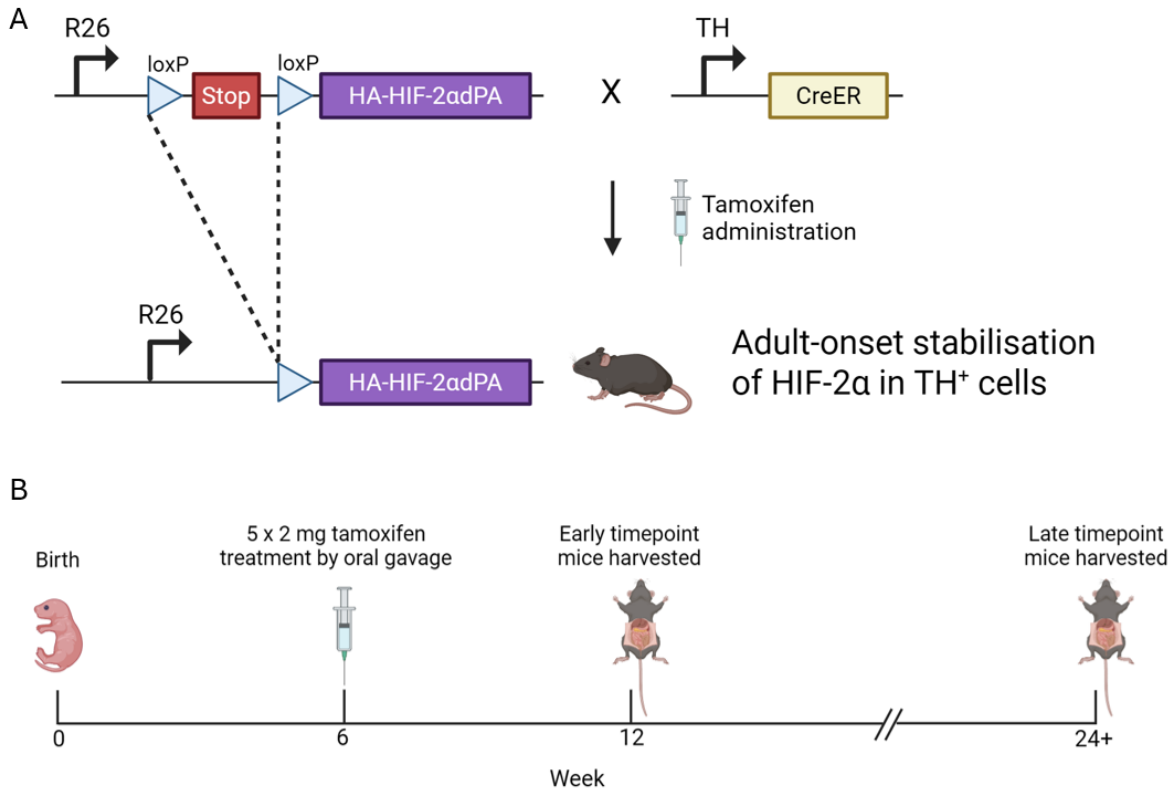

Figure 3.1. Schematic illustrating the adult-onset *Hif-2αdPA* mouse model and experimental timeline. (A) Mice expressing the *Hif-2αdPA* construct at the Rosa26 (R26) locus preceded by a lox-stop-lox sequence, with loxP sites represented by arrowheads, were crossed with mice expressing

tamoxifen-inducible CreER recombinase under the tyrosine hydroxylase (TH) promoter. Tamoxifen-induced Cre-mediated excision of the stop sequence in TH^+ cells of mice expressing both alleles results in stabilisation of HIF-2α. The *Hif-2dPA* constructs contains a hemagglutinin (HA) tag at the N terminus. **(B)** Mice were given 2 mg tamoxifen daily for 5 consecutive days at 6 weeks of age. Mice were harvested and tissues were collected at an early timepoint (6 weeks after the final tamoxifen dose) and a late timepoint (>24 weeks after the final dose). Figures generated with biorender.com.

3.2.2 *Confirmation of adult-onset Hif-2αdPA expression*

To confirm expression of the *Hif-2αdPA* construct in TH^+ tissues following tamoxifen administration, an immunoblot for the hemagglutinin (HA) tag encoded within the *Hif-2αdPA* construct was performed. As described in the previous chapter, carotid bodies were not used because their small size provides insufficient tissue for immunoblotting. Instead, immunoblotting was performed on adrenal medullae from three adult-onset *Hif-2αdPA* and three tamoxifen-treated control mice harvested at the early time point. HA expression was detected in all three adult-onset *Hif-2αdPA* adrenal medullae but not in control medullae **(Figure 3.2A)**.

Immunohistochemistry for the HA tag was not performed because the available HA antibodies were not effective for this application, as established previously. Instead, sections were stained using an antibody against HIF-2α. No nuclear signal was observed in chromaffin cells from control mice, whereas nuclear HIF-2α staining (brown) was evident in the majority of cells within the adrenal medulla of adult-onset *Hif-2αdPA* mice **(Figure 3.2B)**. As HIF-2α is a transcription factor whose canonical activity occurs in the nucleus, its nuclear localisation is consistent with the presence of stabilised HIF-2α within the appropriate cellular compartment. Brown cytoplasmic staining was also observed in both genotypes and was considered background staining rather than specific HIF-2α localisation.

Together, detection of the construct-specific HA tag by immunoblotting and increased nuclear HIF-2α staining by immunohistochemistry provide evidence of successful tamoxifen-induced recombination and HIF-2α stabilisation in the adult-onset *Hif-2αdPA* mice. Although these analyses do not directly quantify recombination, HA expression in all three adult-onset *Hif-2αdPA* adrenal medullae and widespread nuclear HIF-2α staining are consistent with efficient recombination.

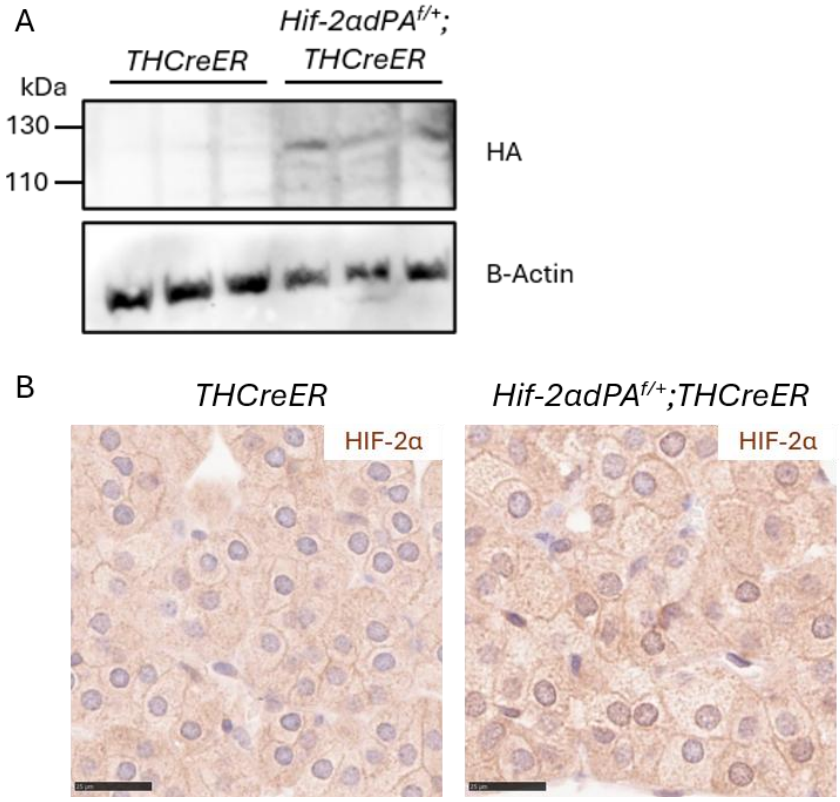

Figure 3.2. HIF-2α protein stabilisation in adrenal medullae of control versus adult-onset *Hif-2αdPA* mice. (A) Immunoblot for hemagglutinin (HA) or β-actin confirming HA-tagged *Hif-2αdPA* transgene expression in the adrenal medulla from adult-onset *Hif-2αdPA* (*Hif-2αdPA$^{f/+}$;THCreER*), but not control (*THCreER*), mice (n = 3 mice per genotype, with one mouse per lane). **(B)** HIF-2α immunohistochemistry showing nuclear HIF-2α protein (brown) stabilisation in chromaffin cells from the adrenal medulla of adult-onset *Hif-2αdPA,* but not control (left), mice. Scale bars represent 0.025 mm.

3.2.3 *Adult-onset Hif-2αdPA stabilisation does not cause an increase in carotid body volume or hypoxic ventilatory response*

Having confirmed successful expression of the *Hif-2αdPA* construct following tamoxifen-administration, carotid body morphology and function was then examined in the adult-onset *Hif-2αdPA* mice. Mice were analysed at two timepoints post-tamoxifen administration: an early timepoint to corresponding to the six-week period of HIF-2α stabilisation in the developmental *Hif-2αdPA* mice, and a later timepoint to assess longer-term effects of adult-onset HIF-2α stabilisation. As demonstrated in chapter 2, developmental stabilisation of HIF-2α in the carotid body confers an almost 5-fold increase in its volume by adulthood **(Figure 2.4)**. To test whether this is also the case with adult-onset stabilisation of HIF-2α, immunohistochemistry for chromogranin A (CgA) and tyrosine hydroxylase (TH) was performed on sections throughout the carotid bifurcation of adult-onset *Hif-2αdPA* and control mice at both the early and late timepoints post-tamoxifen **(Figure 3.3A)**. TH is expressed in neuroendocrine tissue, including surrounding sympathetic ganglia, whereas CgA expression is restricted to carotid body glomus cells. Therefore, the area of tissue positive for CgA was quantified and used to estimate carotid body volume. This revealed no significant differences in the volume of the carotid bodies from control and adult-onset *Hif-2αdPA* mice at both the early and late timepoints following tamoxifen administration **(Figure 3.3B)**. However, if anything, the adult-onset *Hif-2αdPA* carotid body volume appeared to be reduced compared with controls at the late timepoint. Therefore, the carotid body hyperplasia observed in *Hif-2αdPA* mice requires developmental stabilisation of HIF-2α and cannot be recapitulated by HIF-2α stabilisation initiated in adulthood.

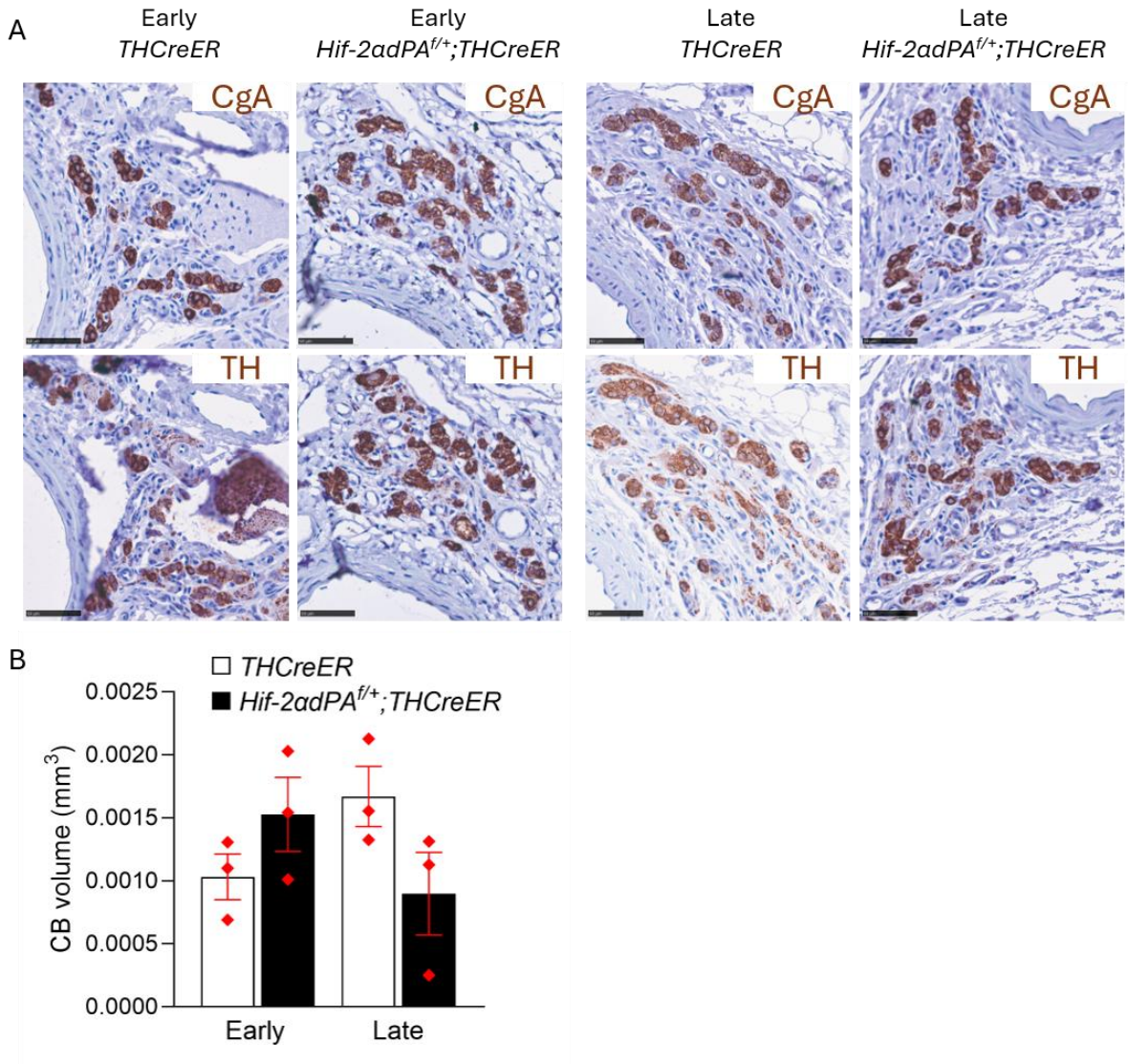

Figure 3.3. Adult-onset stabilisation of HIF-2α does not alter carotid body volume. (A) Representative images of chromogranin A (CgA) and tyrosine hydroxylase (TH) immunohistochemistry in carotid body sections from control (*THCreER*) and adult-onset *Hif-2αdPA* (*Hif-2αdPA$^{f/+}$;THCreER*) mice harvested at the early and late timepoints following tamoxifen administration. Scale bars = 0.1 mm. **(B)** Carotid body (CB) volume quantification Data are presented as mean ± SEM and were analysed by one-way ANOVA with Šídák's multiple comparisons test, no statistical differences were detected.

Developmental stabilisation of HIF-2α alters carotid body function, causing enhanced ventilatory responses to acute hypoxia. To assess whether this is also a developmental phenotype, or whether adult-onset stabilisation of HIF-2α is sufficient to cause an enhanced

hypoxic ventilatory response (HVR), the HVR in adult-onset *Hif-2αdPA* mice was assessed by plethysmography. At both the early and late timepoints post-tamoxifen in male and female mice, there were no significant differences in the magnitude of the acute ventilatory response between adult-onset *Hif-2αdPA* and control mice to 10% O_2/3% CO_2, or to 10% O_2 or 3% CO_2 alone **(Figure 3.4)**. Although non-significant, female adult-onset *Hif-2αdPA* mice at the late timepoint appeared to have a reduced HVR compared with control mice. However, only two mice of each genotype were available for analysis at this timepoint, precluding reliable assessment of whether this difference was reproducible. Therefore, adult-onset stabilisation of HIF-2α is not sufficient to confer an increase in carotid body size or function, suggesting a developmental role of HIF-2α in conferring both the increase in size and function of the *Hif-2αdPA* carotid body.

Females

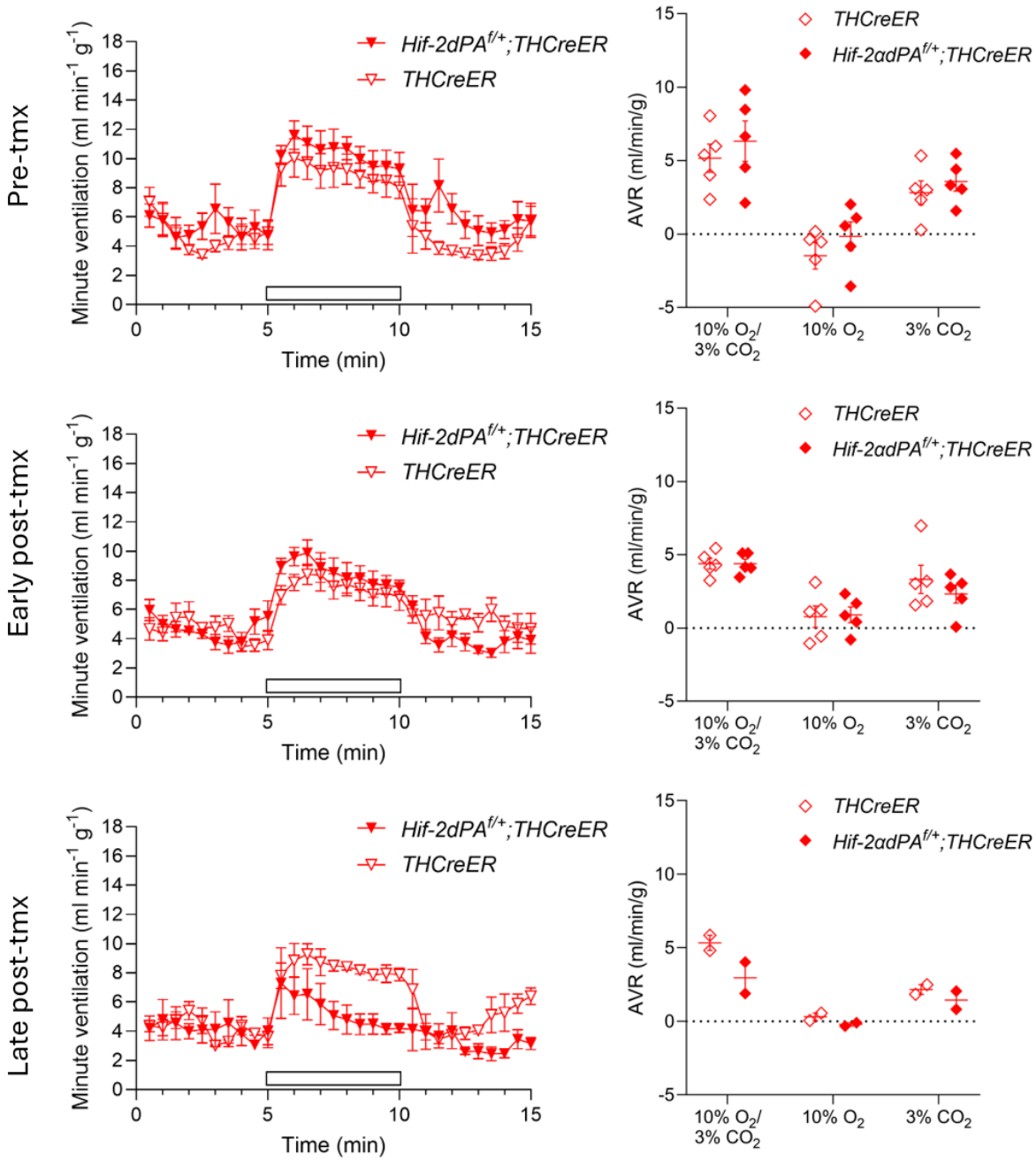
Pre-tmx
Early post-tmx
Late post-tmx
Minute ventilation (ml min-1 g-1)
Time (min)
Hif-2dPAf/+;THCreER
THCreER
AVR (ml/min/g)
10% O2/ 3% CO2
10% O2
3% CO2

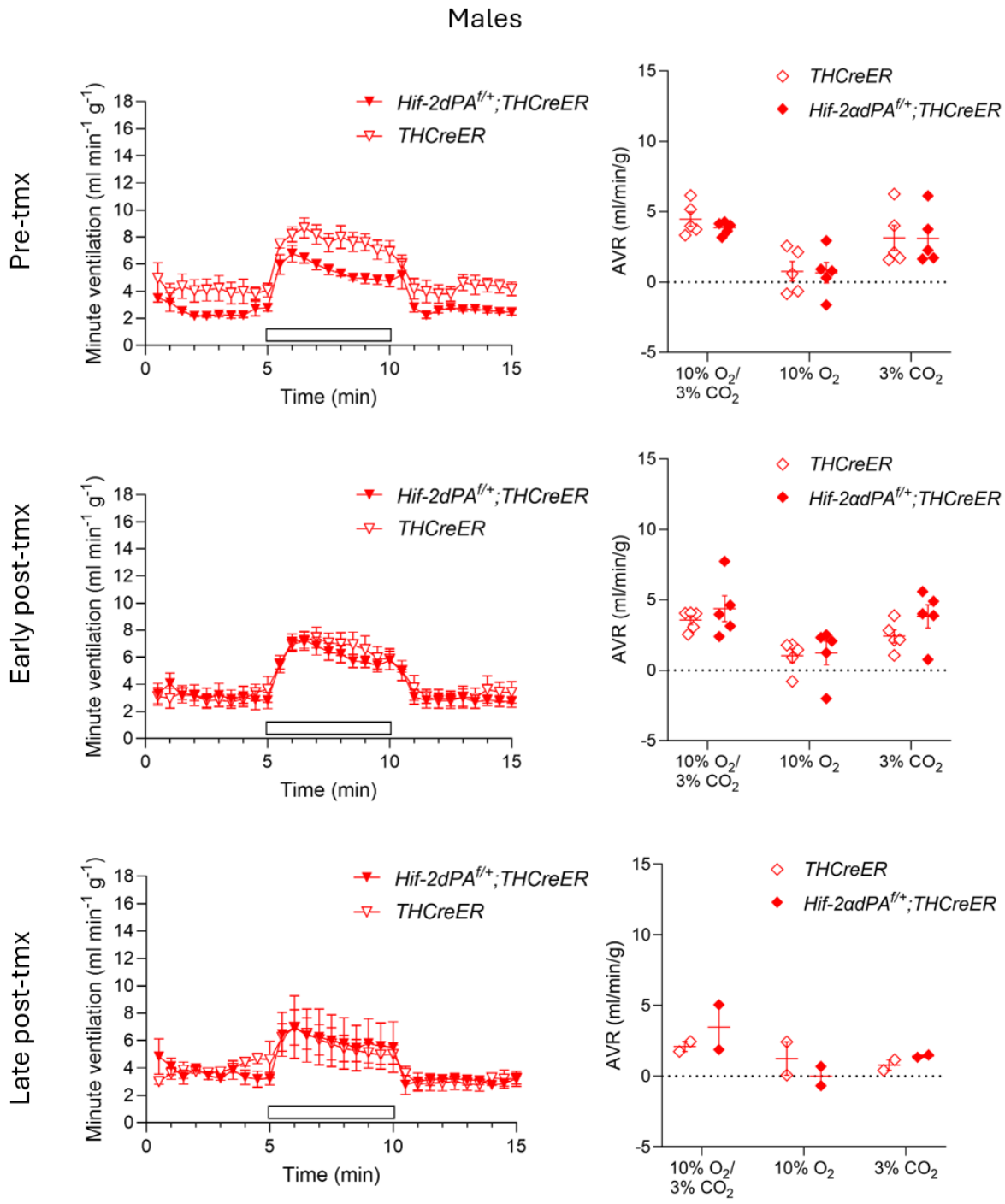

Figure 3.4. Adult-onset *Hif-2αdPA* mice do not have an enhanced hypoxic ventilatory response to 10% O_2/3% CO_2. (A) Ventilatory responses to five minutes of 10% O_2/3% CO_2 (white bars) in male and female mice, n = 5 females and males per genotype were assessed pre-tamoxifen and at the early post-tamoxifen timepoint, n = 2 females and males per genotype were assessed at the late post-tamoxifen timepoint. **(B)** AVRs to each hypoxic stimuli. Data were compared between genotypes for each hypoxic stimuli by Holm-Sidak's multiple comparisons tests, no statistically significant differences were observed.

3.2.4 *Adult-onset Hif-2αdPA does not confer an immature gene expression profile or acute oxygen chemosensitivity in chromaffin cells of the adrenal medulla*

Developmental stabilisation of HIF-2α confers an immature chromaffin cell phenotype in adult mice, including a primarily noradrenergic *Pnmt*$^{-}$ adrenal medulla (Chapter 2). This is inversely correlated with expression of *Epas1* and *Rgs5*, such that the majority of adrenal medullary chromaffin cells in *Hif-2αdPA* mice are *Pnmt*$^{-}$/*Epas1*$^{+}$/*Rgs5*$^{+}$, compared with a predominantly *Pnmt*$^{+}$/*Epas1*$^{-}$/*Rgs5*$^{-}$ population in adult wild-type mice. To determine whether adult-onset stabilisation of HIF-2α is sufficient to induce this immature gene expression profile in the adrenal medulla, *in situ* hybridisation for *Pnmt*, *Epas1* and *Rgs5* was performed on adrenal sections from adult-onset *Hif-2αdPA* and control mice harvested at the early and late timepoints following tamoxifen administration.

In control adrenal medullae at both timepoints, *Pnmt* was widely expressed, while *Epas1* and *Rgs5* expression was restricted to small clusters of *Pnmt*$^{-}$ cells **(Figure 3.5)**. Adult-onset expression of *Hif-2αdPA* did not alter this pattern at either timepoint, with the majority of chromaffin cells expressing *Pnmt*, but not *Epas1* or *Rgs5*, with only small clusters of *Pnmt*$^{-}$/*Epas1*$^{+}$/*Rgs5*$^{+}$ cells, predominantly located at the periphery of the medulla. Although the proportion of cells expressing *Rgs5* was not increased in the adult-onset *Hif-2αdPA* medullae, the intensity of staining appeared darker, potentially indicating increased expression within these cells. Therefore, adult-onset stabilisation of HIF-2α did not alter the distribution of *Pnmt*, *Epas1* or *Rgs5* expression within the adrenal medulla, suggesting that developmental HIF-2α activity is required to establish the immature chromaffin cell gene expression profile.

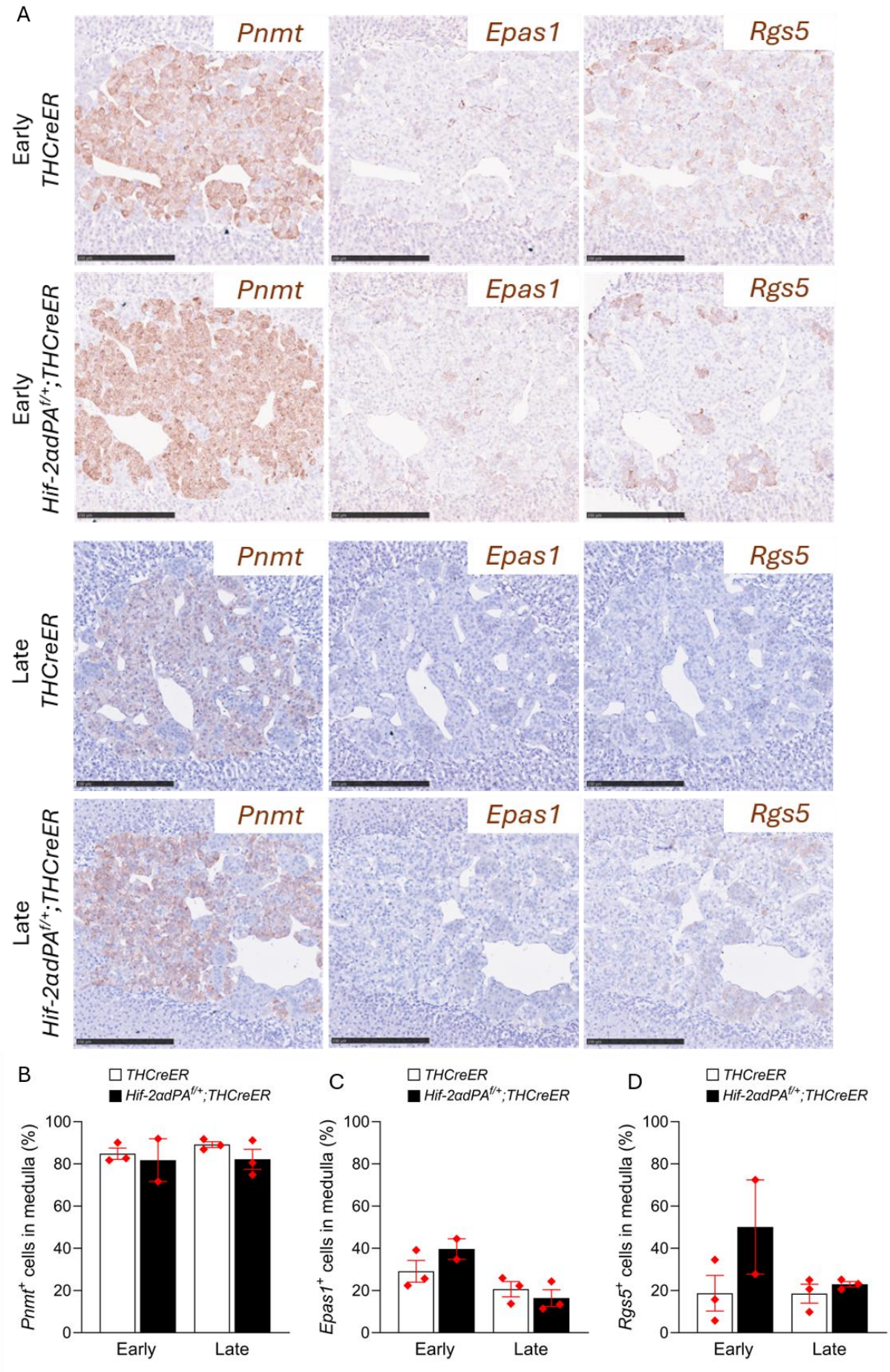
A
Pnmt
Epas1
Rgs5
Early THCreER
Early Hif-2αdPA^f/+;THCreER
Late THCreER
Late Hif-2αdPA^f/+;THCreER
B
C
D
THCreER
Hif-2αdPA^f/+;THCreER
Pnmt+ cells in medulla (%)
Epas1+ cells in medulla (%)
Rgs5+ cells in medulla (%)
0
20
40
60
80
100
Early
Late

Figure 3.5. Adult-onset HIF-2α stabilisation does alter gene expression in the adrenal medulla. **(A)** *Pnmt*, *Epas1* and *Rgs5* mRNA signal (brown) in the adrenal medulla from adjacent sections from control (*THCreER*) and adult-onset *Hif-2αdPA* (*Hif-2αdPA$^{f/+}$;THCreER*) mice harvested at the early and late timepoints following tamoxifen administration. Scale bars = 0.0.25 mm, n = 3 mice of each genotype. Quantification of the percentage of cells within the medulla expressing *Pnmt* **(B)**, *Epas1* **(C)** and *Rgs5* **(D)**. Data are presented as mean ± SEM and were analysed by one-way ANOVA with Šídák's multiple comparisons test, no statistically significant differences were observed.

Consistent with the retention of an immature gene expression profile, including increased expression of the carotid body-enriched genes *Epas1* and *Rgs5*, developmental HIF-2α stabilisation causes retention of acute oxygen chemosensitivity in the adult adrenal medulla (Chapter 2). To determine whether adult-onset stabilisation of HIF-2α is sufficient to confer this property, mice expressing the genetically encoded calcium indicator GCaMP6f (encoded by *Ai95*) were used (*Hif-2αdPA$^{f/+}$;Ai95$^{f/+}$;THCreER* versus *Ai95$^{f/+}$;THCreER* controls). Adrenal slices from these mice were exposed to hypoxic solutions of graded oxygen concentrations and changes in GCaMP6f fluorescence were measured. *Ai95$^{f/+}$;THCreER* adrenal medullae showed comparable increases in fluorescence in response to high K^+ to those observed in *Ai95$^{f/+}$;THCre* medullae, confirming robust GCaMP6f expression under the control of THCreER **(Figure 2.8B and 3.6A)**. GCaMP6f expression was also widespread across the medullae (data not shown), providing evidence of effective recombination.

As observed in *Ai95$^{f/+}$;THCre* adrenal medullae, the majority of cells in *Ai95$^{f/+}$;THCreER* adrenal medullae at both the early and late timepoints post-tamoxifen administration showed no increase in fluorescence in response to solutions equilibrated at 10, 5 or 1% oxygen, and only a small increase in florescence in response to anoxia **(Figure 3.6A and B)**. A similar lack of response was observed in *Hif-2αdPA$^{f/+}$;Ai95$^{f/+}$;THCreER* adrenal medullae at both timepoints **(Figure 3.6A and B)**. Therefore, adult-onset HIF-2α stabilisation was not sufficient to confer acute oxygen chemosensitivity on the adrenal medulla, suggesting that HIF-2α

activity during development is required for persistent oxygen chemosensitivity in adult chromaffin cells.

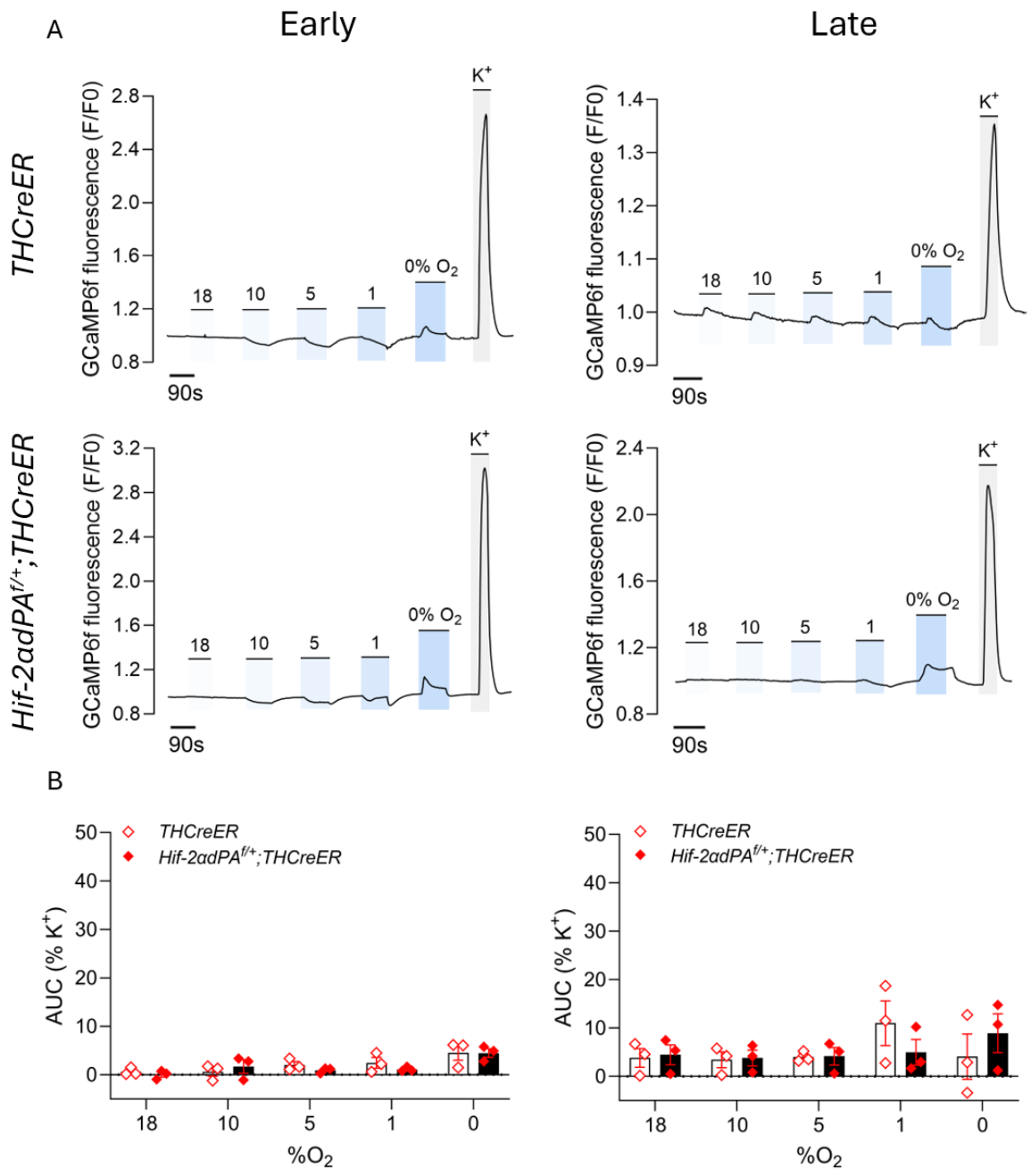

Figure 3.6. Adult-onset HIF-2α stabilisation does not confer oxygen chemosensitivity on the adrenal medulla. (A) Representative traces showing F/F_0 fluorescence in the K^+-responsive region of adrenal gland slices from control (*THCreER*) and adult-onset *Hif-2αdPA* (*Hif-2αdPA$^{f/+}$;THCreER*) mice harvested at the early and late timepoints following tamoxifen administration exposed to graded hypoxia (numbers represent % O_2) and 45mM K^+, including 18% O_2 as a sham control. **(B)** Area under

curve (AUC) graphs of each hypoxic or sham stimulus shown in (A), as a % of the AUC for K^+, n = 3 mice of each genotype.

3.2.5 *Adult-onset Hif-2αdPA does not induce re-establishment of the organ of Zuckerkandl*

Developmental stabilisation of HIF-2α also results in retention of the organ of Zuckerkandl, a major site of foetal chromaffin cells that normally regresses in mice during the first week after birth. To determine whether adult-onset HIF-2α stabilisation is sufficient to induce this foetal chromaffin cell phenotype in adulthood, immunohistochemistry for CgA and TH was performed on sections spanning the abdominal aorta from adult-onset *Hif-2αdPA* and control mice. As expected, no clusters of chromaffin cells co-expressing CgA and TH were present in control mice **(Figure 3.7).** Similarly, adult-onset *Hif-2αdPA* mice harvested at both the early and late timepoints did not possess CgA^+TH^+ chromaffin cell clusters in this region, indicating that adult-onset stabilisation of HIF-2α is not sufficient to re-establish the foetal organ of Zuckerkandl in adulthood **(Figure 3.7)**.

Together with the absence of changes in chromaffin cell gene expression and acute oxygen chemosensitivity in the adrenal medulla, these findings demonstrate that the foetal-like phenotypes observed following developmental stabilisation of HIF-2α cannot be recapitulated by adult-onset HIF-2α stabilisation, suggesting that HIF-2α must be active during development to maintain the immature chromaffin cell phenotype in adult mice.

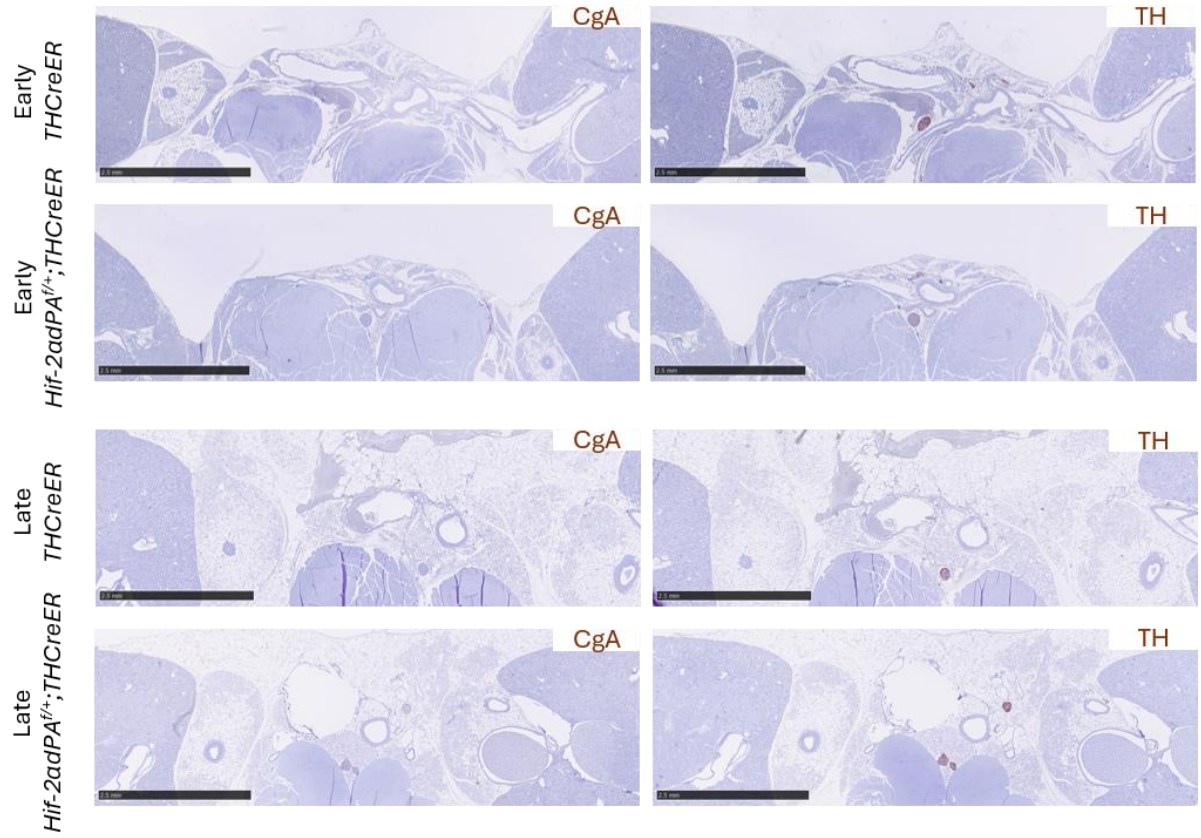

Figure 3.7. Adult-onset HIF-2α stabilisation does not induce re-establishment of the organ of Zuckerkandl. Representative images of chromogranin A (CgA) and tyrosine hydroxylase (TH) immunohistochemistry, which stain chromaffin cells, in transverse sections from the abdominal aorta region of control (*THCreER*) and adult-onset *Hif-2αdPA* (*Hif-2αdPA$^{f/+}$;THCreER*) mice harvested at the early and late timepoints following tamoxifen administration. The organ of Zuckerkandl is not present in any of these mice.

3.2.6 *Hif-2αdPA DNA binding mutant mouse model*

The *Hif-2αdPA* construct described in the previous chapter stabilises HIF-2α in TH$^+$ chromaffin cells, resulting in foetal-like, paraganglioma-like phenotypes. To determine whether these phenotypes require the transcriptional activity of HIF-2α, a modified *Hif-2αdPA* construct was generated in which residues S19-R27, encompassing part of the basic helix-loop-helix DNA binding domain, was deleted (Ming Zhang, Fraydoon Rastinejand) (**Figure 3.8A**). The resulting mHIF-2αΔ19–27 construct was co-expressed with mARNT and successfully purified

as a heterodimeric complex, with both proteins co-eluting as a defined peak during size-exclusion chromatography, indicating that deletion of this region does not substantially impair HIF-2α–ARNT heterodimer formation (performed by MZ) **(Figure 3.8B)**. HRE binding was subsequently assessed by fluorescence polarization using 6-Fam (6-carboxyfluorescein)-labelled double-stranded HRE DNA (MZ). In this assay, free DNA undergoes rapid rotational diffusion and exhibits low polarisation, whereas binding to the HIF-2α–ARNT complex slows its rotation and increases fluorescence polarisation. Wild-type HIF-2α–ARNT showed robust HRE binding, with an apparent K_d of approximately 3.5 nM, whereas the HIF-2αΔ19–27–ARNT complex showed no detectable HRE binding, comparable to the PAS-domain negative control **(Figure 3.8C)**. Together, these results demonstrate that deletion of residues S19–R27 selectively abolishes HRE recognition without disrupting HIF-2α–ARNT heterodimerization *in vitro*.

A

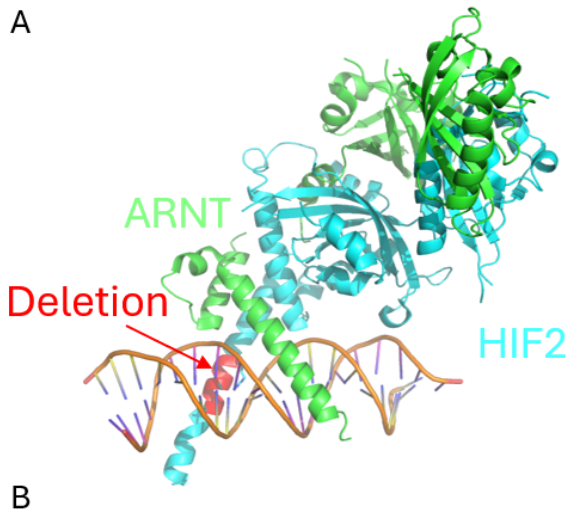
ARNT
Deletion
HIF2

B

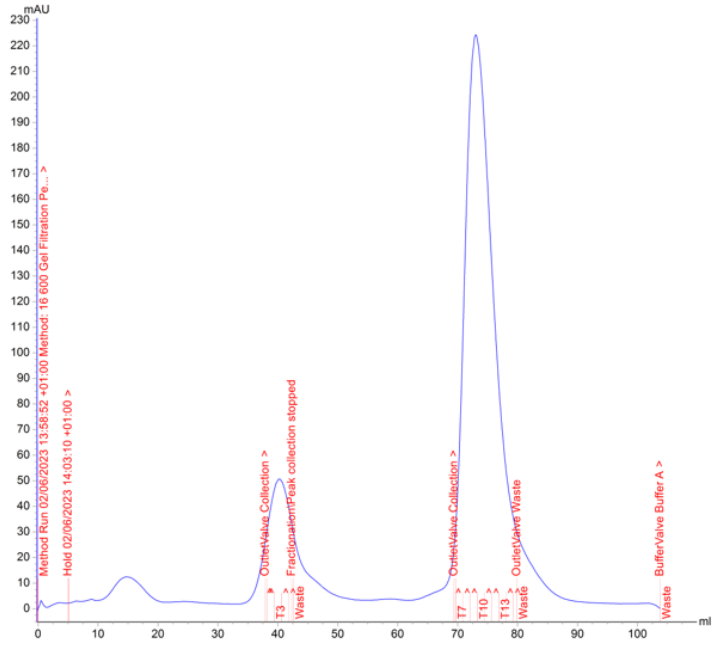
mAU
Method Run 02/06/2023 13:58:52 +01:00 Method: 16 600 Gel Filtration Pe... >
Hold 02/06/2023 14:03:10 +01:00 >
OutletValve Collection >
FractionalomPeak collection stopped
OutletValve Collection >
OutletValve Waste
BufferValve Buffer A >
T3 >
Waste
T7 >
T10 >
T13 >
Waste
Waste
ml

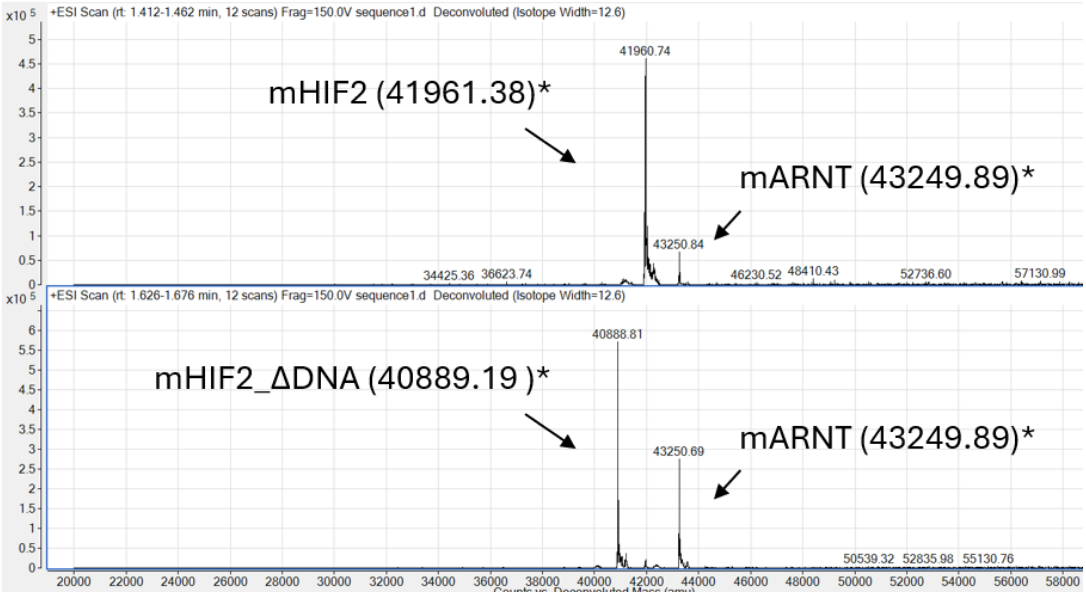
+ESI Scan (rt: 1.412-1.462 min, 12 scans) Frag=150.0V sequence1.d Deconvoluted (Isotope Width=12.6)
41960.74
mHIF2 (41961.38)*
mARNT (43249.89)*
43250.84
34425.36
36623.74
46230.52
48410.43
52736.60
57130.99
+ESI Scan (rt: 1.626-1.676 min, 12 scans) Frag=150.0V sequence1.d Deconvoluted (Isotope Width=12.6)
40888.81
mHIF2_ΔDNA (40889.19)*
mARNT (43249.89)*
43250.69
50539.32
52835.98
55130.76

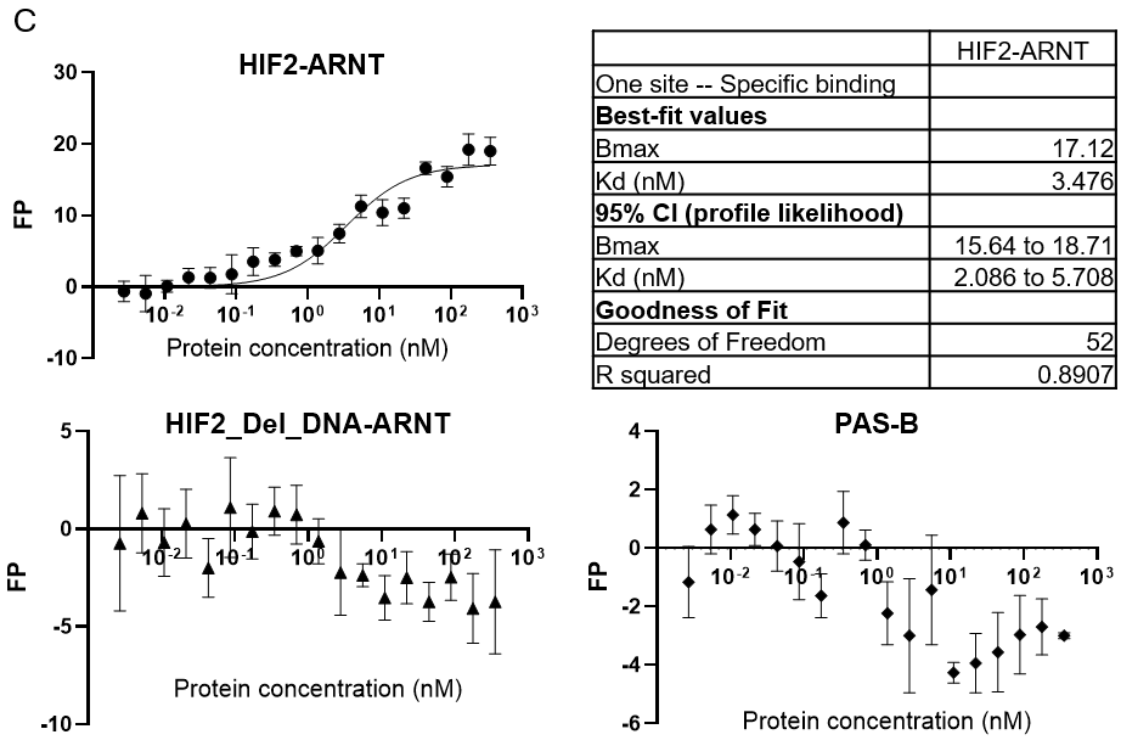

	HIF2-ARNT
One site -- Specific binding	
Best-fit values	
Bmax	17.12
Kd (nM)	3.476
95% CI (profile likelihood)	
Bmax	15.64 to 18.71
Kd (nM)	2.086 to 5.708
Goodness of Fit	
Degrees of Freedom	52
R squared	0.8907

Figure 3.8. *Hif-2αdPA* DNA binding mutant construct. (A) Structural representation of the HIF-2α protein (blue) bound to ARNT (green) interacting with a DNA molecule. The region of the HIF-2α protein which is deleted in the *Hif-2αdPA* DNA binding mutant construct (S19-R27) is shown in red. **(B)** Size-exclusion chromatography (SEC) (top) and intact mass analysis (bottom) of the HIF-2α Δ19–27–ARNT complex. HIF-2αΔ19–27 and ARNT co-eluted in a single SEC peak (a smaller, earlier peak at ~40 mL lies in the void region). Intact mass spectra of wild-type HIF-2α–ARNT and HIF-2αΔ19–27–ARNT showed peaks corresponding to the expected molecular masses of HIF-2α, HIF-2α Δ19–27 and ARNT. **(C)** Fluorescence polarization analysis of wild-type HIF-2α–ARNT, HIF-2α Δ19–27–ARNT and the PAS-domain negative control binding to 6-FAM-labelled double-stranded HRE DNA. The fitted binding curve for wild-type HIF-2α–ARNT gave an apparent K_d of approximately 3.5 nM, while no detectable binding was observed for HIF-2αΔ19–27–ARNT or the PAS-domain control. These experiments and analyses were performed by MZ.

Mice were engineered to express this mutated *Hif-2αdPA* construct under the control of the Rosa26 promoter and preceded by a lox-stop-lox sequence (R26-LSL-Hif-2αdPA DNA binding mutant). This prevents expression of the construct in cells unless Cre recombinase is also present to excise the STOP codon, allowing tissue-specific induction. These mice were crossed with THCre mice to generate offspring with stable expression of transcriptionally inactive *Hif-*

2αdPA in TH^+ chromaffin tissues, known as *Hif-2αdPA DNA binding mutant*$^{f/+}$*;THCre* (hereafter referred to as *Hif-2αdPA* DNA binding mutant) mice (**Figure 3.9**). Comparison of these mice with wild-type and transcriptionally active *Hif-2αdPA* (R26-LSL-*Hif-2αdPA*$^{f/+}$*;THCre*) mice enabled investigation of whether the carotid body and chromaffin cell phenotypes described previously in the *Hif-2αdPA* mice (Chapter 2) require the DNA binding domain of HIF-2α to be intact, thereby determining the extent to which HIF-2α transcriptional activity contributes to these phenotypes.

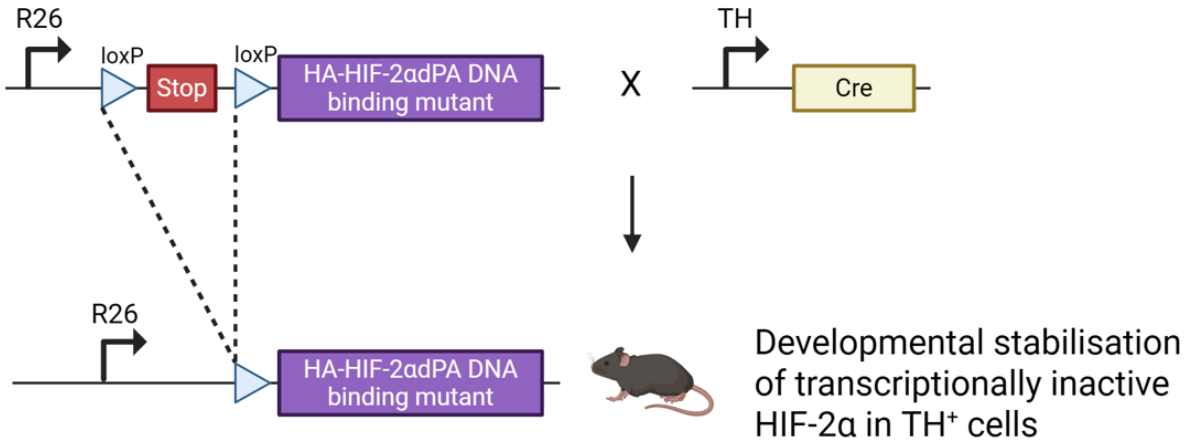

Figure 3.9. *Hif-2αdPA* DNA binding mutant mice. Mice expressing the *Hif-2αdPA* DNA binding mutant construct at the Rosa26 (R26) locus preceded by a lox-stop-lox sequence, with loxP sites represented by arrowheads, were crossed with mice expressing Cre recombinase under the tyrosine hydroxylase (TH) promoter. Cre-mediated excision of the stop sequence in TH^+ cells of mice expressing both alleles results in developmental stabilisation of transcriptionally inactive HIF-2α in these cells. The *Hif-2dPA* DNA binding mutant construct contains a hemagglutinin (HA) tag at the N terminus. Figure generated with biorender.com.

3.2.7 *Confirmation of Hif-2αdPA DNA binding mutant construct expression in the adrenal medulla*

To determine whether the HIF-2α DNA binding mutant construct was expressed at a comparable level to the transcriptionally competent *Hif-2αdPA* construct used in Chapter 2,

protein expression was assessed in chromaffin tissue. Like the *Hif-1αdPA* and *Hif-2αdPA* constructs described previously, the *Hif-2αdPA* DNA binding mutant construct contains an N-terminal HA tag, providing a construct-specific marker of protein expression. Due to the small size of the carotid body, insufficient tissue could be obtained for reliable immunoblotting. Instead, adrenal medullae were used as a source of chromaffin tissue. Immunoblotting for HA was performed on adrenal medullae from three mice of each genotype: *Hif-2αdPA* DNA binding mutant, *Hif-2αdPA* and wild-type. HA protein was detected in the adrenal medullae from both *Hif-2αdPA* and *Hif-2αdPA* DNA binding mutant mice, but not in wild-type controls **(Figure 3.10A)**. The HA-positive bands migrated at approximately 120 kDA, consistent with the expected weight of the HIF-2α constructs with post-translational modifications(W. Y. Kim et al., 2006). The band intensities appeared broadly comparable between the *Hif-2αdPA* and *Hif-2αdPA* DNA binding mutant samples, although one *Hif-2αdPA* DNA binding mutant sample showed stronger HA signal. This suggests that the *Hif-2αdPA* DNA binding mutant construct is expressed at a similar level to *Hif-2αdPA*.

Immunohistochemistry was used to assess HIF-2α expression in the carotid body and adrenal medulla **(Figure 3.10B)**. In wild-type mice, glomus cells in the carotid body showed relatively little intense nuclear HIF-2α staining (brown) beyond the diffuse background staining characteristic of the antibody used (PM8). In contrast, intense nuclear HIF-2α staining was evident in the majority of carotid body glomus cells from both *Hif-2αdPA* and *Hif-2αdPA* DNA binding mutant mice. Similarly, HIF-2α staining was weak or absent in the nuclei of adrenal medullary chromaffin cells from wild-type mice, with only faint, diffuse background staining observed **(Figure 3.10B)**. In contrast, strong nuclear HIF-2α staining was observed in the adrenal medullae of *Hif-2αdPA* mice and nuclear HIF-2α staining was detected in the adrenal medulla of *Hif-2αdPA* DNA binding mutant mice. Although the nuclear staining appeared less intense in the *Hif-2αdPA* DNA binding mutant adrenal medulla than in the *Hif-2αdPA* adrenal

medulla, overall background staining was also reduced in the mutant tissue. Therefore, this difference may reflect technical variation between samples, such as differences in DAB development time, rather than reduced HIF-2α expression.

Together, the HA immunoblot and HIF-2α immunohistochemistry confirm stable nuclear expression of HIF-2α in neuroendocrine tissues of *Hif-2αdPA* DNA binding mutant mice at a level broadly comparable to the transcriptionally competent *Hif-2αdPA* construct. Therefore, comparison between mice expressing these constructs provides a model in which the contribution of the DNA binding domain of HIF-2α, and consequently HIF-2α-dependent transcription, to the carotid body and chromaffin cell phenotypes can be assessed.

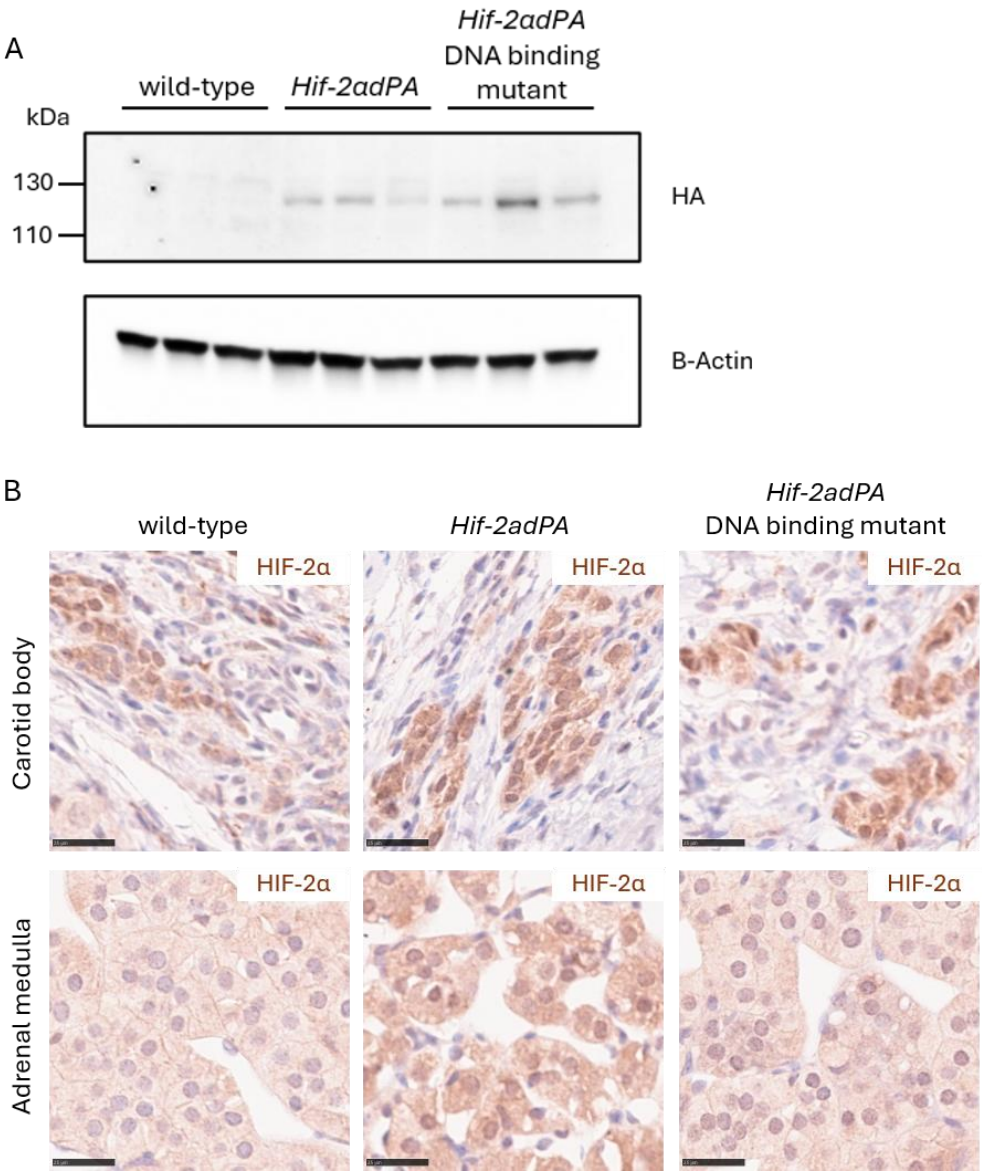

Figure 3.10. HIF-2α protein stabilisation in chromaffin tissues of wild-type versus *Hif-2αdPA* versus *Hif-2αdPA* DNA binding mutant mice. (A) Immunoblot for hemagglutinin (HA) or β-actin confirming HA-tagged *Hif-2αdPA* transgene expression in the adrenal medulla from *Hif-2αdPA* and *Hif-2αdPA* DNA binding mutant, but not wild-type, mice (n = 3 mice per genotype, with one mouse per lane). **(B)** HIF-2α immunohistochemistry showing nuclear HIF-2α protein (brown) stabilisation in the carotid body and adrenal medulla of *Hif-2αdPA* and *Hif-2αdPA* DNA binding mutant, but not wild-type, adult mice. Scale bars represent 0.025 mm.

3.2.8 *Reversion of carotid body hyperplasia and the enhanced hypoxic ventilatory response in Hif-2αdPA DNA binding mutant mice*

Developmental stabilisation of HIF-2α through expression of the *Hif-2αdPA* construct causes an increase in carotid body volume (Chapter 2). To determine whether this hyperplastic phenotype requires the transcriptional activity of HIF-2α, carotid bodies from *Hif-2αdPA* DNA binding mutant mice were examined. Immunohistochemistry for CgA and TH was performed on sections spanning the carotid bifurcation. As discussed earlier, TH is also expressed in the surrounding sympathetic ganglia, whereas CgA staining more specifically marks the carotid body. Therefore, the area of CgA^+ tissue was quantified to estimate carotid body volume. Consistent with the findings described in Chapter 2, carotid bodies from *Hif-2αdPA* mice were larger than those from age- and sex-matched wild-type controls, with a 3.5-fold increase in estimated volume **(Figure 3.11A and B)**. In contrast, carotid bodies from *Hif-2αdPA* DNA binding mutant mice only exhibited a modest 1.7-fold increase in estimated volume compared with wild-type mice **(Figure 3.11A and B)**. Therefore, preventing HIF-2α DNA binding largely reversed the carotid body hyperplasia observed following developmental HIF-2α stabilisation, suggesting that HIF-2α-dependent transcription is required for the majority of this phenotype.

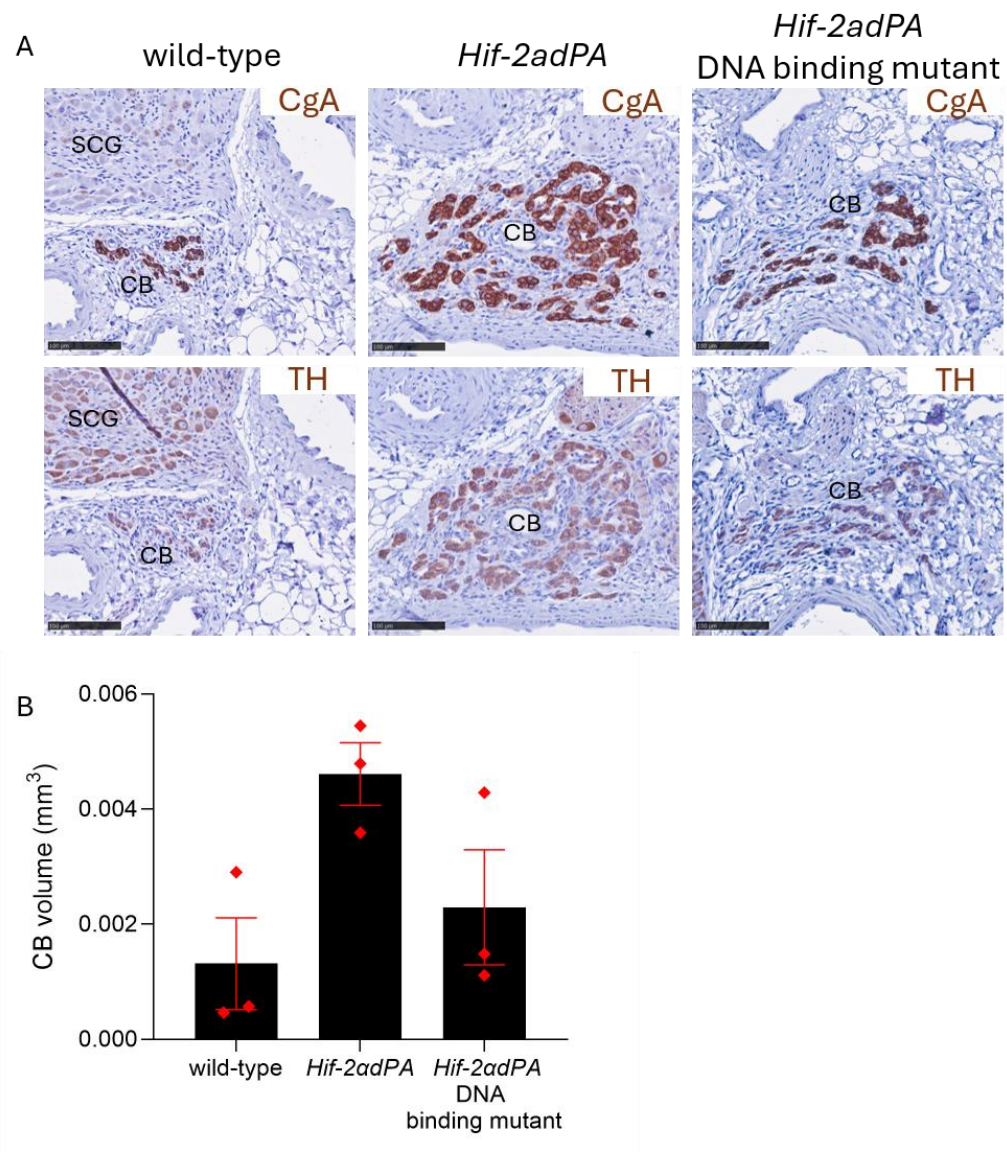

Figure 3.11. HIF-2α DNA binding is necessary for the enlarged carotid bodies seen in *Hif-2αdPA* mice. (A) Representative images of chromogranin A (CgA) and tyrosine hydroxylase (TH) immunohistochemistry in carotid body sections from wild-type, *Hif-2αdPA* and *Hif-2αdPA* DNA binding mutant mice. Scale bars = 0.1 mm. CB = carotid body, SCG = superior cervical ganglion. **(B)** Volume quantification of carotid bodies from wild-type, *Hif-2αdPA* and *Hif-2αdPA* DNA binding mutant mice. Data are presented as mean ± SEM and were analysed by one-way ANOVA with Tukey's multiple comparisons test, differences were not statistically significant.

Developmental stabilisation of HIF-2α also alters carotid body function, with *Hif-2αdPA* mice exhibiting an enhanced ventilatory response to acute hypoxic exposure compared with wild-type controls, in line with their increased carotid body size. To determine whether the DNA

binding domain of HIF-2α is required for this enhanced HVR, ventilatory responses to acute hypoxia were assessed by plethysmography **(Figure 3.12A and B)**. Consistent with the findings presented in Chapter 2, female *Hif-2αdPA* mice showed a trend towards increased HVR to 10% O_2/3% CO_2 compared with wild-type mice, although the difference did not reach statistical significance in this dataset **(Figure 3.12A)**. Male *Hif-2αdPA* mice similarly exhibited a small, but insignificant, increase in ventilatory response to 10% O_2/3% CO_2 compared to wild-type mice **(Figure 3.12A)**. In contrast, neither female nor male *Hif-2αdPA* DNA binding mutant differed from wild-type controls in their ventilatory response to 10% O_2/3% CO_2 **(Figure 3.12A)**. No differences were observed in the acute ventilatory responses to 10% O_2 or 3% CO_2 alone between male or female mice of any genotype **(Figure 3.12B)**. Therefore, these findings suggest that an intact DNA binding domain, and thus the transcriptional activity of HIF-2α, is required for the enhanced HVR associated with developmental HIF-2α stabilisation. Together with the observed effects on carotid body volume, this supports a role for HIF-2α-dependent transcription in both the structural and functional carotid body phenotypes in *Hif-2αdPA* mice.

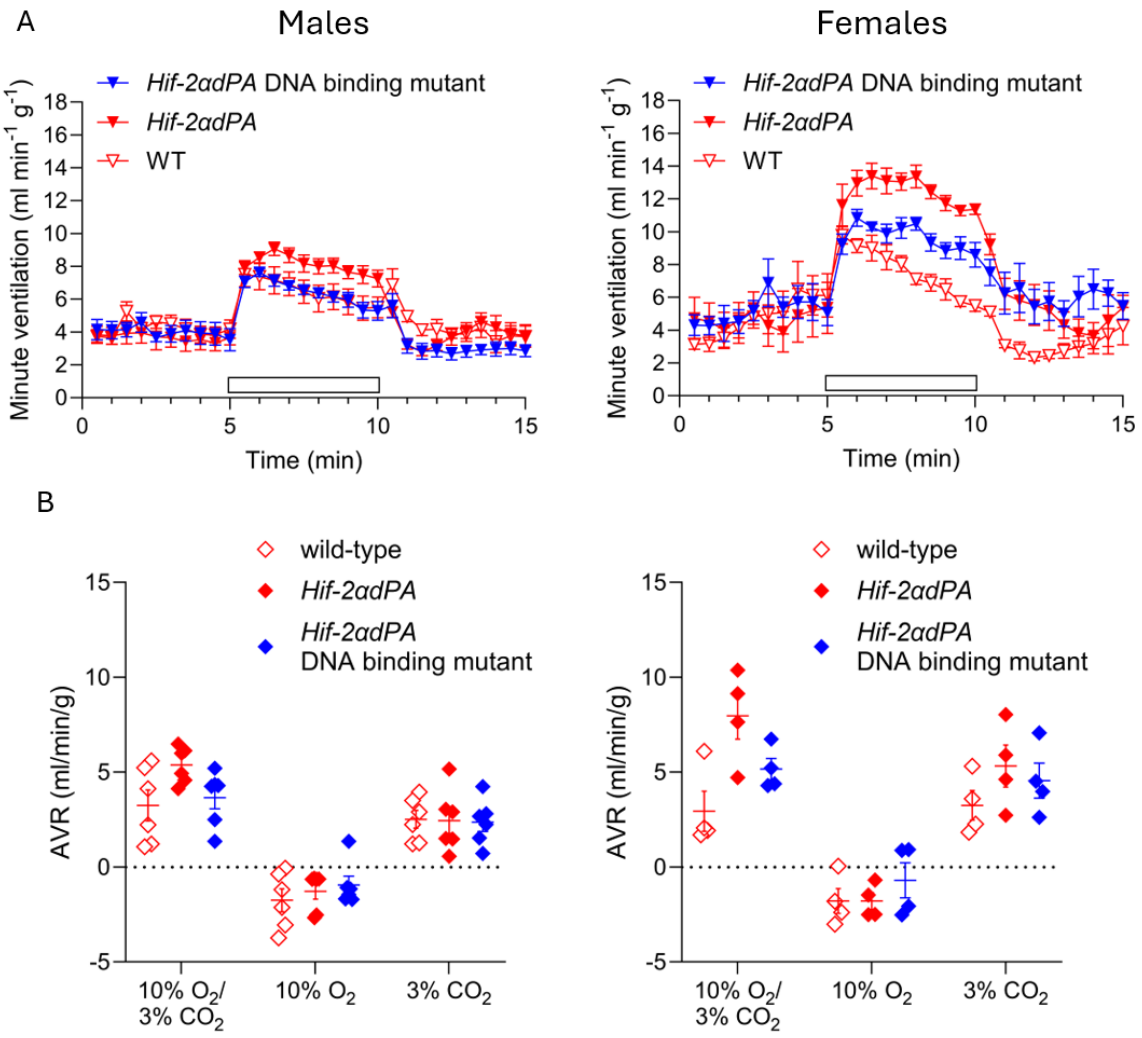

Figure 3.12. *Hif-2αdPA* DNA binding mutant mice do not have an enhanced hypoxic ventilatory response to 10% O_2/3% CO_2. (A) Ventilatory responses to 5 minutes of 10% O_2/3% CO_2 (white bars) in male and female mice, n = 4 females and 6 males of each genotype. **(B)** AVRs to each hypoxic stimuli. Data were compared between genotypes for each hypoxic stimuli by Holm-Sidak's multiple comparisons tests, no differences were statistically significant.

3.2.9 *Reversion of the switch towards immature gene expression and retention of oxygen chemosensitivity in Hif-2αdPA DNA binding mutant mice*

During development, wild-type adrenal medullae acquire expression of *Pnmt*, the enzyme that converts noradrenaline to adrenaline, and lose their ability to directly sense acute hypoxia (Prange-Barczynska et al., 2024; Thompson et al., 1997). As demonstrated in Chapter 2,

developmental stabilisation of HIF-2α causes retention of this immature chromaffin cell state; adult *Hif-2αdPA* mice have a primarily noradrenergic (*Pnmt*$^{-}$) gene expression profile in the adult adrenal medulla, with increased expression of the carotid body-enriched genes *Epas1* and *Rgs5*, as well as retained oxygen chemosensitivity. Therefore, gene expression in the *Hif-2αdPA* DNA binding mutant adrenal medulla was investigated to assess whether the transcriptional activity of HIF-2α plays a role in the retention of these immature chromaffin cell phenotypes.

In situ hybridisation for *Pnmt*, *Epas1* and *Rgs5* showed that the majority of chromaffin cells in the *Hif-2αdPA* DNA binding mutant adrenal medulla express *Pnmt* but do not express *Epas1* or *Rgs5* **(Figure 3.13)**, similar to adrenal medullae from wild-type mice. This confirms that the transcriptional activity of HIF-2α is necessary for the retention of an immature gene expression profile in the adult *Hif-2αdPA* adrenal medulla described in Chapter 2. Lack of upregulation of the HIF-2α target gene *Rgs5* also provides evidence that the *Hif-2αdPA* DNA binding mutant construct successfully blocks the transcriptional activity of the overexpressed HIF-2α.

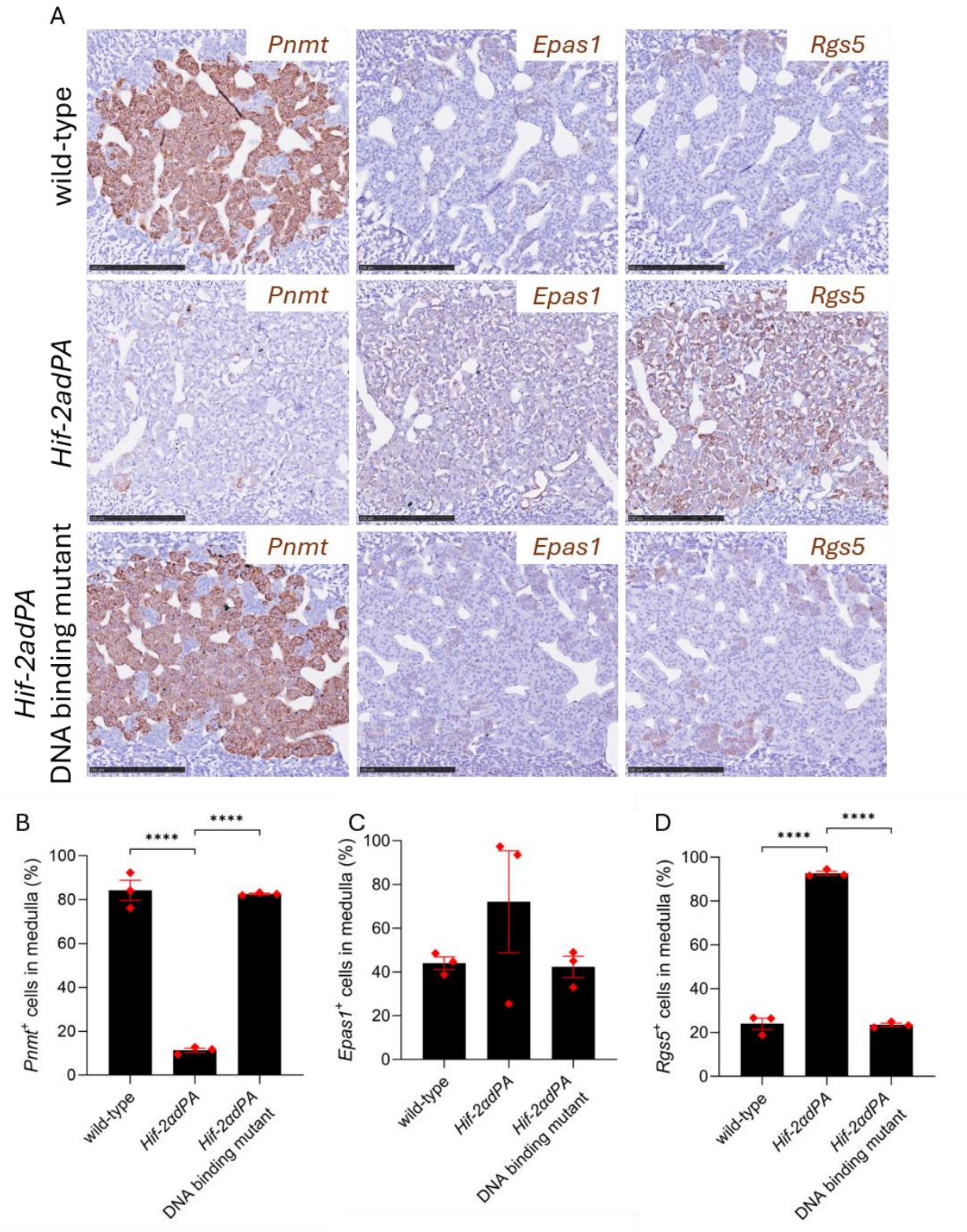

Figure 3.13. The transcriptional activity of HIF-2α is necessary for the gene expression switch seen in the *Hif-2αdPA* adrenal medulla. (A) *Pnmt*, *Epas1* and *Rgs5* mRNA signal (brown) in the adrenal medulla from adjacent sections of adult wild-type, *Hif-2αdPA* and *Hif-2αdPA* DNA binding mutant adrenal glands. The majority of chromaffin cells in the wild-type and *Hif-2αdPA* DNA binding

mutant adrenal medulla are *Pnmt*$^{+}$*/Epas1*$^{-}$*/Rgs5*$^{-}$, whereas the *Hif-2αdPA* adrenal medulla has a majority *Pnmt*$^{-}$*/Epas1*$^{+}$*/Rgs5*$^{+}$ cell population. Scale bars = 0.25 mm, n = 3 mice of each genotype. Quantification of the percentage of cells within the medulla expressing *Pnmt* **(B)**, *Epas1* **(C)** and *Rgs5* **(D)**. Data are presented as mean ± SEM and were analysed by one-way ANOVA with Tukey's multiple comparisons test, **** $p < 0.0001$.

The upregulation of the carotid body-enriched genes *Epas1* and *Rgs5* in the adult *Hif-2αdPA* adrenal medulla is associated with the retention of acute oxygen chemosensitivity, a property which is almost completely lost postnatally in the adrenal medulla of wild-type mice (Chapter 2) (Prange-Barczynska et al., 2024; Thompson et al., 1997). To assess whether the transcriptional activity of HIF-2α is necessary for oxygen sensing, adrenal slices from mice expressing both the *Hif-2αdPA* DNA binding mutant construct and the genetically encoded calcium indicator GCaMP6f, were tested in the perfusion setup described earlier. Consistent with the findings in Chapter 2, adrenal medullae from wild-type mice exhibited increases in florescence to 45 mM K^{+}, which acts as a positive control for cell excitability, but did not respond to acute hypoxic stimuli (10, 5 and 1% O_2, small responses to anoxia were seen), whereas mice expressing *Hif-2αdPA* reproducibly showed rapid, graded increases in florescence in response to decreasing oxygen tensions, demonstrating their ability to respond to acute hypoxia **(Figure 3.14A and B)**. In contrast, adrenal medullae from *Hif-2αdPA* DNA binding mutant mice expressing GCaMP6f did not show any increases in florescence to acute hypoxic stimuli, suggesting that HIF-2α likely needs to be transcriptionally active in order to confer retention of acute oxygen chemosensitivity in the adult adrenal medulla of pseudohypoxic mice.

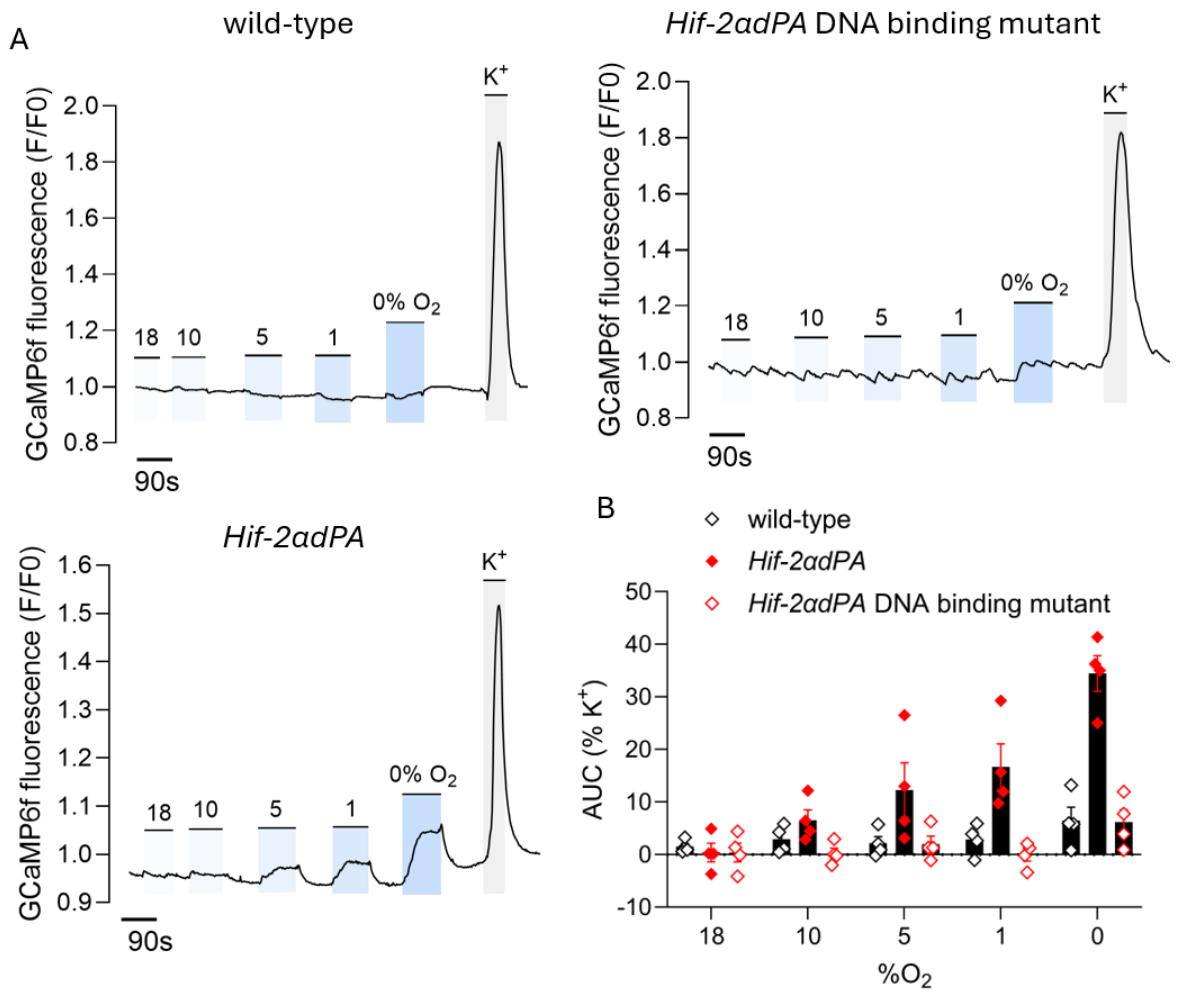

Figure 3.14. HIF-2α DNA binding is necessary for acute oxygen chemosensitivity in the *Hif-2αdPA* adult adrenal medulla. (A) Representative traces showing F/F_0 fluorescence in the K^+-responsive region of wild-type, *Hif-2αdPA* and *Hif-2αdPA* DNA binding mutant adrenal gland slices exposed to graded hypoxia (numbers represent % O_2) and 45mM K^+, including 18% O_2 as a sham control. **(B)** Area under curve (AUC) graphs of each hypoxic or sham stimulus shown in (A), as a % of the AUC for K^+, n = 3 mice of each genotype.

3.2.10 *Hif-2αdPA DNA binding mutant mice do not retain the organ of Zuckerkandl into adulthood*

In addition to an immature gene expression profile and retention of acute oxygen chemosensitivity in the adult adrenal medulla, *Hif-2αdPA* mice also retain an oxygen-chemosensitive organ of Zuckerkandl into adulthood (Chapter 2). To determine whether this

phenotype requires HIF-2α DNA binding, the abdominal aorta region from adult *Hif-2αdPA* DNA binding mutant mice was dissected and immunohistochemistry for CgA and TH was performed on sections spanning this region. Like adult wild-type mice, these mice did not retain any $CgA^{+}TH^{+}$ chromaffin cell structures in the abdominal aorta region **(Figure 3.15)**, indicating that HIF-2α DNA binding is required for retention of the foetal organ of Zuckerkandl following developmental HIF-2α stabilisation.

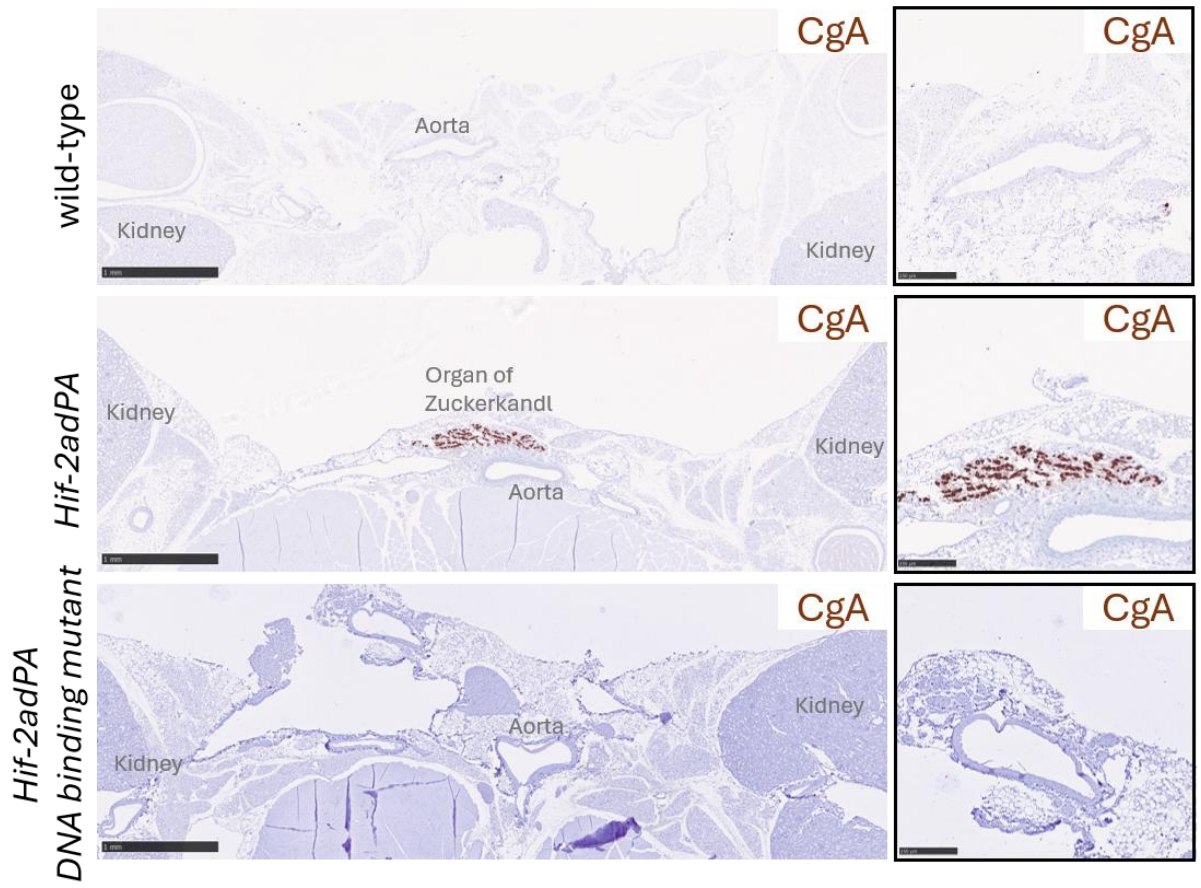

Figure 3.15. HIF-2α DNA binding is necessary for retention of the organ of Zuckerkandl in adult *Hif-2αdPA* mice. Representative images of CgA immunohistochemistry, which stains chromaffin cells, in transverse sections from the abdominal aorta region of adult wild-type, *Hif-2αdPA* and *Hif-2αdPA* DNA binding mutant mice. The organ of Zuckerkandl is present in *Hif-2αdPA* mice, but not in wild-type or *Hif-2αdPA* DNA binding mutant mice.

Together with the findings for carotid body morphology, HVR, chromaffin cell gene expression and oxygen chemosensitivity, these results suggest that the glomus and chromaffin cell phenotypes induced by developmental HIF-2α stabilisation require its transcriptional activity. Therefore, HIF-2α-dependent transcription is required not only for changes in cell-specific gene expression, but also for the associated changes in tissue morphology and retention of acute oxygen chemosensitivity.

3.3 **Discussion**

This chapter investigated the mechanisms by which stabilisation of HIF-2α confers foetal-like, paraganglioma-like neuroendocrine cell phenotypes. In particular, two questions were explored: (1) whether HIF-2α activity must occur during development to establish these phenotypes, and (2) whether the canonical transcriptional activity of HIF-2α is required, or whether other mechanisms may also contribute. Adult-onset stabilisation of HIF-2α did not reproduce the foetal-like, paraganglioma-like neuroendocrine phenotypes induced by developmental HIF-2α stabilisation. Developmental stabilisation of transcriptionally inactive HIF-2α also failed to recapitulate these phenotypes. Together, these findings suggest that HIF-2α acts during development to establish a neuroendocrine cell state associated with persistent oxygen chemosensitivity in chromaffin cells, and that this effect requires its ability to regulate gene transcription.

The finding that HIF-2α stabilisation during development, but not in adulthood, produced foetal-like, paraganglioma-like neuroendocrine phenotypes in adult mice indicates that these phenotypes are influenced by developmental HIF-α activity. This is consistent with several lines of evidence implicating developmental HIF-α activity in pseudohypoxic pheochromocytoma and paraganglioma. In these tumours, mutations affecting HIF signalling

are frequently inherited through the germline (Dahia, 2014; Favier et al., 2015). Likewise, somatic *EPAS1* mutations arise during early development (Buffet et al., 2014; Welander, Andreasson, Juhlin, et al., 2014; Z. Zhuang et al., 2012), raising the possibility that the consequences of HIF pathway dysregulation may depend on the developmental timing of HIF-2α activation within the affected cell. Further support comes from patients with chronic hypoxemia associated with cyanotic congenital heart disease (CCHD), who have an increased risk of pheochromocytoma and paraganglioma (Opotowsky et al., 2015). The phenotype of these tumours varies according to when hypoxaemia begins; recent clinical data showed that patients with CCHD who experienced hypoxaemia from birth predominantly developed sympathetic, catecholamine-secreting tumours, whereas those who did not experience hypoxaemia until childhood or early adulthood more frequently developed parasympathetic carotid body tumours (Arenillas et al., 2025). These findings are consistent with an early developmental period during which hypoxia signalling pathways may exert distinct effects on susceptible sympathetic cells.

Experimental models further support a role for HIF-2α in establishing neuroendocrine cell identity during development. Developmental HIF-2α stabilisation causes chromaffin cells to retain characteristics of the immature or foetal state that are normally lost during maturation, including reduced *Pnmt* expression, retention of the organ of Zuckerkandl and oxygen chemosensitivity (Coupland, 1965; Thompson et al., 1997). Conversely, adult-onset inactivation of *Phd2* does not reproduce the retention of an immature gene expression profile in the adrenal medulla, despite retaining the capacity to induce HIF-2α target genes such as *Rgs5* and *Vegfa* (Eckardt et al., 2021). Consistent with these observations, this chapter demonstrates that the developmental timing of HIF-2α stabilisation is critical for inducing foetal-like, paraganglioma-like neuroendocrine phenotypes. Together, these findings support a model in which HIF-2α activity during development programmes neuroendocrine cells to

retain an immature state, establishing a cellular context that persists into adulthood and potentially increases susceptibility to pseudohypoxic pheochromocytoma and paraganglioma. This raises the possibility that defining the developmental processes underlying this susceptibility, particularly in individuals with inherited predisposition, could ultimately inform approaches to earlier intervention or prevention.

Although the absence of neuroendocrine cell phenotypes following adult-onset HIF-2α stabilisation supports a requirement for developmental HIF-2α activity, a number of caveats of the adult-onset *HIF-2αdPA* model must be considered. First, recombination efficiency between the *HIF-2αdPA$^{f/+}$;THCre* and *HIF-2αdPA$^{f/+}$;THCreER* models was not directly compared. This comparison would be useful to determine whether differences in the extent of *HIF-2αdPA* expression contributed to differences in the phenotype between the models, and therefore to establish more directly whether comparable HIF-2α stabilisation had been achieved. However, HIF-2α immunohistochemistry in the adult-onset *HIF-2αdPA* adrenal medulla indicated substantial and widespread HIF-2α stabilisation following tamoxifen treatment. Furthermore, the GCaMP6f-expressing mice provide an indication of recombination efficiency, as GCaMP6f expression is driven by the same tamoxifen-inducible THCreER system used to activate *HIF-2αdPA*. The widespread expression of GCaMP6f throughout the adrenal medulla therefore provides additional evidence that recombination occurred efficiently in the adult-onset *HIF-2αdPA* model.

A second consideration is that adult-onset *THCreER*-mediated recombination will stabilise HIF-2α only in cells expressing TH at the time of tamoxifen administration. This population may not be identical to the population of cells that expressed TH during development, as some cells may transiently express TH during earlier stages of development and subsequently downregulate it. Consequently, the developmental THCre model may stabilise HIF-2α in a

wider population of cells than the adult-onset THCreER model, and these additional cells could contribute to the phenotypes observed following developmental HIF-2α stabilisation. This possibility could be addressed using a lineage tracing strategy, such as a Cre-dependent tdTomato reporter in the developmental and adult-onset models. Direct comparison of the labelled cells would establish whether the HIF-2α is stabilised in the same neuroendocrine cell populations in both models. If the populations overlap, this would provide stronger evidence that the developmental timing of HIF-2α stabilisation is responsible for the neuroendocrine cell phenotypes, whereas if the developmental model labels a substantially broader cell population, differences in cellular targeting would need to be considered as an alternative explanation for the lack of neuroendocrine cell phenotypes in the adult-onset *Hif-2αdPA* mice.

The second mechanistic question investigated in this chapter was whether HIF-2α may contribute to the foetal-like, paraganglioma-like neuroendocrine phenotypes through mechanisms that extend beyond its canonical activity as a transcription factor. Several observations suggested that this possibility should be considered. First, *Epas1* is highly expressed in the carotid body relative to its dimerisation partners *Arnt* and *Arnt2* (Gao, Bonilla-Henao, et al., 2017; Zhou et al., 2016). If HIF-2α activity in the carotid body depends exclusively on forming transcriptionally active complexes with ARNT/ARNT2, it might be expected that the expression of these components would be more closely matched. Second, combined genetic inactivation of *Arnt*/*Arnt2* in mice produced milder ventilatory, carotid body proliferative and hematopoietic adaptations to hypoxia compared with equivalent *Epas1* inactivation (MPB, TB, PJR, unpublished observations). If all HIF-2α phenotypes were mediated through ARNT/ARNT2-dependent transcription, loss of both dimerisation partners might be expected to phenocopy *Epas1* loss more closely. Finally, mice carrying the S305M mutation in the HIF-2α PAS-B domain exhibit a hypomorphic ventilatory response despite retaining HIF-2α expression, stability and its ability to heterodimerise with HIF-2β (Cheng et

al., 2020), suggesting that HIF-2α may influence physiological responses through properties beyond heterodimerisation and transcriptional regulation. Together, these findings raised the possibility that HIF-2α functions may not be fully explained by canonical DNA-dependent transcription, providing a rationale for testing whether non-transcriptional functions of HIF-2α contribute to the developmental neuroendocrine phenotype. However, the findings presented in this chapter indicate that HIF-2α transcriptional activity is required for the neuroendocrine phenotypes examined here. Loss of transcriptional activity in the *Hif-2αdPA* construct prevented the development of the foetal-like and paraganglioma-like glomus and chromaffin cell phenotypes, indicating that these developmental effects of HIF-2α depend on its ability to regulate gene expression.

However, as with the adult-onset *Hif-2αdPA* model, given the absence of neuroendocrine phenotypes in mice expressing the transcriptionally inactive *HIF-2αdPA* construct, it is important to consider caveats associated with this model. The mutation introduced into the DNA binding domain of the *HIF-2αdPA* construct may have altered HIF-2α function in addition to its ability to bind HREs. For example, the mutation could potentially reduce HIF-2α protein stability, or alter its subcellular localisation, protein conformation or interactions with other proteins compared with the transcriptionally competent *HIF-2αdPA* construct. Any of these effects could potentially prevent the mutant HIF-2α protein from reproducing the neuroendocrine phenotypes, independent of the effect on DNA binding. However, comparable levels of HIF-2α protein were observed by both HIF-2α immunohistochemistry and immunoblotting for the HA tag on the construct, arguing against substantially reduced protein stability as an explanation for the phenotype. Furthermore, the nuclear localisation of HIF-2α observed by immunohistochemistry provides evidence that the transcriptionally inactive protein reaches the cellular compartment in which HIF-2 regulates gene expression, suggesting that altered localisation is also an unlikely explanation for the absence of the phenotype.

However, these experiments cannot completely exclude more subtle effects of the DNA binding mutation on HIF-2α protein structure or protein-protein interactions. Further experiments, such as complementary genetic approaches targeting HIF-2α transcriptional activity, or analysis of the recruitment of HIF-2α and associated transcriptional machinery to target loci, could help distinguish loss of DNA binding from other consequences of the mutation. Nevertheless, the available evidence supports a requirement for HIF-2α transcriptional activity in the foetal-like, paraganglioma-like neuroendocrine phenotypes, whilst acknowledging that the model cannot completely exclude additional effects of the DNA binding mutation. This provides a rationale for identifying the downstream transcriptional programmes that underlie these phenotypes.

Previous bulk RNA sequencing of carotid bodies and adrenal medullae from mice with developmental *Phd2* inactivation (*Phd2ko*) provides evidence for several candidate pathways underlying the retention of oxygen chemosensitivity in the *Phd2ko* adrenal medulla (Prange-Barczynska et al., 2024). The majority of genes upregulated following *Phd2* inactivation in the adrenal medulla were expressed at higher levels in the carotid body than in the wild-type adrenal medulla, indicating that HIF pathway activation shifts the transcriptional profile of chromaffin cells towards that of carotid body cells. These included genes involved in mitochondrial energy metabolism, such as *Cox4i2* and *Ndufa4l2*, which encode atypical components of the cytochrome c oxidase complex that may influence mitochondrial responses to oxygen availability, as well as genes involved in G protein signalling that have also been implicated in pathways that modulate oxygen chemosensitivity, such as *Rgs5* (Prange-Barczynska et al., 2024). Because the carotid body is a specialised oxygen sensor, upregulation of these carotid body-enriched genes provides candidate genes and pathways that may contribute to oxygen chemosensitivity in chromaffin cells. However, the *Hif-2αdPA* model provides a more direct system for investigating HIF-2α-dependent transcription because HIF-2α is selectively stabilised, whereas *Phd2* inactivation may have broader effects on HIF-

dependent and HIF-independent pathways. In particular, *Phd2* inactivation also leads to stabilisation of HIF-1α, meaning that transcriptional changes observed in the *Phd2ko* model cannot be attributed specifically to HIF-2α.

Furthermore, interpreting transcriptional changes in the adrenal medulla is complicated by its cellular heterogeneity. The adrenal medulla contains distinct adrenergic and noradrenergic chromaffin cell populations, and the developmental stabilisation of HIF-2α is associated with a shift towards the noradrenergic population. Therefore, bulk RNA sequencing cannot distinguish transcriptional changes within individual cell populations from changes in their relative abundance. Single cell or spatial transcriptomic approaches could instead resolve these changes at cellular resolution. Single-cell RNA sequencing would identify HIF-2α-dependent transcriptional changes within distinct chromaffin cell populations, such as the noradrenergic and adrenergic populations, allowing changes in gene expression to be separated from changes in cell composition. Spatial transcriptomics would provide complementary information by retaining the anatomical organisation of these populations. This may be particularly informative because adrenergic chromaffin cells predominantly occupy the centre of the adult wild-type adrenal medulla, whereas noradrenergic cells occur in clusters around its periphery, with this distribution reversed following developmental HIF-2α stabilisation. Therefore, spatial transcriptomics could determine whether HIF-2α-dependent transcriptional programmes are associated with specific anatomical regions. Together, these approaches could build on the findings of this chapter by using the developmental *HIF-2αdPA* mouse model to define the cell type-specific transcriptional programmes through which developmental HIF-2α activity establishes the foetal-like, paraganglioma-like state and enables the persistence of oxygen chemosensitivity in the adrenal medulla.

Chapter 4

TH-RESTRICTED MUTATIONS IN BOTH ALLELES OF SDHB CONFER IMMATURE CHROMAFFIN CELL PHENOTYPES IN MICE.

4.1 **Introduction**

Pheochromocytomas and paragangliomas are neuroendocrine tumours that arise from chromaffin cells of the adrenal gland and autonomic paraganglia. They are among the most highly heritable human tumours, with approximately 40% of cases carrying germline mutations in one of several known susceptibility genes (Dahia, 2014; Favier et al., 2015). Of the remaining sporadic cases, around one third also harbour somatic mutations in these same genes (Lenders et al., 2014). These susceptibility genes can be broadly classified into three molecular clusters based on the signalling pathways they affect, with cluster one, also known as the pseudohypoxic cluster, comprising genes that directly (cluster 1B) or indirectly (cluster 1A) regulate HIF signalling (Fishbein et al., 2017). Previous work has generated mouse models targeting components of the HIF pathway directly, representative of cluster 1B tumours, including inactivation of *Phd2* and expression of constitutively active HIF-2α (Eckardt et al., 2021; Fielding et al., 2018; Hodson et al., 2016; Prange-Barczynska et al., 2024) (Chapter 2). This chapter builds upon these studies by investigating genetic alterations that indirectly influence HIF signalling, characteristic of cluster 1A tumours, in particular in succinate dehydrogenase B (SDHB), as these are among the most common and most metastatic mutations associated with these tumours (Brouwers et al., 2006; Gimenez-Roqueplo et al., 2023).

The most common genes mutated in pseudohypoxic pheochromocytomas and paragangliomas are those encoding subunits of SDH, with germline mutations in SDHx underlying approximately 15% of all pheochromocytomas and paragangliomas (Benn et al., 2018). SDH

is an enzyme located in the inner mitochondrial membrane which forms part of both the Krebs cycle and the electron transport chain, coupling these stages of cellular respiration (Rustin et al., 2002; Rutter et al., 2010). It is composed of four subunits: A, B, C, and D **(Figure 4.1)**. SDHA and SDHB form a hydrophilic tail which projects into the mitochondrial matrix. SDHA catalyses the conversion of succinate to fumarate, reducing FAD to $FADH_2$ and releasing electrons to SDHB. SDHB is an iron-sulfur protein which transfers these electrons to SDHC and SDHD. SDHC and SDHD are hydrophobic anchorage subunits embedded in the inner mitochondrial membrane. Together, they form the binding site for ubiquinone which accepts these electrons to become reduced to ubiquinol.

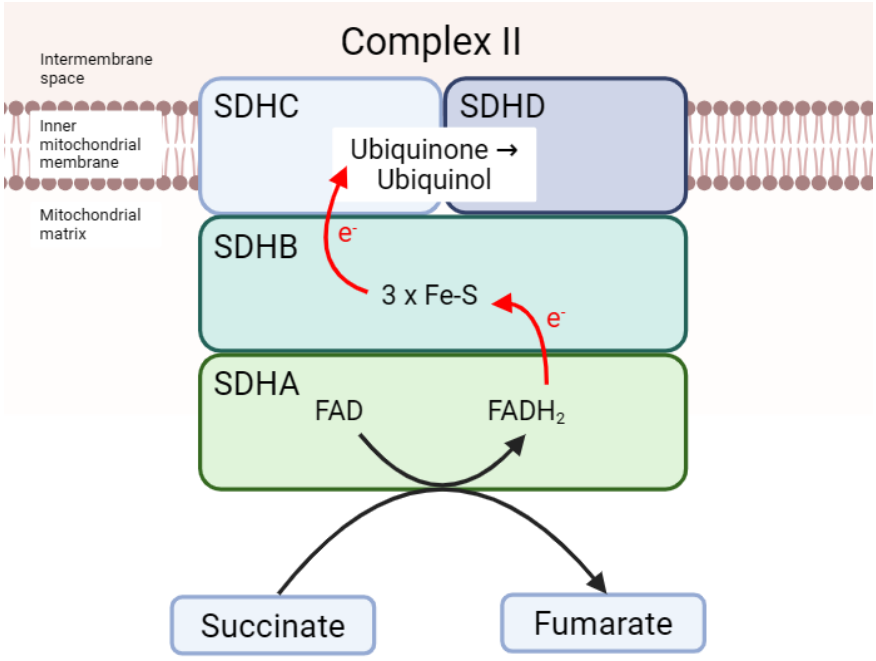

Figure 4.1. Schematic representation of succinate dehydrogenase. Succinate dehydrogenase (SDH) catalyses the oxidation of succinate to fumarate as part of the Krebs cycle, while simultaneously transferring electrons to ubiquinone, which is reduced to ubiquinol. SDH is composed of four subunits: SDHA, SDHB, SDHC and SDHD. SDHA contains the FAD cofactor responsible for the oxidation of succinate, while SDHB contains three iron-sulfur (Fe-S) clusters that mediate electron transfer. SDHC and SDHD form the membrane-anchoring domain within the inner mitochondrial membrane and provide the binding site for ubiquinone.

Mutations in all four *SDH* subunits have been identified in pheochromocytomas and paragangliomas (Evenepoel et al., 2015). These include missense, nonsense, frameshift, and splice site mutations. Mutations in each of the SDH subunits are associated with different tumour phenotypes, including location, prevalence, aggressiveness, and risk of malignancy (Andrews et al., 2018; Jochmanova et al., 2017). *SDHA* mutations are rare and found mainly in extra-adrenal paragangliomas. *SDHC* mutations are also rare and are most often associated with benign head and neck paragangliomas. *SDHD* mutations are also associated with head and neck paragangliomas and are commonly inherited in a paternal autosomal dominant manner. Patients with *SDHD* mutations often have multiple tumours. Finally, *SDHB* mutations are the most common germline mutations underlying familial pheochromocytomas and paragangliomas. They are primarily found in extra-adrenal paragangliomas but can also cause adrenal pheochromocytomas. Unlike *SDHD* mutations, they carry a low risk of developing multiple tumours but are associated with a high risk of aggressiveness, rapid progression, and metastasis.

Oncogenic mutations in any one of the SDH subunits (SDHA, SDHB, SDHC or SDHD), together with loss of the remaining functional allele, can result in loss of SDH activity and consequent accumulation of succinate. Because of its structural similarity with 2-oxoglutarate (2-OG), succinate can act as an oncometabolite by binding to the active site of 2-OG-dependent dioxygenases, leading to competitive inhibition of these enzymes. However, this is a large family of over 60 enzymes including prolyl hydroxylases (PHDs) and ten-eleven translocation (TET) dioxygenases, and the specific 2-OG-dependent dioxygenase(s) whose inhibition by accumulation of succinate to initiate oncogenesis remains unclear (Fletcher & Coleman, 2020; Yang et al., 2012). Inhibition of PHD enzymes causes stabilisation of HIF-α, driving transcription of a wide range of genes which promote cancer cell survival and growth such as

ones involved in angiogenesis, proliferation and glycolysis (Nguyen & Duran, 2016). Inhibition of TET enzymes promotes epigenetic changes, including DNA hypermethylation (Rasmussen & Helin, 2016). DNA hypermethylation and HIF-2α activation are both necessary to drive the epithelial-to-mesenchymal transition and metastatic phenotype in SDHB-deficient cells, suggesting these processes act synergistically to cause development and progression of aggressive *SDHB*-mutated tumours (Morin et al., 2020b). In line with this, HIF-2α protein stabilisation is increased in *Sdhb*$^{-/-}$ cells, whereas despite causing similar levels of succinate accumulation, HIF-2α stabilisation is not observed in *Sdhd*$^{-/-}$ cells (Goncalves et al., 2021). This suggests that the oncogenic mechanisms underlying tumours with mutations in different subunits of SDH may differ. As *SDHB* mutations are the most common germline alterations underlying pheochromocytomas and paragangliomas and carry the highest risk of aggressive, metastatic disease (Amar et al., 2021), understanding the mechanisms by which they cause tumourigenesis, including identifying the 2-OG-dependent dioxygenases whose inhibition contributes to tumour development, is of significant clinical interest. This requires animal models of SDHB-deficient pheochromocytomas and paragangliomas.

Several laboratories have attempted to generate these but with limited success to date. Lepoutre-Lussey et al. (2015) attempted to overcome the embryonic lethality associated with ubiquitous SDH loss by conditionally deleting exon 2 of *Sdhb* in neuroendocrine cells of mice using an exogenous rat tyrosine hydroxylase (TH) promoter driven Cre, or in the adrenal medulla using a human prostate-specific antigen (PSA) Cre (Lepoutre-Lussey et al., 2016; Piruat et al., 2004). Exon 2 encodes part of the 2Fe-2S iron-sulfur cluster domain of SDHB; its deletion introduces a frameshift and premature stop codon, resulting in a truncated protein[10]. Similarly, Armstrong et al. (2022) conditionally deleted exon 3 of SDHB, which also encodes part of the 2Fe-2S iron-sulfur cluster and the beginning of the 4Fe-4S domain, in TH^{+} cells using the same rat TH promoter-driven Cre recombinase (JAX #008601) (Armstrong et al.,

2022). Therefore, across these mouse models, *Sdhb* deletion was achieved using THCre with either exon 2 or 3 excision, or PSACre with exon 2 excision. Although these models demonstrated increased succinate accumulation, consistent with loss of SDH function, they did not develop frank pheochromocytomas or paragangliomas.

THCre-mediated recombination was reported to be incomplete in the above mouse models; only 60% of cells in the adrenal medullae from *Sdhb$^{f/f}$;THCre* mice expressing the mT/mG Cre-reporter, which emits green florescence upon Cre-mediated recombination, were GFP^{+}, while immunoblotting on this tissue showed modest remaining SDHB expression (Armstrong et al., 2022). Consequently, insufficient Cre expression in this THCre line may underlie the lack of frank tumours in these mice. Therefore, in this chapter, mice expressing TH-IRES-Cre (Lindeberg et al., 2004) (the THCre used in the *Phd2ko* and *Hif-2αdPA* mouse models described in this thesis) were bred with mice carrying loxP sites flanking exon 2 of the endogenous *Sdhb* allele (Letouzé et al., 2013) in an attempt to generate an effective mouse model to study the effect of SDHB inactivation in the context of pheochromocytomas and paragangliomas. TH-IRES-Cre is a transgenic mouse line developed by Lindeberg et al. (2004) where Cre recombinase is expressed from the endogenous mouse *Th* locus via an internal ribosome entry sequence (IRES) inserted into the 3'-untranslated region, thereby coupling Cre expression to endogenous *Th* transcription (Lindeberg et al., 2004). These breedings resulted in offspring expressing both TH-IRES-Cre (hereafter referred to as THCre) and either one or two *Sdhb*-floxed alleles (*Sdhb$^{f/+}$;THCre* and *Sdhb$^{f/f}$;THCre*), to investigate the effects of loss of one or two copies of *Sdhb*. TH-restricted excision of exon 2 causes a frameshift, leading to a premature stop codon and truncation of the protein such that SDHB is inactivated in cells of the sympathoadrenal system.

In inherited paragangliomas, however, one copy of the SDHx gene is mutated in the germline whilst the other allele acquires a loss-of-function mutation such as loss of chromosome 1p somatically, i.e. loss of heterozygosity (Gimenez-Roqueplo et al., 2003). To more closely recapitulate this, mice were generated with one allele of *Sdhb* inactivated in the germline. This was attempted by using either: a null *Sdhb* allele (the same deletion of exon 2 as described above but in all tissues i.e. $Sdhb^{+/-}$) or using a germline point mutation in *Sdhb* (V142F). V142F is the mouse equivalent of the valine-to-phenylalanine substitution mutation at codon 140 of *SDHB* (V140F), a variant found clinically in patients and associated with highly aggressive paragangliomas (Flynn et al., 2025; Richter et al., 2019). These mice were bred with $Sdhb^{f/+}$*;THCre* mice so that the second allele of *Sdhb* in these two mouse models was floxed under the control of THCre.

Investigation of these mice revealed that those carrying mutations in both alleles of *Sdhb* (i.e. $Sdhb^{f/f}$*;THCre*, $Sdhb^{f/-}$*;THCre* or $Sdhb^{f/V142F}$*;THCre* mice) exhibited morphological and transcriptomic abnormalities in the carotid body and adrenal medulla, as well as retention of the organ of Zuckerkandl which was sensitive to acute hypoxia. These features resemble the immature glomus and chromaffin cell phenotypes described in Chapter 2 in the *Hif-2αdPA* and *Phd2ko* mouse models and may represent a pre-malignant state. However, these mice were significantly runted and did not survive beyond eight weeks of age. This prevented aging the mice to test whether these abnormalities would progress to frank tumours over time. Therefore, further refinement of the mouse models is necessary to enable assessment of tumour development over a longer timescale.

4.2 **Results**

4.2.1 *Mouse models with mutations in Sdhb*

To investigate the effects of SDHB inactivation in neuroendocrine tissues, genetically modified mice with tyrosine hydroxylase (TH)-restricted mutations in *Sdhb* were generated. This was achieved by crossing mice carrying loxP sites flanking exon 2 of the endogenous *Sdhb* gene (Letouzé et al., 2013) with mice expressing Cre recombinase under the control of the endogenous mouse *Th* promoter (Lindeberg et al., 2004) to obtain *Sdhb*$^{f/+}$*;THCre* and *Sdhb*$^{f/f}$*;THCre* mice. Exon 2 contains part of the sequence encoding the 2Fe-2S iron-sulfur cluster and is a common site of genetic variants in human pheochromocytomas and paragangliomas (C. Liu et al., 2023). Excision of exon 2 by Cre recombinase in TH$^+$ cells yields mRNA with a premature stop codon and hence truncation of the SDHB protein (Letouzé et al., 2013). Initial experiments examined mice with one or two floxed alleles of *Sdhb* (*Sdhb*$^{f/+}$*;THCre* and *Sdhb*$^{f/f}$*;THCre*) in order to investigate the effects of SDHB inactivation in TH$^+$ tissues. However, in pheochromocytomas and paragangliomas, one mutant allele of *Sdhb* is inherited in the germline whilst the other allele is inactivated somatically in affected cells (i.e. loss of heterozygosity). Therefore, to more closely recapitulate the clinical condition, mice were generated with either one germline null allele of *Sdhb* (exon 2 loss and truncation of the protein) or one allele carrying the clinical *Sdhb* V142F point mutation. This is equivalent to the human *SDHB* V140F variant located in exon 4 of *SDHB*, which is associated with highly metastatic pheochromocytomas and paragangliomas (Flynn et al., 2025; Richter et al., 2019). The other allele of *Sdhb* in both of these mice was floxed such that it is inactivated in TH$^+$ tissues. This resulted in *Sdhb*$^{f/-}$*;THCre* or *Sdhb*$^{f/V142F}$*;THCre* mice, in which one copy of *Sdhb* is germline for either a null or a point mutation for *Sdhb* (mimicking germline inheritance), whilst the other copy is inactivated in TH$^+$ tissues (to mimic the 'second hit'). *Sdhb*$^{f/f}$*;THCre*, *Sdhb*$^{f/-}$*;THCre* and *Sdhb*$^{f/V142F}$*;THCre* mice were examined against wild-type and

Sdhb$^{f/+}$*;THCre* mice to assess the effects of SDHB inactivation. The mouse models with mutations in Sdhb are summarised in **Figure 4.2**.

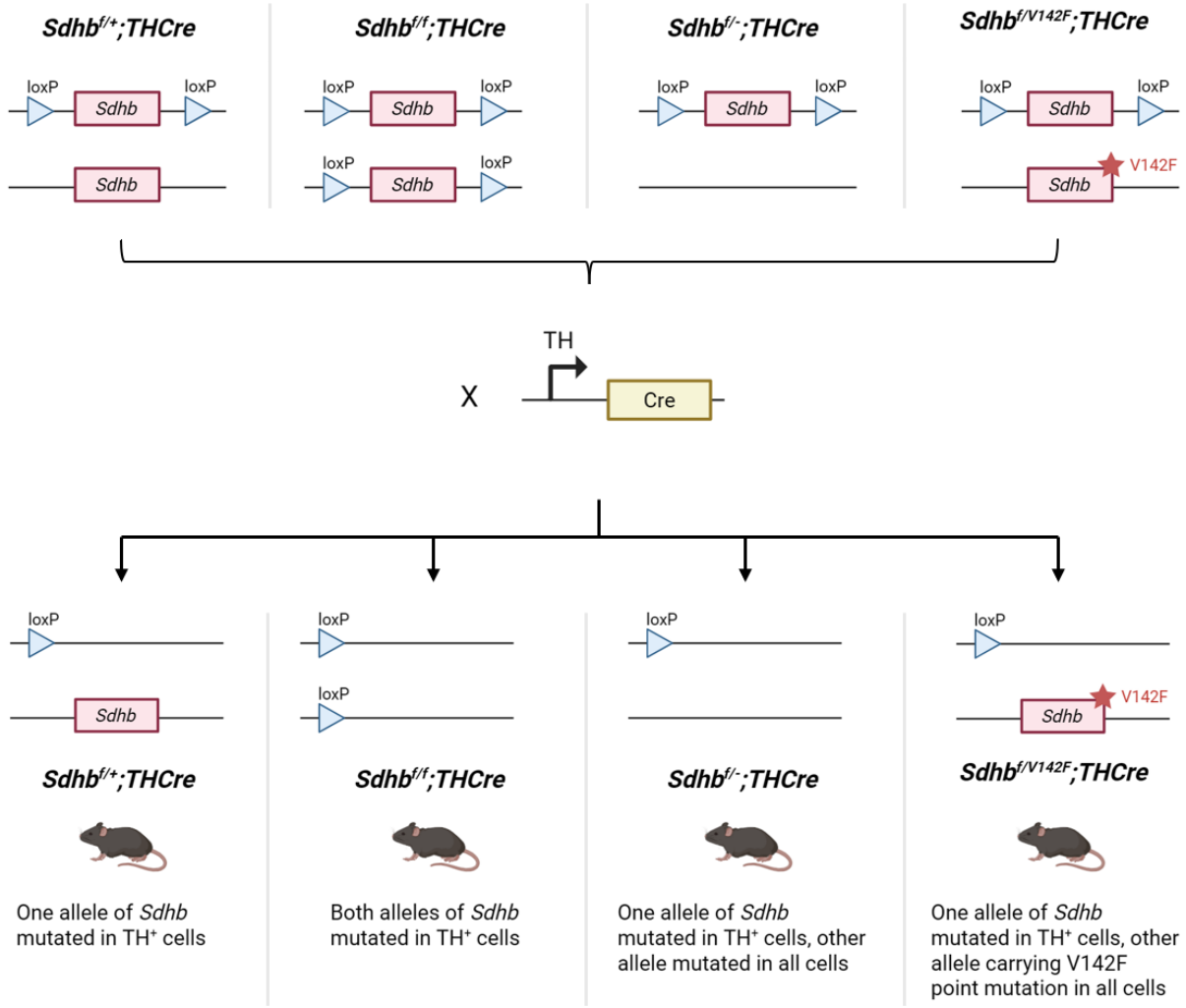

Figure 4.2. Schematic summarising the mouse models with mutations in *Sdhb*. Mice expressing one allele of *Sdhb* with loxP sites (represented by arrowheads) flanking exon 2, and the other allele either wild-type, floxed, null or containing the V142F point mutation, were crossed with mice expressing Cre recombinase under the tyrosine hydroxylase (TH) promoter. Cre-mediated excision of exon 2 of *Sdhb* in TH$^+$ cells of offspring results in mice with developmental mutations in either one or both alleles of *Sdhb* in these cells.

4.2.2 *Mice with mutations in both alleles of Sdhb are runted*

Mice with mutations in both copies of *Sdhb* (*Sdhb$^{f/f}$;THCre*, *Sdhb$^{f/-}$;THCre* and *Sdhb$^{f/V142F}$;THCre*) were significantly smaller than age- and sex-matched wild-type and *Sdhb$^{f/+}$;THCre* mice (**Figure 4.3)**. At six weeks of age, body weight was reduced by approximately 40% in males and 30% in females carrying mutations in both copies of *Sdhb*. The extent of growth restriction was similar across these three genotypes, indicating that the V142F point mutation produced a phenotype comparable to exon 2 deletion in this model. Attempts to increase body weight by providing a high calorie mash diet were unsuccessful, and mice became increasingly sick so had to be culled at approximately eight weeks of age. Therefore, mutation of both, but not a single, copy of *Sdhb* in TH^{+} tissues resulted in severe growth restriction and premature mortality.

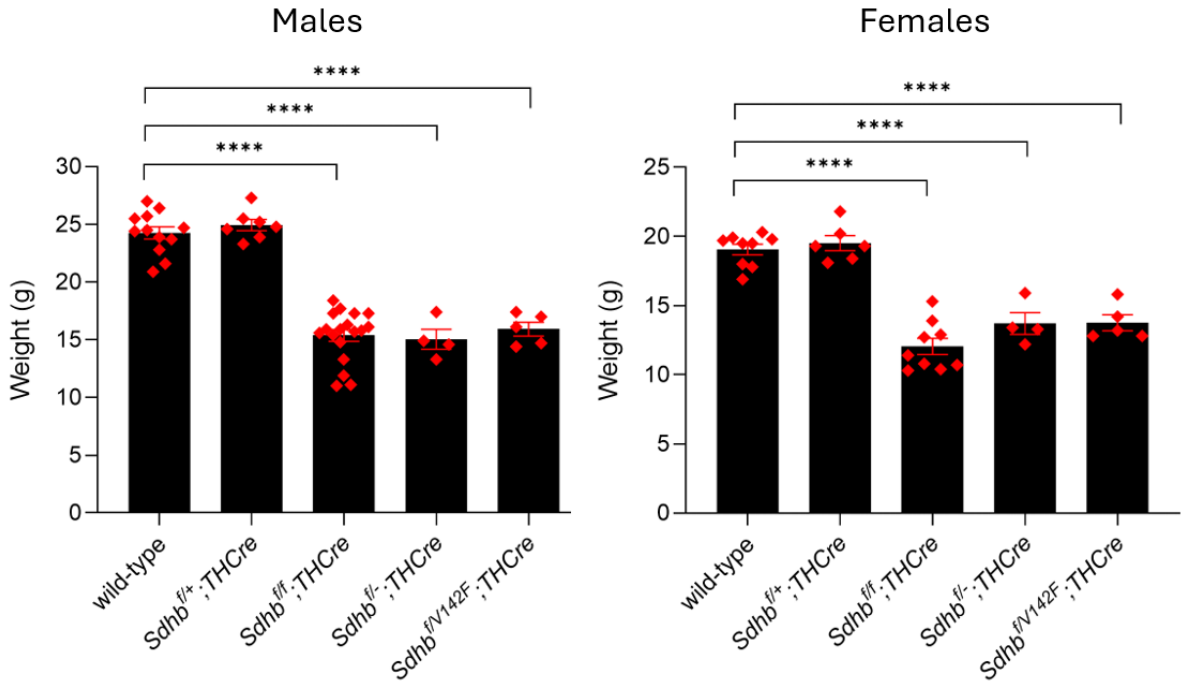

Figure 4.3. Mice with mutations in both alleles of *Sdhb* were runted compared to wild-type and heterozygous littermates. Bar graphs showing the weights of six-week-old male (left) and female (right) wild-type, *Sdhb$^{f/+}$;THCre*, *Sdhb$^{f/f}$;THCre*, *Sdhb$^{f/-}$;THCre and Sdhb$^{f/V142F}$;THCre* mice. Data are

presented as mean ± SEM and were analysed by one-way ANOVA with Tukey's multiple comparisons test, **** $p < 0.0001$

4.2.3 *Confirmation of SDHB loss in the mouse models with mutations in Sdhb*

To assess SDHB expression in mice with genetic mutations in *Sdhb*, immunohistochemistry for SDHB was performed in TH^+ tissues: the carotid body (**Figure 4.4A**) and adrenal gland (**Figure 4.4B**). This revealed strong cytoplasmic staining for SDHB in glomus cells of the wild-type carotid body, reflecting the mitochondrial localisation of SDHB. SDHB protein was detected, but the intensity of staining was weaker in the carotid body from mice with TH-restricted loss of one copy of *Sdhb* (*Sdhb$^{f/+}$;THCre*) and in *Sdhb$^{f/-}$;THCre* mice. SDHB protein appeared to be less strongly expressed in *Sdhb$^{f/f}$;THCre* and *Sdhb$^{f/V142F}$;THCre* carotid bodies.

In wild-type adrenal glands, the medulla showed cytoplasmic SDHB staining, although the intensity of this staining was weaker than in the adrenal cortex, possibly due to a higher mitochondrial density in cortical cells than medullary chromaffin cells. In the *Sdhb$^{f/+}$;THCre* adrenal medulla, immunostaining for SDHB was present but fainter than in the wild-type medulla, suggesting partial but incomplete loss of protein expression. Last, in the adrenal glands from *Sdhb$^{f/f}$;THCre*, *Sdhb$^{f/-}$;THCre* and *Sdhb$^{f/V142F}$;THCre* mice, the medulla lacked positive staining for SDHB. In the adrenal cortex, there was strong cytoplasmic staining in animals irrespective of genotype, confirming TH-restriction of the *Sdhb* mutations and protein loss.

This immunohistochemistry suggests that genetic mutation of both copies of *Sdhb* resulted in protein loss in a tissue restricted manner. The extent of SDHB protein loss was somewhat unexpected in the *Sdhb$^{f/V142F}$;THCre* mice as only one allele of *Sdhb* in these mice encodes the

truncated protein whilst the other harbours a point mutation, suggesting that the V142F mutation may be sufficient to cause SDHB protein instability.

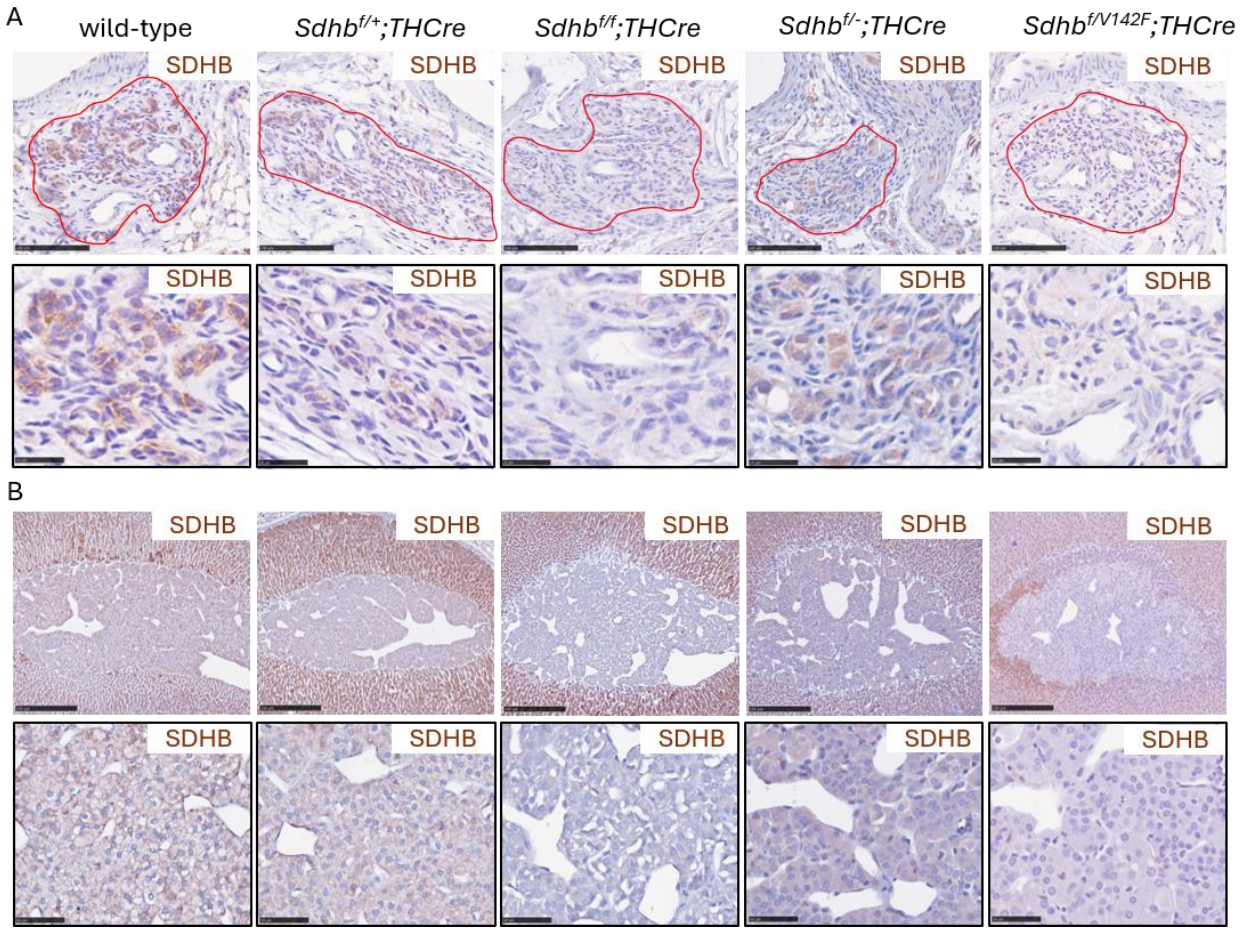

Figure 4.4. TH-restricted loss of SDHB protein expression in the carotid body and adrenal medulla from mice with mutations in *Sdhb*. (A) Representative images of immunohistochemistry for SDHB (brown) in the carotid body from wild-type, *Sdhb$^{f/+}$;THCre*, *Sdhb$^{f/f}$;THCre*, *Sdhb$^{f/-}$;THCre and Sdhb$^{f/V142F}$;THCre* mice. Red lines outline the carotid body. Higher magnification images are shown below outlined in black. Scale bars = 0.1 mm on lower magnification images and 0.025 mm on higher magnification inserts in black boxes below. **(B)** SDHB immunohistochemistry on the adrenal glands from these mice. SDHB protein expression is reduced in the adrenal medulla of mice with mutations in both alleles of *Sdhb* (*Sdhb$^{f/f}$;THCre*, *Sdhb$^{f/-}$;THCre and Sdhb$^{f/V142F}$;THCre*), but retained in the adrenal cortex across all genotypes.

4.2.4 *Carotid body morphology is altered in mice with mutations in both alleles of Sdhb*

To determine whether genetic mutation of *Sdhb* affects carotid body size or morphology, carotid bodies from mice of all genotypes were examined by immunohistochemistry for chromogranin A (CgA) and tyrosine hydroxylase (TH). Sections spanning the carotid bifurcation were stained to identify carotid body glomus cells and the volume of TH^+ and CgA^+ tissue was estimated from the stained area across serial sections. There were no differences in TH^+ tissue volume between wild-type, *Sdhb$^{f/+}$;THCre, Sdhb$^{f/f}$;THCre*, *Sdhb$^{f/-}$;THCre* and *Sdhb$^{f/V142F}$;THCre* carotid bodies (**Figure 4.5A and C)**. However, marked differences in cellular morphology were observed between genotypes **(Figure 4.5A and B)**. In wild-type and *Sdhb$^{f/+}$;THCre* carotid bodies, glomus cells showed the expected co-expression of CgA and TH. In contrast, glomus cells from mice with mutations in both alleles of *Sdhb* (*Sdhb$^{f/f}$;THCre*, *Sdhb$^{f/-}$;THCre* and *Sdhb$^{f/V142F}$;THCre*) retained TH expression and glomus-like morphology, but many lacked detectable CgA expression. Accordingly, CgA^+ tissue volume was significantly reduced compared with wild-type carotid bodies (**Figure 4.5B and D**), consistent with an altered or less differentiated glomus cell phenotype. In addition, many glomus cells in these mice exhibited evidence of 'cellular clearing', characterised by clear regions within the cytoplasm that were negative for CgA and TH and remained unstained by the haematoxylin counterstain. Therefore, mutation of both *Sdhb* alleles altered the phenotype and morphology of carotid body glomus cells, characterised by reduced CgA expression and cellular clearing, without affecting overall carotid body volume.

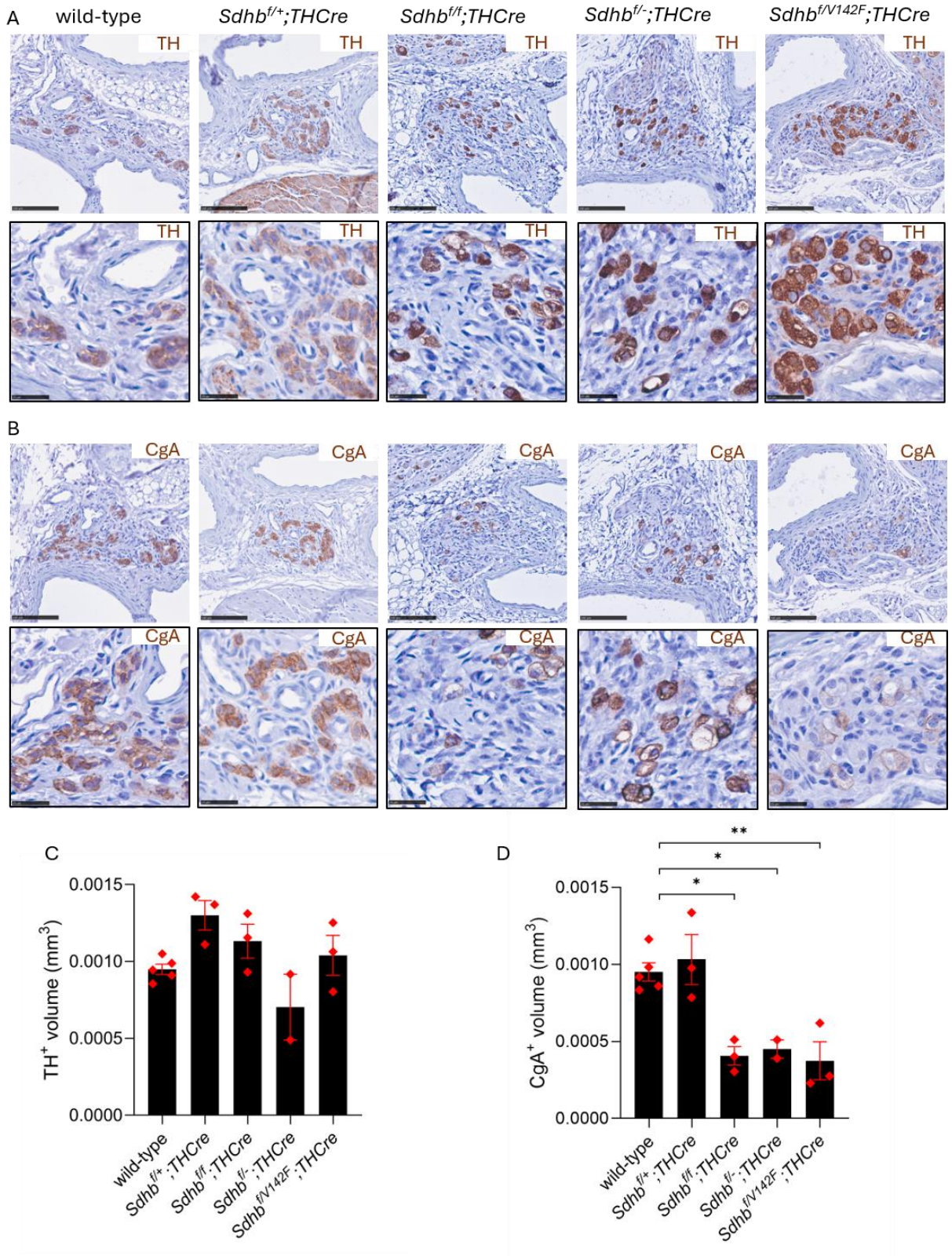

Figure 4.5. SDHB inactivation causes altered glomus cell morphology and reduced chromogranin A expression the carotid body. (A) Representative images of tyrosine hydroxylase (TH) immunohistochemistry (brown) on sections containing the carotid body. Scale bars represent 0.01 mm on lower magnification images and 0.0025 mm on higher magnification inserts outlined in black boxes.

(B) Chromogranin A (CgA) immunohistochemistry (brown) showing reduced CgA expression and abnormal glomus cell clearing in the carotid bodies from *Sdhb$^{f/f}$;THCre*, *Sdhb$^{f/-}$;THCre and Sdhb$^{f/V142F}$;THCre*, but not wild-type and *Sdhb$^{f/+}$;THCre* mice. **(C)** and **(D)** Quantification of carotid body volume calculated from TH^+ (C) and CgA^+ (D) cell areas. Data are presented as mean ± SEM and were analysed by one-way ANOVA with Tukey's multiple comparisons test, * $p < 0.05$, ** $p < 0.01$.

4.2.5 *Mice with mutations in both alleles of Sdhb are unable to tolerate acute hypoxia*

Given the altered carotid body morphology in mice with mutations in both copies of *Sdhb*, the ventilatory response to hypoxia was assessed by whole-body plethysmography as a measure of carotid body function. Mice were placed in airtight chambers and sequentially exposed to five minutes of room air, five minutes of hypoxia and a further five minutes of room air. Hypoxic challenges included 10% O_2, 10% O_2 and 3% CO_2 to counteract the hypercapnia associated with hyperventilation, and 3% CO_2 alone, as described in earlier chapters. There were no significant differences in the ventilatory responses to any of the gas mixtures between the wild-type and *Sdhb$^{f/+}$;THCre* mice in either males or females **(Figure 4.6)**. Plethysmography was also attempted in two *Sdhb$^{f/f}$;THCre* mice. However, both mice exhibited a rapid reduction in breathing rate to near zero following exposure to 10% O_2, accompanied by marked behavioural signs of distress, including repetitive circling within the plethysmography chamber. Both animals were immediately removed from the chambers, after which breathing rate recovered upon re-exposure to normoxia and the animals returned to their baseline behaviour. In accordance with animal welfare requirements, no further mice with mutations in both alleles of *Sdhb*, including *Sdhb$^{f/-}$;THCre* and *Sdhb$^{f/V142F}$;THCre*, were subjected to plethysmography. Therefore, loss of a single *Sdhb* allele in TH^+ tissue did not affect the hypoxic ventilatory response, whereas mice with mutations in both *Sdhb* alleles were unable to tolerate the 10% O_2 challenge. This severe response is consistent with the morphological abnormalities observed in the carotid body glomus cells from mice with mutations in both alleles of *Sdhb*.

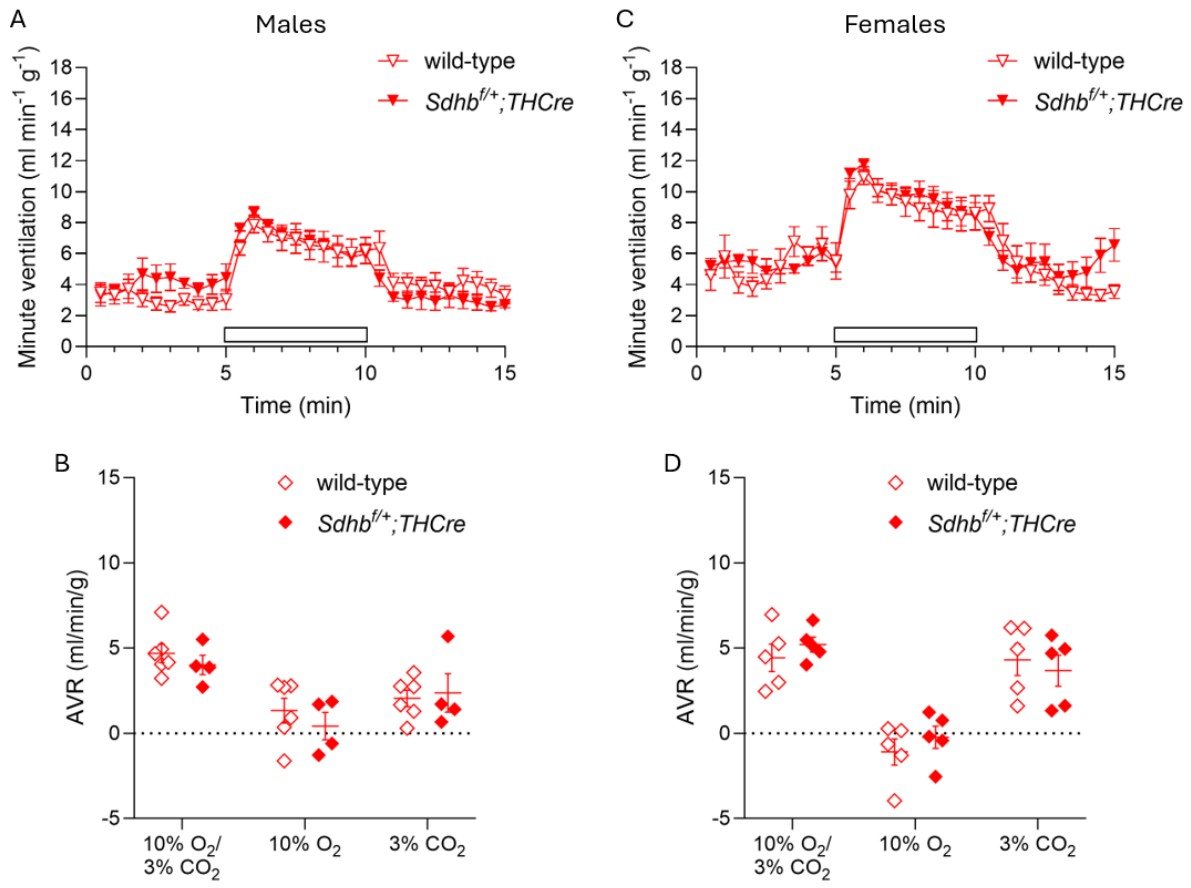

Figure 4.6. The hypoxic ventilatory response in wild-type and *Sdhb$^{f/+}$;THCre* mice. (A) and **(C)** Ventilatory responses to five minutes of 10% O_2/3% CO_2 (white bars) in male and female mice, n = 5 females and males of each genotype. **(B)** and **(D)** The acute ventilatory response (AVR) to each hypoxic stimuli. Data were compared between genotypes for each hypoxic stimuli by Holm-Sidak's multiple comparisons tests. No significant differences were observed.

4.2.6 *Reduction in Chromogranin A expression in the adrenal medulla of mice with mutations in both alleles of Sdhb*

The adrenal medulla is the site of pheochromocytomas. It is composed of chromaffin cells which, like the carotid body, express both CgA, a protein involved in the generation of neurosecretory granules, and TH, the rate-limiting enzyme in catecholamine synthesis. Therefore, to visualise these chromaffin cells in mice carrying mutations in *Sdhb* and wild-type controls, immunohistochemistry for CgA and TH was performed on sections throughout their

adrenal medullae **(Figure 4.7A and B)**. The adrenal glands from these mice appeared grossly similar, with no differences in the TH^+ area of the medulla between genotypes (**Figure 4.7C**). However, CgA expression was significantly reduced in mice with mutations in both alleles of *Sdhb*. In wild-type and *Sdhb$^{f/+}$;THCre* mice, all chromaffin cells in the adrenal medulla showed strong expression of both CgA and TH. By contrast, adrenal medullae from *Sdhb$^{f/f}$;THCre*, *Sdhb$^{f/-}$;THCre* and *Sdhb$^{f/V142F}$;THCre* mice showed strong expression of TH in all chromaffin cells, but weak-to-no expression of CgA in some chromaffin cells, particularly around the edge of the medulla at the corticomedullary junction. Quantification revealed that the CgA^+ area of adrenal medullae from *Sdhb$^{f/f}$;THCre*, *Sdhb$^{f/-}$;THCre* and *Sdhb$^{f/V142F}$;THCre* mice was significantly smaller than that of wild-type mice (**Figure 4.7D**), similar to the reduced expression of CgA in TH^+ carotid body glomus cells of these mice. Therefore, mutations in both alleles of *Sdhb* lead to reduced CgA expression in a proportion of TH^+ cells in both the carotid body and adrenal medulla, potentially indicating impaired differentiation of neuroendocrine cells.

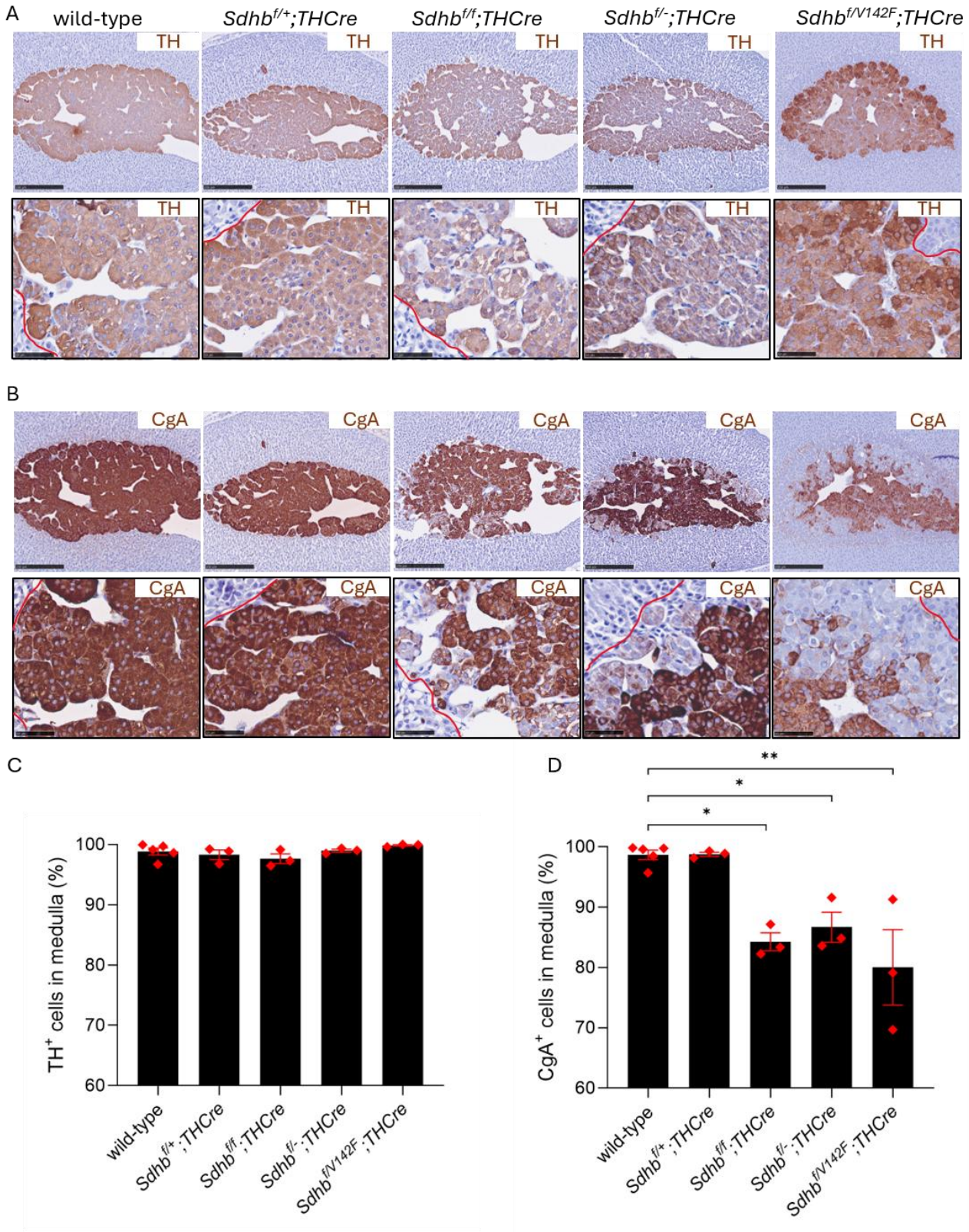

Figure 4.7. Normal tyrosine hydroxylase but reduced chromogranin A expression in the adrenal medulla of mice with mutations in both alleles of *Sdhb*. Representative images of immunohistochemistry for tyrosine hydroxylase (TH) **(A)** and chromogranin A (CgA) **(B)** in adrenal

glands from wild-type, *Sdhb$^{f/+}$;THCre*, *Sdhb$^{f/f}$;THCre*, *Sdhb$^{f/-}$;THCre and Sdhb$^{f/V142F}$;THCre* mice. Scale bars represent 0.25 mm on lower magnification images and 0.05 mm on higher magnification inserts outlined in black boxes. Red lines outline the corticomedullary junction. **(C)** and **(D)** Percentage of TH^+ (C) and CgA^+ (D) cells in the adrenal medulla Data are presented as mean ± SEM and were analysed by one-way ANOVA with Tukey's multiple comparisons test, * $p < 0.05$, ** $p < 0.01$.

4.2.7 *Mutations in both alleles of Sdhb results in an immature gene expression profile in the adrenal medulla*

Downregulation of phenylethanolamine N-methyltransferase (PNMT), the enzyme that converts noradrenaline to adrenaline, has been reported in pseudohypoxic pheochromocytomas, including those with mutations in *SDHB*, leading to an immature noradrenergic secretory profile (Burnichon et al., 2011; Eisenhofer et al., 2001; S. E. Lee et al., 2016). To test whether *Pnmt* expression was altered in the adrenal medulla of mice carrying *Sdhb* mutations, *in situ* hybridisation was performed on adrenal sections. In wild-type adrenal medullae, the majority of chromaffin cells expressed *Pnmt*, consistent with the mature adrenergic secretory profile of the adult adrenal medulla and data from previous chapters, whereas no *Pnmt* signal was detected in the adrenal cortex **(Figure 4.8A and B).** Within the medulla, *Pnmt* expression was largely mutually exclusive with expression of *Epas1*, the gene encoding HIF-2α, and the HIF-2α target gene *Rgs5* **(Figure 4.8A, C and D)**. A similar pattern was observed in *Sdhb$^{f/+}$;THCre* mice, in which the majority of medullary chromaffin cells were *Pnmt$^+$/Epas1$^-$/Rgs5$^-$*, while a smaller population, typically clustered around the edges of the medulla, were *Pnmt$^-$/Epas1$^+$/Rgs5$^+$* **(Figure 4.8A-D)**.

In contrast, all three genotypes with mutations in both alleles of *Sdhb* (*Sdhb$^{f/f}$;THCre*, *Sdhb$^{f/-}$;THCre* and *Sdhb$^{f/V142F}$;THCre*) showed a significant reduction in the proportion of chromaffin cells expressing *Pnmt* **(Figure 4.8A and B)**. There was no corresponding significant increase

in the percentage of medullary chromaffin cells expressing *Epas1* and *Rgs5* **(Figure 4.8A, C and D).** However, *Rgs5* staining appeared stronger in the *Rgs5*$^{+}$ population of biallelic *Sdhb* mutant adrenal medullae than in wild-type and *Sdhb*$^{f/+}$*;THCre* mice, suggesting increased expression in cells where it is present **(Figure 4.8A)**. Together, these findings demonstrate that mutation of both alleles of *Sdhb* shifts the adrenal medullary gene expression profile towards a *Pnmt*$^{-}$, noradrenergic phenotype, characteristic of less mature chromaffin cells. The qualitative increase in *Rgs5* is consistent with activation of HIF-2α-associated transcription, although the quantitative data does not demonstrate a broad increase in the proportion of cells expressing this. Notably, residual *Pnmt* expression in the *Sdhb* mutant adrenal medullae was frequently observed in clusters of chromaffin cells located near venous sinusoids (**Figure 4.8A**). This spatial distribution is consistent with the possibility that local increases in oxygenation may promote expression of this gene.

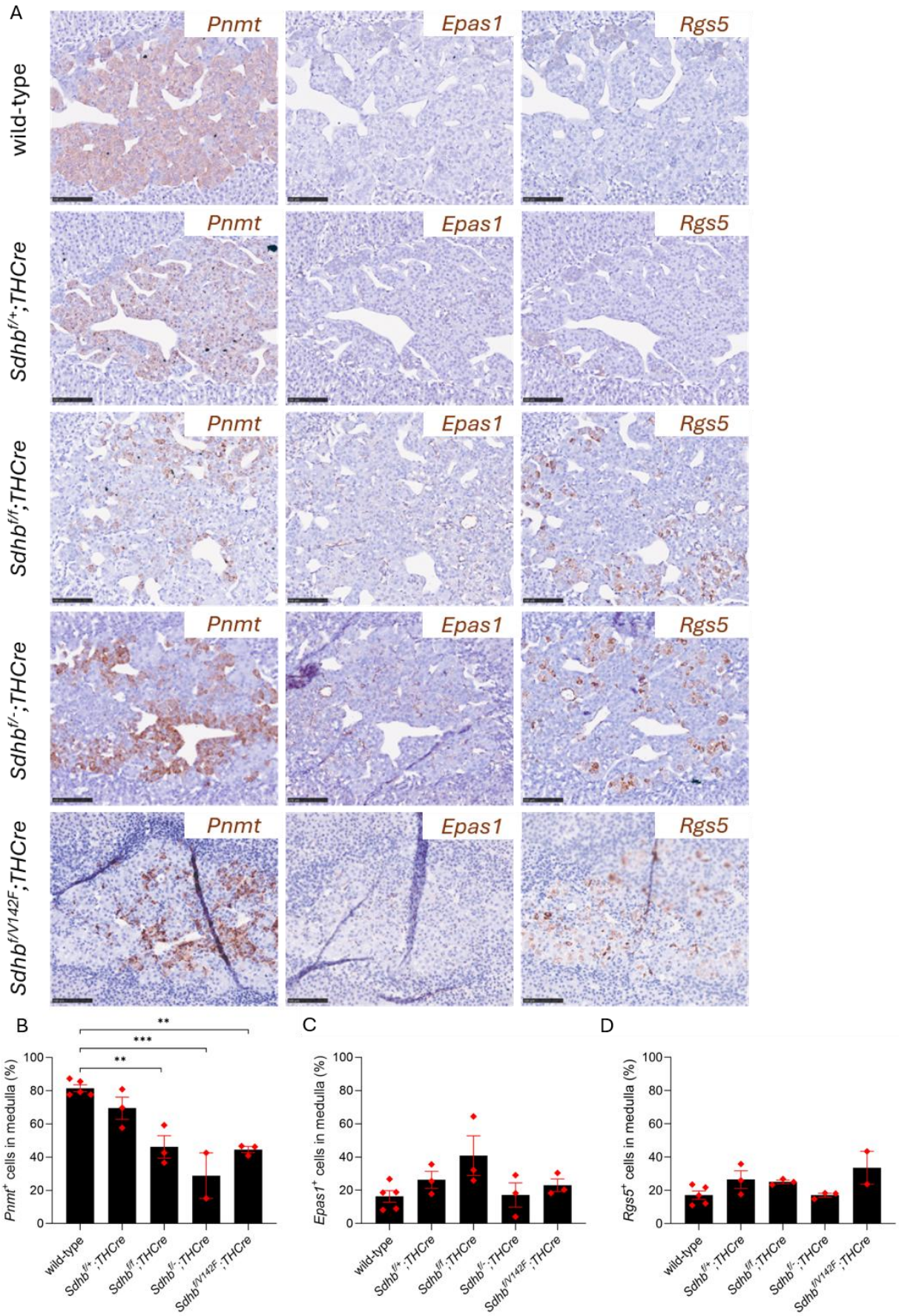
A
wild-type
Sdhb f/+;THCre
Sdhb f/f;THCre
Sdhb f/-;THCre
Sdhb f/V142F;THCre
Pnmt
Epas1
Rgs5
B
C
D
Pnmt+ cells in medulla (%)
Epas1+ cells in medulla (%)
Rgs5+ cells in medulla (%)
0
20
40
60
80
100
**
***
wild-type
Sdhb f/+;THCre
Sdhb f/f;THCre
Sdhb f/-;THCre
Sdhb f/V142F;THCre

Figure 4.8. A shift towards immature gene expression in adrenal medullae from mice with mutations in both alleles of *Sdhb*. (A) Representative images showing *Pnmt*, *Epas1* and *Rgs5* mRNA signal (brown) in the adrenal medulla from adjacent sections of adult wild-type, *Sdhb$^{f/+}$;THCre*, *Sdhb$^{f/f}$;THCre*, *Sdhb$^{f/-}$;THCre and Sdhb$^{f/V142F}$;THCre* adrenal glands. Scale bars = 0.1 mm. Graphs showing the percentage of medullary chromaffin cells expressing *Pnmt* **(B)**, *Epas1* **(C)** and *Rgs5* **(D)**. Data are presented as mean ± SEM and were analysed by one-way ANOVA with Tukey's multiple comparisons test, ** $p < 0.01$, *** $p < 0.001$.

4.2.8 *The adrenal medulla from mice with mutations in both alleles of Sdhb is unresponsive to acute hypoxia*

The adult adrenal medulla is not typically oxygen chemosensitive (García-Fernández et al., 2007; Prange-Barczynska et al., 2024; Thompson et al., 1997). However, since mutations in both alleles of *Sdhb* reduced expression of *Pnmt*, with possible induction of *Rgs5* in the adult adrenal medulla (a carotid body enriched gene that is associated with oxygen chemosensitivity (Prange-Barczynska et al., 2024)), it was next investigated whether this tissue was similarly oxygen chemosensitive. To achieve this, adrenal slices from adult mice with mutations in both alleles of *Sdhb* expressing the genetically encoded calcium indicator GCaMP6f (*Ai95$^{f/+}$*) (*Sdhb$^{f/f}$;Ai95$^{f/+}$;THCre* and *Sdhb$^{f/V142F}$; Ai95$^{f/+}$;THCre*), as well as control mice also expressing GCaMP6f (*Ai95$^{f/+}$;THCre*), were examined. It was not possible to test *Sdhb$^{f/-}$; Ai95$^{f/+}$;THCre* mice (and only a low number of *Sdhb$^{f/V142F}$; Ai95$^{f/+}$;THCre* mice) due to the difficulties in breeding and maintaining mice with mutations in both alleles of *Sdhb* caused by their severe runting phenotype and premature mortality.

Prior to conducting this experiment, the laboratory protocol for assessing tissue responses to hypoxia was refined: instead of exposing tissue to hypoxic stimuli of 10, 5, 1 and 0% oxygen, tissues were continuously perfused with the same buffer solution while the oxygen tension was gradually reduced from atmospheric oxygen levels to near zero then back up to atmospheric

levels. Importantly, the exact oxygen level of the solution at the point it flowed over the tissue was measured in real time using an oxygen dipping probe. The response of wild-type carotid bodies to acute hypoxia using the old and new method is shown to demonstrate the difference in data obtained from each **(Figure 4.9)**. The carotid body was used as it serves as a positive control for oxygen chemosensitivity. **Figure 4.9A** shows the data obtained from the old setup, which allows analysis of the magnitude of the fluorescence response to each discreet hypoxic stimuli, and the shape of the response over the 90-second-long exposures. However, this approach does not provide information on the responsiveness to levels of hypoxia other than 10, 5, 1 and 0% oxygen. Therefore, the setup of these fluorescent microscopy experiments was improved to generate data such as that shown in **Figure 4.9B**. A key advantage of this protocol is that it allows precise determination of the oxygen tension at which the tissue first responds to hypoxia. Therefore, this improved approach was used for subsequent experiments analysing tissue responsiveness to acute hypoxia.

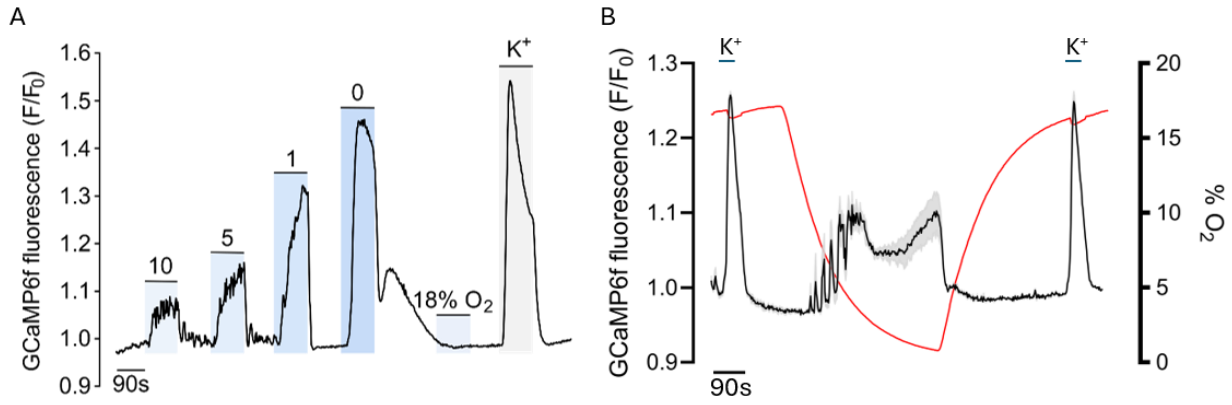

Figure 4.9. Example traces of the fluorescent response of GCaMP6f-expressing carotid bodies exposed to hypoxia using the previous and current methodologies. (A) A representative trace showing F/F_0 fluorescence in the K^+-responsive cells of an *Ai95$^{f/+}$;THCre* carotid body exposed to graded hypoxia (numbers represent % O_2) and 45mM K^+, including 18% O_2 as a sham control, as per the old methodology. **(B)** A representative trace showing F/F_0 fluorescence in the K^+-responsive cells of an *Ai95$^{f/+}$;THCre* carotid body exposed to gradual de-oxygenation to below 1% O_2 then subsequent

re-oxygenation (oxygen % is represented by the red line and shown on the y-axis) and 45mM K^+, as per the updated methodology.

Adrenal glands were dissected from GCaMP6f-expressing mice with mutations in both alleles of *Sdhb* and controls and sliced using a vibratome. Slices were then placed under the florescence microscope and perfused with CO_2-buffered saline solution. Before exposing the tissue to hypoxia, a 30-second exposure to 45 mM K^+ solution was used as a positive control to confirm that the cells were viable and excitable (**Figure 4.10A**). Adrenal medullae from all genotypes exhibited large increases in fluorescence in response to high K^+. Consistent with data from earlier chapters, the majority of chromaffin cells in the wild-type adrenal medulla did not respond to hypoxia, as indicated by the absence of changes in fluorescence intensity during hypoxic stimulation (**Figure 4.10B**). Similarly, the majority of chromaffin cells in adrenal medullae from mice carrying mutations in both copies of *Sdhb* showed no change in florescence in response to acute hypoxia (**Figure 4.10C**). The proportion of hypoxia-responsive cells was within the expected range for a wild-type medulla, and the magnitude of responses in the few cells that showed a response was small. Therefore, *Sdhb* inactivation was not sufficient to confer acute oxygen chemosensitivity on the adult adrenal medulla, despite the reduction in *Pnmt* and partial increase in *Rgs5* observed. This finding is consistent with the less pronounced gene expression changes observed following *Sdhb* inactivation compared with those seen in the *Phd2ko* and *Hif-2αdPA* medullae.

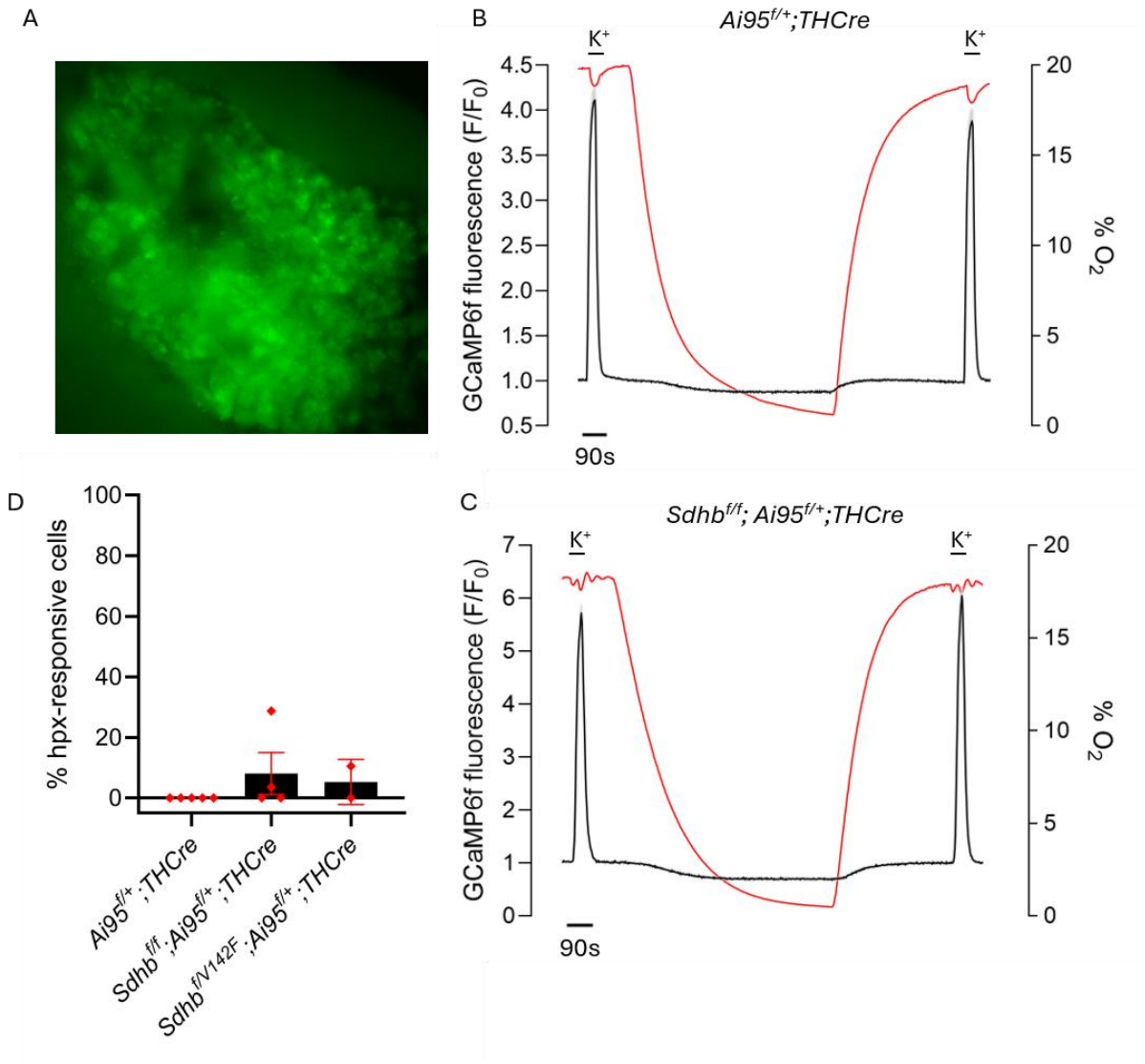

Figure 4.10. Mutation of both alleles of *Sdhb* does not confer acute oxygen chemosensitivity in the adult adrenal medulla. (A) Representative image showing GFP fluorescence in the adrenal medulla of an adrenal gland slice exposed to 45mM K^+ from a mouse expressing GCaMP6f (*Ai95$^{f/+}$;THCre*). **(B) and (C)** Representative traces showing F/F_0 fluorescence in K^+-responsive cells of *Ai95$^{f/+}$;THCre* (B) and *Sdhb$^{f/f}$;Ai95$^{f/+}$;THCre* (C) adrenal gland slices exposed to hypoxia (represented by the red line, % oxygen shown on the y-axis) and 45mM K^+. **(D)** Percentage of cells in the *Ai95$^{f/+}$;THCre, Sdhb$^{f/f}$;Ai95$^{f/+}$;THCre* and *Sdhb^{fV142F};Ai95$^{f/+}$;THCre* adrenal gland slices that showed an increase in florescence in response to hypoxia. Data are presented as mean ± SEM.

4.2.9 *Mutation of both alleles of Sdhb causes retention of the organ of Zuckerkandl in adult mice*

Mutation of both alleles of *Sdhb* causes a shift towards immature glomus and chromaffin cell phenotypes in the carotid body and adrenal medulla. Given that the main site of catecholamine production during development is the organ of Zuckerkandl, which then regresses postnatally (Schober et al., 2013; West et al., 1953), it was next assessed whether developmental inactivation of *Sdhb* confers retention of this foetal organ into adulthood. The abdominal aorta region was dissected from *Sdhb$^{f/+}$;THCre*, *Sdhb$^{f/f}$;THCre*, *Sdhb$^{f/-}$;THCre* and *Sdhb$^{f/V142F}$;THCre* mice and wild-type controls. These were fixed, embedded and sectioned in their entirety, from the base to the top of the kidneys, and immunohistochemistry for CgA and TH was performed throughout to detect chromaffin cells. Consistent with earlier chapters, adult wild-type mice did not possess an organ of Zuckerkandl, evidenced by the absence of any CgA^+TH^+ chromaffin cell clusters in this region. Similarly, adult *Sdhb$^{f/+}$;THCre* mice also lacked CgA^+TH^+ chromaffin cell clusters along the abdominal aorta, indicating that they do not retain their organ of Zuckerkandl in adulthood. In contrast, in all genotypes with mutations in both alleles of *Sdhb* (*Sdhb$^{f/f}$;THCre*, *Sdhb$^{f/-}$;THCre* and *Sdhb$^{f/V142F}$;THCre*), clusters of chromaffin cells forming a structure resembling the organ of Zuckerkandl were detected along the abdominal aorta **(Figure 4.11A and B)**. The volume of this tissue was estimated by quantifying the area of CgA^+ tissue across sections throughout the abdominal region **(Figure 4.11B)**. In summary, biallelic, but not monoallelic, mutation of *Sdhb* is sufficient to confer retention of the organ of Zuckerkandl in adult mice.

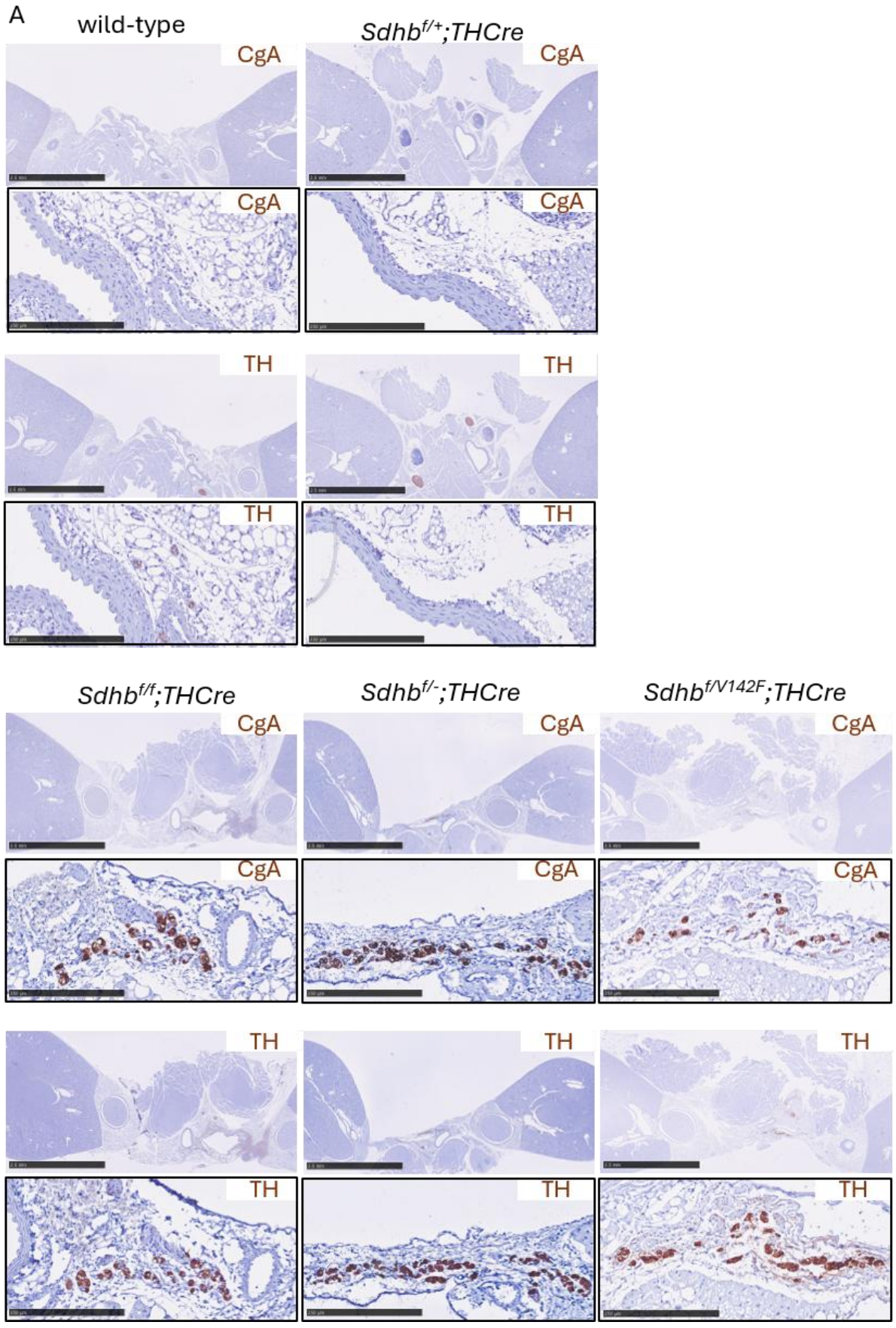
A
wild-type
Sdhb^f/+;THCre
Sdhb^f/f;THCre
Sdhb^f/-;THCre
Sdhb^f/V142F;THCre
CgA
TH

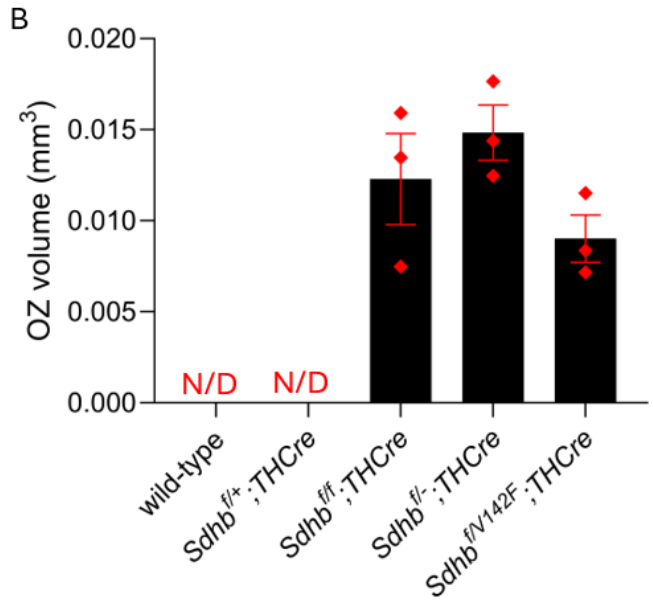

Figure 4.11. The organ of Zuckerkandl is retained in adult mice with mutations in both alleles of *Sdhb*. **(A)** Representative images of chromogranin A (CgA) immunohistochemistry, which stains chromaffin cells, in transverse sections from the abdominal aorta region from adult wild-type, *Sdhb$^{f/+}$;THCre*, *Sdhb$^{f/f}$;THCre*, *Sdhb$^{f/-}$;THCre and Sdhb$^{f/V142F}$;THCre* mice. Scale bars represent 2.5 mm on lower magnification images and 0.25 mm on higher magnification inserts in black boxes. (B) Volume quantification of the organ of Zuckerkandl (OZ) across the genotypes. The organ of Zuckerkandl was present in *Sdhb$^{f/f}$;THCre*, *Sdhb$^{f/-}$;THCre and Sdhb$^{f/V142F}$;THCre* mice, but was not detected (N/D) in wild-type and *Sdhb$^{f/+}$;THCre* mice. Data are presented as mean ± SEM.

4.2.10 *The retained organ of Zuckerkandl in mice with mutations in both alleles of Sdhb mice expresses carotid body marker genes and responds to acute hypoxia*

Given its prominent role in foetal catecholamine production, it has previously been hypothesised that the foetal organ of Zuckerkandl may respond directly to changes in oxygen availability, analogous to the oxygen-sensitive glomus cells of the adult carotid body (Brundin, 1966; Hervonen & Korkala, 1972; Tian et al., 1998). To test whether this is the case in the retained organ of Zuckerkandl in mice with mutations in both alleles of *Sdhb*, expression of genes associated with oxygen chemosensitivity in the carotid body was first examined. This

includes: *Epas1*, which encodes HIF-2α; *Rgs5*, a HIF target gene which acts as a negative regulator of G protein-coupled receptors; and atypical mitochondrial subunits such as *Cox4i2*. *In situ* hybridization for these transcripts revealed the presence of *Epas1*, *Rgs5* and *Cox4i2* mRNA in the retained organ of Zuckerkandl from *Sdhb$^{f/f}$;THCre*, *Sdhb$^{f/-}$;THCre* and *Sdhb$^{f/V142F}$;THCre* mice **(Figure 4.12)**, suggesting that like the wild-type carotid body, the organ of Zuckerkandl in these animals may also be oxygen chemosensitive. Differences in staining intensity between genotypes, particularly the very low *Cox4i2* signal, likely reflects variation in tissue freshness at the time of *in situ* hybridisation, given the high sensitivity of this technique to tissue quality.

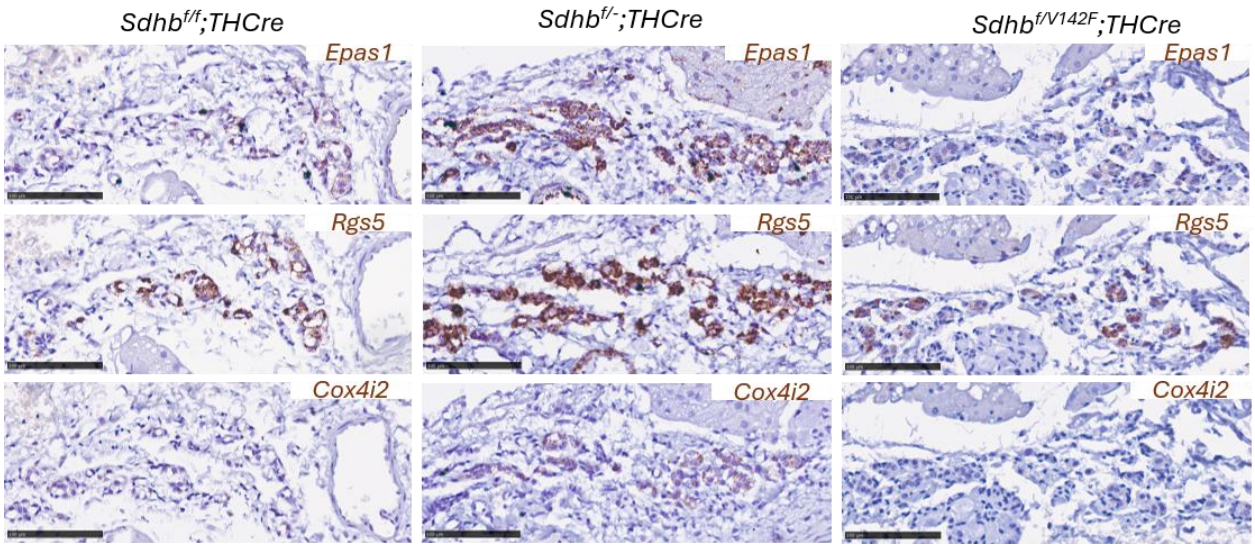

Figure 4.12. Expression of carotid body-enriched genes in the organ of Zuckerkandl from adult mice with mutations in both alleles of *Sdhb*. *In situ* hybridisation for *Epas1*, *Rgs5* and *Cox4i2* mRNA in the organ of Zuckerkandl from adult *Sdhb$^{f/f}$;THCre*, *Sdhb$^{f/-}$;THCre and Sdhb$^{f/V142F}$;THCre* mice. Scale bars = 0.1 mm.

The responsiveness of the organ of Zuckerkandl from mice with mutations in *Sdhb* to acute hypoxia was tested using mice expressing the genetic calcium indicator GCaMP6f (*Sdhb$^{f/f}$;Ai95$^{f/+}$;THCre*, *Sdhb$^{f/-}$;Ai95$^{f/+}$;THCre* and *Sdhb$^{f/V142F}$;Ai95$^{f/+}$;THCre*). The low number

of *Sdhb*$^{f/-}$;*Ai95*$^{f/+}$;*THCre* and *Sdhb*$^{f/V142F}$;*Ai95*$^{f/+}$;*THCre* mice included in these experiments reflects the difficulties associated with breeding and maintaining these mice due to their severe runting and early death, as described earlier in the chapter. Following harvest, the abdominal region was dissected and the organ of Zuckerkandl was subdissected. The response of the tissue to acute hypoxia was then assessed using the florescence microscope and superfusion system described above. Cells that exhibited an increase in fluorescence during the initial 30-second exposure to 45mM K^+ solution were selected for analysis. A proportion of these cells (quantified in **Figure 4.13C**) exhibited an increase in florescence in response to decreasing oxygen tension. This response was sustained throughout the duration of hypoxia and returned to baseline upon reoxygenation **(Figure 4.13B)**, demonstrating that the retained organ of Zuckerkandl in mice with mutations in both alleles of *Sdhb* is acutely oxygen chemosensitive. The oxygen tension eliciting half maximal fluorescence (P_{50}) was calculated as a measure of the sensitivity of the organ of Zuckerkandl to acute hypoxia (**Figure 4.13D**). Together, these findings demonstrate that TH-restricted mutations in both alleles of *Sdhb* are sufficient to promote retention of the organ of Zuckerkandl in adult mice, which both expresses carotid body-enriched genes and is responsive to acute hypoxia.

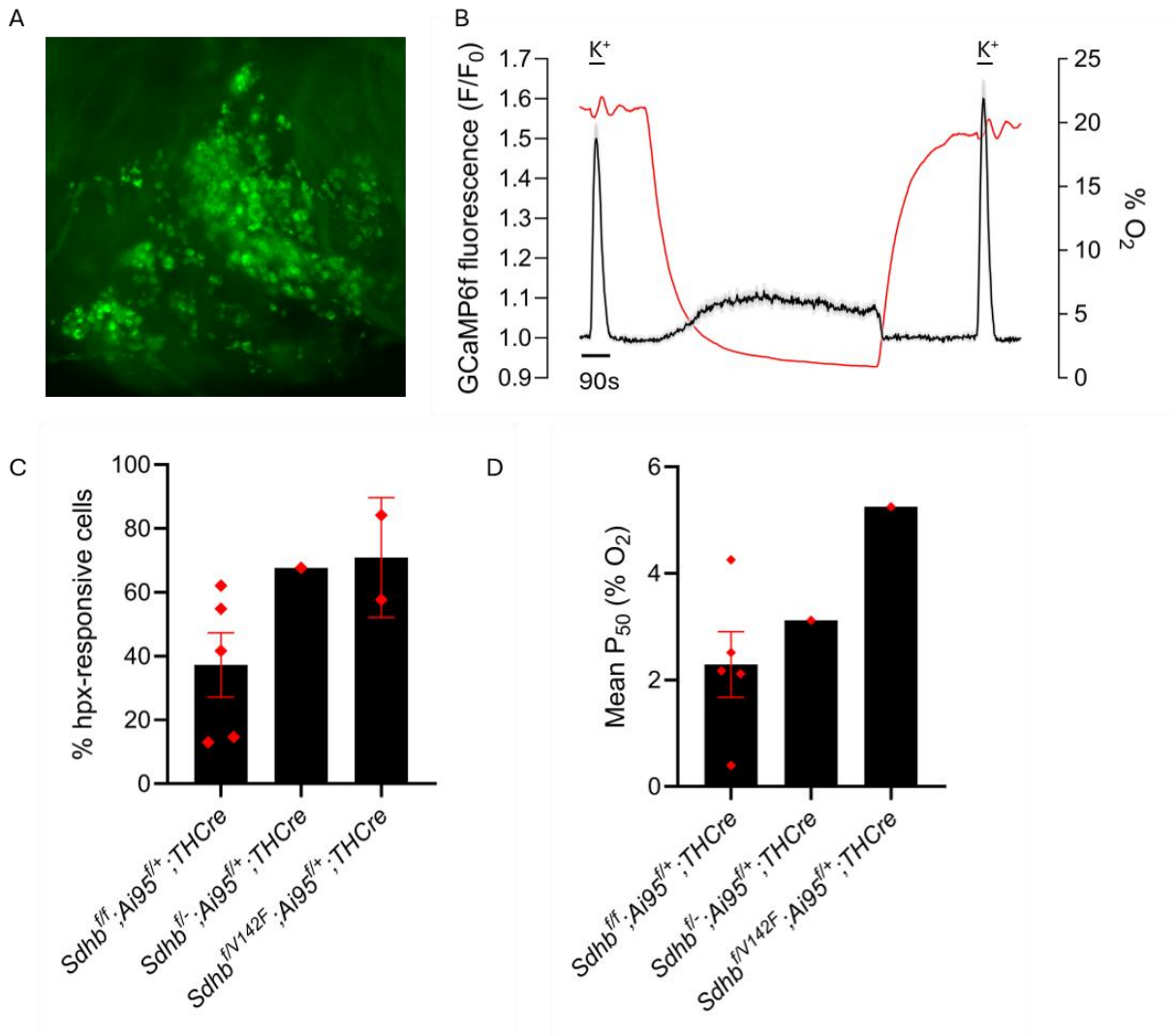

Figure 4.13. The retained organ of Zuckerkandl in mice with mutations in both alleles of *Sdhb* is oxygen chemosensitive. (A) A representative image of the organ of Zuckerkandl exposed to 45nM K^+ as a positive control for cell excitability. **(B)** A representative trace showing F/F_0 fluorescence in the K^+-responsive cells from an *Sdhb$^{f/f}$;Ai95$^{f/+}$;THCre* organ of Zuckerkandl exposed to hypoxia. Oxygen tension is shown in red. **(C)** Percentage of cells in the organ of Zuckerkandl from *Ai95$^{f/+}$;THCre, Sdhb$^{f/f}$;Ai95$^{f/+}$;THCre* and *Sdhb$^{f/V142F}$;Ai95$^{f/+}$;THCre* mice which showed an increase in florescence in response to hypoxia. Data are presented as mean ± SEM. **(D)** Mean P_{50} (oxygen tension at which 50% of the maximal fluorescence response was achieved) in the organ of Zuckerkandl from *Sdhb$^{f/f}$;Ai95$^{f/+}$;THCre, Sdhb$^{f/-}$;Ai95$^{f/+}$;THCre* and *Sdhb$^{f/V142F}$;Ai95$^{f/+}$;THCre* mice.

4.3 **Discussion**

This chapter aimed to develop a mouse model of SDHB-deficient pheochromocytoma and paraganglioma by generating mice with TH-restricted mutations in *Sdhb*. Although these mice did not develop frank tumours, they exhibited morphological and molecular abnormalities, consistent with retention of immature chromaffin cells. These included a shift towards an immature gene expression profile, characterised by loss of *Pnmt* and CgA expression, and retention of the oxygen chemosensitive organ of Zuckerkandl into adulthood. However, the mice were runted and died by approximately eight weeks of age, such that they could not be aged to determine whether paraganglioma formation would occur with time.

Other laboratories have previously attempted to develop TH-restricted SDHB-deficient mouse models of pheochromocytomas and paragangliomas (Armstrong et al., 2022; Lepoutre-Lussey et al., 2016). Like the mice described in this chapter, these models did not develop frank tumours. However, milder morphological phenotypes such as retention of immature chromaffin cells were not assessed. In contrast to the previously reported models, the mice described in this chapter also exhibited marked growth deficiency. Therefore, despite comparable TH-restricted *Sdhb* inactivation, the mice generated in this study appear to have a distinct phenotype. Differences in *Sdhb* allele configuration are unlikely to account for these differences as both the previous and current studies examined mice carrying either two floxed *Sdhb* alleles (*Sdhb$^{f/f}$;THCre*) or one floxed and one null allele (*Sdhb$^{f/-}$;THCre*). Furthermore, no clear phenotypic differences were identified between the *Sdhb$^{f/f}$;THCre*, *Sdhb$^{f/-}$;THCre* and *Sdhb$^{f/V142F}$;THCre* models in this chapter, further suggesting that *Sdhb* allele configuration is unlikely to explain these phenotypic differences. A more likely explanation may be the use of different THCre alleles. Previous studies used the randomly integrated rat exogenous THCre line (JAX #008601), whereas the present study used the mouse endogenous TH-IRES-Cre line

(Lindeberg et al., 2004). These lines differ in their genomic configuration and regulation and may therefore produce differences in the level, onset and cellular pattern of Cre recombinase expression, resulting in differences in the extent and timing of exon 2 excision. The earlier work reported incomplete THCre-driven recombination in the adrenal medulla, raising the possibility that the JAX #008601 THCre leaves a sufficient proportion of chromaffin cells with functional SDHB to prevent the phenotypes observed in the present study (Armstrong et al., 2022). However, testing this hypothesis would require direct comparison of the two THCre lines, including assessment of the onset and level of Cre expression, recombination efficiency, SDHB protein loss and succinate accumulation.

An interesting observation of this work was that the V124F point mutation in *Sdhb* resulted in a similar degree of SDHB protein loss in the carotid body and adrenal medulla as complete loss of exon 2 and protein truncation, as evidenced by the immunohistochemistry shown in Figure 4.4. Consistent with this, mice carrying the V142F point mutation in one allele of *Sdhb*, with the second allele floxed and conditionally deleted under the control of THCre, developed phenotypes that were as severe as those observed with complete inactivation of both *Sdhb* alleles (either two floxed alleles or one floxed and one germline-null allele). All three mouse models exhibited comparable runting and similar immature chromaffin cell phenotypes. This suggests that the V142F point mutation is sufficient to cause substantial SDHB protein instability, resulting in functional loss of SDH activity comparable to that caused by truncating mutations. This is consistent with previous work in HeLa cells, in which the loss of SDH function associated with a variety of common *Sdhb* missense variants was attributed to increased degradation of the mutant protein (Yang et al., 2012). Furthermore, cells transfected with the V140F SDHB variant, the human equivalent of the mouse V142F mutation, showed almost complete loss of SDH enzyme function, evidenced by a markedly elevated succinate-to-fumarate ratio (S. Lee et al., 2026). In humans, the V140F variant is classified as pathogenic

and has been associated with metastatic pheochromocytomas and paragangliomas (Richter et al., 2019). Together, these findings demonstrate that this point mutation is sufficient to severely disrupt SDH function, which, in humans, can contribute to tumorigenesis.

Mice with TH-restricted mutations in both alleles of *Sdhb* described in this chapter exhibited immature chromaffin cell phenotypes similar to those previously reported in other mouse models of pseudohypoxic pheochromocytoma and paraganglioma (*Phd2ko* and *Hif-2αdPA*). This includes loss of *Pnmt* expression in the adrenal medulla and retention of the oxygen chemosensitive organ of Zuckerkandl in adult mice, suggesting that HIF-2α activation may act as a common mechanism underlying these paraganglioma-like phenotypes. However, the phenotype of the mice with mutations in *Sdhb* was less pronounced than that of the *Phd2ko* and *Hif-2αdPA* mice, with less extensive *Pnmt* loss and a lack of oxygen chemosensitivity in the adrenal medulla, a smaller retained organ of Zuckerkandl and no carotid body hyperplasia.

Conversely, these mice exhibited an additional feature of neuroendocrine cell immaturity compared to *Phd2ko* and *Hif-2αdPA* mice, with a reduction in CgA expression in both carotid body glomus cells and adrenal medullary chromaffin cells. These differences suggest that mechanisms in addition to HIF-2α activation may contribute to the phenotype of the mice with mutations in *Sdhb*. In particular, *Sdhb* inactivation results in succinate accumulation which inhibits 2-OG-dependent dioxygenases other than PHD enzymes, including TET and Jumonji domain-containing demethylases. Consistent with this, work in $Sdhb^{-/-}$ immortalised mouse chromaffin cells showed that pseudohypoxia and TET inhibition act synergistically to drive the epithelial-to-mesenchymal transition and metastatic phenotype associated with loss of SDHB (Morin et al., 2020a). Therefore, a similar interaction may underlie the reduction in CgA in the carotid bodies and adrenal medullae of mice with *Sdhb* mutations. The milder *Pnmt*, adrenal oxygen chemosensitivity and organ of Zuckerkandl phenotypes in the mice with mutations in

Sdhb may also reflect qualitative or quantitative differences in HIF signalling between the models: *Hif-2αdPA* drives overexpression of a constitutively stable human HIF-2α protein, whereas *Phd2* and *Sdhb* inactivation lead to stabilisation of endogenous mouse HIF-2α together with other HIF-α isoforms, including HIF-1α. Overall, these findings suggest that while HIF-2α activation likely drives the shared immature chromaffin cell phenotype observed across the different pseudohypoxic mouse models, both variations in degree of HIF activation and/or additional HIF-independent mechanisms may contribute to the distinct phenotypes observed in the mice with mutations in *Sdhb*.

Another interesting difference between mice with mutations in *Sdhb* and the previously described pseudohypoxic models is the spatial pattern of *Pnmt* expression in the adrenal medulla. Although *Pnmt* expression was broadly reduced in the adrenal medulla from mice with mutations in both alleles of *Sdhb*, clusters of chromaffin cells, particularly those surrounding blood vessels, retained *Pnmt* expression. This distribution raises the possibility that local oxygen availability may influence the extent of HIF-2α stabilisation in *Sdhb*-deficient chromaffin cells. If succinate accumulation causes partial rather than complete inhibition of PHD activity, increased oxygen availability in the chromaffin cells surrounding sinusoids may permit residual PHD-mediated HIF hydroxylation and consequently lower HIF-2α protein expression in these cells. If increased HIF-2α activity is responsible for the absence of *Pnmt* expression in pseudohypoxic chromaffin cells, this could explain why cells surrounding the sinusoids acquire *Pnmt* expression, whereas those further from the sinusoids do not. In contrast, loss of *Pnmt* expression is more extensive in *Phd2ko* and *Hif-2αdPA* mice, with the minority populations of $Pnmt^{+}$ cells typically located around the corticomedullary junction rather than the venous sinusoids. In *Hif-2αdPA* mice, stabilised HIF-2α is overexpressed in all TH^{+} cells, such that differences in local oxygen availability are unlikely to substantially influence HIF-2α stability. In *Phd2ko* mice, PHD2 is absent, so increased oxygenation should have little effect

on HIF-2α hydroxylation and degradation, although the remaining PHD isoforms could still be affected by local differences in oxygenation. This difference in the mechanisms of HIF-2α stabilisation may therefore explain why this pattern of *Pnmt* expression around vascularisation was seen in the adrenal medullae from mice with mutations in both alleles of *Sdhb*, but not from *Phd2ko* or *Hif-2αdPA* mice. Alternatively, this may reflect changes independent of HIF-2α stabilisation in the *Sdhb*-inactivated mice, as discussed earlier in relation to CgA loss.

The severe growth restriction in mice with mutations in both alleles of *Sdhb* represents an important caveat when interpreting their immature chromaffin cell phenotypes. In particular, phenotypes such as retention of the organ of Zuckerkandl into adulthood could reflect a general developmental delay associated with growth restriction, rather than a direct consequence of succinate accumulation and its proposed oncometabolite activity. The mechanism underlying this runting is unknown, although loss of SDH activity in TH^+ catecholaminergic cells in the brain, including those in the substantia nigra, ventral tegmental area, and hypothalamus, leading to impaired catecholamine signalling may play a role. Dopaminergic signalling in the substantia nigra is involved in movement (Salvatore, 2024), so impaired signalling here may have affected the ability of these mice to stand on their hind legs and feed, while the ventral tegmental area is involved in reward and motivation (Geisler & Hayes, 2023), leading to decreased appetite and feeding behaviour. Furthermore, the hypothalamus produces growth hormone-releasing hormone (GHRH) which stimulates the anterior pituitary gland to produce and secrete growth hormone into the bloodstream (Hiller-Sturmhofel & Bartke, 1998). Therefore, impaired energy production and catecholamine signalling in these TH^+ cell types may cause growth restriction in mice with mutations in both alleles of *Sdhb*. Interestingly, TH-restricted inactivation of *Sdhc* conversely causes obesity in aging mice, suggesting that inactivation of *Sdhb* versus *Sdhc* has different effects on SDH activity, leading to different downstream effects of these mutations (Al Khazal et al., 2021). Regardless of the underlying

mechanism, runting represents an important caveat as it prevents the mice from being aged sufficiently to determine whether tumourigenesis occurs over time. A potential approach to overcome this limitation would be to induce inactivation of *Sdhb* during development using an inducible THCre recombinase (i.e. THCreER) with a submaximal dose of tamoxifen administered perinatally.

Chapter 5

DEVELOPMENTAL STABILISATION OF HIF-2A CONFERS RETENTION OF A PRE-NEOPLASTIC ORGAN OF ZUCKERKANDL.

5.1 **Introduction**

Work presented in previous chapters, together with work conducted prior to this thesis, has demonstrated that developmental pseudohypoxic mutations, including HIF-2α gain-of-function, loss of the HIF prolyl hydroxylase PHD2, and inactivation of the Krebs cycle enzyme succinate dehydrogenase B (SDHB), all result in retention of immature chromaffin cells in adult mice (Eckardt et al., 2021; Prange-Barczynska et al., 2024). Notably, all three mouse models retain an organ of Zuckerkandl in adulthood. This is a chromaffin cell structure located along the abdominal aorta which is typically only present in neonates (Coupland, 1965). It was first described by Emil Zuckerkandl in 1901 and is the largest accumulation of extra-adrenal chromaffin cells (Zuckerkandl, 1901). These cells originate from the neural crest and produce, store and secrete catecholamines, primarily noradrenaline, through regulated exocytosis of catecholamine-containing secretory vesicles. During foetal development, the organ of Zuckerkandl contributes to cardiovascular homeostasis by releasing catecholamines into the circulation in response to physiological stressors such as hypoxia (West et al., 1953). Circulating noradrenaline acts primarily through α_1-adrenergic receptors on vascular smooth muscle cells to induce vasoconstriction, thereby increasing systemic vascular resistance and, consequently, arterial blood pressure. The organ of Zuckerkandl subsequently undergoes regression postnatally and is typically absent in adult mammals (Schober et al., 2013). In humans, it reaches its maximum size at approximately three years of age before regressing, whereas in mice, it is lost within weeks after birth (Subramanian & Maker, 2006). The

mechanism of its regression is poorly understood, although autophagy is thought to play a central role (Schober et al., 2013). In parallel, the adrenal medulla matures and becomes the principal source of circulating catecholamines in adulthood (Otlyga et al., 2025).

The organ of Zuckerkandl is of particular interest in the context of hypoxia signalling for multiple reasons. First, its physiological function in the foetus is believed to involve the production and secretion of catecholamines into the circulation in response to hypoxic stress. Studies in foetal lambs demonstrated increased plasma noradrenaline levels in response to acute hypoxia (Jones & Robinson, 1975), while experiments in newborn rabbits showed that hypoxia stimulated catecholamine release from extra-adrenal chromaffin bodies but not the adrenal medulla (Brundin, 1966). Noradrenaline promotes peripheral vasoconstriction through vascular α_1-adrenergic receptors, thereby redistributing oxygenated blood towards critical organs with high metabolic demand, such as the foetal brain and heart. Second, the organ of Zuckerkandl expresses very high levels of *Epas1*, the gene encoding HIF-2α (Tian et al., 1998). Consistent with a role for HIF-2α in the hypoxia-responsive catecholaminergic system, *EPAS1* was shown to colocalise with tyrosine hydroxylase (TH) in cells of the sympathoadrenal system in the developing chicken embryo (Favier et al., 1999). Furthermore, mice with global deletion of *Epas1* exhibited pronounced bradycardia, reduced catecholamine levels and embryonic lethality at mid-gestation (Tian et al., 1998), supporting an important role for HIF-2α in the development and function of the catecholaminergic system. Third, developmental pseudohypoxic mutations that result in TH-restricted activation of HIF-2α, either through expression of a constitutively-active HIF-2α construct, *Hif-2αdPA*, or inactivation of *Phd2* or *Sdhb*, cause retention of the organ of Zuckerkandl in adult mice (Chapters 2 and 4) (Prange-Barczynska et al., 2024). This suggests that aberrant HIF-2α activity during the developmental window interferes with normal regression of this organ. Finally, although rare in most types of cancer, mutations affecting the HIF pathway are strongly associated with organ of Zuckerkandl

paragangliomas. A retrospective study of patients with organ of Zuckerkandl paragangliomas showed that 11/14 (79%) harboured mutations in SDH subunits, including nine with mutations in *SDHB* and two with mutations in *SDHD* (Lodish et al., 2010). This included nonsense, missense, deletions, frameshift and splice site mutations, including one patient with the V140F *SDHB* point mutation modelled in Chapter 3. Tumours at this location were associated with aggressive behaviour and a high incidence of metastatic disease, consistent with the recognised phenotype of SDHB-associated paragangliomas. There is also a reported case of an organ of Zuckerkandl paraganglioma harbouring a somatic gain-of-function mutation in *EPAS1* (Abdullah et al., 2017). Chronic systemic hypoxia, including in congenital cyanotic heart disease (CCHD), has also been associated with an increased risk of abdominal paragangliomas (Opotowsky et al., 2015). Together, these findings suggest that the organ of Zuckerkandl is linked to hypoxia biology in two distinct but potentially related ways: it contributes to the foetal hypoxic response through secretion of catecholamines, whilst aberrant hypoxic signalling during development results in its retention into adulthood where it may represent a susceptible cell population for tumourigenesis. This raises the possibility that the mechanisms underlying oxygen sensing in the organ of Zuckerkandl may contribute both to its normal developmental regression and to its susceptibility to paraganglioma development.

This chapter therefore investigated whether the organ of Zuckerkandl is acutely oxygen sensitive and whether it retains this ability to sense hypoxia after birth, how this capacity changes during its normal postnatal regression, and whether environmental hypoxia is sufficient to prevent this regression. In addition, the potential relationship between the retained organ of Zuckerkandl and tumorigenesis was examined in aged pseudohypoxic mice. This work provides direct evidence of oxygen chemosensitivity in the neonatal organ of Zuckerkandl, and shows that this oxygen-sensing capacity declines alongside the expression of HIF-2α target genes before morphological regression of the organ. Furthermore, this chapter

demonstrates that exposure to environmental hypoxia, like pseudohypoxia, prevents the regression of the organ of Zuckerkandl. Together, these findings suggest that HIF-2α signalling contributes to the maintenance of both the electrophysiological function and the retention of the organ of Zuckerkandl. Clusters of cells expressing cyclin D1 were identified in the organ of Zuckerkandl from aged pseudohypoxic mice, suggesting the presence of a potentially pre-neoplastic cell population. Finally, proliferating organ of Zuckerkandl paragangliomas were observed in a proportion of aged *Phd2ko* mice, providing evidence of a link between the persistence of the organ of Zuckerkandl and tumour formation, as well as a potential mouse model for investigating tumour initiation and evaluating therapeutic strategies.

5.2 **Results**

5.2.1 *Reduced HIF target gene expression in the wildtype organ of Zuckerkandl over the postnatal period*

The organ of Zuckerkandl is a foetal chromaffin cell structure that undergoes postnatal regression. Previous work demonstrated a reduction in the size of the organ of Zuckerkandl between postnatal day 0 (P0, the day of birth), P7 and P21 (Prange-Barczynska et al., 2024). To determine whether changes in organ size occur during the earlier perinatal period, wild-type mice were harvested at embryonic day 18 (E18), P0 and P3. The abdominal region, including the kidneys, aorta, inferior vena cava, renal arteries and ureters, was dissected, fixed and sectioned transversely. Immunohistochemistry for chromogranin A (CgA) and tyrosine hydroxylase (TH) was performed on sequential sections to detect the presence of chromaffin cells. In this region, structures positive for TH but lacking CgA staining were identified as sympathetic ganglia, allowing these to be distinguished from CgA-positive chromaffin tissue.

The volume of the organ of Zuckerkandl was estimated by quantifying the area of CgA-positive tissue across the serial sections. Despite the expected postnatal regression of this tissue, no significant difference in estimated organ of Zuckerkandl volume was observed between E18, P0 and P3 (**Figure 5.1A**). Therefore, within the timepoints examined, the overall volume of CgA-positive tissue remained relatively consistent.

It was hypothesised that the increase in oxygen availability associated with birth would be accompanied by reduced expression of HIF and its downstream targets. Expression of *Epas1* and selected HIF target genes was therefore examined in the organ of Zuckerkandl across these perinatal timepoints. *In situ* hybridisation was performed using probes against: *Epas1*, which encodes HIF-2α, *Rgs5*, which encodes regulator of G protein signalling, *Vegfa*, which encodes vascular endothelial growth factor A, and *Cox4i2*, which encodes an atypical cytochrome c oxidase subunit (**Figure 5.1B**). At E18, strong expression of *Epas1* was detected throughout the organ of Zuckerkandl, accompanied by strong expression of the HIF-2α target genes *Rgs5* and *Vegfa*, with weaker but readily detectible expression of *Cox4i2*. At P0, *Epas1* remained detectable across the organ of Zuckerkandl, although the signal appeared reduced compared with E18. A corresponding reduction in expression of the HIF-2α target genes was also observed, with the decrease particularly apparent for *Vegfa* and *Cox4i2*. By P3, expression of *Epas1*, *Rgs5*, *Vegfa* and *Cox4i2* in the wild-type organ of Zuckerkandl appeared further reduced.

Taken together, these findings demonstrate that although the estimated volume of the organ of Zuckerkandl did not significantly change between E18 and P3, expression of *Epas1* and several HIF-2α target genes decreased progressively following birth. This is consistent with a reduction in HIF-2α signalling following the increase in oxygen availability at birth, occurring before detectable changes in the overall volume of the organ of Zuckerkandl.

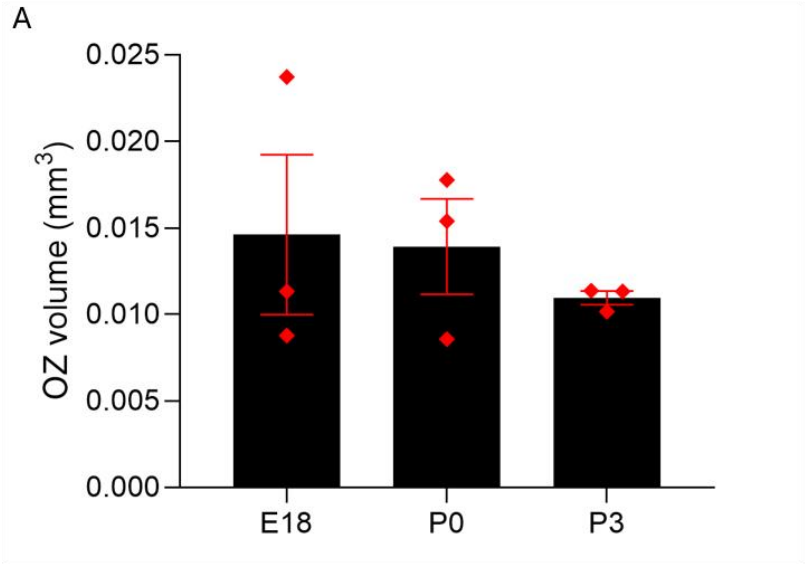
A
0.025
0.020
0.015
0.010
0.005
0.000
OZ volume (mm3)
E18
P0
P3

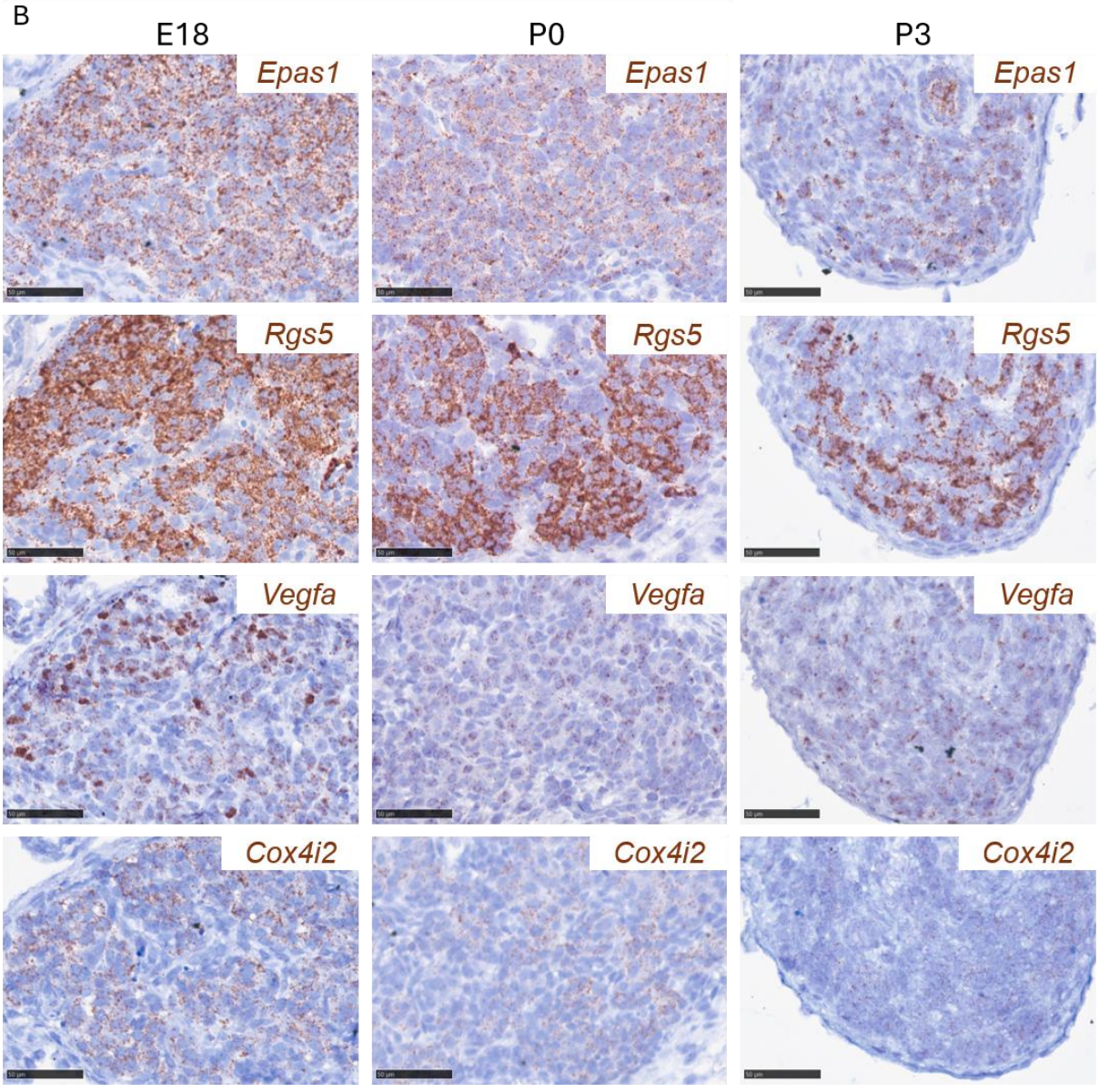
B
E18
P0
P3
Epas1
Epas1
Epas1
Rgs5
Rgs5
Rgs5
Vegfa
Vegfa
Vegfa
Cox4i2
Cox4i2
Cox4i2

Figure 5.1. Organ of Zuckerkandl volume and gene expression over the perinatal period. (A) Volume quantification of the organ of Zuckerkandl (OZ) in n = 3 wild-type mice harvested at embryonic day 18 (E18), postnatal day 0 (P0) and postnatal day 3 (P3). Data are presented as mean ± SEM and were analysed by a one-way ANOVA with Tukey's multiple comparisons test, differences were not significant. **(B)** Representative images of *in situ* hybridisation using probes against *Epas1*, *Rgs5*, *Vegfa* and *Cox4i2* on organ of Zuckerkandl tissue from wild-type mice harvested at these timepoints. Scale bars = 0.05 mm.

5.2.2 *The neonatal wild-type organ of Zuckerkandl is responsive to acute hypoxia*

The neonatal organ of Zuckerkandl secretes catecholamines in response to physiological stressors such as hypoxia (Brundin, 1966; Jones & Robinson, 1975). However, the temporal dynamics and cellular mechanisms underlying this response are not well characterised. In particular, it is unclear whether hypoxia directly activates exocytosis from chromaffin cells of the foetal organ of Zuckerkandl on a rapid timescale, similar to the oxygen chemosensitivity in the carotid body, or whether it instead alters catecholamine production to induce noradrenaline production through transcriptional or metabolic pathways. Therefore, to assess the electrophysiological response to hypoxia in these cells, wild-type mice expressing GCaMP6f under the control of the tyrosine hydroxylase promoter (*Ai95*$^{f/+}$*;THCre*) were used. This allowed tissue-restricted visualisation of Ca^{2+} activity in the organ of Zuckerkandl. The abdominal region from mice at embryonic day 18 (E18), P0 (the day of birth) and postnatal day three (P3) was dissected and the organ of Zuckerkandl was sub-dissected. The tissue was then placed under the fluorescent microscope and tested in the perfusion system described in the previous chapter. Cells which showed an increase in florescence in response to 45mM K^+ were deemed electrically excitable and selected for analysis (a representative image of the fluorescent response to K^+ is shown in **Figure 5.2A**).

Chromaffin cells in the organ of Zuckerkandl from wild-type mice at all three neonatal timepoints (E18, P0 and P3) showed gradual increases in GFP fluorescence in response to decreasing oxygen levels in the perfusate (illustrated by the representative trace in **Figure 5.2B** and in **Figure 5.2C**). Furthermore, upon reoxygenation, the level of GFP fluorescence dropped back to baseline levels, showing these hypoxia responses are reversible **(Figure 5.2B)**. The percentage of electrically excitable cells which responded to hypoxia varied between animals but was not statistically different between developmental timepoints **(Figure 5.2D)**. This variability may indicate that only a subset of organ of Zuckerkandl chromaffin cells are responsive to hypoxia, with the proportion of responsive cells varying between animals. Alternatively, as TH expression is not exclusive to chromaffin cells, some of the electrically excitable TH^+ cells recorded may represent another cell type, such as sympathetic ganglia, which are unresponsive to acute hypoxia.

Although the organ of Zuckerkandl from all three neonatal timepoints responded to acute hypoxia, the precise oxygen tension at which a fluorescent response was elicited varied between the different timepoints (**Figure 5.2D**). The organ of Zuckerkandl from mice harvested at E18 responded to the mildest levels of hypoxia, with an average P_{50} of 10% O_2. This sensitivity progressively decreased with age to 9% at P0 and 4% at P3. This suggests that the sensitivity of the oxygen chemosensing response in the organ of Zuckerkandl may decrease over time, prior to involution of the tissue. Together, this work provides the first molecular evidence that the neonatal organ of Zuckerkandl is directly oxygen chemosensitive, and demonstrates that HIF target gene expression and sensitivity to acute hypoxia decrease before the organ has fully regressed.

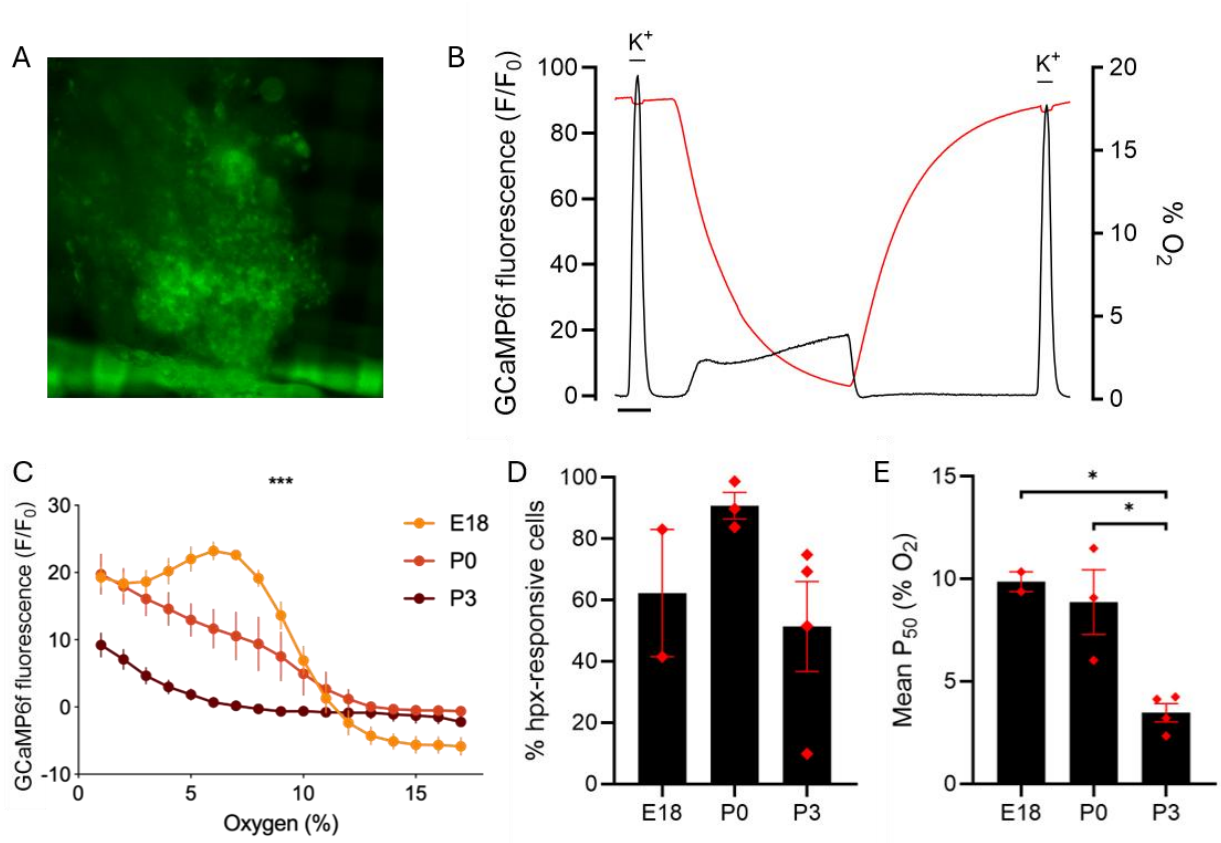

Figure 5.2. Oxygen chemosensitivity in the neonatal organ of Zuckerkandl decreases after birth. **(A)** Representative image showing GFP fluorescence in the organ of Zuckerkandl exposed to 45mM K^+ from a neonatal mouse expressing GCaMP6f (*Ai95*$^{f/+}$*;THCre*). **(B)** A representative trace showing F/F_0 fluorescence in the K^+-responsive cells from a neonatal (P0) organ of Zuckerkandl exposed to hypoxia. Oxygen tension is shown in red. **(C)** Non-linear regression of the fluorescent response to different oxygen tensions in the organ of Zuckerkandl from E18, P0 and P3 mice. p = 0.000649 (two-way ANOVA, column effect). **(D)** % of K^+-responsive cells that responded to hypoxia in the organ of Zuckerkandl across the neonatal timepoints. Data are presented as mean ± SEM. **(E)** Mean P_{50} (% of oxygen at which 50% of the maximal fluorescence response was achieved) in the organ of Zuckerkandl across the neonatal timepoints. Data are presented as mean ± SEM and analysed by one-way ANOVA with Tukey's multiple comparison's test, * $p < 0.05$.

5.2.3 *Comparison of the retained organ of Zuckerkandl in adult mice with developmental pseudohypoxic mutations*

Previous work has demonstrated that mice with developmental, TH-restricted HIF-2α-activating mutations retain their organ of Zuckerkandl in adulthood. This includes *Phd2ko* mice, *Hif-2αdPA* mice, and mice with mutations in both alleles of *Sdhb*. On the other hand, adult *Hif-1αdPA, Hif-2αdPA* DNA binding mutant and adult-onset *Hif-2αdPA* mice do not possess an organ of Zuckerkandl, suggesting that: its retention is dependent on the HIF-2α isoform; the transcriptional activity of HIF-2α is necessary for its maintenance; activation of HIF-2α must occur during the developmental period.

To further investigate the similarities and differences between the three pseudohypoxic mouse models with a retained organ of Zuckerkandl, the size and cellular morphology of this tissue were compared. *Sdhb$^{f/f}$;THCre* mice are used in these comparisons as the chromaffin cell phenotypes observed in all three mouse models with mutations in both alleles of *Sdhb* were indistinguishable (Chapter 4). Immunohistochemistry for TH and CgA was performed on sections throughout the abdominal region of the pseudohypoxic mice and the area of tissue expressing CgA was calculated to approximate the volume of the organ of Zuckerkandl. The organ of Zuckerkandl from *Phd2ko* mice was the largest, with an average volume of 0.125 (± 0.0234) mm^3, compared to 0.0536 (± 0.0129) mm^3 in *Hif-2αdPA* mice and 0.0123 (± 0.00251) mm^3 in *Sdhb$^{f/f}$;THCre* mice (**Figure 5.3C**).

The cellular morphology of the organ of Zuckerkandl chromaffin cells also differed between genotypes. In the retained organ of Zuckerkandl from *Phd2ko* and *Sdhb$^{f/f}$;THCre* mice, clear gaps in the cytosol of the chromaffin cells were present which did not stain for CgA or the haematoxylin counterstain (**Figure 5.3A**). In contrast, chromaffin cells in the *Hif-2αdPA* organ of Zuckerkandl did not exhibit this clear cell phenotype. Therefore, while all three

pseudohypoxic mouse models retain an organ of Zuckerkandl in adulthood, there are morphological differences in this tissue depending on the underlying mutation. These may reflect quantitative differences in the degree of HIF-2α activation between the models, or qualitative differences such as activation of HIF-1α signalling or other non-HIF targets in the *Phd2ko* and *Sdhb$^{f/f}$;THCre* mice.

To assess stabilisation of HIF-2α within the retained organ of Zuckerkandl in each of the pseudohypoxic models, immunohistochemistry for HIF-2α was also performed on the organ of Zuckerkandl from *Hif-2αdPA*, *Phd2ko* and *Sdhb$^{f/f}$;THCre* mice. This confirmed nuclear expression of HIF-2α in the majority of organ of Zuckerkandl chromaffin cells in all three pseudohypoxic genotypes (**Figure 5.3C**). However, while it allowed detection of stabilised HIF-2α protein, the sensitivity of HIF-2α immunohistochemistry was insufficient to detect quantitative differences in the level of HIF-2α stabilisation. Therefore, these findings demonstrate that HIF-2α is stabilised in the retained organ of Zuckerkandl across all three pseudohypoxic models, but cannot exclude whether differences in the degree of HIF-2α stabilisation, or stabilisation of HIF-1α or other non-HIF substrates, underlie the morphological differences observed.

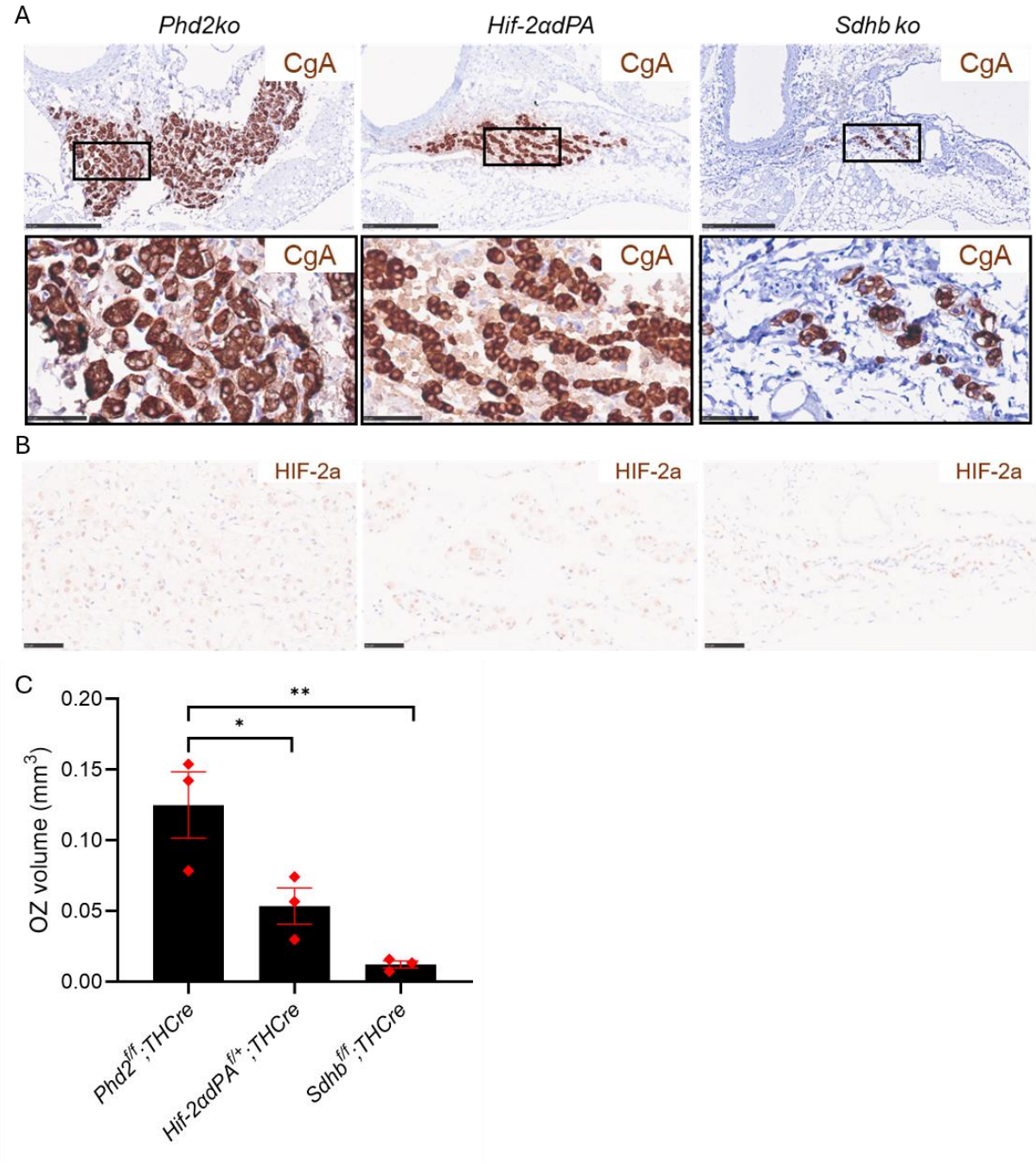

Figure 5.3. Comparison of the retained organ of Zuckerkandl across pseudohypoxic genotypes. **(A)** Representative images of chromogranin A (CgA) immunohistochemistry in transverse sections from the abdominal aorta region of adult *Phd2ko*, *Hif-2αdPA* and *Sdhb* mutant mice. Scale bars represent 0.25 mm on lower magnification images and 0.05 mm on high magnification inserts in black boxes below. **(B)** Representative images of HIF-2α immunohistochemistry in the organ of Zuckerkandl from these mice. Scale bars = 0.05 mm **(C)** Volume quantification of the organ of Zuckerkandl in n = 3 adult mice of each genotype Data are presented as mean ± SEM and were analysed by one-way ANOVA with Tukey's multiple comparisons, ** $p < 0.01$, * $p < 0.5$.

5.2.4 *Environmental hypoxia during the early postnatal period is sufficient to cause retention of the organ of Zuckerkandl*

It was next assessed whether environmental hypoxia, rather than genetic pseudohypoxia, during the perinatal period is sufficient to cause retention of the organ of Zuckerkandl in wild-type mice. Litters of three-day-old wild-type mice were placed into a normobaric hypoxia chamber at 10% oxygen and kept here for 19 days. 10% oxygen was selected in line with previous experiments in this laboratory (Bishop et al., 2013; Cheng et al., 2020; Fielding et al., 2018; Hodson et al., 2016); this is a similar level of oxygen to that at 19,000 feet above sea level (i.e. the top of Mount Kilimanjaro), so is a severe hypoxic stimulus. Mice were placed in the hypoxia chamber at three days old as placing pregnant mothers into hypoxia shortly before birth resulted in mothers cannibalising their pups. After 19 days in the hypoxia chamber, around half of the pups had died so the remaining mice were taken out of hypoxia and harvested (**Figure 5.4A**). Age-matched wild-type mice which were not exposed to hypoxia were also harvested as normoxic controls. The abdominal regions from these mice were dissected, fixed, processed and embedded in paraffin. Immunohistochemistry for CgA and TH was performed on sequential sections throughout to detect the presence of chromaffin cells.

In the normoxic control mice, the organ of Zuckerkandl had almost completely regressed by 22 days old, with only a few chromaffin cells detected in this region (**Figure 5.4B**). On the other hand, significantly more $CgA^{+}TH^{+}$ chromaffin cells were present in the abdominal region of the wild-type mice that were exposed to hypoxia in the postnatal period. These chromaffin cells formed a cluster along the abdominal aorta, indicating the presence of a retained organ of Zuckerkandl. The volume of the organ of Zuckerkandl from the normoxic and hypoxic mice was estimated by calculating the area of tissue positive for CgA on sequential sections

throughout the abdominal region. This confirmed that the volume of the organ of Zuckerkandl in the mice exposed to perinatal hypoxia was significantly greater than age-matched normoxic control mice (**Figure 5.4C**). Therefore, environmental exposure to 10% oxygen during the postnatal period, like developmental pseudohypoxic mutations, is sufficient to confer retention of the organ of Zuckerkandl.

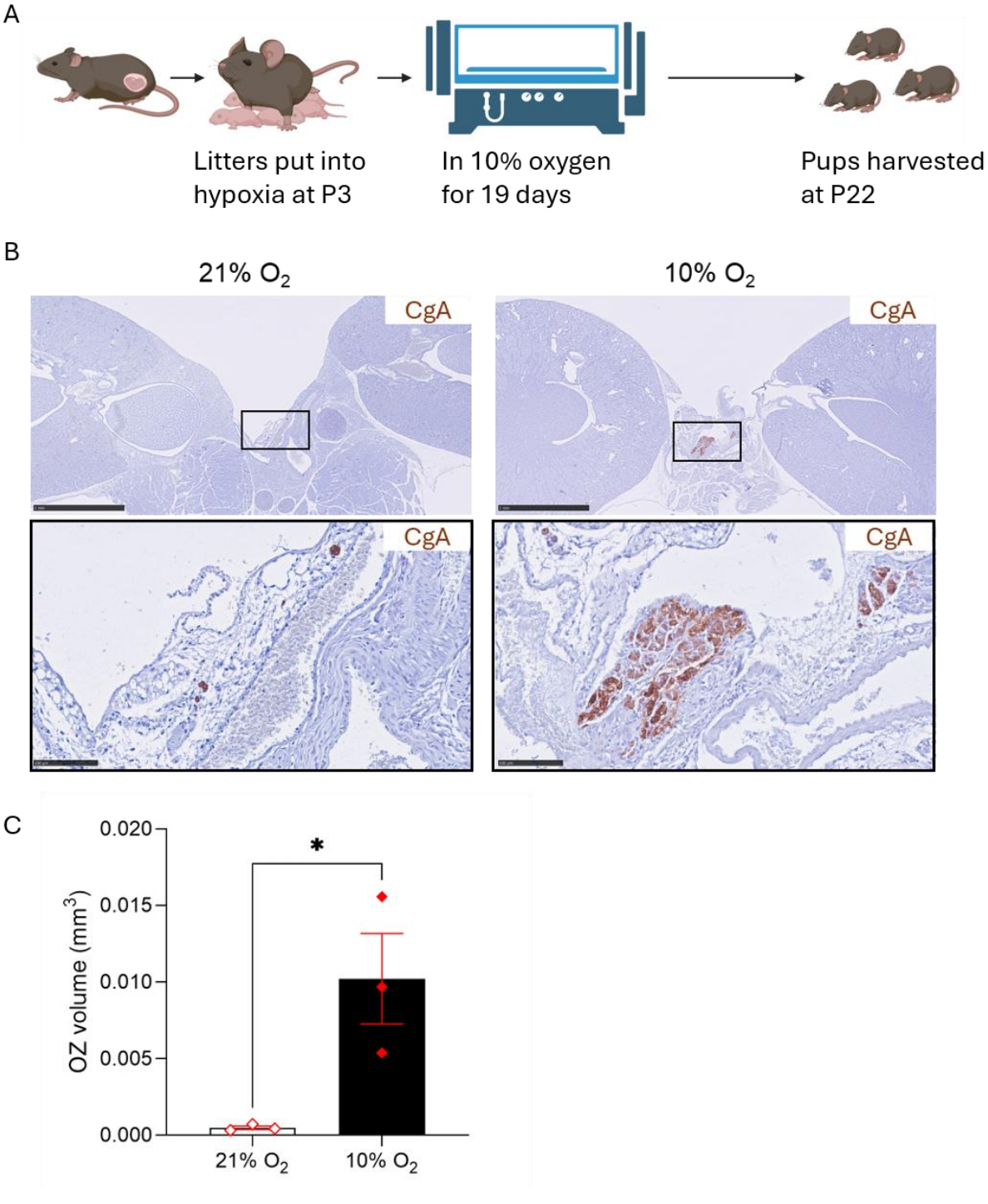

Figure 5.4. Exposure to 10% oxygen during the postnatal period is sufficient to confer retention of the organ of Zuckerkandl. (A) Schematic showing the experimental design. Mice were put into the hypoxia chamber at 10% oxygen at P3 then taken out and harvested at P22. Figure was made using biorender.com. **(B)** Representative images of chromogranin A (CgA) immunohistochemistry in transverse sections from the abdominal aorta region of mice kept in normoxic conditions (left) versus mice kept in 10% oxygen (right) during this postnatal period. Scale bars = 1 mm on lower magnification images and 0.1 mm on higher magnification images in black boxes below. **(C)** Volume quantification of the organ of Zuckerkandl in n = 3 control and hypoxic mice. Data are presented as mean ± SEM and were analysed by unpaired t-test, * $p < 0.5$.

5.2.5 *Interaction between environmental hypoxia and pseudohypoxia*

Clinical observations suggest that chronic systemic hypoxaemia may modify the effects of pseudohypoxic mutations and promote paraganglioma development. Patients with congenital cyanotic heart disease (CCHD) have an increased risk of developing pheochromocytomas and paragangliomas (Opotowsky et al., 2015), and *EPAS1* gain-of-function mutations are markedly enriched in CCHD-associated tumours (Arenillas et al., 2025; Vaidya et al., 2018). Furthermore, in a cohort of patients with pheochromocytomas and paragangliomas, approximately one third also had an underlying hypoxaemia-associated haemoglobin disorder (Mancini et al., 2024; Vaidya et al., 2018).

To determine whether environmental hypoxia similarly modifies the effect of pseudohypoxia in the postnatal retention of the organ of Zuckerkandl, *Phd2ko* mice were exposed to 10% oxygen in the normobaric hypoxia chamber from P3 to P22. This genotype was selected based on mouse availability. At P22, mice were harvested and, as described above, the abdominal region was immunostained for CgA and TH to assess the presence and volume of the organ of Zuckerkandl. Postnatal hypoxia resulted in a significant, approximately four-fold reduction in organ of Zuckerkandl volume in *Phd2ko* mice compared with age-matched *Phd2ko* mice maintained under normoxic conditions (**Figure 5.5A and B**). Nevertheless, the organ of

Zuckerkandl in hypoxic *Phd2ko* mice remained approximately 2.5-fold larger than that of hypoxic wild-type mice (**Figure 5.4C**). Therefore, environmental hypoxia substantially attenuated the enlargement of the organ of Zuckerkandl caused by *Phd2* inactivation but did not completely reverse the pseudohypoxic phenotype.

These findings suggest that environmental hypoxia modifies, rather than simply enhances, the effect of pseudohypoxia on postnatal retention of the organ of Zuckerkandl. In *Phd2ko* mice, hypoxic exposure substantially reduced the volume of the retained organ of Zuckerkandl, despite the association of chronic systemic hypoxia with increased pheochromocytoma and paraganglioma risk and enrichment of gain-of-function *EPAS1* mutations in human tumours. Therefore, the effects of environmental hypoxia on the developmental phenotype produced by pseudohypoxia are not necessarily concordant with its association with tumour susceptibility in humans and may depend on the precise genetic mutation.

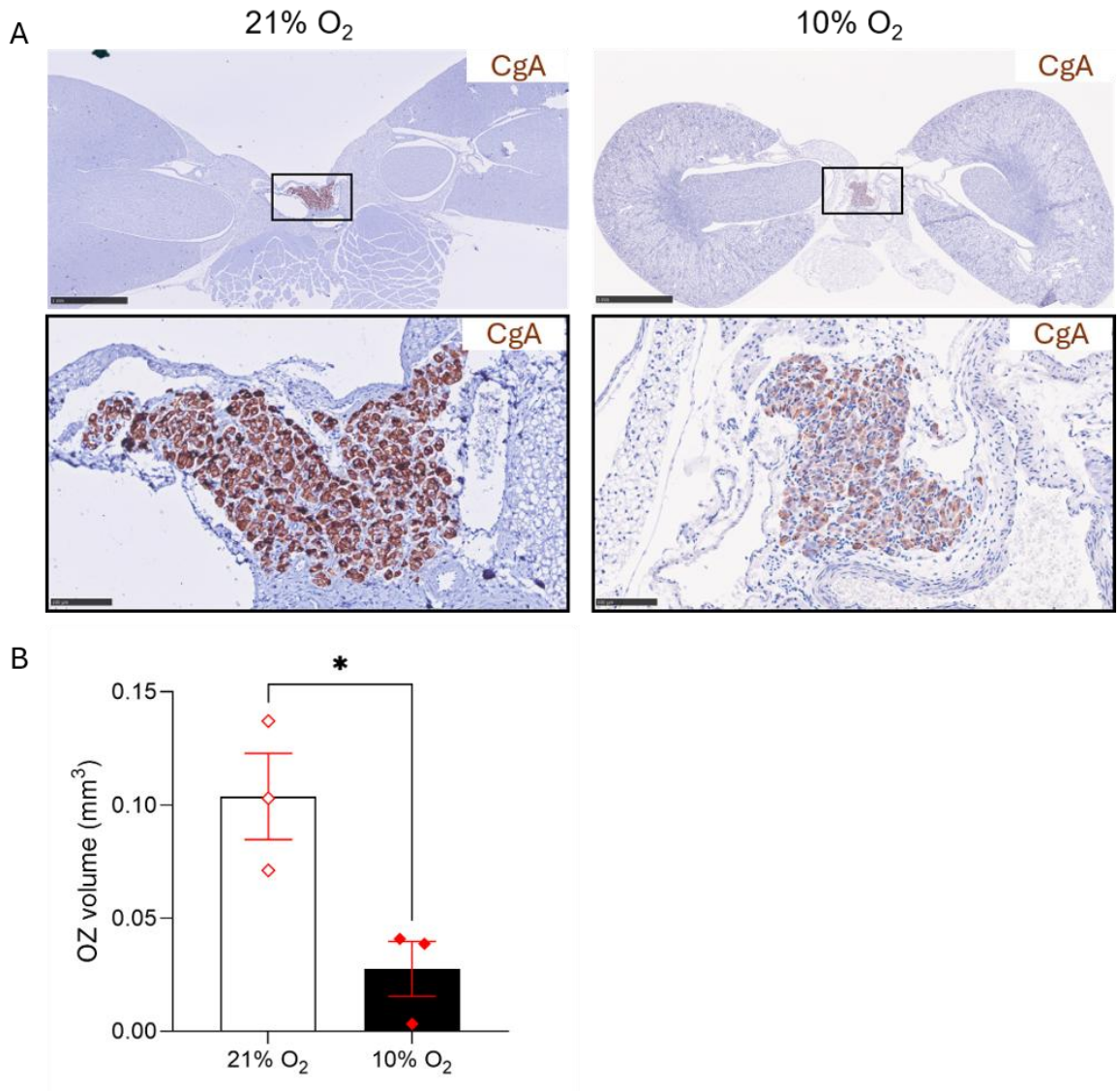

Figure 5.5. Exposure to 10% oxygen during the postnatal period causes a smaller organ of Zuckerkandl in *Phd2ko* mice. (A) Representative images of chromogranin A (CgA) immunohistochemistry in transverse sections from the abdominal aorta region of *Phd2ko* mice kept in normoxic conditions (left) versus mice kept in 10% oxygen (right) during this postnatal period. Scale bars = 1 mm on lower magnification images and 0.1 mm on higher magnification images in black boxes below. **(B)** Volume quantification of the organ of Zuckerkandl in n = 3 control and hypoxic mice. Data are presented as mean ± SEM and were analysed by unpaired t-test, * $p < 0.5$.

5.2.6 *A proportion of aged Phd2ko mice develop proliferating organ of Zuckerkandl paragangliomas*

The *Hif-2αdPA*, *Phd2ko* and *Sdhb*-inactivated mouse models described in this thesis were developed with the aim to model pseudohypoxic pheochromocytomas and paragangliomas. In previous experiments, these mice have been harvested at approximately 6-8-weeks-old to represent adulthood. All three pseudohypoxic models mice retain their organ of Zuckerkandl at this timepoint but do not exhibit frank tumours. To assess whether these developmental pseudohypoxic mutations could lead to paraganglioma tumorigenesis over time, cohorts of *Phd2ko* and *Hif-2αdPA* mice were aged. Mice with mutations in both alleles of *Sdhb* could not be maintained beyond approximately eight weeks of age due to severe runting and weakness, preventing assessment of tumour development over time in this model.

The *Phd2ko* and *Hif-2αdPA* cohorts were harvested once the mice had reached at least 16 months of age; this timepoint was selected to allow sufficient time for tumour development. The abdominal regions were serially sectioned and immunostained for CgA and TH, both established markers of chromaffin cells. Expression of CgA enabled distinction of chromaffin tissue from surrounding TH^+ sympathetic ganglia. All aged pseudohypoxic mice examined possessed a retained organ of Zuckerkandl. In addition, 2/8 *Phd2$^{f/f}$;THCre* and 2/8 *Phd2$^{f/-}$;THCre* mice developed lesions contiguous with, or near to, the retained organ of Zuckerkandl that expressed both CgA and TH (**Figure 5.6 and Table 5.1**). These lesions were classified as organ of Zuckerkandl paragangliomas based on their increased size, cellular organisation, vascular architecture and altered chromaffin cell morphology. The tumours displayed a characteristic nested or Zellballen-like organisation of chromaffin cells, surrounded by vascular cells identified by CD31 immunostaining (**Figure 5.6C**). This organisation is consistent with the histological architecture used to identify human paragangliomas, in which nests of

chromaffin cells are separated by an extensive vascular network (Guilmette & Sadow, 2019). These lesions exhibited altered chromaffin cell morphology compared with the retained non-tumour organ of Zuckerkandl, with no evidence of cellular clearing (**Figure 5.6C**). In several cases, tumour tissue and retained non-tumour organ of Zuckerkandl were present on the same section and were directly contiguous, allowing the distinct morphology of the tumour and adjacent non-tumour tissue to be observed **(Figure 5.6D)**.

No frank organ of Zuckerkandl paragangliomas were detected in the abdominal region of ten aged *Hif-2αdPA* mice (**Table 5.1**). An abnormality characterised by a cluster of ectopic chromaffin cells separate from the retained organ of Zuckerkandl was observed in one mouse but was not classified as a tumour because it lacked the nested conformation and cellular morphology observed in the frank tumours. Given the limited size of the aged cohorts, which was constrained by the timescale of this thesis, this data does not exclude the possibility that *Hif-2αdPA* mice can develop frank organ of Zuckerkandl paragangliomas, although the absence of tumours in this cohort suggests that if they occur, they may be relatively uncommon. Therefore, this chapter demonstrates the first pseudohypoxic mouse model of frank paragangliomas in the aged *Phd2ko* mice.

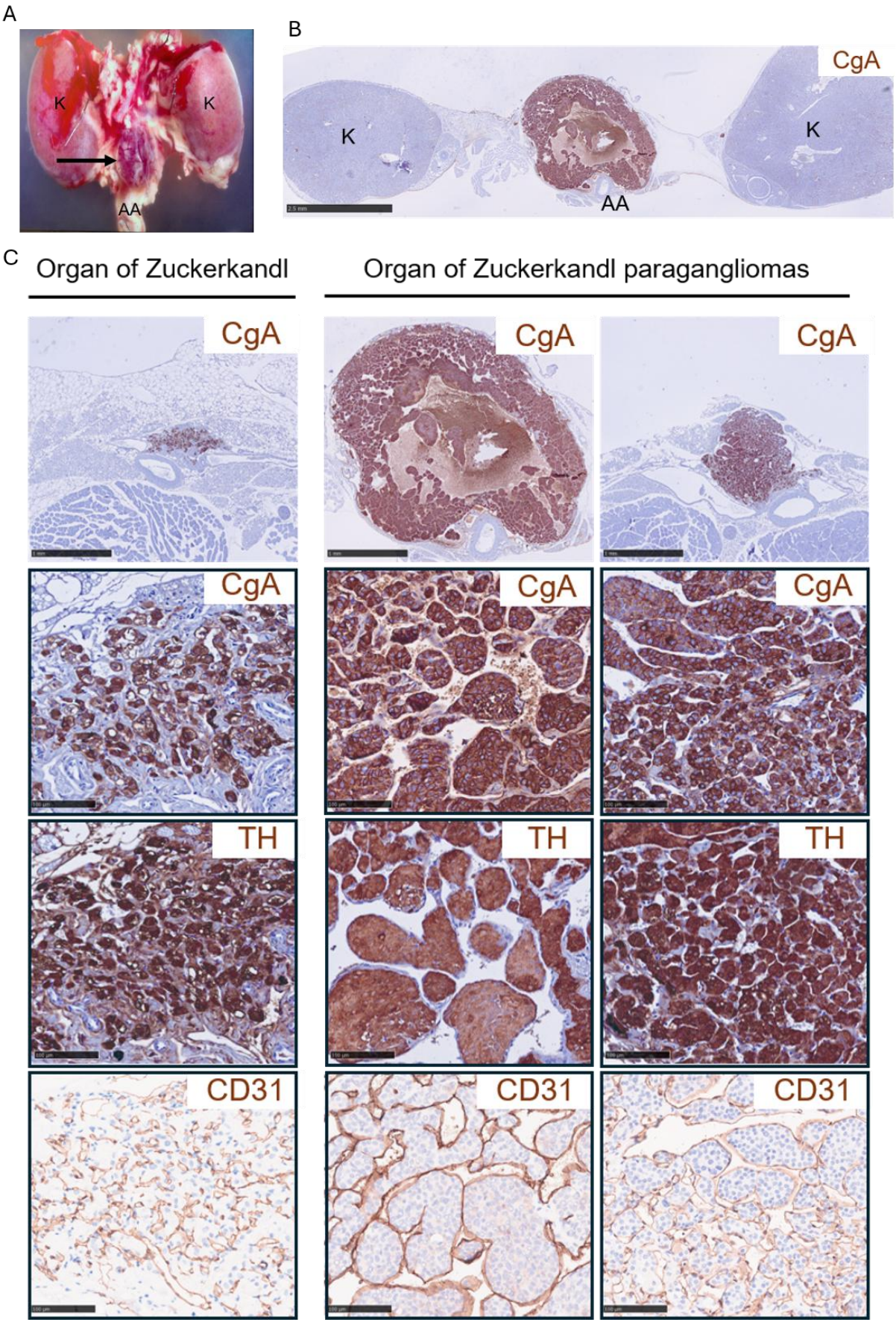
A
K
K
AA
B
CgA
K
K
AA
C
Organ of Zuckerkandl
Organ of Zuckerkandl paragangliomas
CgA
CgA
CgA
CgA
CgA
CgA
TH
TH
TH
CD31
CD31
CD31

D

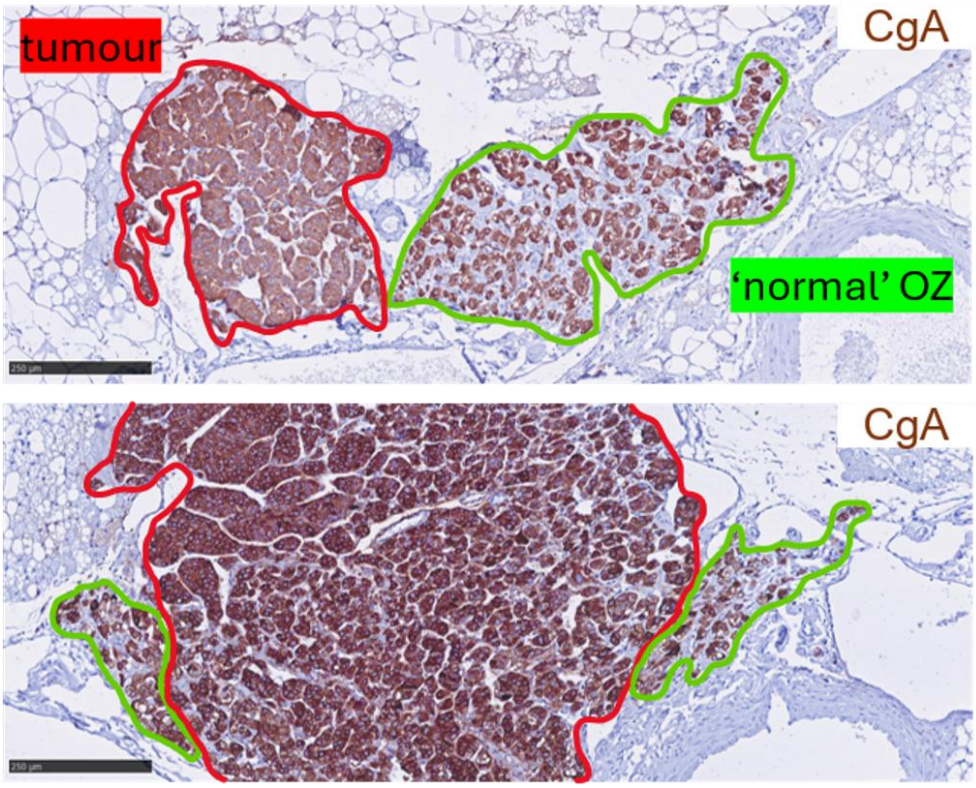

Figure 5.6. Development of organ of Zuckerkandl paragangliomas in aged *Phd2ko* mice. (A) Macroscopic image showing a large organ of Zuckerkandl paraganglioma (arrow) in an aged *Phd2ko* mouse. K = kidneys, AA = abdominal aorta. **(B)** Chromogranin A (CgA) immunohistochemistry on a transverse section of the abdominal aorta region shown in (A), showing the large organ of Zuckerkandl paraganglioma. K = kidney, AA = abdominal aorta. **(C)** Representative images of CgA, tyrosine hydroxylase (TH) and CD31 immunohistochemistry in a non-neoplastic retained organ of Zuckerkandl from an aged *Phd2ko* mouse (left panel) versus organ of Zuckerkandl paragangliomas from two aged *Phd2ko* mice (right). Scale bars = 1 mm on top row images and 0.1 mm on images below in black boxes. **(D)** CgA immunohistochemistry on sections demonstrating organ of Zuckerkandl paragangliomas (outlined in red) contiguous to non-neoplastic organ of Zuckerkandl tissue (outlined in green).

Genotype	Incidence in females	Incidence in males
Phd2$^{f/-}$;THCre	2/6	0/2
Phd2$^{f/f}$;THCre	2/8	0/0
Hif-2adPA$^{f/+}$;THCre	0/7 (but 1 abnormal)	0/3

Table 5.1 Incidence of organ of Zuckerkandl paragangliomas in aged pseudohypoxic mice by genotype and sex. Incidence is expressed as the number of mice with organ of Zuckerkandl paragangliomas out of the total number of mice examined for each genotype and sex. One female *Hif-2αdPA* mouse exhibited an abnormal organ of Zuckerkandl which did not meet the criteria for frank organ of Zuckerkandl paragangliomas.

5.2.7 *HIF-2α and HIF target gene expression in the frank organ of Zuckerkandl paragangliomas*

Having identified organ of Zuckerkandl paragangliomas in aged *Phd2ko* mice, HIF-2α expression was examined to determine whether the tumours retained evidence of pseudohypoxic HIF pathway activation. Immunohistochemistry for HIF-2α was performed on tumour sections and age- and genotype-matched non-tumour organ of Zuckerkandl control tissue. This enabled assessment of persistent HIF-2α stabilisation in the paragangliomas and comparison with HIF-2α expression in the retained non-tumour organ of Zuckerkandl. Nuclear HIF-2α staining was detected in the majority of chromaffin cells in both the non-tumour organ of Zuckerkandl from aged *Phd2ko* mice and in the frank organ of Zuckerkandl paragangliomas (**Figure 5.7**). However, the DAB staining intensity appeared stronger in the tumours than in the control tissue, suggesting increased HIF-2α stabilisation.

To determine whether the increased HIF-2α stabilisation in the tumours corresponded with increased expression of HIF-2α target genes, expression of *Rgs5*, *Vegfa* and *Cox4i2* was assessed in the paragangliomas and non-tumour organ of Zuckerkandl from age-matched mice. *Rgs5* encodes a GTPase-activating protein, *Vegfa* promotes angiogenesis, and *Cox4i2* encodes an atypical mitochondrial subunit which is enriched in the oxygen chemosensitive carotid body. *In-situ* hybridisation revealed mRNA transcript expression of all three genes in the non-tumour organ of Zuckerkandl and in the organ of Zuckerkandl paragangliomas from age-matched *Phd2ko* mice (**Figure 5.7**). The intensity of signal for the HIF-2α target genes appeared stronger

in the tumours compared with non-tumour control tissue, consistent with increased HIF-2α activity, although quantitative RNA detection methods would be required to confirm differences in transcript abundance.

Together, these findings demonstrate that a proportion of aged *Phd2ko* mice develop organ of Zuckerkandl paragangliomas. These tumours retain strong nuclear HIF-2α expression and expression of HIF-2α target genes, consistent with persistent pseudohypoxic activation of the HIF pathway following *Phd2* loss.

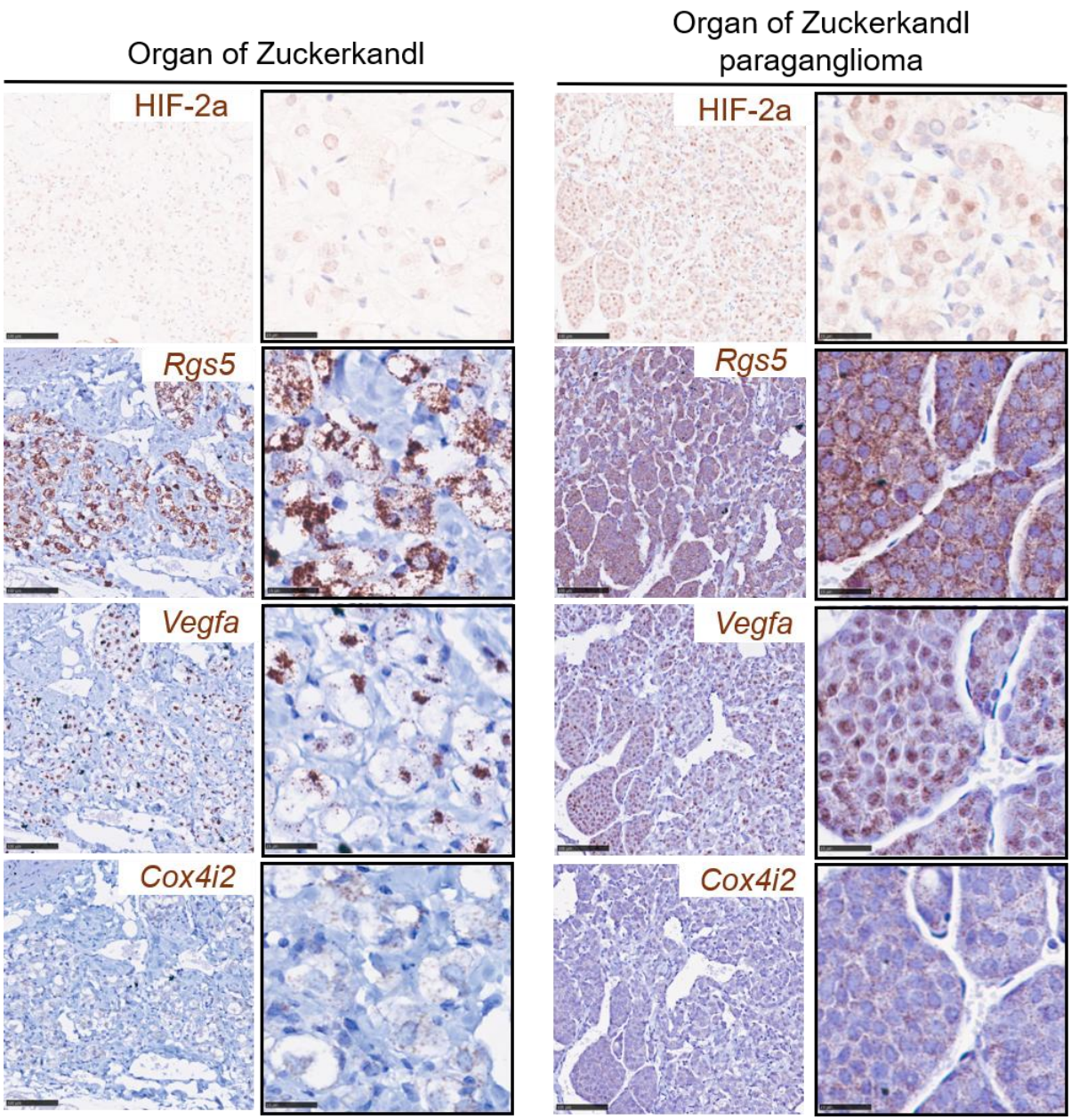

Figure 5.7. HIF-2α and HIF-2α target gene expression in the non-neoplastic organ of Zuckerkandl versus an organ of Zuckerkandl paraganglioma. Representative images showing immunohistochemistry for HIF-2α (protein) and *in situ* hybridisation for *Rgs5*, *Vegfa* and *Cox4i2* (mRNA) in a non-neoplastic organ of Zuckerkandl (left) versus an organ of Zuckerkandl paraganglioma (right), both from aged *Phd2ko* mice. Scale bars = 0.01 mm on lower magnification images and 0.025 mm on higher magnification images (outlined in black boxes).

5.2.8 *Increased proliferation markers in the frank organ of Zuckerkandl paragangliomas*

To determine whether the development of organ of Zuckerkandl paragangliomas was associated with increased cellular proliferation, the expression of proliferation markers was compared between the paragangliomas and the non-tumour organ of Zuckerkandl from aged *Phd2ko* mice. Ki67 is expressed during the G1, S, G2 and mitotic phases of the cell cycle but strongly downregulated during G0. The percentage of cells in a tumour which are expressing Ki67, known as the Ki67 index, is commonly used as a marker of tumour cell proliferation, and higher levels of Ki67 are generally associated with more aggressive disease (Scholzen & Gerdes, 2000). Immunohistochemistry using an antibody against Ki67 revealed very few cells expressing Ki67 in the non-tumour organ of Zuckerkandl from aged *Phd2ko* mice. In contrast, nuclear expression of Ki67 was detected in a proportion of cells in the organ of Zuckerkandl paragangliomas (**Figure 5.8A and B**), suggesting increased proliferative activity in the tumour tissue. The very low proportion of $Ki67^+$ cells in one tumour was attributable to weak staining that did not meet the detection threshold, rather than an absence of Ki67 expression. This contrasts with the non-tumour tissue, in which Ki67 expression was not visibly detected.

Cyclin D1, encoded by *CCND1*, was also assessed as another marker of cell proliferation. Cyclin D1 drives progression of the cell cycle from the G1 to S phase through binding to cyclin-dependent kinase 4 (CDK4) and CDK6, leading to phosphorylation of the retinoblastoma protein (RB) and activation of E2F transcription factor. Cyclin D1 was of particular interest as it is a direct HIF-2 transcriptional target in VHL-deficient clear cell renal cell carcinoma (ccRCC), and a germline ccRCC susceptibility locus has been identified in a HIF-responsive distal enhancer of CCND1 (Schödel et al., 2012). *In situ* hybridisation revealed low levels of *Ccnd1* mRNA transcript expression throughout the non-tumour organ of Zuckerkandl versus increased *Ccnd1* mRNA expression throughout the organ of Zuckerkandl paragangliomas

(**Figure 5.8A**). Immunohistochemistry demonstrated that cyclin D1 protein expression was also increased in the organ of Zuckerkandl paragangliomas compared to the non-tumour organ of Zuckerkandl (**Figure 5.8A**). Quantification of DAB-positive staining demonstrated nuclear cyclin D1 protein expression in 13.2 (± 9.04) % of cells in the non-tumour organ of Zuckerkandl, compared to 72.9 (± 7.89) % of tumour cells (**Figure 5.8C**).

Together with the increased Ki67 expression, the increase in cyclin D1 mRNA and protein in the organ of Zuckerkandl paragangliomas suggests that the tumours contain a greater proportion of cells undergoing active cell cycle progression than the age-matched non-tumour organ of Zuckerkandl. The proportion of cells expressing cyclin D1 was substantially greater than those expressing Ki67 in both tumour and control tissue, potentially reflecting differences in the cell cycle stages where these markers are expressed, or non-proliferative functions of cyclin D1.

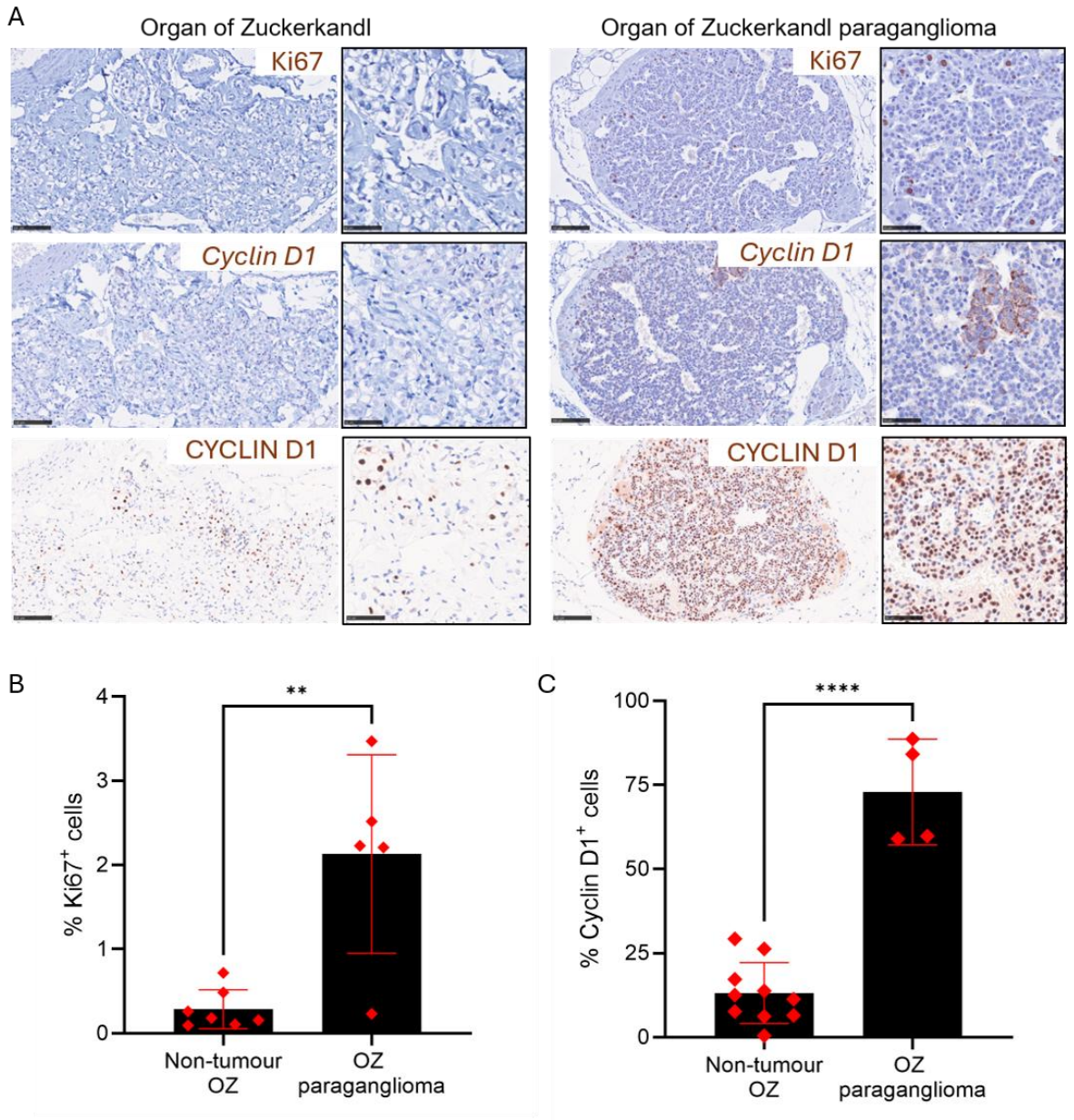

Figure 5.8. Increased expression of proliferation markers in the frank organ of Zuckerkandl paragangliomas versus the non-neoplastic organ of Zuckerkandl from age-matched *Phd2ko* mice. **(A)** Representative images of immunohistochemistry for Ki67 (top) and *in situ* hybridisation (middle) and immunohistochemistry (bottom) for cyclin D1 in the non-neoplastic organ of Zuckerkandl (left) compared to organ of Zuckerkandl paragangliomas (right) from aged *Phd2ko* mice. Scale bars = 0.1 mm on lower magnification images and 0.05 mm on higher magnification inserts (outlined in black boxes). **(B)** % of cells with nuclear Ki67 staining in the non-neoplastic organ of Zuckerkandl (OZ) versus organ of Zuckerkandl paragangliomas. n = 4 mice had organ of Zuckerkandl paragangliomas but one mouse had two distinct regions of tumour which were stained for Ki67. Data are presented as mean ± SEM and were analysed by an unpaired t-test, ** $p < 0.01$. **(B)** % of cells with nuclear cyclin D1 protein staining by immunohistochemistry in the non-neoplastic organ of Zuckerkandl (OZ) versus

organ of Zuckerkandl paragangliomas. Data are presented as mean ± SEM and were analysed by an unpaired t-test, **** $p < 0.0001$.

5.2.9 *The non-tumour organ of Zuckerkandl from aged Phd2ko mice contains clusters of cyclin D1-expressing cells*

Although cyclin D1 expression was lower in the non-tumour organ of Zuckerkandl from aged *Phd2ko* mice than in the organ of Zuckerkandl paragangliomas, the presence of cyclin D1 mRNA and protein in the non-tumour tissue raised the possibility that a proportion of these chromaffin cells may be proliferative. To determine whether cyclin D1 was also expressed in the organ of Zuckerkandl of young adult mice and whether its expression changed with age, immunohistochemistry was performed on tissue from young adult and aged *Phd2ko* mice (**Figure 5.9A**).

Cyclin D1 expression was detected in the organ of Zuckerkandl at both ages, although staining appeared more intense in aged tissue. Therefore, the number of cells with nuclear cyclin D1 staining was quantified using two intensity thresholds: a 'weak' threshold to identify cells expressing any detectable cyclin D1 and a 'strong' threshold to identify cells with higher levels of expression. Approximately 25% of organ of Zuckerkandl chromaffin cells were positive at the weak threshold in both young adult and aged *Phd2ko* mice, indicating that the proportion of cells expressing detectable cyclin D1 was similar at the two ages (**Figure 5.9B**). However, the intensity and spatial distribution of staining differed between age groups. In young adult tissue, cyclin D1-positive cells generally showed faint staining and were distributed throughout the organ, whereas in aged *Phd2ko* mice, positive cells showed stronger staining and frequently appeared in clusters, or 'rests'. Quantification of the number of cells within cyclin D1-positive clusters, with clusters defined as two or more cells with boundaries less than 0.5 μm apart, showed a significant increase in the cluster size in aged compared to young adult *Phd2ko* mice

(p = 0.03) **(Figure 5.9C)** (analysis performed by Jeremy Nielsen). Therefore, although the proportion of chromaffin cells expressing any detectable cyclin D1 remained similar, aging in *Phd2ko* mice was associated with increased intensity of cyclin D1 expression and greater clustering of cyclin D1-positive cells. These clusters may represent local populations with increased proliferative potential and could therefore indicate the emergence or expansion of a proliferative, pre-neoplastic population within the non-tumour organ of Zuckerkandl with age, potentially representing an early stage in paraganglioma development.

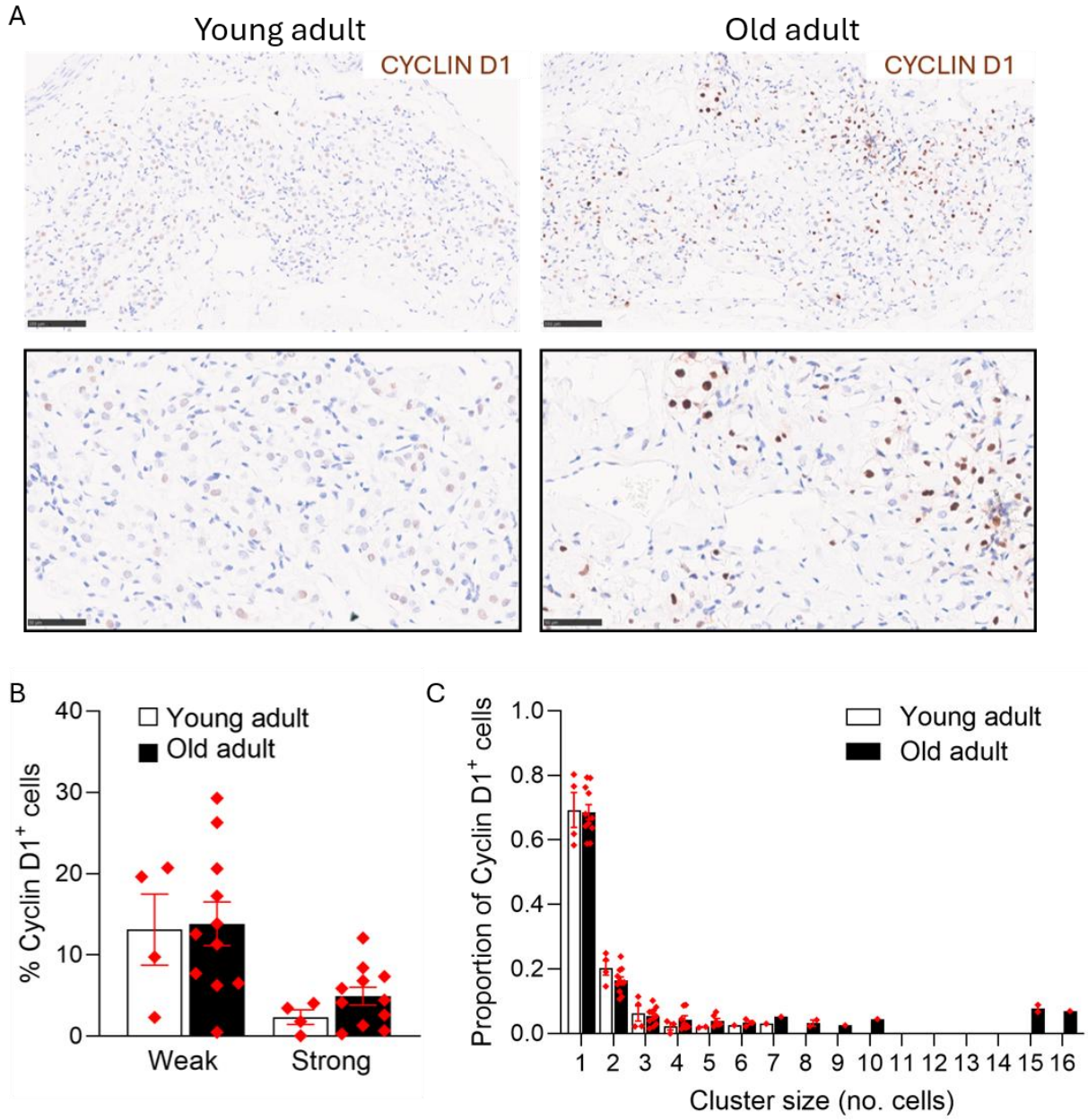

Figure 5.9. 'Rests' of cyclin D1-expressing cells in the retained organ of Zuckerkandl from aged, but not young adult, *Phd2ko* mice. (A) Representative images of cyclin D1 immunohistochemistry on the retained, non-tumour organ of Zuckerkandl from young adult *Phd2ko* mice versus aged *Phd2ko* mice. Scale bars = 0.1 mm on lower magnification images and 0.05 mm on higher magnification inserts below outlined in black boxes. **(B)** % of cells expressing cyclin D1 in the retained organ of Zuckerkandl from young adult versus old adult *Phd2ko* mice using a weak and strong detection threshold in QuPath. Data are presented as mean ± SEM and were analysed by one-way ANOVA with Šídák's multiple comparisons test. **(C)** Quantification of the cluster size of cyclin $D1^+$ cells, with a cluster defined as two or more cells with boundaries less than 0.5 μm apart. Statistical analysis was performed using a two-sided Kolmogorov-Smirnov test in the R statistical software (v4.6.1), $p = 0.03$.

5.3 **Discussion**

This chapter provides further investigation into the organ of Zuckerkandl, a foetal chromaffin cell structure which typically regresses after development. Acute oxygen chemosensitivity was shown in the organ of Zuckerkandl from wild-type mice across three neonatal timepoints, with the sensitivity of this response decreasing post-birth prior to the complete physical regression of this tissue. Furthermore, this chapter demonstrates, for the first time, that environmental hypoxia in the postnatal period is sufficient to confer retention of the organ of Zuckerkandl, similar to the pseudohypoxic mutations detailed earlier in this thesis. Moreover, this chapter describes the first incidence of frank organ of Zuckerkandl paragangliomas in a pseudohypoxic mouse model, providing a useful model of investigation into the human tumour syndrome. These tumours contained high levels of the HIF target gene and cell cycle marker cyclin D1, indicating active proliferation. Clusters of cyclin D1-expressing cells were also detected in the non-neoplastic organ of Zuckerkandl from aged mice, suggesting the emergence of potentially pre-neoplastic populations of cells in this tissue over time.

A limitation of the environmental hypoxia experiments described in this chapter is that the level of hypoxia was more severe than is physiologically relevant to most human populations. Mice

were exposed to 10% oxygen, corresponding to the oxygen availability at an altitude of almost 6,000 meters above sea level. While 10% oxygen induces robust physiological responses, it is substantially more severe than the degree of hypoxia experienced by populations living at high altitude locations and may not accurately model the milder chronic hypoxaemia observed in many human disease states. It will therefore be important to determine whether the retention of the organ of Zuckerkandl persists at lower, more physiologically relevant levels of hypoxia, such as 12-15% O_2, which more closely reflect the oxygen availability at inhabited high-altitude locations. Furthermore, in these experiments mice were exposed to hypoxia in the postnatal period, whereas prenatal hypoxaemia is of considerable interest given that altered HIF signalling during development influences the persistence of the organ of Zuckerkandl and, potentially, susceptibility to paraganglioma formation in later life. Using a higher oxygen tension may permit extending the timeline of hypoxia to cover the prenatal period without compromising survival of the pups. An additional question is whether HIF activity is only required during the perinatal window to confer retention of the organ of Zuckerkandl, or whether continued HIF activity is necessary for its maintenance in adulthood. This could be addressed by exposing mice to hypoxia during the perinatal period and subsequently returning them to normoxia for a defined window of time before harvest. Collectively, these experiments would establish the physiological range over which hypoxia promotes the retention of the organ of Zuckerkandl and may have clinical relevance for individuals carrying pseudohypoxic paragangliomas susceptibility variants. In particular, they could help determine whether exposure to severe hypoxia during pregnancy or early life exacerbates the incidence of tumour formation.

Despite the caveats of the current experiments, retention of the organ of Zuckerkandl in mice following developmental hypoxia or pseudohypoxia may have important implications for human physiology. If similar retention occurs in humans exposed to chronic hypoxaemia

during development, either as a consequence of pseudohypoxic mutations, hypoxaemia-causing pathology or residence at high altitude, this could result in persistent alterations in catecholamine production into adulthood. The organ of Zuckerkandl is a source of circulating noradrenaline. Therefore, its retention may cause an increase in the absolute concentration of noradrenaline in the blood and alter the relative balance of circulating catecholamines. Given that noradrenaline acts predominantly through α1-adrenergic receptors on vascular smooth muscle cells to promote vasoconstriction, increased noradrenaline from the organ of Zuckerkandl could contribute to increased vascular resistance and hypertension, affecting vascular workload and sympathetic tone. Furthermore, pseudohypoxic mice retained other immature chromaffin cell phenotypes in adulthood, including reduced *Pnmt* expression in the adrenal medulla. As PNMT catalyses the conversion of noradrenaline to adrenaline, increased noradrenaline production and reduced adrenaline production from the adrenal medulla may further exacerbate this shift in catecholamine balance. Therefore, *Pnmt* expression in the adrenal medulla of mice exposed to postnatal environmental hypoxia should also be assed to determine whether, like mice with pseudohypoxic mutations, their immature chromaffin cell phenotype extends beyond retention of the organ of Zuckerkandl. Furthermore, measurement of circulating catecholamines in the pseudohypoxic and hypoxic mice would establish whether the observed phenotypes translate into altered systemic catecholamine balance and provide further insight into their potential long-term cardiovascular consequences.

As well as potential cardiovascular implications, aberrant retention of the organ of Zuckerkandl in humans may increase susceptibility to paraganglioma development. The identification of organ of Zuckerkandl paragangliomas in aged *Phd2ko* mice, which retain their organ of Zuckerkandl into adulthood, raises the possibility that this ectopically retained tissue serves as a cellular substrate from which tumours can arise. This is supported by the anatomical location of these tumours, which often occurred contiguously with the non-tumour organ of

Zuckerkandl. A similar relationship between persistent embryological tissues and tumorigenesis has been described in other contexts, including notochordal remnants which can give rise to chordoma (Barber et al., 2021). However, lineage tracing studies will be required to determine whether paragangliomas arise directly from the retained organ of Zuckerkandl. Specifically, *Phd2* mutant mice could be crossed with a tdTomato reporter line under the control of a chromaffin cell-specific Cre driver to permanently label chromaffin cells and their descendants during development. Detection of tdTomato within tumour cells in aged mice would support a developmental chromaffin cell origin and, together with their anatomical contiguity with the retained organ of Zuckerkandl, would provide evidence that retained organ of Zuckerkandl tissue serves as a cellular substrate for tumour development. THCre would not be optimal for this purpose as TH is expressed in both chromaffin cells and sympathetic ganglia. Instead, a driver with greater specificity for the chromaffin cell lineage would be preferable.

The cyclin D1-positive chromaffin cell rests observed in the non-tumour organ of Zuckerkandl from aged pseudohypoxic mice may represent a pre-neoplastic population. The mechanisms underlying their emergence and expansion remain unclear and could involve the acquisition of secondary mutations or, given the frequency of these rests, clonal expansion of progenitor-like cell populations. This is of particular interest given that *CCND1* is a HIF-responsive gene in VHL-deficient renal cell carcinoma (RCC), where HIF-2α regulates *CCND1* through a distal enhancer, and genetic variation at the 11q13.3 RCC susceptibility locus influences HIF binding to this enhancer, and consequently cyclin D1 expression (Schödel et al., 2012). Furthermore, in human pheochromocytomas and paragangliomas, those with direct HIF-2α-activating mutations had significantly higher expression of *CCND1* compared to other common driver mutations (Toledo et al., 2013). However, cyclin D1-expressing rests were present in the organ of Zuckerkandl from all aged pseudohypoxic mice examined (data for *Hif-2αdPA* mice not

shown), whereas paragangliomas developed in only 25% of aged *Phd2ko* mice and none of the aged *Hif-2αdPA* mice. This suggests that cyclin D1 expression alone is insufficient to drive neoplastic transformation and that additional events are required for paraganglioma tumorigenesis. The absence of tumours in the aged *Hif-2αdPA* mice may reflect differences in the *Phd2ko* and *Hif-2αdPA* mouse models that influence this transformation, such as quantitative differences in HIF stabilisation or qualitative differences resulting from *Phd2* loss, which also stabilises HIF-1α and may alter other non-HIF substrates. Alternatively, the absence of tumours in *Hif-2αdPA* mice may reflect the limited cohort size and relatively low incidence of tumour development. Further work, including lineage tracing and transcriptional characterisation of the cyclin D1-positive cells, is required to determine whether these clusters represent a true pre-neoplastic population, and to define the mechanism underlying their transition to paraganglioma. This may have clinical relevance by identifying early cellular or molecular targets for preventing tumour development in individuals with inherited pseudohypoxic mutations who may retain their organ of Zuckerkandl.

The organ of Zuckerkandl paragangliomas in aged *Phd2ko* mice provide a useful model for investigating tumorigenesis and evaluating potential therapies. However, the low incidence and late onset of these tumours limit its utility. Increasing tumour susceptibility could therefore improve this model. One approach could be concurrent inactivation of HIF-1α. Although in the paragraph above, stabilisation of HIF-1α was proposed to promote paraganglioma tumorigenesis in *Phd2ko* mice, there is evidence that it may conversely act as a tumour suppressor. Shen et al. (2011) showed that this is the case in clear cell renal cell carcinoma (ccRCC); they found that HIF-1α was frequently deleted or functionally disrupted in renal carcinoma cells, whilst restoration of HIF-1α supressed tumour cell proliferation and tumour growth (Shen et al., 2011). In chromaffin cells, previous work showed that, while aged wild-type and *Phd2ko* mice did not develop pheochromocytomas, concurrent TH-restricted *Phd2*

and *Hif-1α* knockout resulted in the formation of chromaffin cell nodules in the adrenal medulla in 3/11 aged mice (Eckardt et al., 2021). Additionally, in a single aged TH-restricted *Phd2* and *Hif-1α* double-knockout mouse, examination revealed the presence of an organ of Zuckerkandl paraganglioma (i.e. 1/1 incidence) (data not shown). However, a much larger cohort will be necessary to determine whether deletion of HIF-1α reliably increases the incidence of paragangliomas. Alternatively, overexpression of oncogenes such as CCND1 or MYC in parallel with pseudohypoxic mutations could increase incidence or accelerate tumour onset, particularly given the high cyclin D1 expression in the *Phd2ko* organ of Zuckerkandl paragangliomas and the potentially pre-neoplastic cyclin $D1^{+}$ chromaffin cell rests identified in the non-tumour organ of Zuckerkandl from aged pseudohypoxic mice. A third hypothesised mechanism of sensitising mice to tumorigenesis is exposure to environmental hypoxia. Individuals with CCHD have an approximately five-fold increased risk of paragangliomas (Vaidya et al., 2018) and somatic gain-of-function mutations in *EPAS1* are enriched in these patients with both CCHD and paragangliomas, with an incidence of 80% compared to only 5-6% in the general paraganglioma population (Arenillas et al., 2025; Dahia, 2014). Furthermore, in a cohort of 40 patients with pheochromocytomas and paragangliomas with underlying *EPAS1* mutations, at least one third also had a haemoglobin disorder such as sickle cell disease, sickle cell trait or haemoglobin C disease (Mancini et al., 2024). This suggests that chronic hypoxaemia and *EPAS1*-driven pseudohypoxia may act synergistically to promote tumourigenesis of pheochromocytomas and paragangliomas. However, this chapter demonstrated a converse interaction between pseudohypoxia and hypoxia; *Phd2ko* mice exposed to hypoxia in the postnatal period had a smaller organ of Zuckerkandl compared to mice of the same genotype which remained in normoxia. This may reflect a dose-dependent effect of HIF signalling, whereby additional environmental hypoxia pushes HIF activity beyond the level that supports retention of the organ of Zuckerkandl and instead selects against

Phd2ko chromaffin cells. The interaction may therefore depend on the precise pseudohypoxic mutation, as the *EPAS1* mutations enriched in patients with chronic hypoxaemia differ mechanistically from *Phd2* inactivation, which also stabilises HIF-1α. Therefore, further work is necessary to determine how the magnitude and nature of HIF signalling influences the interaction between hypoxia, pseudohypoxia and paraganglioma tumorigenesis.

Despite the low incidence and late onset of the frank organ of Zuckerkandl paragangliomas, if the retained organ of Zuckerkandl is truly the origin of organ of Zuckerkandl paragangliomas, it provides a more tractable model for pharmacological investigations. First, it would be interesting to investigate whether belzutifan, a HIF-2α antagonist which is clinically licenced to treat renal cell carcinomas and recently received FDA approval for unresectable pheochromocytomas and paragangliomas (Jimenez et al., 2025), induces regression of the retained organ of Zuckerkandl in adult pseudohypoxic mice. A reduction in tissue size or in the number of cells expressing cyclin D1 would suggest that continued HIF-2α activity is necessary for maintenance of the organ of Zuckerkandl, providing a rationale for investigating belzutifan as an early intervention in individuals carrying inherited pseudohypoxic paraganglioma susceptibility variants as this could potentially reduce the pool of persistent chromaffin cells that may serve as tumour precursors. It would also be valuable to investigate whether belzutifan treatment could prevent retention of the organ of Zuckerkandl in perinatal mice exposed to hypoxia. As retention of the organ of Zuckerkandl is proposed to be dependent on HIF-2α, inhibition during this period may restore its typical regression, providing further mechanistic insights into the role of HIF-2α signalling in maintaining this tissue and establishing whether this pathway represents a potential therapeutic target during early life.

As well as targeting HIF-2α, a prominent feature of pseudohypoxic paragangliomas is their elevated expression of cell cycle promoters. Therefore, these represent another potential

therapeutic avenue. Treatment of mice with clinically licensed CDK4/6 inhibitors could be used to determine whether inhibition of cyclin D1-CDK4/6 signalling prevents maintenance of the organ of Zuckerkandl in wild-type mice exposed to postnatal hypoxia and/or promotes regression of the adult organ of Zuckerkandl in pseudohypoxic mice. This would provide further insight into the role of cyclin D1 in the maintenance of the organ of Zuckerkandl and its potential association with the proposed pre-neoplastic cell population. Importantly, repurposing clinically licenced drugs such as CDK4/6 inhibitors, rather than developing novel therapeutic agents, could significantly reduce the time and cost associated with development of a new therapeutic agent. Furthermore, belzutifan resistance has been documented in HIF-2-dependent ccRCC, and CDK4/6 inhibition has retained anti-tumour activity in preclinical HIF-2 inhibitor-resistant VHL-deficient models, providing a rationale for investigating this combination in pseudohypoxic paraganglioma (Nicholson et al., 2019; Shirole et al., 2025).

Chapter 6

FINAL DISCUSSION

This thesis demonstrates that HIF-2α activity during development regulates neuroendocrine cell fate, with stabilisation of HIF-2α sufficient to confer retention of foetal-like, paraganglioma-like chromaffin cells into adulthood (Chapter 2). Previous work in mice with inactivation of *Phd2* (*Phd2ko*) demonstrated these phenotypes (Eckardt et al., 2021; Fielding et al., 2018; Prange-Barczynska et al., 2024), but the present work shows that HIF-2α itself is sufficient, rather than HIF-1α or other PHD2-dependent targets. These findings extend a broader body of evidence implicating HIF-2α in hypoxia-responsive neuroendocrine tissues. HIF-2α is highly expressed in the foetal organ of Zuckerkandl chromaffin cells and adult carotid body glomus cells, where it is required for normal development and hypoxic responses (Gao, Bonilla-Henao, et al., 2017; Macias et al., 2018; Tian et al., 1998). HIF-2α also contributes to ventilatory acclimatisation to sustained hypoxia, with both genetic and pharmacological inhibition impairing this response (Hodson et al., 2016). More recently, the selective HIF-2α antagonist belzutifan has demonstrated clinical activity in established pheochromocytomas and paragangliomas (Jimenez et al., 2025), further supporting an important role for HIF-2α signalling in these tumours. These observations, together with the association of activating *EPAS1* mutations with pheochromocytomas and paragangliomas (Abdullah et al., 2017; Comino-Méndez et al., 2013; Welander, Andreasson, Brauckhoff, et al., 2014; Z. Zhuang et al., 2012) support a key role for HIF-2α in linking developmental oxygen sensing, neuroendocrine cell fate and tumour susceptibility.

This thesis subsequently investigated the mechanisms through which HIF-2α activity confers the foetal-like, paraganglioma-like neuroendocrine phenotype. Previous studies have suggested that HIF-2α may have functions beyond its canonical role as a transcription factor acting

through heterodimerisation with ARNT. Combined loss of *Arnt* and *Arnt2* only mildly impairs carotid body proliferative and ventilatory responses to hypoxia (MPB, PJR and TB, unpublished observations) compared to ablation in *Epas1* null mice. Further, the S305M point mutation in the ligand binding pocket of the PAS B domain of HIF-2α, which does not disrupt heterodimerisation with ARNT, impairs physiological responses to hypoxia (Cheng et al., 2020). Together, these findings raise the possibility that HIF-2α has functions that are not fully explained by conventional HIF-2α-ARNT transcriptional activity, including functions involving alternative binding partners other than ARNT, such as BMAL1, which has recently been shown to form an active transcriptional complex with HIF-2α (Ruan et al., 2025).

However, work in this thesis demonstrated that, for the glomus and chromaffin cell phenotypes described in *Hif-2αdPA* mice, HIF-2α transcriptional activity is essential as stabilisation of transcriptionally inactive Hif-2α did not reproduce these phenotypes (Chapter 3). HIF-2α-dependent transcription provides a plausible mechanism for establishing the cellular machinery required for oxygen chemosensitivity. In particular, *Cox4i2* and *Ndufa4l2*, which encode atypical mitochondrial components associated with cytochrome c oxidase, are enriched in oxygen-sensitive carotid body glomus cells and are induced in HIF-2α-dependent oxygen-chemosensitive chromaffin cells (Moreno-Domínguez et al., 2020; Ortega-Sáenz et al., 2020). These proteins are proposed to alter the properties of mitochondrial complex IV such that mitochondrial respiration becomes more sensitive to changes in oxygen availability. COX4I2, together with HIGD1C, has been shown to contribute to the increased oxygen sensitivity of complex IV, providing a potential mechanism by which changes in oxygen availability are translated into alterations in mitochondrial electron transport and redox state. Such mitochondrial signals could then contribute to inhibition of oxygen-sensitive K^+ channels, membrane depolarisation, Ca^{2+} entry and vesicle exocytosis. Therefore, HIF-2α-dependent

transcription may establish the mitochondrial machinery that couples a reduction in oxygen availability to the rapid response characteristic of oxygen chemosensitive neuroendocrine cells.

A further mechanistic insight from this thesis is that HIF-2α activity must occur during development to confer the foetal-like neuroendocrine phenotype, whereas stabilisation of HIF-2α in adulthood does not produce the same changes (Chapter 3). This indicates that HIF-2α does not simply act as an ongoing determinant of neuroendocrine cell identity, but instead influences cell fate during development, establishing a persistent immature state that cannot be reproduced by equivalent HIF-2α activation later in life. This developmental requirement may also be relevant to tumourigenesis. Somatic gain-of-function mutations in *EPAS1* occur in pheochromocytomas and paragangliomas and can represent early, clonally selected events in tumourigenesis. In patients with cyanotic congenital heart disease (CCHD), *EPAS1* mutations are highly enriched and hypoxaemia has been proposed to positively select *EPAS1* mutant cells during early life, with some tumours developing many years after the period of hypoxaemia (Arenillas et al., 2025). Similar associations between chronic hypoxic states and *EPAS1*-mutated tumours have also been reported in patients with haemoglobinopathies (Mancini et al., 2024).

The clinical use of the HIF-2α antagonist belzutifan to treat established pheochromocytomas and paragangliomas provides an important distinction from these developmental findings. Developmental HIF-2α activation establishes a persistent immature chromaffin cell state, whereas equivalent activation in adult chromaffin cells does not recreate that state. By contrast, the response of established pheochromocytomas and paragangliomas to belzutifan indicates that ongoing HIF-2α signalling can remain therapeutically relevant after tumour formation. Therefore, the developmental effects of HIF-2α stabilisation and its role in tumour maintenance may represent distinct biological processes.

The observation that developmental HIF-2α stabilisation causes retention of the foetal organ of Zuckerkandl prompted the question of whether physiological activation of the same pathway by environmental hypoxia could produce a similar phenotype. This thesis demonstrates that postnatal hypoxia prolongs the persistence of the organ of Zuckerkandl beyond the period in which it would normally regress (Chapter 5), suggesting that HIF-2α activation may provide a common mechanism through which environmental hypoxia and pseudohypoxia maintain this foetal neuroendocrine tissue. Although the retained organ of Zuckerkandl itself is not a paraganglioma, its persistence provides an ectopic population of immature chromaffin cells that could be susceptible to subsequent tumourigenesis. This raises the possibility that chronic hypoxia during development may confer susceptibility to organ of Zuckerkandl paragangliomas, analogous to the established association between hypoxia and pheochromocytomas and paragangliomas at other sites. Carotid body paragangliomas are more prevalent in populations living at high altitude (Gonzalez-Urquijo et al., 2022; S. Kumar et al., 2024; Saldana et al., 1973), while patients with CCHD have an increased incidence of pheochromocytomas and paragangliomas, including sympathetic tumours arising from adrenal and extra-adrenal chromaffin tissues (Arenillas et al., 2025; Opotowsky et al., 2015). However, whether developmental chronic hypoxia increases susceptibility to paragangliomas arising specifically from retained organ of Zuckerkandl tissue is not established.

Notably, the anatomical distribution of CCHD-associated tumours appears to vary with the timing of hypoxaemia, with a higher proportion of secretory tumours arising from sympathetic chromaffin tissues in patients who experience hypoxaemia from birth, compared with a greater proportion of carotid body paragangliomas in those who develop hypoxaemia later (Arenillas et al., 2025). This observation suggests that the timing of hypoxaemia may influence the distribution of neuroendocrine tumours, although the underlying mechanism is unclear. The findings of this thesis provide one example of how developmental hypoxia can alter

neuroendocrine tissue by prolonging maintenance of the foetal organ of Zuckerkandl, but whether similar effects occur in other oxygen-responsive neuroendocrine tissue remains unknown. Examining other neuroendocrine tissues from mice exposed to perinatal hypoxia could determine whether developmental hypoxia produces similar changes across tissues, or whether its effects are tissue-specific.

An unexpected finding from the perinatal hypoxia experiments was that hypoxic exposure reduces the size of the retained organ of Zuckerkandl in *Phd2ko* mice (Chapter 5). Therefore, rather than increasing or simply maintaining the phenotype produced by *Phd2* inactivation, additional environmental hypoxia promoted involution of the organ of Zuckerkandl. This suggests that the relationship between HIF activity and chromaffin cell fate is not necessarily linear, and that the magnitude or context of HIF-α activity may influence the resulting phenotype. A similar principle has been proposed in VHL-associated disease, in which different *VHL* mutations are associated with distinct clinical manifestations, consistent with differences in the extent or context of HIF pathway dysregulation (S.-J. Liu et al., 2018). Determining whether postnatal hypoxia produces the same effect on the organ of Zuckerkandl size in *Hif-2αdPA* and *Sdhb* deficient mice would establish whether the involution observed in *Phd2ko* mice is specific to the mechanism of HIF activation or instead reflects differences in the level or cellular context of HIF signalling. Notably, this response appears distinct from the relationship between genetic and environmental hypoxia suggested in CCHD-associated pheochromocytomas and paragangliomas, in which *EPAS1* mutations are frequent and have been suggested to undergo positive selection in hypoxic tissues (Arenillas et al., 2025). Whereas additional environmental hypoxia attenuated the developmental phenotype caused by *Phd2* inactivation in this thesis, the CCHD-associated tumour data raises the possibility that hypoxia and constitutive HIF-2α activation can instead cooperate to promote tumour

development. Defining why these responses differ could provide insight into how the level and cellular context of HIF-2α activation influence chromaffin cell fate and tumour susceptibility.

A key finding of this thesis is the identification of the first mouse model of frank pseudohypoxic paraganglioma, which develop in aged *Phd2ko* mice (Chapter 5). This model provides an opportunity to investigate the progression from persistent immature chromaffin tissue to tumourigenesis, including the earliest stages of tumour development, disease progression and response to treatment. In addition, if the malignant chromaffin cells retain functional oxygen chemosensitivity, establishing a cell line from these highly proliferative tumours could provide a useful system for investigating the molecular mechanisms underlying oxygen sensing in chromaffin cells. A limitation of the aged *Phd2ko* model is the relatively low incidence and late age of onset of tumours. Increasing tumour incidence or accelerating tumour development through further modifications could therefore enhance its experimental utility. Conversely, these features also provide an opportunity to investigate the factors that determine why only a subset of retained chromaffin cells progress to malignancy.

A further priority for future work is to determine whether tumorigenesis can be reproduced in other genetic models of pseudohypoxia. In particular, *VHL* and *SDHx* mutations are more common in pheochromocytomas and paragangliomas (Fishbein et al., 2017), so mouse models of these mutations would provide complementary systems with greater clinical relevance. The *Sdhb* models described in this thesis (Chapter 4) are particularly informative because SDHB loss is likely to influence tumorigenesis through both HIF-dependent and HIF-independent mechanisms (Morin et al., 2020a). As succinate accumulation following SDH loss can alter multiple cellular processes in addition to stabilising HIF, comparison of *Sdhb*-deficient mice with models in which HIF signalling is directly activated can help to distinguish phenotypes that are shared as a consequence of HIF activation from those that are specific to SDH dysfunction. However, mice with biallelic *Sdhb* mutations developed in this thesis were

markedly runted and unwell so could not be aged to determine whether they develop tumours. Inducing *Sdhb* inactivation later in development, for example using a tamoxifen-inducible CreER system and a lower dose of tamoxifen to reduce recombination efficiency, may help dissociate the effects of SDH loss on growth and viability from its tumorigenic effects, potentially allowing these mice to be aged to assess tumour development.

Beyond establishing models of frank tumorigenesis, lineage-tracing approaches could be used to define the early cellular events linking persistent developmental chromaffin cells to tumour formation. In particular, identifying molecular features that distinguish the rests of proliferative cells identified within the retained organ of Zuckerkandl of aged pseudohypoxic mice without frank tumours (Chapter 5) could enable these cells to be selectively labelled before tumour development. Subsequent analysis of tumours for labelled descendants could then determine whether these rests represent genuine pre-neoplastic populations. Demonstrating this would provide an experimentally tractable intermediate stage of tumour development that could be studied without waiting for fully established tumours to arise. These cells could subsequently be used in genetic or pharmacological screens to identify pathways required for their persistence or progression, followed by assessment of whether candidate compounds can eliminate them. This could ultimately identify strategies for preventing tumour initiation in individuals with inherited pheochromocytoma and paraganglioma susceptibility.

Taken together, the findings of this thesis demonstrate that developmental HIF-2α activity is an important determinant of neuroendocrine cell fate. HIF-2α-dependent transcription establishes a cellular programme associated with immature chromaffin cell identity and oxygen responsiveness, and activation of this pathway during development is sufficient to promote persistence of this phenotype into adulthood. Finally, the development of paragangliomas in aged pseudohypoxic mice provides a direct link between persistence of this developmental cell

state and tumour formation, establishing a model in which the interaction between developmental cell fate, oxygen sensing and tumour susceptibility can be investigated.

Chapter 7

Materials and methods

7.1 **Materials and chemicals**

Phosphate Buffered Saline (PBS) was prepared in-house as 1.37 M NaCl, 26.8 mM KCl, 46.7 mM $Na_2HPO_4.7H_2O$, 14.7 mM KH_2PO_4 in double distilled water (ddH_2O). PBS-T is 1% v/v Tween20 in PBS.

7.2 **Ethical approval**

All animal protocols were approved by the University of Oxford Medical Science Division Ethical Review Committee, authorised by project and personal licences, and are compliant with the UK Home Office Animals (Scientific Procedures) Act 1986.

7.3 **Animals**

Mice with a C57BL/6 genetic background were used for all experiments. Genetically modified mice were bred on this background. Mice were housed in the Wellcome Trust Functional Genetics Facility in individually ventilated cages on a 12-hour light/dark cycle with constant access to food and water. Both male and female mice, aged 2-3 months, were used for experiments unless age is otherwise stated. Age-and sex-matched controls were used for all experiments. Littermate controls were used where possible.

7.4 **Genotyping**

Ear biopsies were obtained from all mice at approximately three weeks of age for genotyping and identification. Biopsies were digested overnight at 55 °C in Proteinase K buffer containing 2% SDS (Sigma), 0.02 M EDTA, pH 8.0 (Invitrogen), 0.05 M Tris, pH 8.0 (Invitrogen) and 488 $\mu g \cdot ml^{-1}$ Proteinase K (Meridian Bioscience). Samples were cooled at 4 °C for 30 minutes, after which saturated NaCl in ddH_2O was added to precipitate protein contaminants. Samples

were incubated for a further 10 minutes at 4 °C before centrifugation at 10,000 rpm for 10 minutes. The supernatant was transferred to a fresh tube and mixed with isopropanol at a 1:1 ratio, followed by incubation at 4 °C for 30 minutes to precipitate the DNA. Samples were centrifuged at 13,000 rpm for 30-60 minutes, after which the isopropanol was removed and the DNA pellets were dried at 45 °C. DNA pellets were resuspended in 50 µl nuclease free water (Invitrogen). Genotypes were determined by PCR amplification of target regions within the alleles of interest. The primers used are listed in **Table 8.1**. Taq DNA Polymerase (Qiagen) or BioTaq DNA polymerase (Meridian Bioscience) was used according to the manufacturer's instructions.

Genotype	**Source/Reference**	**Primers**
Hif-1αdPA$^{f/+}$	Kim et al. (2006) The Jackson Laboratory Stock No: 009673	8832: CCGGTAGAATTCCTGCAGGTCGAGGG oIMR3621: CGTGATCTGCAACTCCAGTC oIMR8546: GGAGCGGGAGAAATGGATATG
Hif-2αdPA$^{f/+}$	Kim et al. (2006) The Jackson Laboratory Stock No: 009674	24500: CAGGACAACGCCCACACA 37895: TCTGAAAACGAGTCCGAAGC 37896: GTCGCAGGGATGAGTGAAGT oIMR9020: AAGGGAGCTGCAGTGGAGTA
Hif-2αdPA DNA binding mutant$^{f/+}$	Ben Davies (The Francis Crick Institute)	LR 3 F: AAGGAGTAGCTCGGAGAGG LR 3 R: GCTCCACCTGTGTAAGTCCC LR 5-3 F: GGTGGAAAATGGCCGCTTTT LR 5-3 R: GCTCCACCTGTGTAAGTCCC
Sdhb$^{f/f}$ Sdhb$^{f/-}$	Letouzé et al. (2013)	SDHB F: CCATGCCAGTAACCCCAGAATTGG SDHB R: GTCCCACCTCACTGTAGGTCAC
Sdhb$^{f/V142F}$	Ben Davies (The Francis Crick Institute)	Sdhb-F3: GGTACATCCTCTGTTAGCGCA R_Sdhb_hindIII: CCAAAGAAGCTGTGAAGCTT

Phd2$^{f/f}$ *Phd2*$^{f/-}$	Takeda et al. (2006)	P2MPLEXfw1: TTGCAGTGTGCAACAGTCAG P2MPLEXwtrv1: CACGGGGAACTCTGATTCAT P2MPLEXkorv1:CCAAAATCACCAATCTAGAATAACTTC
Ai95$^{f/+}$	The Jackson Laboratory Stock No: 024105	oIMR9021: CCGAAAATCTGTGGGAAGTC oIMR 9020: AAGGGAGCTGCAGTGGAGTA 19908: ACGAGTCGGATCTCCCTTTG
THCre *THCreER*	Lindeberg et al. (2004)	creJun-fw: CGGTCGATGCAACGAGTGATGAG G creJun-rv: CCAGAGACGGAAATCCATCGCTC G CreJUNfw: CTCATACCAGTTCGCACAGGCGG C CreJUNrv: CCGCTAGCACTCACGTTGGTAGG C

Table 7.1 PCR primers used for genotyping.

7.5 **Tamoxifen administration**

20 mg/ml tamoxifen (MP Biomedicals) stock solution was prepared in corn oil with 10% ethanol (Li et al., 2010). Mice expressing inducible THCreER were administered 2 mg tamoxifen by oral gavage once daily for five consecutive days. Mice were weighed daily to monitor for weight loss.

7.6 **Plethysmography**

To measure tidal volume and respiratory rate, awake, unrestrained mice were weighed and placed into whole body plethysmograph chambers (600 mL; Model PLY4211; Buxco). Mice were allowed to acclimatise in unsealed chambers for 30 minutes, after which the chambers were sealed and supplied with medical air at a flow rate of 1.5 L/min for 5 minutes before recording commenced. Mice were then exposed to 1.5 L/min 10% O_2, 10% O_2/3% CO_2 and 3% CO_2 (balance nitrogen) for five minute periods. Medical air was administered for 5 minutes before and after each stimulus, and mice were allowed to rest in unsealed chambers for 15 minutes between recordings.

Minute ventilation was calculated and normalised to the animal's body weight, and values were plotted over time. The acute ventilatory response (AVR) to each respiratory challenge was calculated by subtracting the average minute ventilation during the last minute of room air from the average minute ventilation during the first stable minute of the stimulus, excluding the first 30 seconds following stimulus onset.

7.7 **Postnatal hypoxia**

Litters of mice at postnatal day 3 were placed into a normobaric altitude chamber with gas composition altered using Everest Summit II hypoxicators (Hypoxico) (Bishop et al., 2013). They remained in their standard housing cages with lids removed and oxygen levels were gradually decreased from room air to 10% oxygen over the course of a day. Mice were checked every day and mothers were given mash to eat as well as normal access to food pellets and water. Mice were removed from the altitude chambers at postnatal day 21 then immediately culled by carbon dioxide overdose.

7.8 **Immunohistochemistry**

Mice were culled by overdose of isoflurane (Zoetis) and perfuse fixed with 5 ml phosphate buffered saline (PBS) then 5 ml 4% paraformaldehyde (Sigma). Their carotid bifurcations, adrenal glands and abdominal regions (including the kidneys and aorta) were dissected and immersion fixed in 4% paraformaldehyde/PBS (Sigma) overnight. These tissues were then transferred into 70% ethanol and stored at 4 °C. Tissues were processed by dehydration in ascending ethanol concentrations (70%, 90% then 100%), before submersion in Histo-Clear II (National Diagnostics) then paraffin wax at 60 °C in an automated tissue processor (Excelsior AS, Thermo Scientific). These tissues were then embedded in paraffin, sectioned at 4 μm thickness using an RM135 microtome (Leica Biosystems) and placed in polysine-coated slides (VWR).

Tissues were stained for: chromogranin A (CgA) (1:500, ab68271, Abcam); Tyrosine Hydroxylase (TH) (1:5000, NB300-109, Novus Biologicals); CD31 (1:100, ab28364, Abcam); SDHB (1:1000, HPA002868, Sigma-Aldrich); and counterstained with modified Harris Haematoxylin (Epredia). Briefly, slides were washed twice in xylene (MP Biomedicals) to remove paraffin then rehydrated in 100%, 90% then 70% ethanol. They were then placed in Antigen Retrieval Solution (Dako) within a pressure cooker for 10 minutes. Following antigen retrieval, slides were allowed to cool for 30-60 minutes before incubation with Peroxidase Block (Dako) for 5 minutes. Slides were then washed in PBS-T, followed by incubation with the relevant primary antibody overnight at 4 °C. The following day, slides were washed in PBS-T and incubated with an HRP-conjugated anti-rabbit secondary antibody for 30 minutes. Following further washing in PBS-T, 3,3'-diaminobenzidine (DAB) chromogen (Dako) was added for 10 minutes to detect signal. The reaction was stopped with tap water and tissues were counterstained with modified Harris Haematoxylin then mounted with coverslips using DPX Mountant (VWR).

HIF-2α immunohistochemistry was performed as previously described in Prange-Barczynska et al. (2024)(Prange-Barczynska et al., 2024). Sections were deparaffinised, rehydrated and subjected to antigen retrieval using Dako Antigen Retrieval Solution in a pressure cooker for 30 minutes. Sections were then blocked for non-specific protein binding and avidin and biotin binding before incubation with anti-HIF-2α primary antibody (PM8 (Wiesener et al., 2003); 1:3000) overnight at 4°C. Indirect detection was performed using sequential incubations with an HRP-conjugated anti-rabbit secondary antibody (Dako; 30 minutes, room temperature), a biotin-conjugated anti-HRP tertiary antibody (Rockland 200-4638-0100; 1:250; 2 hours, room temperature) and HRP-conjugated Streptavidin (BD Pharmingen 551321; 1 hour, room temperature). Slides were developed using DAB chromogen for 1.5 minutes, counterstained with haematoxylin and mounted using DPX Mountant as described above.

Stained slides were scanned with the Nanozoomer S210 side scanner (Hamamatsu) and visualised on NDP.View2 software (Hamamatsu).

Carotid body and organ of Zuckerkandl volume was estimated by drawing around the chromogranin A (CgA)-positive area of tissue on NDP.View2 on stained slides and averaging the area of consecutive stained slides to estimate the area of intermediate non-stained slides. The sum of the areas was then multiplied by the tissue thickness to calculate tissue volume.

CgA-positive area in the adrenal medulla (Chapter 4) and Ki67 and cyclin D1 expression in the organ of Zuckerkandl (Chapter 5) were quantified from immunohistochemically stained tissue sections using QuPath (version 0.5.1) (Bankhead et al., 2017). The tissue was manually drawn around to generate a region of interest (ROI) and DAB-positive cells within this region were identified using the Positive Cell Selection feature. The percentage of positive cells was calculated as the number of DAB-positive cells divided by the total number of cells detected within the ROI, multiplied by 100. The same detection and classification parameters were applied consistently across all samples.

Clustering analysis of cyclin D1-positive cells was performed in QuPath (v0.7.0) by JN. Cyclin D1-positive nuclei were detected in the region of the organ of Zuckerkandl using automated cell detection, for which the optical threshold for cyclin D1-positive nuclei was determined manually for each image by an investigator blinded to age. Clusters of positive cells were determined using a custom QuPath Groovy script, with a cluster defined as two or more cells with boundaries less than 0.5 μm apart. Statistical analysis was performed using a two-sided Kolmogorov-Smirnov test in the R statistical software (v4.6.1).

7.9 *In situ* hybridisation

Tissues were prepared and sectioned as described above for immunohistochemistry. Transcripts were detected on adjacent sections using the RNAscope 2.5 HD BROWN assay (Advanced

Cell Diagnostics) and the following probes: *Pnmt* (426421)*, Epas1* (314371), *Rgs5* (430181), *Cox4i2* (497901), *Ndufa4l2* (816431), *Higd1c* (537761), *Vegfa* (436961) and *Ccnd1* (442671) and counterstained with modified Harris Haematoxylin (Epredia).

The percentage of $mRNA^+$ tissue was quantified using QuPath (version 0.5.1) as described above. The detection threshold was maintained consistently across samples wherever possible, with adjustments made where necessary to account for variation in background haematoxylin staining between runs.

7.10 **Tissue preparation for calcium imaging**

Tissues were dissected and placed into ice-cold PBS. Carotid bodies and organ of Zuckerkandl tissue were then subdissected and placed on a nylon mesh (Warner Instruments) in F12 media (Gibco) with Foetal Bovine Serum (Gibco), Penicillin/Streptomycin and L-Glutamine, and stored in an incubator at 37°C, 5% CO_2 until imaging. Adrenal glands were embedded in 4% low melting point agarose (BP1360, Fisher Scientific) dissolved in Tyrode's saline + HEPES (25 mM $NaHCO_3$, 117 mM NaCl, 1 mM NaH_2PO_4, 11 mM D-Glucose, 4.5 mM KCl, 1 mM $MgCl_2$ and 25 mM HEPES) and sliced at 150 µm thickness using a VT100S Vibratome (Leica). Slices were placed in F12 media and stored in an incubator at 37 °C, 5% CO_2 for at least an hour before imaging.

7.11 **Fluorescent calcium imaging**

Live tissues were imaged in a custom-built perfusion system using a wide-field Leica DMi8 microscope (Leica Microsystems CMS), configured with a pE340fura light source (CoolLED), a GFP filter cube (excitation filter 470 ± 40 nm, 495 nm dichroic mirror, emission filter 525 ± 50 nm) and a monochrome Prime 95B camera (Photometrics).

For experiments in Chapters 2 and 3, buffer solutions (25 mM $NaHCO_3$, 117 mM NaCl, 1 mM NaH_2PO_4, 11 mM D-Glucose, 4.5 mM KCl (or 45 mM for high K^+ solution), 1 mM $MgCl_2$)

were prepared and bubbled with gasses using 3-channel Gas Blender mixers (100 Series, MCQ instruments) for at least two hours prior to imaging to achieve the desired oxygen concentrations. Gas mixtures are shown in **Table 8.2**. Solutions were kept in a water bath at 37 °C. Immediately prior to imaging, $CaCl_2$ was added to the solutions to a final concentration of 1 mM to prevent calcium carbonate precipitation and 1.2 g sodium sulphite was added to the anoxia solution to act as an oxygen scavenger. Tissues were then placed in the perfusion chamber and immobilised using an anchor (2HD-22CL/15, Warner Instruments). Control solution (18% O_2) was perfused over the tissue then test solutions were applied for 90 seconds (30 seconds for K^+ solution) with at least 120 seconds of control solution in between. GFP images were taken every two seconds with a 40x objective (HC PL FLUOTAR 40x/1.30 OIL 340 nm, Leica Microsystems CMS) for the carotid body and organ of Zuckerkandl, or a 10x objective (N PLAN 10x/0.25 achromatic corrected objective, Leica Microsystems CMS) for adrenal gland slices. Raw data was analysed using Fiji ImageJ software (NIH). Average GFP fluorescence intensity in the region of interest selected was measured across all of the images and plotted against time, normalised to the background fluorescence (F/F_0), and background corrected against a non-K^+ responsive region of tissue.

Test solution	**Compressed air**	**N_2**	**CO_2**
Control and 45 mM K^+	95%	0%	5%
10% O_2	50%	45%	5%
5% O_2	25%	70%	5%
1% O_2 and anoxia	2%	93%	5%

Table 7.2 Gas mixtures used for Ca^{2+} imaging of fresh tissues.

For experiments in Chapters 4 and 5, the same buffer and K^+ solutions were prepared and bubbled as per the control in **Table 8.1**. $CaCl_2$ was added to the solutions to a final

concentration of 1 mM before imaging the tissue, as described above. The buffer solution was initially perfused over the tissue for 90 seconds, followed by 30 seconds of K^+ solution, then back to the control buffer solution. After a further 90 seconds, the gas composition bubbling the buffer solution was changed to 0% compressed air and 95% N_2. The tissue was perfused with this buffer solution until the oxygen concentration in the perfusate at the tissue reached <1%, as measured using an OXY-1 SMA Compact Fiber Optic Oxygen Meter (PreSens, SACJ0003000249). Once the oxygen concentration had fallen below 1%, the gas composition was returned to 95% compressed air and 0% N_2 and tissue imaging continued until the oxygen concentration had returned to baseline. A further 30 second application of K^+ solution was then performed. Data was analysed as described above.

7.12 **Hemagglutinin immunoblotting**

Tissues were dissected, lysed in sodium dodecyl sulfate (SDS) lysis buffer (50mM Tris pH 6.8, 2% SDS, 10% glycerol) and sonicated to homogeneity. Samples were normalised for protein concentration using a BCA assay (Pierce, Thermo Fisher Scientific), then mixed with Laemmli sample buffer. Proteins were separated by SDS-polyacrylamide gel electrophoresis then transferred onto a polyvinylidene difluoride membrane (Immobilon-P, Millipore). This was blocked in 4% fat free milk (w/v in phosphate buffered saline, PBS, containing 0.1% Tween20) then incubated overnight with HRP-conjugated HA (3F10, Sigma Aldrich) diluted 1:500 in milk. Chemiluminescence substrate (West Dura, 34076, Thermo Fisher Scientific) was added and bound antibody was detected using a ChemiDoc XRS+ imaging system (BioRad). β-actin (ab49900, Abcam) was used as a loading control.

7.13 **Statistical analysis**

All quantitative analysis were plotted and statistical analysis were carried out in GraphPad Prism 10.0.2. Statistical tests are detailed in the figure legends and data are represented on bar charts as mean ± SEM.

BIBLIOGRAPHY

Abdullah, A. E., Guerin, C., Imperiale, A., Barlier, A., Battini, S., Pertuit, M., Roche, P., Essamet, W., Vaisse, B., Pacak, K., Sebag, F., & Taïeb, D. (2017). Paraganglioma of the organ of Zuckerkandl associated with a somatic HIF2α mutation: A case report. *Oncology Letters*, *13*(3), 1083–1086. https://doi.org/10.3892/ol.2017.5599

Adams, M. (1996). The non-neurogenic catecholamine response of the fetal adrenal to hypoxia is dependent on activation of voltage sensitive Ca2+ channels. *Developmental Brain Research*, *94*(2), 182–189. https://doi.org/10.1016/0165-3806(96)00054-5

Aitken, M. L., Franklin, J. L., Pierson, D. J., & Schoene, R. B. (1986). Influence of body size and gender on control of ventilation. *Journal of Applied Physiology*, *60*(6), 1894–1899. https://doi.org/10.1152/jappl.1986.60.6.1894

Akkuratova, N., Faure, L., Kameneva, P., Kastriti, M. E., & Adameyko, I. (2022). Developmental heterogeneity of embryonic neuroendocrine chromaffin cells and their maturation dynamics. *Frontiers in Endocrinology*, *13*. https://doi.org/10.3389/fendo.2022.1020000

al Khazal, F., Kang, S., Nelson Holte, M., Choi, D., Singh, R., Ortega-Sáenz, P., López-Barneo, J., & Maher, L. J. (2021). Unexpected obesity, rather than tumorigenesis, in a conditional mouse model of mitochondrial complex II deficiency. *The FASEB Journal*, *35*(2). https://doi.org/10.1096/fj.202002100R

al Subhi, A. R., Boyle, V., & Elston, M. S. (2022). Systematic Review: Incidence of Pheochromocytoma and Paraganglioma Over 70 Years. *Journal of the Endocrine Society*, *6*(9). https://doi.org/10.1210/jendso/bvac105

Albadari, N., Deng, S., & Li, W. (2019). The transcriptional factors HIF-1 and HIF-2 and their novel inhibitors in cancer therapy. *Expert Opinion on Drug Discovery*, *14*(7), 667–682. https://doi.org/10.1080/17460441.2019.1613370

Amar, L., Pacak, K., Steichen, O., Akker, S. A., Aylwin, S. J. B., Baudin, E., Buffet, A., Burnichon, N., Clifton-Bligh, R. J., Dahia, P. L. M., Fassnacht, M., Grossman, A. B., Herman, P., Hicks, R. J., Januszewicz, A., Jimenez, C., Kunst, H. P. M., Lewis, D., Mannelli, M., … Lussey-Lepoutre, C. (2021). International consensus on initial screening and follow-up of asymptomatic SDHx mutation carriers. *Nature Reviews Endocrinology*, *17*(7), 435–444. https://doi.org/10.1038/s41574-021-00492-3

Amorim-Pires, D., Peixoto, J., & Lima, J. (2016). Hypoxia Pathway Mutations in Pheochromocytomas and Paragangliomas. *Cytogenetic and Genome Research*, *150*(3–4), 227–241. https://doi.org/10.1159/000457479

Andrews, K. A., Ascher, D. B., Pires, D. E. V., Barnes, D. R., Vialard, L., Casey, R. T., Bradshaw, N., Adlard, J., Aylwin, S., Brennan, P., Brewer, C., Cole, T., Cook, J. A., Davidson, R., Donaldson, A., Fryer, A., Greenhalgh, L., hodgson, S. v, Irving, R., … Maher, E. R. (2018). Tumour risks and genotype–phenotype correlations associated with germline variants in succinate dehydrogenase subunit genes *SDHB* , *SDHC* and *SDHD*. *Journal of Medical Genetics*, *55*(6), 384–394. https://doi.org/10.1136/jmedgenet-2017-105127

Appelhoff, R. J., Tian, Y.-M., Raval, R. R., Turley, H., Harris, A. L., Pugh, C. W., Ratcliffe, P. J., & Gleadle, J. M. (2004). Differential function of the prolyl hydroxylases PHD1, PHD2, and PHD3 in the regulation of hypoxia-inducible factor. *The Journal of Biological Chemistry*, *279*(37), 38458–38465. https://doi.org/10.1074/jbc.M406026200

Aragonés, J., Schneider, M., van Geyte, K., Fraisl, P., Dresselaers, T., Mazzone, M., Dirkx, R., Zacchigna, S., Lemieux, H., Jeoung, N. H., Lambrechts, D., Bishop, T., Lafuste, P., Diez-Juan, A., Harten, S. K., van Noten, P., de Bock, K., Willam, C., Tjwa, M., … Carmeliet, P. (2008). Deficiency or inhibition of oxygen sensor Phd1 induces hypoxia tolerance by reprogramming basal metabolism. *Nature Genetics*, *40*(2), 170–180. https://doi.org/10.1038/ng.2007.62

Arenillas, C., Celada, L., Ruiz-Cantador, J., Calsina, B., Datta, D., García-Galea, E., Fasani, R., Moreno-Cárdenas, A. B., Alba-Linares, J. J., Miranda-Barrio, B., Martínez-Montes, Á. M., Alvarez-Escola, C., Lecumberri, B., González García, A., K. Flores, S., Esquivel, E., Ding, Y., Peitzsch, M., Robles-Guirado, J.-Á., … Toledo, R. A. (2025). Convergent Genetic Adaptation in Human Tumors Developed Under Systemic Hypoxia and in Populations Living at High Altitudes. *Cancer Discovery*, *15*(5), 1037–1062. https://doi.org/10.1158/2159-8290.CD-24-0943

Arias-Mayenco, I., González-Rodríguez, P., Torres-Torrelo, H., Gao, L., Fernández-Agüera, M. C., Bonilla-Henao, V., Ortega-Sáenz, P., & López-Barneo, J. (2018). Acute O2 Sensing: Role of Coenzyme QH2/Q Ratio and Mitochondrial ROS Compartmentalization. *Cell Metabolism*, *28*(1), 145-158.e4. https://doi.org/10.1016/j.cmet.2018.05.009

Armstrong, N., Storey, C. M., Noll, S. E., Margulis, K., Soe, M. H., Xu, H., Yeh, B., Fishbein, L., Kebebew, E., Howitt, B. E., Zare, R. N., Sage, J., & Annes, J. P. (2022). SDHB knockout and succinate accumulation are insufficient for tumorigenesis but dual SDHB/NF1 loss yields SDHx-like pheochromocytomas. *Cell Reports*, *38*(9), 110453. https://doi.org/10.1016/j.celrep.2022.110453

Arsenault, P. R., Pei, F., Lee, R., Kerestes, H., Percy, M. J., Keith, B., Simon, M. C., Lappin, T. R. J., Khurana, T. S., & Lee, F. S. (2013). A Knock-in Mouse Model of Human PHD2 Gene-associated Erythrocytosis Establishes a Haploinsufficiency Mechanism. *Journal of Biological Chemistry*, *288*(47), 33571–33584. https://doi.org/10.1074/jbc.M113.482364

Baashar, A., & Alsahafi, Z. (2026). The carotid body role in oxygen sensing: Anatomy, neurovascular organization, and structural bases of chemotransduction. *Experimental Lung Research*, *52*(1), 154–166. https://doi.org/10.1080/01902148.2026.2694801

Bankhead, P., Loughrey, M. B., Fernández, J. A., Dombrowski, Y., McArt, D. G., Dunne, P. D., McQuaid, S., Gray, R. T., Murray, L. J., Coleman, H. G., James, J. A., Salto-Tellez, M., & Hamilton, P. W. (2017). QuPath: Open source software for digital pathology image analysis. *Scientific Reports*, *7*(1), 16878. https://doi.org/10.1038/s41598-017-17204-5

Barber, S. M., Sadrameli, S. S., Lee, J. J., Fridley, J. S., Teh, B. S., Oyelese, A. A., Telfeian, A. E., & Gokaslan, Z. L. (2021). Chordoma—Current Understanding and Modern Treatment Paradigms. *Journal of Clinical Medicine*, *10*(5), 1054. https://doi.org/10.3390/jcm10051054

ben Aim, L., Maher, E. R., Cascon, A., Barlier, A., Giraud, S., Ercolino, T., Pigny, P., Clifton-Bligh, R. J., Mirebeau-Prunier, D., Mohamed, A., Favier, J., Gimenez-Roqueplo, A.-P., Schiavi, F., Toledo, R. A., Dahia, P. L., Robledo, M., Bayley, J. P., & Burnichon, N. (2022). International initiative for a curated *SDHB* variant database improving the diagnosis of hereditary paraganglioma and pheochromocytoma. *Journal of Medical Genetics*, *59*(8), 785–792. https://doi.org/10.1136/jmedgenet-2020-107652

Benn, D. E., Gimenez-Roqueplo, A.-P., Reilly, J. R., Bertherat, J., Burgess, J., Byth, K., Croxson, M., Dahia, P. L. M., Elston, M., Gimm, O., Henley, D., Herman, P., Murday, V., Niccoli-Sire, P., Pasieka, J. L., Rohmer, V., Tucker, K., Jeunemaitre, X., Marsh, D. J., … Robinson, B. G. (2006). Clinical Presentation and Penetrance of Pheochromocytoma/Paraganglioma Syndromes. *The Journal of Clinical Endocrinology & Metabolism*, *91*(3), 827–836. https://doi.org/10.1210/jc.2005-1862

Benn, D. E., Zhu, Y., Andrews, K. A., Wilding, M., Duncan, E. L., Dwight, T., Tothill, R. W., Burgess, J., Crook, A., Gill, A. J., Hicks, R. J., Kim, E., Luxford, C., Marfan, H., Richardson, A. L., Robinson, B., Schlosberg, A., Susman, R., Tacon, L., … Clifton-Bligh, R. J. (2018). Bayesian approach to determining penetrance of pathogenic SDH variants. *Journal of Medical Genetics*, *55*(11), 729–734. https://doi.org/10.1136/jmedgenet-2018-105427

Berra, E., Benizri, E., Ginouvès, A., Volmat, V., Roux, D., & Pouysségur, J. (2003). HIF prolyl-hydroxylase 2 is the key oxygen sensor setting low steady-state levels of HIF-1alpha in normoxia. *The EMBO Journal*, *22*(16), 4082–4090. https://doi.org/10.1093/emboj/cdg392

Bilton, R. L., & Booker, G. W. (2003). The subtle side to hypoxia inducible factor (HIFα) regulation. *European Journal of Biochemistry*, *270*(5), 791–798. https://doi.org/10.1046/j.1432-1033.2003.03446.x

Biscoe, T. J., Sampson, S. R., & Purves, M. J. (1967). Stimulus Response Curves of Single Carotid Body Chemoreceptor Afferent Fibres. *Nature*, *215*(5101), 654–655. https://doi.org/10.1038/215654a0

Bisgard, G. E. (2000). Carotid body mechanisms in acclimatization to hypoxia. *Respiration Physiology*, *121*(2–3), 237–246. https://doi.org/10.1016/S0034-5687(00)00131-6

Bishop, T., Gallagher, D., Pascual, A., Lygate, C. A., de Bono, J. P., Nicholls, L. G., Ortega-Saenz, P., Oster, H., Wijeyekoon, B., Sutherland, A. I., Grosfeld, A., Aragones, J., Schneider, M., van Geyte, K., Teixeira, D., Diez-Juan, A., Lopez-Barneo, J., Channon, K. M., Maxwell, P. H., … Ratcliffe, P. J. (2008). Abnormal Sympathoadrenal Development and Systemic Hypotension in *PHD3* $^{-/-}$ Mice. *Molecular and Cellular Biology*, *28*(10), 3386–3400. https://doi.org/10.1128/MCB.02041-07

Bishop, T., Talbot, N. P., Turner, P. J., Nicholls, L. G., Pascual, A., Hodson, E. J., Douglas, G., Fielding, J. W., Smith, T. G., Demetriades, M., Schofield, C. J., Robbins, P. A., Pugh, C. W., Buckler, K. J., & Ratcliffe, P. J. (2013). Carotid body hyperplasia and enhanced ventilatory responses to hypoxia in mice with heterozygous deficiency of PHD2. *The Journal of Physiology*, *591*(14), 3565–3577. https://doi.org/10.1113/jphysiol.2012.247254

Black, A. M. S., McCloskey, D. I., & Torrance, R. W. (1971). The responses of carotid body chemoreceptors in the cat to sudden changes of hypercapnic and hypoxic stimuli. *Respiration Physiology*, *13*(1), 36–49. https://doi.org/10.1016/0034-5687(71)90063-6

Bondarenko, N. S., Murtazina, A. R., Dil'mukhametova, L. K., Ikonopistseva, M. A., Volina, E. v., & Ugrumov, M. v. (2016). Secretory activity of the brain and peripheral organs: Spontaneous and stimulated release of noradrenaline in the ontogenesis of rats. *Doklady Biochemistry and Biophysics*, *467*(1), 153–156. https://doi.org/10.1134/S1607672916020204

Bournaud, R., Hidalgo, J., Yu, H., Girard, E., & Shimahara, T. (2007). Catecholamine secretion from rat foetal adrenal chromaffin cells and hypoxia sensitivity. *Pflügers Archiv - European Journal of Physiology*, *454*(1), 83–92. https://doi.org/10.1007/s00424-006-0185-z

Brouwers, F. M., Eisenhofer, G., Tao, J. J., Kant, J. A., Adams, K. T., Linehan, W. M., & Pacak, K. (2006). High Frequency of *SDHB* Germline Mutations in Patients with Malignant Catecholamine-Producing Paragangliomas: Implications for Genetic Testing. *The Journal of Clinical Endocrinology & Metabolism*, *91*(11), 4505–4509. https://doi.org/10.1210/jc.2006-0423

Bruick, R. K., & McKnight, S. L. (2001). A Conserved Family of Prolyl-4-Hydroxylases That Modify HIF. *Science*, *294*(5545), 1337–1340. https://doi.org/10.1126/science.1066373

Brundin, T. (1966). Storage and in vitro Release Rate of Catecholamines from Granules Isolated from Preaortal Paraganglia and Adrenals of Newborn Rabbits. *Acta Physiologica Scandinavica*, *66*(4), 406–409. https://doi.org/10.1111/j.1748-1716.1966.tb03217.x

Buckler, K. J. (1997). A novel oxygen-sensitive potassium current in rat carotid body type I cells. *The Journal of Physiology*, *498*(3), 649–662. https://doi.org/10.1113/jphysiol.1997.sp021890

Buckler, K. J. (2015). TASK channels in arterial chemoreceptors and their role in oxygen and acid sensing. *Pflügers Archiv - European Journal of Physiology*, *467*(5), 1013–1025. https://doi.org/10.1007/s00424-015-1689-1

Buckler, K. J., & Turner, P. J. (2013). Oxygen sensitivity of mitochondrial function in rat arterial chemoreceptor cells. *The Journal of Physiology*, *591*(14), 3549–3563. https://doi.org/10.1113/jphysiol.2013.257741

Buckler, K. J., & Vaughan-Jones, R. D. (1994). Effects of hypoxia on membrane potential and intracellular calcium in rat neonatal carotid body type I cells. *The Journal of Physiology*, *476*(3), 423–428. https://doi.org/10.1113/jphysiol.1994.sp020143

Buckler, K. J., Williams, B. A., & Honore, E. (2000). An oxygen-, acid- and anaesthetic-sensitive TASK-like background potassium channel in rat arterial chemoreceptor cells. *The Journal of Physiology*, *525*(1), 135–142. https://doi.org/10.1111/j.1469-7793.2000.00135.x

Buffet, A., Burnichon, N., Favier, J., & Gimenez-Roqueplo, A.-P. (2020b). An overview of 20 years of genetic studies in pheochromocytoma and paraganglioma. *Best Practice & Research Clinical Endocrinology & Metabolism*, *34*(2), 101416. https://doi.org/10.1016/j.beem.2020.101416

Buffet, A., Smati, S., Mansuy, L., Ménara, M., Lebras, M., Heymann, M.-F., Simian, C., Favier, J., Murat, A., Cariou, B., & Gimenez-Roqueplo, A.-P. (2014). Mosaicism in *HIF2A* -Related Polycythemia-Paraganglioma Syndrome. *The Journal of Clinical Endocrinology & Metabolism*, *99*(2), E369–E373. https://doi.org/10.1210/jc.2013-2600

Burnichon, N., Vescovo, L., Amar, L., Libé, R., de Reynies, A., Venisse, A., Jouanno, E., Laurendeau, I., Parfait, B., Bertherat, J., Plouin, P.-F., Jeunemaitre, X., Favier, J., & Gimenez-Roqueplo, A.-P. (2011). Integrative genomic analysis reveals somatic mutations in pheochromocytoma and paraganglioma. *Human Molecular Genetics*, *20*(20), 3974–3985. https://doi.org/10.1093/hmg/ddr324

Calsina, B., Piñeiro-Yáñez, E., Martínez-Montes, Á. M., Caleiras, E., Fernández-Sanromán, Á., Monteagudo, M., Torres-Pérez, R., Fustero-Torre, C., Pulgarín-Alfaro, M., Gil, E., León, R., Jiménez, S., García-Martín, S., Martin, M. C., Roldán-Romero, J. M., Lanillos, J., Mellid, S., Santos, M., Díaz-Talavera, A., … Robledo, M. (2023). Genomic and immune landscape Of metastatic pheochromocytoma and paraganglioma. *Nature Communications*, *14*(1), 1122. https://doi.org/10.1038/s41467-023-36769-6

Carbone, E., Borges, R., Eiden, L. E., García, A. G., & Hernández-Cruz, A. (2019). Chromaffin Cells of the Adrenal Medulla: Physiology, Pharmacology, and Disease. *Comprehensive Physiology*, *9*(4), 1443–1502. https://doi.org/10.1002/j.2040-4603.2019.tb00098.x

Cardones, A. R., & Banez, L. L. (2006). VEGF inhibitors in cancer therapy. *Current Pharmaceutical Design*, *12*(3), 387–394. https://doi.org/10.2174/138161206775201910

Carroll, J. L., & Kim, I. (2005). Postnatal development of carotid body glomus cell O2 sensitivity. *Respiratory Physiology & Neurobiology*, *149*(1–3), 201–215. https://doi.org/10.1016/j.resp.2005.04.009

Cascón, A., Calsina, B., Monteagudo, M., Mellid, S., Díaz-Talavera, A., Currás-Freixes, M., & Robledo, M. (2023). Genetic bases of pheochromocytoma and paraganglioma. *Journal of Molecular Endocrinology*, *70*(3). https://doi.org/10.1530/JME-22-0167

Chang, A. J., Ortega, F. E., Riegler, J., Madison, D. v., & Krasnow, M. A. (2015). Oxygen regulation of breathing through an olfactory receptor activated by lactate. *Nature*, *527*(7577), 240–244. https://doi.org/10.1038/nature15721

Chen, J., He, L., Liu, X., Dinger, B., Stensaas, L., & Fidone, S. (2007). Effect of the endothelin receptor antagonist bosentan on chronic hypoxia-induced morphological and physiological changes in rat carotid body. *American Journal of Physiology-Lung Cellular and Molecular Physiology*, *292*(5), L1257–L1262. https://doi.org/10.1152/ajplung.00419.2006

Chen, T.-W., Wardill, T. J., Sun, Y., Pulver, S. R., Renninger, S. L., Baohan, A., Schreiter, E. R., Kerr, R. A., Orger, M. B., Jayaraman, V., Looger, L. L., Svoboda, K., & Kim, D. S. (2013). Ultrasensitive fluorescent proteins for imaging neuronal activity. *Nature*, *499*(7458), 295–300. https://doi.org/10.1038/nature12354

Chen, Y., Tipoe, G. L., Liong, E., Leung, P., Lam, S.-Y., Iwase, R., Tjong, Y.-W., & Fung, M.-L. (2002). Chronic hypoxia enhances endothelin-1-induced intracellular calcium elevation in rat carotid body chemoreceptors and up-regulates ETA receptor expression. *Pflügers Archiv - European Journal of Physiology*, *443*(4), 565–573. https://doi.org/10.1007/s00424-001-0728-2

Cheng, X., Prange-Barczynska, M., Fielding, J. W., Zhang, M., Burrell, A. L., Lima, J. D. C. C., Eckardt, L., Argles, I. L. A., Pugh, C. W., Buckler, K. J., Robbins, P. A., Hodson, E. J., Bruick, R. K., Collinson, L. M., Rastinejad, F., Bishop, T., & Ratcliffe, P. J. (2020). Marked and rapid effects of pharmacological HIF-2α antagonism on hypoxic ventilatory control. *Journal of Clinical Investigation*, *130*(5), 2237–2251. https://doi.org/10.1172/JCI133194

Clifford, S. C. (2001). Contrasting effects on HIF-1alpha regulation by disease-causing pVHL mutations correlate with patterns of tumourigenesis in von Hippel-Lindau disease. *Human Molecular Genetics*, *10*(10), 1029–1038. https://doi.org/10.1093/hmg/10.10.1029

Colinas, O., Moreno-Domínguez, A., Ortega-Sáenz, P., & López-Barneo, J. (2023). *Constitutive Expression of Hif2α Confers Acute O2 Sensitivity to Carotid Body Glomus Cells* (pp. 153–162). https://doi.org/10.1007/978-3-031-32371-3_17

Comino-Méndez, I., de Cubas, A. A., Bernal, C., Álvarez-Escolá, C., Sánchez-Malo, C., Ramírez-Tortosa, C. L., Pedrinaci, S., Rapizzi, E., Ercolino, T., Bernini, G., Bacca, A., Letón, R., Pita, G., Alonso, M. R., Leandro-García, L. J., Gómez-Graña, Á., Inglada-Pérez, L., Mancikova, V., Rodríguez-Antona, C., … Cascón, A. (2013). Tumoral EPAS1 (HIF2A) mutations explain sporadic pheochromocytoma and paraganglioma in the absence of erythrocytosis. *Human Molecular Genetics*, *22*(11), 2169–2176. https://doi.org/10.1093/hmg/ddt069

Cornfield, D. N., Stevens, T., McMurtry, I. F., Abman, S. H., & Rodman, D. M. (1994). Acute hypoxia causes membrane depolarization and calcium influx in fetal pulmonary artery smooth muscle cells. *American Journal of Physiology-Lung Cellular and Molecular Physiology*, *266*(4), L469–L475. https://doi.org/10.1152/ajplung.1994.266.4.L469

Coupland, R. E. (1965). *The natural history of the chromaffin cell*.

Covello, K. L., Kehler, J., Yu, H., Gordan, J. D., Arsham, A. M., Hu, C.-J., Labosky, P. A., Simon, M. C., & Keith, B. (2006). HIF-2α regulates Oct-4: effects of hypoxia on stem cell function, embryonic development, and tumor growth. *Genes & Development*, *20*(5), 557–570. https://doi.org/10.1101/gad.1399906

Crona, J., Lamarca, A., Ghosal, S., Welin, S., Skogseid, B., & Pacak, K. (2019). Genotype–phenotype correlations in pheochromocytoma and paraganglioma: a systematic review and individual patient meta-analysis. *Endocrine-Related Cancer*, *26*(5), 539–550. https://doi.org/10.1530/ERC-19-0024

Crona, J., Taïeb, D., & Pacak, K. (2017). New Perspectives on Pheochromocytoma and Paraganglioma: Toward a Molecular Classification. *Endocrine Reviews*, *38*(6), 489–515. https://doi.org/10.1210/er.2017-00062

Cubiella, T., Alba-Linares, J. J., San-Juan-Guardado, J., Suarez-Priede, A., Gómez-Suárez, N., Tous, M., Bancos, I., Villabona, C., Serrano, T., Tena, I., del Olmo, M., Forga, L., Valdés, N., Fraga, M. F., & Chiara, M.-D. (2026). Epigenetic and metabolic rewiring in metastatic pheochromocytomas and paragangliomas driven by SDHB mutations. *Communications Biology*, *9*(1), 266. https://doi.org/10.1038/s42003-026-09543-9

Czyzyk-Krzeska, M. F., Bayliss, D. A., Lawson, E. E., & Millhorn, D. E. (1992). Regulation of Tyrosine Hydroxylase Gene Expression in the Rat Carotid Body by Hypoxia. *Journal of Neurochemistry*, *58*(4), 1538–1546. https://doi.org/10.1111/j.1471-4159.1992.tb11376.x

Dahia, P. L. M. (2014). Pheochromocytoma and paraganglioma pathogenesis: learning from genetic heterogeneity. *Nature Reviews Cancer*, *14*(2), 108–119. https://doi.org/10.1038/nrc3648

Dahia, P. L. M., Ross, K. N., Wright, M. E., Hayashida, C. Y., Santagata, S., Barontini, M., Kung, A. L., Sanso, G., Powers, J. F., Tischler, A. S., Hodin, R., Heitritter, S., Moore, F., Dluhy, R., Sosa, J. A., Ocal, I. T., Benn, D. E., Marsh, D. J., Robinson, B. G., … Stiles, C. D. (2005). A HIF1alpha regulatory loop links hypoxia and mitochondrial signals in pheochromocytomas. *PLoS Genetics*, *1*(1), 72–80. https://doi.org/10.1371/journal.pgen.0010008

de Castro, F. (1926). Sur la structure et l'innervation de la glande intercarotidienne de l'homme et des mammifères et sur un nouveau système d'innervation autonome du nerf glossopharyngien. *Trabajos Del Laboratorio de Investigaciones Biológicas de La Universidad de Madrid*, *24*, 365–432.

de Castro, F. (1928). Sur la structure et l'innervation du sinus carotidien de l'homme et des mammifères: nouveaux faits sur l'innervation et la fonction du glomus caroticum. *Trabajos Del Laboratorio de Investigaciones Biológicas de La Universidad de Madrid*, *25*, 330–380.

de Castro, F. (2009). *The Discovery of Sensory Nature of the Carotid Bodies – Invited Article* (pp. 1–18). https://doi.org/10.1007/978-90-481-2259-2_1

de Kock, L. L. (1951). Histology of the Carotid Body. *Nature*, *167*(4250), 611–612. https://doi.org/10.1038/167611b0

Dhillon, D. P., Barer, G. R., & Walsh, M. (1984). THE ENLARGED CAROTID BODY OF THE CHRONICALLY HYPOXIC AND CHRONICALLY HYPOXIC AND HYPERCAPNIC RAT: A MORPHOMETRIC ANALYSIS. *Quarterly Journal of Experimental Physiology*, *69*(2), 301–317. https://doi.org/10.1113/expphysiol.1984.sp002807

Diao, X., Ye, F., Zhang, M., Ren, X., Tian, X., Lu, J., Sun, X., Hou, Z., Chen, X., Li, F., Zhuang, J., Ding, H., Peng, C., Rastinejad, F., Luo, C., & Wu, D. (2022). Identification of oleoylethanolamide as an endogenous ligand for HIF-3α. *Nature Communications*, *13*(1), 2529. https://doi.org/10.1038/s41467-022-30338-z

Douglas, C. G., Haldane, J. S., Henderson, Y., & Schneider, E. C. (1913). VI. Physiological observations made on Pike's Peak, Colorado, with special reference to adaptation to low barometric pressures. *Philosophical Transactions of the Royal Society of London. Series B, Containing Papers of a Biological Character*, *203*(294–302), 185–318. https://doi.org/10.1098/rstb.1913.0006

Eckardt, L., Prange-Barczynska, M., Hodson, E. J., Fielding, J. W., Cheng, X., Lima, J. D. C. C., Kurlekar, S., Douglas, G., Ratcliffe, P. J., & Bishop, T. (2021). Developmental role of PHD2 in the pathogenesis of pseudohypoxic pheochromocytoma. *Endocrine-Related Cancer*, *28*(12), 757–772. https://doi.org/10.1530/ERC-21-0211

Eisenhofer, G., Walther, M. M., Huynh, T.-T., Li, S.-T., Bornstein, S. R., Vortmeyer, A., Mannelli, M., Goldstein, D. S., Linehan, W. M., Lenders, J. W. M., & Pacak, K. (2001). Pheochromocytomas in von Hippel-Lindau Syndrome and Multiple Endocrine Neoplasia Type 2 Display Distinct Biochemical and Clinical Phenotypes. *The Journal of Clinical Endocrinology & Metabolism*, *86*(5), 1999–2008. https://doi.org/10.1210/jcem.86.5.7496

Ema, M., Taya, S., Yokotani, N., Sogawa, K., Matsuda, Y., & Fujii-Kuriyama, Y. (1997). A novel bHLH-PAS factor with close sequence similarity to hypoxia-inducible factor 1α regulates the *VEGF* expression and is potentially involved in lung and vascular development. *Proceedings of the National Academy of Sciences*, *94*(9), 4273–4278. https://doi.org/10.1073/pnas.94.9.4273

Epstein, A. C. R., Gleadle, J. M., McNeill, L. A., Hewitson, K. S., O'Rourke, J., Mole, D. R., Mukherji, M., Metzen, E., Wilson, M. I., Dhanda, A., Tian, Y.-M., Masson, N., Hamilton, D. L., Jaakkola, P., Barstead, R., Hodgkin, J., Maxwell, P. H., Pugh, C. W., Schofield, C. J., & Ratcliffe, P. J. (2001). C. elegans EGL-9 and Mammalian Homologs Define a Family of Dioxygenases that Regulate HIF by Prolyl Hydroxylation. *Cell*, *107*(1), 43–54. https://doi.org/10.1016/S0092-8674(01)00507-4

Evenepoel, L., Papathomas, T. G., Krol, N., Korpershoek, E., de Krijger, R. R., Persu, A., & Dinjens, W. N. M. (2015). Toward an improved definition of the genetic and tumor spectrum associated with SDH germ-line mutations. *Genetics in Medicine*, *17*(8), 610–620. https://doi.org/10.1038/gim.2014.162

Favier, J., Amar, L., & Gimenez-Roqueplo, A.-P. (2015). Paraganglioma and phaeochromocytoma: from genetics to personalized medicine. *Nature Reviews Endocrinology*, *11*(2), 101–111. https://doi.org/10.1038/nrendo.2014.188

Favier, J., Brière, J.-J., Burnichon, N., Rivière, J., Vescovo, L., Benit, P., Giscos-Douriez, I., de Reyniès, A., Bertherat, J., Badoual, C., Tissier, F., Amar, L., Libé, R., Plouin, P.-F., Jeunemaitre, X., Rustin, P., & Gimenez-Roqueplo, A.-P. (2009b). The Warburg Effect Is Genetically Determined in Inherited Pheochromocytomas. *PLoS ONE*, *4*(9), e7094. https://doi.org/10.1371/journal.pone.0007094

Favier, J., & Gimenez-Roqueplo, A.-P. (2010). Pheochromocytomas: The (pseudo)-hypoxia hypothesis. *Best Practice & Research Clinical Endocrinology & Metabolism*, *24*(6), 957–968. https://doi.org/10.1016/j.beem.2010.10.004

Favier, J., Kempf, H., Corvol, P., & Gasc, J.-M. (1999). Cloning and expression pattern of EPAS1 in the chicken embryo. *FEBS Letters*, *462*(1–2), 19–24. https://doi.org/10.1016/S0014-5793(99)01476-3

Feil, R., Brocard, J., Mascrez, B., LeMeur, M., Metzger, D., & Chambon, P. (1996). Ligand-activated site-specific recombination in mice. *Proceedings of the National Academy of Sciences*, *93*(20), 10887–10890. https://doi.org/10.1073/pnas.93.20.10887

Fernández-Agüera, M. C., Gao, L., González-Rodríguez, P., Pintado, C. O., Arias-Mayenco, I., García-Flores, P., García-Pergañeda, A., Pascual, A., Ortega-Sáenz, P., & López-Barneo, J. (2015). Oxygen Sensing by Arterial Chemoreceptors Depends on Mitochondrial Complex I Signaling. *Cell Metabolism*, *22*(5), 825–837. https://doi.org/10.1016/j.cmet.2015.09.004

Fieber, L. A., & McCleskey, E. W. (1993). L-type calcium channels in type I cells of the rat carotid body. *Journal of Neurophysiology*, *70*(4), 1378–1384. https://doi.org/10.1152/jn.1993.70.4.1378

Fielding, J. W., Hodson, E. J., Cheng, X., Ferguson, D. J. P., Eckardt, L., Adam, J., Lip, P., Maton-Howarth, M., Ratnayaka, I., Pugh, C. W., Buckler, K. J., Ratcliffe, P. J., & Bishop, T. (2018). PHD2 inactivation in Type I cells drives HIF-2α-dependent multilineage hyperplasia and the formation of paraganglioma-like carotid bodies. *The Journal of Physiology*, *596*(18), 4393–4412. https://doi.org/10.1113/JP275996

Fishbein, L., Leshchiner, I., Walter, V., Danilova, L., Robertson, A. G., Johnson, A. R., Lichtenberg, T. M., Murray, B. A., Ghayee, H. K., Else, T., Ling, S., Jefferys, S. R., de Cubas, A. A., Wenz, B., Korpershoek, E., Amelio, A. L., Makowski, L., Rathmell, W. K., Gimenez-Roqueplo, A.-P., … Zmuda, E. (2017). Comprehensive Molecular Characterization of Pheochromocytoma and Paraganglioma. *Cancer Cell*, *31*(2), 181–193. https://doi.org/10.1016/j.ccell.2017.01.001

Fishbein, L., & Wilkerson, M. D. (2018). Chromaffin cell biology: inferences from The Cancer Genome Atlas. *Cell and Tissue Research*, *372*(2), 339–346. https://doi.org/10.1007/s00441-018-2795-0

Flamme, I., Fröhlich, T., von Reutern, M., Kappel, A., Damert, A., & Risau, W. (1997). HRF, a putative basic helix-loop-helix-PAS-domain transcription factor is closely related to hypoxia-inducible factor-1α and developmentally expressed in blood vessels. *Mechanisms of Development*, *63*(1), 51–60. https://doi.org/10.1016/S0925-4773(97)00674-6

Fletcher, S. C., & Coleman, M. L. (2020). Human 2-oxoglutarate-dependent oxygenases: nutrient sensors, stress responders, and disease mediators. *Biochemical Society Transactions*, *48*(5), 1843–1858. https://doi.org/10.1042/BST20190333

Flores, S. K., Estrada-Zuniga, C. M., Thallapureddy, K., Armaiz-Peña, G., & Dahia, P. L. M. (2021). Insights into Mechanisms of Pheochromocytomas and Paragangliomas Driven by Known or New Genetic Drivers. *Cancers*, *13*(18), 4602. https://doi.org/10.3390/cancers13184602

Flynn, A., Pattison, A. D., Balachander, S., Boehm, E., Bowen, B., Dwight, T., Rossello, F. J., Hofmann, O., Martelotto, L., Zethoven, M., Kirschner, L. S., Else, T., Fishbein, L., Gill, A. J., Tischler, A. S., Giordano, T., Prodanov, T., Noble, J. R., Reddel, R. R., … Tothill, R. W. (2025). Multi-omic analysis of SDHB-deficient pheochromocytomas and paragangliomas identifies metastasis and treatment-related molecular profiles. *Nature Communications*, *16*(1), 2632. https://doi.org/10.1038/s41467-025-57595-y

Fong, G.-H., & Takeda, K. (2008). Role and regulation of prolyl hydroxylase domain proteins. *Cell Death & Differentiation*, *15*(4), 635–641. https://doi.org/10.1038/cdd.2008.10

Forster, H. v., Bisgard, G. E., & Klein, J. P. (1981). Effect of peripheral chemoreceptor denervation on acclimatization of goats during hypoxia. *Journal of Applied Physiology*, *50*(2), 392–398. https://doi.org/10.1152/jappl.1981.50.2.392

Friedrich, G., & Soriano, P. (1991). Promoter traps in embryonic stem cells: a genetic screen to identify and mutate developmental genes in mice. *Genes & Development*, *5*(9), 1513–1523. https://doi.org/10.1101/gad.5.9.1513

Furlan, A., Dyachuk, V., Kastriti, M. E., Calvo-Enrique, L., Abdo, H., Hadjab, S., Chontorotzea, T., Akkuratova, N., Usoskin, D., Kamenev, D., Petersen, J., Sunadome, K., Memic, F., Marklund, U., Fried, K., Topilko, P., Lallemend, F., Kharchenko, P. v, Ernfors, P., & Adameyko, I. (2017). Multipotent peripheral glial cells generate neuroendocrine cells of the adrenal medulla. *Science (New York, N.Y.)*, *357*(6346). https://doi.org/10.1126/science.aal3753

Ganfornina, M. D., Pérez-García, M. T., Gutiérrez, G., Miguel-Velado, E., López-López, J. R., Marín, A., Sánchez, D., & González, C. (2005). Comparative gene expression profile of mouse carotid body and adrenal medulla under physiological hypoxia. *The Journal of Physiology*, *566*(2), 491–503. https://doi.org/10.1113/jphysiol.2005.088815

Gao, L., Bonilla-Henao, V., García-Flores, P., Arias-Mayenco, I., Ortega-Sáenz, P., & López-Barneo, J. (2017). Gene expression analyses reveal metabolic specifications in acute O_2 -sensing

chemoreceptor cells. *The Journal of Physiology*, *595*(18), 6091–6120. https://doi.org/10.1113/JP274684

Gao, L., González-Rodríguez, P., Ortega-Sáenz, P., & López-Barneo, J. (2017). Redox signaling in acute oxygen sensing. *Redox Biology*, *12*, 908–915. https://doi.org/10.1016/j.redox.2017.04.033

García-Fernández, M., Mejías, R., & López-Barneo, J. (2007). Developmental changes of chromaffin cell secretory response to hypoxia studied in thin adrenal slices. *Pflügers Archiv - European Journal of Physiology*, *454*(1), 93–100. https://doi.org/10.1007/s00424-006-0186-y

Geisler, C. E., & Hayes, M. R. (2023). Metabolic hormone action in the VTA: Reward-directed behavior and mechanistic insights. *Physiology & Behavior*, *268*, 114236. https://doi.org/10.1016/j.physbeh.2023.114236

Gelman, D. M., Noaín, D., Avale, M. E., Otero, V., Low, M. J., & Rubinstein, M. (2003). Transgenic mice engineered to target Cre/loxP-mediated DNA recombination into catecholaminergic neurons. *Genesis*, *36*(4), 196–202. https://doi.org/10.1002/gene.10217

Gimenez-Roqueplo, A.-P., Favier, J., Rustin, P., Rieubland, C., Crespin, M., Nau, V., Khau Van Kien, P., Corvol, P., Plouin, P.-F., Jeunemaitre, X., & COMETE Network. (2003). Mutations in the SDHB gene are associated with extra-adrenal and/or malignant phaeochromocytomas. *Cancer Research*, *63*(17), 5615–5621.

Gimenez-Roqueplo, A.-P., Robledo, M., & Dahia, P. L. M. (2023). Update on the genetics of paragangliomas. *Endocrine-Related Cancer*, *30*(4). https://doi.org/10.1530/ERC-22-0373

Giussani, D. A. (2016). The fetal brain sparing response to hypoxia: physiological mechanisms. *The Journal of Physiology*, *594*(5), 1215–1230. https://doi.org/10.1113/JP271099

Giussani, D. A., Spencer, J. A., Moore, P. J., Bennet, L., & Hanson, M. A. (1993). Afferent and efferent components of the cardiovascular reflex responses to acute hypoxia in term fetal sheep. *The Journal of Physiology*, *461*(1), 431–449. https://doi.org/10.1113/jphysiol.1993.sp019521

Goncalves, J., Moog, S., Morin, A., Gentric, G., Müller, S., Morrell, A. P., Kluckova, K., Stewart, T. J., Andoniadou, C. L., Lussey-Lepoutre, C., Bénit, P., Thakker, A., Vettore, L., Roberts, J., Rodriguez, R., Mechta-Grigoriou, F., Gimenez-Roqueplo, A.-P., Letouzé, E., Tennant, D. A., & Favier, J. (2021). Loss of SDHB Promotes Dysregulated Iron Homeostasis, Oxidative Stress, and Sensitivity to Ascorbate. *Cancer Research*, *81*(13), 3480–3494. https://doi.org/10.1158/0008-5472.CAN-20-2936

Gonzalez, C., Almaraz, L., Obeso, A., & Rigual, R. (1994). Carotid body chemoreceptors: from natural stimuli to sensory discharges. *Physiological Reviews*, *74*(4), 829–898. https://doi.org/10.1152/physrev.1994.74.4.829

Gonzalez, C., Conde, S. v., Gallego-MartÃn, T., Olea, E., Gonzalez-Obeso, E., Ramirez, M., Yubero, S., Agapito, M. T., Gomez-NiÃ±no, A., Obeso, A., Rigual, R., & Rocher, A. (2014). Fernando de Castro and the discovery of the arterial chemoreceptors. *Frontiers in Neuroanatomy*, *8*. https://doi.org/10.3389/fnana.2014.00025

Gonzalez-Urquijo, M., Viteri-Pérez, V. H., Becerril-Gaitan, A., Hinojosa-Gonzalez, D., Enríquez-Vega, M. E., Soto Vaca Guzmán, I. W., Valda-Ameller, G. E., de Jesús García-Pérez, J., Vaquero-Puerta, C., Jaramillo-Vergara, V. H., Cisneros-Tinoco, M. A., Santoscoy-Ibarra, J. M., Fabiani, M. A., Cárdenas-Figueroa, E. G., Borja-Rojas, V. E., Salinas-Ramos, I. V., Gonzalez-Valladares, A. J., Katherine-Perez, A. C., Bañuelos-Gutierrez, G., … Barajas-Colón, J. Á. (2022). Clinical Characteristics and Surgical Outcomes of Carotid Body Tumors: Data from the Carotid Paraganglioma Cooperative International Registry (CAPACITY) Group. *World Journal of Surgery*, *46*(10), 2507–2514. https://doi.org/10.1007/s00268-022-06663-1

Gray, O. A., Yoo, J., Sobreira, D. R., Jousma, J., Witonsky, D., Sakabe, N. J., Peng, Y.-J., Prabhakar, N. R., Fang, Y., Nobréga, M. A., & di Rienzo, A. (2022). A pleiotropic hypoxia-sensitive *EPAS1* enhancer is disrupted by adaptive alleles in Tibetans. *Science Advances*, *8*(47). https://doi.org/10.1126/sciadv.ade1942

Greer, S. N., Metcalf, J. L., Wang, Y., & Ohh, M. (2012). The updated biology of hypoxia-inducible factor. *The EMBO Journal*, *31*(11), 2448–2460. https://doi.org/10.1038/emboj.2012.125

Gronblad, M., & Eranko, O. (1978). Fine structure of dense-cored vesicles in glomus cells of rat carotid body after fixation with permanganate or glutaraldehyde. *Histochemistry*, *57*(4), 305–312. https://doi.org/10.1007/BF00492666

Gu, Y. Z., Moran, S. M., Hogenesch, J. B., Wartman, L., & Bradfield, C. A. (1998). Molecular characterization and chromosomal localization of a third alpha-class hypoxia inducible factor subunit, HIF3alpha. *Gene Expression*, *7*(3), 205–213.

Guha, A., Musil, Z., Vicha, A., Zelinka, T., Pacak, K., Astl, J., & Chovanec, M. (2019). A systematic review on the genetic analysis of paragangliomas: primarily focused on head and neck paragangliomas. *Neoplasma*, *66*(05), 671–680. https://doi.org/10.4149/neo_2018_181208N933

Guilmette, J., & Sadow, P. M. (2019). A Guide to Pheochromocytomas and Paragangliomas. *Surgical Pathology Clinics*, *12*(4), 951–965. https://doi.org/10.1016/j.path.2019.08.009

Hansen, J. T. (1981). Morphological aspects of secretion in the glomus cell paraneurons of the carotid body: evidence for calcium-dependent exocytosis. *Cytobios*, *32*(126), 79–88.

Heikkilä, M., Pasanen, A., Kivirikko, K. I., & Myllyharju, J. (2011). Roles of the human hypoxia-inducible factor (HIF)-3α variants in the hypoxia response. *Cellular and Molecular Life Sciences*, *68*(23), 3885–3901. https://doi.org/10.1007/s00018-011-0679-5

Hervonen, A., & Korkala, O. (1972a). The Effect of Hypoxia on the Catecholamine Content of Human Fetal Abdominal Paraganglia and Adrenal Medulla. *Acta Obstetricia et Gynecologica Scandinavica*, *51*(1), 17–24. https://doi.org/10.3109/00016347209154963

Hervonen, A., & Korkala, O. (1972b). The Effect of Hypoxia on the Catecholamine Content of Human Fetal Abdominal Paraganglia and Adrenal Medulla. *Acta Obstetricia et Gynecologica Scandinavica*, *51*(1), 17–24. https://doi.org/10.3109/00016347209154963

Heymans, C. (1930). Sinus carotidien et réflexes respiratoires. II. Influences respiratoires réflexes de l'acidose, de l'alcalose, de l'anhydride carbonique, de l'ion hydrogène et de l'anoxémie: sinus carotidiens et échanges respiratoires dans les poumons et au-delà des poumons. *Archives Internationales de Pharmacodynamie et de Thérapie*, *39*, 400–448.

Heymans, C. (1938). Role of the Cardioaortic and Carotid-Sinus Nerves in the Reflex Control of the Respiratory Center. *New England Journal of Medicine*, *219*(5), 157–159. https://doi.org/10.1056/NEJM193808042190503

Heymans, J. F., & Heymans, C. (1927). Sur les modifications directes et sur la regulation reflexe de l'activite du centre respiratoire de la tete isolee du chien. . *Archives Internationales de Pharmacodynamie et de Thérapie*, *33*, 273–370.

Hiller-Sturmhöfel, S., & Bartke, A. (1998). The endocrine system: an overview. *Alcohol Health and Research World*, *22*(3), 153–164.

Hockman, D., Adameyko, I., Kaucka, M., Barraud, P., Otani, T., Hunt, A., Hartwig, A. C., Sock, E., Waithe, D., Franck, M. C. M., Ernfors, P., Ehinger, S., Howard, M. J., Brown, N., Reese, J., & Baker,

C. V. H. (2018). Striking parallels between carotid body glomus cell and adrenal chromaffin cell development. *Developmental Biology*, *444 Suppl 1*(Suppl 1), S308–S324. https://doi.org/10.1016/j.ydbio.2018.05.016

Hodson, E. J., Nicholls, L. G., Turner, P. J., Llyr, R., Fielding, J. W., Douglas, G., Ratnayaka, I., Robbins, P. A., Pugh, C. W., Buckler, K. J., Ratcliffe, P. J., & Bishop, T. (2016). Regulation of ventilatory sensitivity and carotid body proliferation in hypoxia by the PHD2/HIF-2 pathway. *The Journal of Physiology*, *594*(5), 1179–1195. https://doi.org/10.1113/JP271050

Holmes, A. P., Swiderska, A., Nathanael, D., Aldossary, H. S., Ray, C. J., Coney, A. M., & Kumar, P. (2022). Are Multiple Mitochondrial Related Signalling Pathways Involved in Carotid Body Oxygen Sensing? *Frontiers in Physiology*, *13*. https://doi.org/10.3389/fphys.2022.908617

Howard, L. S., & Robbins, P. A. (1995a). Alterations in respiratory control during 8 h of isocapnic and poikilocapnic hypoxia in humans. *Journal of Applied Physiology*, *78*(3), 1098–1107. https://doi.org/10.1152/jappl.1995.78.3.1098

Howard, L. S., & Robbins, P. A. (1995b). Ventilatory response to 8 h of isocapnic and poikilocapnic hypoxia in humans. *Journal of Applied Physiology*, *78*(3), 1092–1097. https://doi.org/10.1152/jappl.1995.78.3.1092

Hu, C.-J., Sataur, A., Wang, L., Chen, H., & Simon, M. C. (2007). The N-Terminal Transactivation Domain Confers Target Gene Specificity of Hypoxia-inducible Factors HIF-1α and HIF-2α. *Molecular Biology of the Cell*, *18*(11), 4528–4542. https://doi.org/10.1091/mbc.e06-05-0419

Hu, C.-J., Wang, L.-Y., Chodosh, L. A., Keith, B., & Simon, M. C. (2003). Differential Roles of Hypoxia-Inducible Factor 1α (HIF-1α) and HIF-2α in Hypoxic Gene Regulation. *Molecular and Cellular Biology*, *23*(24), 9361–9374. https://doi.org/10.1128/MCB.23.24.9361-9374.2003

Huang, J., Zhao, Q., Mooney, S. M., & Lee, F. S. (2002). Sequence Determinants in Hypoxia-inducible Factor-1α for Hydroxylation by the Prolyl Hydroxylases PHD1, PHD2, and PHD3. *Journal of Biological Chemistry*, *277*(42), 39792–39800. https://doi.org/10.1074/jbc.M206955200

Huang, L. E., Arany, Z., Livingston, D. M., & Bunn, H. F. (1996). Activation of Hypoxia-inducible Transcription Factor Depends Primarily upon Redox-sensitive Stabilization of Its α Subunit. *Journal of Biological Chemistry*, *271*(50), 32253–32259. https://doi.org/10.1074/jbc.271.50.32253

Ishiguro, T., Iwase, M., Kanamaru, M., Izumizaki, M., Ohshima, Y., & Homma, I. (2006). Impaired ventilation and metabolism response to hypoxia in histamine H1 receptor-knockout mice. *Respiratory Physiology & Neurobiology*, *154*(3), 331–341. https://doi.org/10.1016/j.resp.2006.01.017

Iturriaga, R., & Alcayaga, J. (2004). Neurotransmission in the carotid body: transmitters and modulators between glomus cells and petrosal ganglion nerve terminals. *Brain Research Reviews*, *47*(1–3), 46–53. https://doi.org/10.1016/j.brainresrev.2004.05.007

Iturriaga, R., Alcayaga, J., Chapleau, M. W., & Somers, V. K. (2021). Carotid body chemoreceptors: physiology, pathology, and implications for health and disease. *Physiological Reviews*, *101*(3), 1177–1235. https://doi.org/10.1152/physrev.00039.2019

Ivan, M., Haberberger, T., Gervasi, D. C., Michelson, K. S., Günzler, V., Kondo, K., Yang, H., Sorokina, I., Conaway, R. C., Conaway, J. W., & Kaelin, W. G. (2002). Biochemical purification and pharmacological inhibition of a mammalian prolyl hydroxylase acting on hypoxia-inducible factor. *Proceedings of the National Academy of Sciences*, *99*(21), 13459–13464. https://doi.org/10.1073/pnas.192342099

Ivan, M., Kondo, K., Yang, H., Kim, W., Valiando, J., Ohh, M., Salic, A., Asara, J. M., Lane, W. S., & Kaelin Jr., W. G. (2001). HIFα Targeted for VHL-Mediated Destruction by Proline Hydroxylation: Implications for O $_2$ Sensing. *Science*, *292*(5516), 464–468. https://doi.org/10.1126/science.1059817

Iyer, N. v., Kotch, L. E., Agani, F., Leung, S. W., Laughner, E., Wenger, R. H., Gassmann, M., Gearhart, J. D., Lawler, A. M., Yu, A. Y., & Semenza, G. L. (1998). Cellular and developmental control of O $_2$ homeostasis by hypoxia-inducible factor 1α. *Genes & Development*, *12*(2), 149–162. https://doi.org/10.1101/gad.12.2.149

Jaakkola, P., Mole, D. R., Tian, Y.-M., Wilson, M. I., Gielbert, J., Gaskell, S. J., Kriegsheim, A. von, Hebestreit, H. F., Mukherji, M., Schofield, C. J., Maxwell, P. H., Pugh, ‡ Christopher W., & Ratcliffe, ‡ Peter J. (2001). Targeting of HIF-α to the von Hippel-Lindau Ubiquitylation Complex by O $_2$ -Regulated Prolyl Hydroxylation. *Science*, *292*(5516), 468–472. https://doi.org/10.1126/science.1059796

Jhawar, S., Arakawa, Y., Kumar, S., Varghese, D., Kim, Y. S., Roper, N., Elloumi, F., Pommier, Y., Pacak, K., & del Rivero, J. (2022). New Insights on the Genetics of Pheochromocytoma and Paraganglioma and Its Clinical Implications. *Cancers*, *14*(3), 594. https://doi.org/10.3390/cancers14030594

Jiang, B. H., Semenza, G. L., Bauer, C., & Marti, H. H. (1996). Hypoxia-inducible factor 1 levels vary exponentially over a physiologically relevant range of O2 tension. *American Journal of Physiology-Cell Physiology*, *271*(4), C1172–C1180. https://doi.org/10.1152/ajpcell.1996.271.4.C1172

Jimenez, C., Andreassen, M., Durand, A., Moog, S., Hendifar, A., Welin, S., Spada, F., Sharma, R., Wolin, E., Ruether, J., Garcia-Carbonero, R., Fassnacht, M., Capdevila, J., del Rivero, J., Iliopoulos, O., Huillard, O., Jang, R., Mai, K., Artamonova, E., … Berruti, A. (2025). Belzutifan for Advanced Pheochromocytoma or Paraganglioma. *New England Journal of Medicine*, *393*(20), 2012–2022. https://doi.org/10.1056/NEJMoa2504964

Jochmanova, I., Wolf, K. I., King, K. S., Nambuba, J., Wesley, R., Martucci, V., Raygada, M., Adams, K. T., Prodanov, T., Fojo, A. T., Lazurova, I., & Pacak, K. (2017). SDHB-related pheochromocytoma and paraganglioma penetrance and genotype–phenotype correlations. *Journal of Cancer Research and Clinical Oncology*, *143*(8), 1421–1435. https://doi.org/10.1007/s00432-017-2397-3

Jones, C. T., & Robinson, R. O. (1975). Plasma catecholamines in foetal and adult sheep. *The Journal of Physiology*, *248*(1), 15–33. https://doi.org/10.1113/jphysiol.1975.sp010960

Jorgensen, K., Song, D., Weinstein, J., Garcia, O. A., Pearson, L. N., Inclán, M., Rivera-Chira, M., León-Velarde, F., Kiyamu, M., Brutsaert, T. D., Bigham, A. W., & Lee, F. S. (2023). High-Altitude Andean H194R *HIF2A* Allele Is a Hypomorphic Allele. *Molecular Biology and Evolution*, *40*(7). https://doi.org/10.1093/molbev/msad162

Kaelin, W. G., & Ratcliffe, P. J. (2008). Oxygen Sensing by Metazoans: The Central Role of the HIF Hydroxylase Pathway. *Molecular Cell*, *30*(4), 393–402. https://doi.org/10.1016/j.molcel.2008.04.009

Kallio, P. J., Pongratz, I., Gradin, K., McGuire, J., & Poellinger, L. (1997). Activation of hypoxia-inducible factor 1α: Posttranscriptional regulation and conformational change by recruitment of the Arnt transcription factor. *Proceedings of the National Academy of Sciences*, *94*(11), 5667–5672. https://doi.org/10.1073/pnas.94.11.5667

Kameda, Y. (1996). Immunoelectron microscopic localization of vimentin in sustentacular cells of the carotid body and the adrenal medulla of guinea pigs. *Journal of Histochemistry & Cytochemistry*, *44*(12), 1439–1449. https://doi.org/10.1177/44.12.8985136

Kameda, Y. (2020). Molecular and cellular mechanisms of the organogenesis and development of the mammalian carotid body. *Developmental Dynamics*, *249*(5), 592–609. https://doi.org/10.1002/dvdy.144

Kameda, Y., Amano, T., & Tagawa, T. (1990). Distribution and ontogeny of chromogranin A and tyrosine hydroxylase in the carotid body and glomus cells located in the wall of the common carotid artery and its branches in the chicken. *Histochemistry*, *94*(6). https://doi.org/10.1007/BF00271988

Kamihara, J., Hamilton, K. v., Pollard, J. A., Clinton, C. M., Madden, J. A., Lin, J., Imamovic, A., Wall, C. B., Wassner, A. J., Weil, B. R., Heeney, M. M., Vargas, S. O., Kaelin, W. G., Janeway, K. A., Perini, R. F., Zojwalla, N. J., Voss, S. D., & DuBois, S. G. (2021). Belzutifan, a Potent HIF2α Inhibitor, in the Pacak–Zhuang Syndrome. *New England Journal of Medicine*, *385*(22), 2059–2065. https://doi.org/10.1056/NEJMoa2110051

Kane, A. D., Kothmann, E., & Giussani, D. A. (2020). Detection and response to acute systemic hypoxia. *BJA Education*, *20*(2), 58–64. https://doi.org/10.1016/j.bjae.2019.10.004

Kantorovich, V., King, K. S., & Pacak, K. (2010). SDH-related pheochromocytoma and paraganglioma. *Best Practice & Research. Clinical Endocrinology & Metabolism*, *24*(3), 415–424. https://doi.org/10.1016/j.beem.2010.04.001

Kastriti, M. E., Kameneva, P., Kamenev, D., Dyachuk, V., Furlan, A., Hampl, M., Memic, F., Marklund, U., Lallemend, F., Hadjab, S., Calvo-Enrique, L., Ernfors, P., Fried, K., & Adameyko, I. (2019). Schwann Cell Precursors Generate the Majority of Chromaffin Cells in Zuckerkandl Organ and Some Sympathetic Neurons in Paraganglia. *Frontiers in Molecular Neuroscience*, *12*. https://doi.org/10.3389/fnmol.2019.00006

Katz, D. M., & Erb, M. J. (1990). Developmental regulation of tyrosine hydroxylase expression in primary sensory neurons of the rat. *Developmental Biology*, *137*(2), 233–242. https://doi.org/10.1016/0012-1606(90)90250-m

Keith, B., & Simon, M. C. (2007). Hypoxia-Inducible Factors, Stem Cells, and Cancer. *Cell*, *129*(3), 465–472. https://doi.org/10.1016/j.cell.2007.04.019

Kim, D., Cavanaugh, E. J., Kim, I., & Carroll, J. L. (2009). Heteromeric TASK-1/TASK-3 is the major oxygen-sensitive background K^+ channel in rat carotid body glomus cells. *The Journal of Physiology*, *587*(12), 2963–2975. https://doi.org/10.1113/jphysiol.2009.171181

Kim, W. Y., Safran, M., Buckley, M. R. M., Ebert, B. L., Glickman, J., Bosenberg, M., Regan, M., & Kaelin, W. G. (2006). Failure to prolyl hydroxylate hypoxia-inducible factor α phenocopies VHL inactivation in vivo. *The EMBO Journal*, *25*(19), 4650–4662. https://doi.org/10.1038/sj.emboj.7601300

Klinger, P., Schietke, R. E., Warnecke, C., Swoboda, B., Wiesener, M., Hennig, F. F., & Gelse, K. (2011). Deletion of the oxygen-dependent degradation domain results in impaired transcriptional activity of hypoxia-inducible factors. *Transcription*, *2*(6), 269–275. https://doi.org/10.4161/trns.2.6.18619

Krapf, R. (1991). [Hypo- and hyperventilation: consequences for acid-base balance]. *Schweizerische Rundschau Fur Medizin Praxis = Revue Suisse de Medecine Praxis*, *80*(40), 1058–1061.

Kumar, P., & Prabhakar, N. R. (2012). Peripheral Chemoreceptors: Function and Plasticity of the Carotid Body. In *Comprehensive Physiology* (pp. 141–219). Wiley. https://doi.org/10.1002/cphy.c100069

Kumar, S., Gupta, N., Thakur, P., Gupta, N., & Bodh, A. (2024). High Altitude Head and Neck Paragangliomas: A First Sub-Himalayan Experience. *OTO Open*, *8*(1). https://doi.org/10.1002/oto2.112

Ladroue, C., Carcenac, R., Leporrier, M., Gad, S., le Hello, C., Galateau-Salle, F., Feunteun, J., Pouysségur, J., Richard, S., & Gardie, B. (2008). PHD2 mutation and congenital erythrocytosis with paraganglioma. *The New England Journal of Medicine*, *359*(25), 2685–2692. https://doi.org/10.1056/NEJMoa0806277

Laidler, P., & Kay, J. M. (1975). A quantitative morphological study of the carotid bodies of rats living at a simulated altitude of 4300 metres. *The Journal of Pathology*, *117*(3), 183–191. https://doi.org/10.1002/path.1711170308

Lando, D., Peet, D. J., Gorman, J. J., Whelan, D. A., Whitelaw, M. L., & Bruick, R. K. (2002). FIH-1 is an asparaginyl hydroxylase enzyme that regulates the transcriptional activity of hypoxia-inducible factor. *Genes & Development*, *16*(12), 1466–1471. https://doi.org/10.1101/gad.991402

Lauweryns, J. M., & Cokelaere, M. (1973). Hypoxia-sensitive neuro-epithelial bodies intrapulmonary secretory neuroreceptors, modulated by the CNS. *Zeitschrift F□r Zellforschung Und Mikroskopische Anatomie*, *145*(4), 521–540. https://doi.org/10.1007/BF00306722

Lee, C.-C., Wu, C.-Y., & Yang, H.-Y. (2020). Discoveries of how cells sense oxygen win the 2019 Nobel Prize in Physiology or medicine. *Biomedical Journal*, *43*(5), 434–437. https://doi.org/10.1016/j.bj.2020.05.019

Lee, P., Chandel, N. S., & Simon, M. C. (2020). Cellular adaptation to hypoxia through hypoxia inducible factors and beyond. *Nature Reviews Molecular Cell Biology*, *21*(5), 268–283. https://doi.org/10.1038/s41580-020-0227-y

Lee, S. E., Oh, E., Lee, B., Kim, Y. J., Oh, D.-Y., Jung, K., Choi, J.-S., Kim, J., Kim, S. J., Yang, J. W., An, J., Oh, Y. L., & Choi, Y.-L. (2016). Phenylethanolamine N-methyltransferase downregulation is associated with malignant pheochromocytoma/paraganglioma. *Oncotarget*, *7*(17), 24141–24153. https://doi.org/10.18632/oncotarget.8234

Lee, S., Needleman, L., Park, J., Schugar, R. C., Guo, Q., Ford, J. M., & Annes, J. P. (2026). Functional characterization of SDHB variants clarifies hereditary pheochromocytoma and paraganglioma risk and genotype-phenotype relationships. *Journal of Clinical Investigation*, *136*(4). https://doi.org/10.1172/JCI198165

Lenders, J. W. M., Duh, Q.-Y., Eisenhofer, G., Gimenez-Roqueplo, A.-P., Grebe, S. K. G., Murad, M. H., Naruse, M., Pacak, K., & Young, W. F. (2014). Pheochromocytoma and Paraganglioma: An Endocrine Society Clinical Practice Guideline. *The Journal of Clinical Endocrinology & Metabolism*, *99*(6), 1915–1942. https://doi.org/10.1210/jc.2014-1498

Lenders, J. W. M., Kerstens, M. N., Amar, L., Prejbisz, A., Robledo, M., Taieb, D., Pacak, K., Crona, J., Zelinka, T., Mannelli, M., Deutschbein, T., Timmers, H. J. L. M., Castinetti, F., Dralle, H., Widimský, J., Gimenez-Roqueplo, A.-P., & Eisenhofer, G. (2020). Genetics, diagnosis, management and future directions of research of phaeochromocytoma and paraganglioma: a position statement and consensus of the Working Group on Endocrine Hypertension of the European Society of Hypertension. *Journal of Hypertension*, *38*(8), 1443–1456. https://doi.org/10.1097/HJH.0000000000002438

Lepoutre-Lussey, C., Thibault, C., Buffet, A., Morin, A., Badoual, C., Bénit, P., Rustin, P., Ottolenghi, C., Janin, M., Castro-Vega, L.-J., Trapman, J., Gimenez-Roqueplo, A.-P., & Favier, J. (2016). From

Nf1 to Sdhb knockout: Successes and failures in the quest for animal models of pheochromocytoma. *Molecular and Cellular Endocrinology*, *421*, 40–48. https://doi.org/10.1016/j.mce.2015.06.027

Letouzé, E., Martinelli, C., Loriot, C., Burnichon, N., Abermil, N., Ottolenghi, C., Janin, M., Menara, M., Nguyen, A. T., Benit, P., Buffet, A., Marcaillou, C., Bertherat, J., Amar, L., Rustin, P., De Reyniès, A., Gimenez-Roqueplo, A.-P., & Favier, J. (2013). SDH Mutations Establish a Hypermethylator Phenotype in Paraganglioma. *Cancer Cell*, *23*(6), 739–752. https://doi.org/10.1016/j.ccr.2013.04.018

Levitsky, K. L., & López-Barneo, J. (2009). Developmental change of T-type Ca^{2+} channel expression and its role in rat chromaffin cell responsiveness to acute hypoxia. *The Journal of Physiology*, *587*(9), 1917–1929. https://doi.org/10.1113/jphysiol.2009.168989

Li, W., Zhao, X., Han, Q., Ren, C., Gao, S., Liu, Y., & Li, X. (2025). Relationship between breast tissue involution and breast cancer. *Frontiers in Oncology*, *15*. https://doi.org/10.3389/fonc.2025.1420350

Li, X., Sutherland, S., Takeda, K., Fong, G.-H., & Lee, F. S. (2010). Integrity of the prolyl hydroxylase domain protein 2:erythropoietin pathway in aging mice. *Blood Cells, Molecules, and Diseases*, *45*(1), 9–19. https://doi.org/10.1016/j.bcmd.2010.03.003

Lindeberg, J., Usoskin, D., Bengtsson, H., Gustafsson, A., Kylberg, A., Söderström, S., & Ebendal, T. (2004). Transgenic expression of Cre recombinase from the tyrosine hydroxylase locus. *Genesis*, *40*(2), 67–73. https://doi.org/10.1002/gene.20065

Lisy, K., & Peet, D. J. (2008). Turn me on: regulating HIF transcriptional activity. *Cell Death & Differentiation*, *15*(4), 642–649. https://doi.org/10.1038/sj.cdd.4402315

Liu, C., Zhou, D., Yang, K., Xu, N., Peng, J., & Zhu, Z. (2023). Research progress on the pathogenesis of the SDHB mutation and related diseases. *Biomedicine & Pharmacotherapy*, *167*, 115500. https://doi.org/10.1016/j.biopha.2023.115500

Liu, S.-J., Wang, J.-Y., Peng, S.-H., Li, T., Ning, X.-H., Hong, B.-A., Liu, J.-Y., Wu, P.-J., Zhou, B.-W., Zhou, J.-C., Qi, N.-N., Peng, X., Zhang, J.-F., Ma, K.-F., Cai, L., & Gong, K. (2018). Genotype and phenotype correlation in von Hippel–Lindau disease based on alteration of the HIF-α binding site in VHL protein. *Genetics in Medicine*, *20*(10), 1266–1273. https://doi.org/10.1038/gim.2017.261

Lodish, M. B., Adams, K. T., Huynh, T. T., Prodanov, T., Ling, A., Chen, C., Shusterman, S., Jimenez, C., Merino, M., Hughes, M., Cradic, K. W., Milosevic, D., Singh, R. J., Stratakis, C. A., & Pacak, K. (2010). Succinate dehydrogenase gene mutations are strongly associated with paraganglioma of the organ of Zuckerkandl. *Endocrine-Related Cancer*, *17*(3), 581–588. https://doi.org/10.1677/ERC-10-0004

López-Barneo, J., González-Rodríguez, P., Gao, L., Fernández-Agüera, M. C., Pardal, R., & Ortega-Sáenz, P. (2016). Oxygen sensing by the carotid body: mechanisms and role in adaptation to hypoxia. *American Journal of Physiology-Cell Physiology*, *310*(8), C629–C642. https://doi.org/10.1152/ajpcell.00265.2015

López-Barneo, J., López-López, J. R., Ureña, J., & Gonzalez, C. (1988). Chemotransduction in the Carotid Body: K^+ Current Modulated by $P O_2$ In Type I Chemoreceptor Cells. *Science*, *241*(4865), 580–582. https://doi.org/10.1126/science.2456613

López-Barneo, J., & Ortega-Sáenz, P. (2022). Mitochondrial acute oxygen sensing and signaling. *Critical Reviews in Biochemistry and Molecular Biology*, *57*(2), 205–225. https://doi.org/10.1080/10409238.2021.2004575

López-Barneo, J., Ortega-Sáenz, P., Pardal, R., Pascual, A., & Piruat, J. I. (2008). Carotid body oxygen sensing. *European Respiratory Journal*, *32*(5), 1386–1398. https://doi.org/10.1183/09031936.00056408

López-López, J. R., & Pérez-García, M. T. (2007). Oxygen sensitive Kv channels in the carotid body. *Respiratory Physiology & Neurobiology*, *157*(1), 65–74. https://doi.org/10.1016/j.resp.2007.01.022

Losman, J.-A., Koivunen, P., & Kaelin, W. G. (2020). 2-Oxoglutarate-dependent dioxygenases in cancer. *Nature Reviews Cancer*, *20*(12), 710–726. https://doi.org/10.1038/s41568-020-00303-3

Macias, D., Cowburn, A. S., Torres-Torrelo, H., Ortega-Sáenz, P., López-Barneo, J., & Johnson, R. S. (2018). HIF-2α is essential for carotid body development and function. *eLife*, *7*. https://doi.org/10.7554/eLife.34681

Macías, D., Fernández-Agüera, M. C., Bonilla-Henao, V., & López-Barneo, J. (2014a). Deletion of the von Hippel–Lindau gene causes sympathoadrenal cell death and impairs chemoreceptor-mediated adaptation to hypoxia. *EMBO Molecular Medicine*, *6*(12), 1577–1592. https://doi.org/10.15252/emmm.201404153

MacKenzie, E. D., Selak, M. A., Tennant, D. A., Payne, L. J., Crosby, S., Frederiksen, C. M., Watson, D. G., & Gottlieb, E. (2007). Cell-Permeating *α* -Ketoglutarate Derivatives Alleviate Pseudohypoxia in Succinate Dehydrogenase-Deficient Cells. *Molecular and Cellular Biology*, *27*(9), 3282–3289. https://doi.org/10.1128/MCB.01927-06

Madani, R., Al-Hashmi, M., Bliss, R., & Lennard, T. W. J. (2007). Ectopic Pheochromocytoma: Does the Rule of Tens Apply? *World Journal of Surgery*, *31*(4), 849–854. https://doi.org/10.1007/s00268-006-0608-1

Mahon, P. C., Hirota, K., & Semenza, G. L. (2001). FIH-1: a novel protein that interacts with HIF-1α and VHL to mediate repression of HIF-1 transcriptional activity. *Genes & Development*, *15*(20), 2675–2686. https://doi.org/10.1101/gad.924501

Mancini, M., Buffet, A., Porte, B., Amar, L., Lussey-Lepoutre, C., Crinière, L., Baudin, E., Meatchi, T., Gimenez-Roqueplo, A., Favier, J., & Burnichon, N. (2024). *EPAS1* -mutated paragangliomas associated with haemoglobin disorders. *British Journal of Haematology*, *204*(3), 1054–1060. https://doi.org/10.1111/bjh.19278

Masson, N., Keeley, T. P., Giuntoli, B., White, M. D., Puerta, M. L., Perata, P., Hopkinson, R. J., Flashman, E., Licausi, F., & Ratcliffe, P. J. (2019). Conserved N-terminal cysteine dioxygenases transduce responses to hypoxia in animals and plants. *Science*, *365*(6448), 65–69. https://doi.org/10.1126/science.aaw0112

Maxwell, P. H., Osmond, M. K., Pugh, C. W., Heryet, A., Nicholls, L. G., Tan, C. C., Doe, B. G., Ferguson, D. J. P., Johnson, M. H., & Ratcliffe, P. J. (1993). Identification of the renal erythropoietin-producing cells using transgenic mice. *Kidney International*, *44*(5), 1149–1162. https://doi.org/10.1038/ki.1993.362

Maxwell, P. H., Wiesener, M. S., Chang, G.-W., Clifford, S. C., Vaux, E. C., Cockman, M. E., Wykoff, C. C., Pugh, C. W., Maher, E. R., & Ratcliffe, P. J. (1999). The tumour suppressor protein VHL targets hypoxia-inducible factors for oxygen-dependent proteolysis. *Nature*, *399*(6733), 271–275. https://doi.org/10.1038/20459

Mazzone, M., Dettori, D., Leite de Oliveira, R., Loges, S., Schmidt, T., Jonckx, B., Tian, Y.-M., Lanahan, A. A., Pollard, P., Ruiz de Almodovar, C., de Smet, F., Vinckier, S., Aragonés, J., Debackere, K., Luttun, A., Wyns, S., Jordan, B., Pisacane, A., Gallez, B., … Carmeliet, P. (2009). Heterozygous

Deficiency of PHD2 Restores Tumor Oxygenation and Inhibits Metastasis via Endothelial Normalization. *Cell*, *136*(5), 839–851. https://doi.org/10.1016/j.cell.2009.01.020

McDonald, D. M., & Mitchell, R. A. (1975). The innervation of glomus cells, ganglion cells and blood vessels in the rat carotid body: A quantitative ultrastructural analysis. *Journal of Neurocytology*, *4*(2), 177–230. https://doi.org/10.1007/BF01098781

Mesa-Ciller, C., Turiel, G., Guajardo-Grence, A., Lopez-Rodriguez, A. B., Egea, J., de Bock, K., Aragonés, J., & Urrutia, A. A. (2023). Unique expression of the atypical mitochondrial subunit NDUFA4L2 in cerebral pericytes fine tunes HIF activity in response to hypoxia. *Journal of Cerebral Blood Flow and Metabolism : Official Journal of the International Society of Cerebral Blood Flow and Metabolism*, *43*(1), 44–58. https://doi.org/10.1177/0271678X221118236

Mete, O., Asa, S. L., Gill, A. J., Kimura, N., de Krijger, R. R., & Tischler, A. (2022). Overview of the 2022 WHO Classification of Paragangliomas and Pheochromocytomas. *Endocrine Pathology*, *33*(1), 90–114. https://doi.org/10.1007/s12022-022-09704-6

Metzen, E., Berchner-Pfannschmidt, U., Stengel, P., Marxsen, J. H., Stolze, I., Klinger, M., Huang, W. Q., Wotzlaw, C., Hellwig-Bürgel, T., Jelkmann, W., Acker, H., & Fandrey, J. (2003). Intracellular localisation of human HIF-1α hydroxylases:implications for oxygen sensing. *Journal of Cell Science*, *116*(7), 1319–1326. https://doi.org/10.1242/jcs.00318

Michiels, C. (2004). Physiological and Pathological Responses to Hypoxia. *The American Journal of Pathology*, *164*(6), 1875–1882. https://doi.org/10.1016/S0002-9440(10)63747-9

Mkrtchian, S., Kåhlin, J., Ebberyd, A., Gonzalez, C., Sanchez, D., Balbir, A., Kostuk, E. W., Shirahata, M., Fagerlund, M. J., & Eriksson, L. I. (2012). The human carotid body transcriptome with focus on oxygen sensing and inflammation – a comparative analysis. *The Journal of Physiology*, *590*(16), 3807–3819. https://doi.org/10.1113/jphysiol.2012.231084

Mojet, M. H., Mills, E., & Duchen, M. R. (1997). Hypoxia-induced catecholamine secretion in isolated newborn rat adrenal chromaffin cells is mimicked by inhibition of mitochondrial respiration. *The Journal of Physiology*, *504 (Pt 1)*(Pt 1), 175–189. https://doi.org/10.1111/j.1469-7793.1997.175bf.x

Moreno-Domínguez, A., Ortega-Sáenz, P., Gao, L., Colinas, O., García-Flores, P., Bonilla-Henao, V., Aragonés, J., Hüttemann, M., Grossman, L. I., Weissmann, N., Sommer, N., & López-Barneo, J. (2020). Acute O $_2$ sensing through HIF2α-dependent expression of atypical cytochrome oxidase subunits in arterial chemoreceptors. *Science Signaling*, *13*(615). https://doi.org/10.1126/scisignal.aay9452

Morin, A., Goncalves, J., Moog, S., Castro-Vega, L.-J., Job, S., Buffet, A., Fontenille, M.-J., Woszczyk, J., Gimenez-Roqueplo, A.-P., Letouzé, E., & Favier, J. (2020a). TET-Mediated Hypermethylation Primes SDH-Deficient Cells for HIF2α-Driven Mesenchymal Transition. *Cell Reports*, *30*(13), 4551-4566.e7. https://doi.org/10.1016/j.celrep.2020.03.022

Mortola, J. P., & Saiki, C. (1996). Ventilatory response to hypoxia in rats: gender differences. *Respiration Physiology*, *106*(1), 21–34. https://doi.org/10.1016/0034-5687(96)00064-3

Mulligan, E., & Lahiri, S. (1981). Dependence of carotid chemoreceptor stimulation by metabolic agents on PaO2 and PaCO2. *Journal of Applied Physiology: Respiratory, Environmental and Exercise Physiology*, *50*(4), 884–891. https://doi.org/10.1152/jappl.1981.50.4.884

Mulligan, E., Lahiri, S., & Storey, B. T. (1981). Carotid body O2 chemoreception and mitochondrial oxidative phosphorylation. *Journal of Applied Physiology*, *51*(2), 438–446. https://doi.org/10.1152/jappl.1981.51.2.438

Murray, T. R., Chen, L., Marshall, B. E., & Macarak, E. J. (1990). Hypoxic Contraction of Cultured Pulmonary Vascular Smooth Muscle Cells. *American Journal of Respiratory Cell and Molecular Biology*, *3*(5), 457–465. https://doi.org/10.1165/ajrcmb/3.5.457

Murtazina, A. R., Nikishina, Yu. O., Bondarenko, N. S., Sapronova, A. Ya., Volina, E. v., & Ugrumov, M. v. (2017). Gene expression and content of enzymes of noradrenaline synthesis in the rat organ of Zuckerkandl at the critical period of morphogenesis. *Doklady Biochemistry and Biophysics*, *474*(1), 200–203. https://doi.org/10.1134/S1607672917030097

Muz, B., de la Puente, P., Azab, F., & Azab, A. K. (2015). The role of hypoxia in cancer progression, angiogenesis, metastasis, and resistance to therapy. *Hypoxia (Auckland, N.Z.)*, *3*, 83–92. https://doi.org/10.2147/HP.S93413

Neumann, H. P. H., Young, W. F., & Eng, C. (2019). Pheochromocytoma and Paraganglioma. *New England Journal of Medicine*, *381*(6), 552–565. https://doi.org/10.1056/NEJMra1806651

Nguyen, T. L., & Durán, R. v. (2016). Prolyl hydroxylase domain enzymes and their role in cell signaling and cancer metabolism. *The International Journal of Biochemistry & Cell Biology*, *80*, 71–80. https://doi.org/10.1016/j.biocel.2016.09.026

Nicholson, H. E., Tariq, Z., Housden, B. E., Jennings, R. B., Stransky, L. A., Perrimon, N., Signoretti, S., Harris, I. S., Endress, J. E., & Kaelin, W. G. (2019). HIF-independent synthetic lethality between CDK4/6 inhibition and VHL loss across species. *Science Signaling*, *12*(601). https://doi.org/10.1126/scisignal.aay0482

Nielsen, A. M., Bisgard, G. E., & Vidruk, E. H. (1988). Carotid chemoreceptor activity during acute and sustained hypoxia in goats. *Journal of Applied Physiology*, *65*(4), 1796–1802. https://doi.org/10.1152/jappl.1988.65.4.1796

Nye, G. A., Ingram, E., Johnstone, E. D., Jensen, O. E., Schneider, H., Lewis, R. M., Chernyavsky, I. L., & Brownbill, P. (2018). Human placental oxygenation in late gestation: experimental and theoretical approaches. *The Journal of Physiology*, *596*(23), 5523–5534. https://doi.org/10.1113/JP275633

Ogasawara, T., Fujii, Y., Kakiuchi, N., Shiozawa, Y., Sakamoto, R., Ogawa, Y., Ootani, K., Ito, E., Tanaka, T., Watanabe, K., Yoshida, Y., Kimura, N., Shiraishi, Y., Chiba, K., Tanaka, H., Miyano, S., & Ogawa, S. (2022). Genetic Analysis of Pheochromocytoma and Paraganglioma Complicating Cyanotic Congenital Heart Disease. *The Journal of Clinical Endocrinology & Metabolism*, *107*(9), 2545–2555. https://doi.org/10.1210/clinem/dgac362

Opotowsky, A. R., Moko, L. E., Ginns, J., Rosenbaum, M., Greutmann, M., Aboulhosn, J., Hageman, A., Kim, Y., Deng, L. X., Grewal, J., Zaidi, A. N., Almansoori, G., Oechslin, E., Earing, M., Landzberg, M. J., Singh, M. N., Wu, F., & Vaidya, A. (2015). Pheochromocytoma and Paraganglioma in Cyanotic Congenital Heart Disease. *The Journal of Clinical Endocrinology & Metabolism*, *100*(4), 1325–1334. https://doi.org/10.1210/jc.2014-3863

O'Rourke, J. F., Tian, Y.-M., Ratcliffe, P. J., & Pugh, C. W. (1999). Oxygen-regulated and Transactivating Domains in Endothelial PAS Protein 1: Comparison with Hypoxia-inducible Factor-1α. *Journal of Biological Chemistry*, *274*(4), 2060–2071. https://doi.org/10.1074/jbc.274.4.2060

Ortega-Sáenz, P., Levitsky, K. L., Marcos-Almaraz, M. T., Bonilla-Henao, V., Pascual, A., & López-Barneo, J. (2010). Carotid body chemosensory responses in mice deficient of TASK channels. *Journal of General Physiology*, *135*(4), 379–392. https://doi.org/10.1085/jgp.200910302

Ortega-Sáenz, P., & López-Barneo, J. (2020). Physiology of the Carotid Body: From Molecules to Disease. *Annual Review of Physiology*, *82*(1), 127–149. https://doi.org/10.1146/annurev-physiol-020518-114427

Ortega-Sáenz, P., Moreno-Domínguez, A., Gao, L., & López-Barneo, J. (2020). Molecular Mechanisms of Acute Oxygen Sensing by Arterial Chemoreceptor Cells. Role of Hif2α. *Frontiers in Physiology*, *11*. https://doi.org/10.3389/fphys.2020.614893

Ortega-Saenz, P., Pardal, R., Garcia-Fernandez, M., & Lopez-Barneo, J. (2003). Rotenone selectively occludes sensitivity to hypoxia in rat carotid body glomus cells. *The Journal of Physiology*, *548*(3), 789–800. https://doi.org/10.1113/jphysiol.2003.039693

Otlyga, E., Otlyga, D., Junemann, O., Krivova, Y., Proshchina, A., Kharlamova, A., Gulimova, V. I., Sonin, G., & Saveliev, S. (2025). Developmental Parallels Between the Human Organs of Zuckerkandl and Adrenal Medulla. *Life*, *15*(8), 1214. https://doi.org/10.3390/life15081214

Pandit, J. J., Huskens, N., O'Donohoe, P. B., Turner, P. J., & Buckler, K. J. (2020). Competitive Interactions between Halothane and Isoflurane at the Carotid Body and TASK Channels. *Anesthesiology*, *133*(5), 1046–1059. https://doi.org/10.1097/ALN.0000000000003520

Pardal, R., Ortega-Sáenz, P., Durán, R., & López-Barneo, J. (2007). Glia-like Stem Cells Sustain Physiologic Neurogenesis in the Adult Mammalian Carotid Body. *Cell*, *131*(2), 364–377. https://doi.org/10.1016/j.cell.2007.07.043

Peng, J., Zhang, L., Drysdale, L., & Fong, G.-H. (2000). The transcription factor EPAS-1/hypoxia-inducible factor 2α plays an important role in vascular remodeling. *Proceedings of the National Academy of Sciences*, *97*(15), 8386–8391. https://doi.org/10.1073/pnas.140087397

Peng, S., Zhang, J., Tan, X., Huang, Y., Xu, J., Silk, N., Zhang, D., Liu, Q., & Jiang, J. (2020). The VHL/HIF Axis in the Development and Treatment of Pheochromocytoma/Paraganglioma. *Frontiers in Endocrinology*, *11*, 586857. https://doi.org/10.3389/fendo.2020.586857

Peng, Y., Cui, C., He, Y., Ouzhuluobu, Zhang, H., Yang, D., Zhang, Q., Bianbazhuoma, Yang, L., He, Y., Xiang, K., Zhang, X., Bhandari, S., Shi, P., Yangla, Dejiquzong, Baimakangzhuo, Duojizhuoma, Pan, Y., … Su, B. (2017). Down-Regulation of *EPAS1* Transcription and Genetic Adaptation of Tibetans to High-Altitude Hypoxia. *Molecular Biology and Evolution*, msw280. https://doi.org/10.1093/molbev/msw280

Pequignot, J.-M., & Hellstrom, S. (1983). Intact and sympathectomized carotid bodies of long-term hypoxic rats. *Virchows Archiv A Pathological Anatomy and Histopathology*, *400*(3), 235–243. https://doi.org/10.1007/BF00612185

Pescador, N., Cuevas, Y., Naranjo, S., Alcaide, M., Villar, D., Landázuri, M. O., & del Peso, L. (2005). Identification of a functional hypoxia-responsive element that regulates the expression of the *egl nine* homologue 3 (*egln3/phd3*) gene. *Biochemical Journal*, *390*(1), 189–197. https://doi.org/10.1042/BJ20042121

Petrova, V., Annicchiarico-Petruzzelli, M., Melino, G., & Amelio, I. (2018). The hypoxic tumour microenvironment. *Oncogenesis*, *7*(1), 10. https://doi.org/10.1038/s41389-017-0011-9

Pietruschka, F. (1985). Calcium influx in cultured carotid body cells is stimulated by acetylcholine and hypoxia. *Brain Research*, *347*(1), 140–143. https://doi.org/10.1016/0006-8993(85)90901-1

Piruat, J. I., Pintado, C. O., Ortega-Sáenz, P., Roche, M., & López-Barneo, J. (2004). The Mitochondrial *SDHD* Gene Is Required for Early Embryogenesis, and Its Partial Deficiency Results

in Persistent Carotid Body Glomus Cell Activation with Full Responsiveness to Hypoxia. *Molecular and Cellular Biology*, *24*(24), 10933–10940. https://doi.org/10.1128/MCB.24.24.10933-10940.2004

Powers, J. F., Cochran, B., Baleja, J. D., Sikes, H. D., Pattison, A. D., Zhang, X., Lomakin, I., Shepard-Barry, A., Pacak, K., Moon, S. J., Langford, T. F., Stein, K. T., Tothill, R. W., Ouyang, Y., & Tischler, A. S. (2020). A xenograft and cell line model of SDH-deficient pheochromocytoma derived from Sdhb+/- rats. *Endocrine-Related Cancer*, *27*(6), 337–354. https://doi.org/10.1530/ERC-19-0474

Prada-Dacasa, P., Urpi, A., Sánchez-Benito, L., Bianchi, P., & Quintana, A. (2020). Measuring Breathing Patterns in Mice Using Whole-body Plethysmography. *BIO-PROTOCOL*, *10*(17). https://doi.org/10.21769/BioProtoc.3741

Prange-Barczynska, M., Jones, H., Sugimoto, Y., Cheng, X., Lima, J., Ratnayaka, I., Douglas, G., Buckler, K., Ratcliffe, P., Keeley, T., & Bishop, T. (2024). Hif-2α programmes oxygen chemosensitivity in chromaffin cells. *Journal of Clinical Investigation*.

Pugh, C. W., Tan, C. C., Jones, R. W., & Ratcliffe, P. J. (1991). Functional analysis of an oxygen-regulated transcriptional enhancer lying 3' to the mouse erythropoietin gene. *Proceedings of the National Academy of Sciences*, *88*(23), 10553–10557. https://doi.org/10.1073/pnas.88.23.10553

Rajakumar, A., & Conrad, K. P. (2000). Expression, Ontogeny, and Regulation of Hypoxia-Inducible Transcription Factors in the Human Placenta1. *Biology of Reproduction*, *63*(2), 559–569. https://doi.org/10.1095/biolreprod63.2.559

Rasmussen, K. D., & Helin, K. (2016). Role of TET enzymes in DNA methylation, development, and cancer. *Genes & Development*, *30*(7), 733–750. https://doi.org/10.1101/gad.276568.115

Ratcliffe, P. J. (2013). Oxygen sensing and hypoxia signalling pathways in animals: the implications of physiology for cancer. *The Journal of Physiology*, *591*(8), 2027–2042. https://doi.org/10.1113/jphysiol.2013.251470

Raval, R. R., Lau, K. W., Tran, M. G. B., Sowter, H. M., Mandriota, S. J., Li, J.-L., Pugh, C. W., Maxwell, P. H., Harris, A. L., & Ratcliffe, P. J. (2005). Contrasting Properties of Hypoxia-Inducible Factor 1 (HIF-1) and HIF-2 in von Hippel-Lindau-Associated Renal Cell Carcinoma. *Molecular and Cellular Biology*, *25*(13), 5675–5686. https://doi.org/10.1128/MCB.25.13.5675-5686.2005

Ravenna, L., Salvatori, L., & Russo, M. A. (2016). <scp>HIF</scp> 3α: the little we know. *The FEBS Journal*, *283*(6), 993–1003. https://doi.org/10.1111/febs.13572

Redlich, A., Pamporaki, C., Lessel, L., Frühwald, M. C., Vorwerk, P., & Kuhlen, M. (2021). Pseudohypoxic pheochromocytomas and paragangliomas dominate in children. *Pediatric Blood & Cancer*, *68*(7). https://doi.org/10.1002/pbc.28981

Richter, S., Gieldon, L., Pang, Y., Peitzsch, M., Huynh, T., Leton, R., Viana, B., Ercolino, T., Mangelis, A., Rapizzi, E., Menschikowski, M., Aust, D., Kroiss, M., Beuschlein, F., Gudziol, V., Timmers, H. J. L. M., Lenders, J., Mannelli, M., Cascon, A., … Klink, B. (2019). Metabolome-guided genomics to identify pathogenic variants in isocitrate dehydrogenase, fumarate hydratase, and succinate dehydrogenase genes in pheochromocytoma and paraganglioma. *Genetics in Medicine*, *21*(3), 705–717. https://doi.org/10.1038/s41436-018-0106-5

Ricketts, C. J., Shuch, B., Vocke, C. D., Metwalli, A. R., Bratslavsky, G., Middelton, L., Yang, Y., Wei, M.-H., Pautler, S. E., Peterson, J., Stolle, C. A., Zbar, B., Merino, M. J., Schmidt, L. S., Pinto, P. A., Srinivasan, R., Pacak, K., & Linehan, W. M. (2012). Succinate Dehydrogenase Kidney Cancer: An Aggressive Example of the Warburg Effect in Cancer. *Journal of Urology*, *188*(6), 2063–2071. https://doi.org/10.1016/j.juro.2012.08.030

Rocher, A., & Aaronson, P. I. (2024). The Thirty-Fifth Anniversary of K+ Channels in O2 Sensing: What We Know and What We Don't Know. *Oxygen*, *4*(1), 53–89. https://doi.org/10.3390/oxygen4010004

Ruan, W., Li, T., Bang, I. H., Lee, J., Deng, W., Ma, X., Luo, C., Du, F., Yoo, S.-H., Kim, B., Li, J., Yuan, X., Figarella, K., An, Y. A., Wang, Y.-Y., Liang, Y., DeBerge, M., Zhang, D., Zhou, Z., … Eltzschig, H. K. (2025). BMAL1–HIF2A heterodimer modulates circadian variations of myocardial injury. *Nature*, *641*(8064), 1017–1028. https://doi.org/10.1038/s41586-025-08898-z

Rustin, P., Munnich, A., & Rötig, A. (2002). Succinate dehydrogenase and human diseases: new insights into a well-known enzyme. *European Journal of Human Genetics*, *10*(5), 289–291. https://doi.org/10.1038/sj.ejhg.5200793

Rutter, J., Winge, D. R., & Schiffman, J. D. (2010). Succinate dehydrogenase – Assembly, regulation and role in human disease. *Mitochondrion*, *10*(4), 393–401. https://doi.org/10.1016/j.mito.2010.03.001

Rychkov, G. Y., Adams, M. B., McMillen, I. C., & Roberts, M. L. (1998). Oxygen-sensing mechanisms are present in the chromaffin cells of the sheep adrenal medulla before birth. *The Journal of Physiology*, *509*(3), 887–893. https://doi.org/10.1111/j.1469-7793.1998.887bm.x

Saldana, M. J., Salem, L. E., & Travezan, R. (1973). High altitude hypoxia and chemodectomas. *Human Pathology*, *4*(2), 251–263. https://doi.org/10.1016/S0046-8177(73)80012-7

Salvatore, M. F. (2024). Dopamine Signaling in Substantia Nigra and Its Impact on Locomotor Function—Not a New Concept, but Neglected Reality. *International Journal of Molecular Sciences*, *25*(2), 1131. https://doi.org/10.3390/ijms25021131

Scheuermann, T. H., Tomchick, D. R., Machius, M., Guo, Y., Bruick, R. K., & Gardner, K. H. (2009). Artificial ligand binding within the HIF2α PAS-B domain of the HIF2 transcription factor. *Proceedings of the National Academy of Sciences*, *106*(2), 450–455. https://doi.org/10.1073/pnas.0808092106

Schober, A., Parlato, R., Huber, K., Kinscherf, R., Hartleben, B., Huber, T. B., Schütz, G., & Unsicker, K. (2013). Cell Loss and Autophagy in the Extra-Adrenal Chromaffin Organ of Zuckerkandl are Regulated by Glucocorticoid Signalling. *Journal of Neuroendocrinology*, *25*(1), 34–47. https://doi.org/10.1111/j.1365-2826.2012.02367.x

Schödel, J., Bardella, C., Sciesielski, L. K., Brown, J. M., Pugh, C. W., Buckle, V., Tomlinson, I. P., Ratcliffe, P. J., & Mole, D. R. (2012). Common genetic variants at the 11q13.3 renal cancer susceptibility locus influence binding of HIF to an enhancer of cyclin D1 expression. *Nature Genetics*, *44*(4), 420–425. https://doi.org/10.1038/ng.2204

Schofield, C. J., & Ratcliffe, P. J. (2004). Oxygen sensing by HIF hydroxylases. *Nature Reviews Molecular Cell Biology*, *5*(5), 343–354. https://doi.org/10.1038/nrm1366

Scholzen, T., & Gerdes, J. (2000). The Ki-67 protein: From the known and the unknown. *Journal of Cellular Physiology*, *182*(3), 311–322. https://doi.org/10.1002/(SICI)1097-4652(200003)182:3<311::AID-JCP1>3.0.CO;2-9

Scortegagna, M., Ding, K., Oktay, Y., Gaur, A., Thurmond, F., Yan, L.-J., Marck, B. T., Matsumoto, A. M., Shelton, J. M., Richardson, J. A., Bennett, M. J., & Garcia, J. A. (2003). Multiple organ pathology, metabolic abnormalities and impaired homeostasis of reactive oxygen species in Epas1−/− mice. *Nature Genetics*, *35*(4), 331–340. https://doi.org/10.1038/ng1266

Seidler, F. J., & Slotkin, T. A. (1985). Adrenomedullary function in the neonatal rat: responses to acute hypoxia. *The Journal of Physiology*, *358*(1), 1–16. https://doi.org/10.1113/jphysiol.1985.sp015536

Semenza, G. L. (2012). Hypoxia-inducible factors in physiology and medicine. *Cell*, *148*(3), 399–408. https://doi.org/10.1016/j.cell.2012.01.021

Semenza, G. L. (2020). The Genomics and Genetics of Oxygen Homeostasis. *Annual Review of Genomics and Human Genetics*, *21*(1), 183–204. https://doi.org/10.1146/annurev-genom-111119-073356

Semenza, G. L., Nejfelt, M. K., Chi, S. M., & Antonarakis, S. E. (1991). Hypoxia-inducible nuclear factors bind to an enhancer element located 3' to the human erythropoietin gene. *Proceedings of the National Academy of Sciences*, *88*(13), 5680–5684. https://doi.org/10.1073/pnas.88.13.5680

Semenza, G. L., & Prabhakar, N. R. (2018). The role of hypoxia-inducible factors in carotid body (patho) physiology. *The Journal of Physiology*, *596*(15), 2977–2983. https://doi.org/10.1113/JP275696

Semenza, G. L., & Wang, G. L. (1992). A Nuclear Factor Induced by Hypoxia via De Novo Protein Synthesis Binds to the Human Erythropoietin Gene Enhancer at a Site Required for Transcriptional Activation. *Molecular and Cellular Biology*, *12*(12), 5447–5454. https://doi.org/10.1128/mcb.12.12.5447-5454.1992

Shen, C., Beroukhim, R., Schumacher, S. E., Zhou, J., Chang, M., Signoretti, S., & Kaelin, W. G. (2011). Genetic and Functional Studies Implicate *HIF1* α as a 14q Kidney Cancer Suppressor Gene. *Cancer Discovery*, *1*(3), 222–235. https://doi.org/10.1158/2159-8290.CD-11-0098

Shirole, N. H., Kesar, D., Lee, Y., Goodale, A., Syamala, S., Kukreja, S., Li, R., Qiu, X., Yu, W., Goldman, S., Cejas, P., Long, H. W., Adelman, K., Doench, J. G., Sellers, W. R., & Kaelin, W. G. (2025). Requirement for Cyclin D1 Underlies Cell-Autonomous HIF2 Dependence in Kidney Cancer. *Cancer Discovery*, *15*(7), 1484–1504. https://doi.org/10.1158/2159-8290.CD-24-1378

Siebenmann, C., & Lundby, C. (2015). Regulation of cardiac output in hypoxia. *Scandinavian Journal of Medicine & Science in Sports*, *25*(S4), 53–59. https://doi.org/10.1111/sms.12619

Skuli, N., Majmundar, A. J., Krock, B. L., Mesquita, R. C., Mathew, L. K., Quinn, Z. L., Runge, A., Liu, L., Kim, M. N., Liang, J., Schenkel, S., Yodh, A. G., Keith, B., & Simon, M. C. (2012). Endothelial HIF-2α regulates murine pathological angiogenesis and revascularization processes. *Journal of Clinical Investigation*, *122*(4), 1427–1443. https://doi.org/10.1172/JCI57322

Slingo, M. E., Turner, P. J., Christian, H. C., Buckler, K. J., & Robbins, P. A. (2014). The von Hippel-Lindau Chuvash mutation in mice causes carotid-body hyperplasia and enhanced ventilatory sensitivity to hypoxia. *Journal of Applied Physiology*, *116*(7), 885–892. https://doi.org/10.1152/japplphysiol.00530.2013

Smith, C. A., Bisgard, G. E., Nielsen, A. M., Daristotle, L., Kressin, N. A., Forster, H. v., & Dempsey, J. A. (1986). Carotid bodies are required for ventilatory acclimatization to chronic hypoxia. *Journal of Applied Physiology*, *60*(3), 1003–1010. https://doi.org/10.1152/jappl.1986.60.3.1003

Smythies, J. A., Sun, M., Masson, N., Salama, R., Simpson, P. D., Murray, E., Neumann, V., Cockman, M. E., Choudhry, H., Ratcliffe, P. J., & Mole, D. R. (2019). Inherent DNA-binding specificities of the HIF-1α and HIF-2α transcription factors in chromatin. *The EMBO Reports*, *20*(1), EMBR201846401. https://doi.org/10.15252/embr.201846401

Sobrino, V., González-Rodríguez, P., Annese, V., López-Barneo, J., & Pardal, R. (2018). Fast neurogenesis from carotid body quiescent neuroblasts accelerates adaptation to hypoxia. *The EMBO Reports*, *19*(3), EMBR201744598. https://doi.org/10.15252/embr.201744598

Soliz, J., Thomsen, J. J., Soulage, C., Lundby, C., & Gassmann, M. (2009). Sex-dependent regulation of hypoxic ventilation in mice and humans is mediated by erythropoietin. *American Journal of Physiology-Regulatory, Integrative and Comparative Physiology*, *296*(6), R1837–R1846. https://doi.org/10.1152/ajpregu.90967.2008

Sowter, H. M., Raval, R. R., Moore, J. W., Ratcliffe, P. J., & Harris, A. L. (2003). Predominant role of hypoxia-inducible transcription factor (Hif)-1alpha versus Hif-2alpha in regulation of the transcriptional response to hypoxia. *Cancer Research*, *63*(19), 6130–6134.

Srirangalingam, U., LeCain, M., Tufton, N., Akker, S. A., Drake, W. M., & Metcalfe, K. (2017). Four generations of SDHB-related disease: complexities in management. *Familial Cancer*, *16*(2), 279–282. https://doi.org/10.1007/s10689-016-9946-9

Subramanian, A., & Maker, V. K. (2006). Organs of Zuckerkandl: their surgical significance and a review of a century of literature. *The American Journal of Surgery*, *192*(2), 224–234. https://doi.org/10.1016/j.amjsurg.2006.02.018

Suresh, S., Rajvanshi, P. K., & Noguchi, C. T. (2020). The Many Facets of Erythropoietin Physiologic and Metabolic Response. *Frontiers in Physiology*, *10*. https://doi.org/10.3389/fphys.2019.01534

Swiderska, A., Coney, A. M., Alzahrani, A. A., Aldossary, H. S., Batis, N., Ray, C. J., Kumar, P., & Holmes, A. P. (2021). Mitochondrial Succinate Metabolism and Reactive Oxygen Species Are Important but Not Essential for Eliciting Carotid Body and Ventilatory Responses to Hypoxia in the Rat. *Antioxidants*, *10*(6), 840. https://doi.org/10.3390/antiox10060840

Takeda, K., Ho, V. C., Takeda, H., Duan, L.-J., Nagy, A., & Fong, G.-H. (2006). Placental but not heart defects are associated with elevated hypoxia-inducible factor alpha levels in mice lacking prolyl hydroxylase domain protein 2. *Molecular and Cellular Biology*, *26*(22), 8336–8346. https://doi.org/10.1128/MCB.00425-06

Talks, K. L., Turley, H., Gatter, K. C., Maxwell, P. H., Pugh, C. W., Ratcliffe, P. J., & Harris, A. L. (2000). The Expression and Distribution of the Hypoxia-Inducible Factors HIF-1α and HIF-2α in Normal Human Tissues, Cancers, and Tumor-Associated Macrophages. *The American Journal of Pathology*, *157*(2), 411–421. https://doi.org/10.1016/S0002-9440(10)64554-3

Tatsumi, K., Pickett, C. K., & Weil, J. v. (1995). Possible role of dopamine in ventilatory acclimatization to high altitude. *Respiration Physiology*, *99*(1), 63–73. https://doi.org/10.1016/0034-5687(94)00084-D

Thompson, R. J., Jackson, A., & Nurse, C. A. (1997). Developmental loss of hypoxic chemosensitivity in rat adrenomedullary chromaffin cells. *The Journal of Physiology*, *498*(2), 503–510. https://doi.org/10.1113/jphysiol.1997.sp021876

Tian, H., Hammer, R. E., Matsumoto, A. M., Russell, D. W., & McKnight, S. L. (1998). The hypoxia-responsive transcription factor EPAS1 is essential for catecholamine homeostasis and protection against heart failure during embryonic development. *Genes and Development*, *12*(21). https://doi.org/10.1101/gad.12.21.3320

Tian, H., McKnight, S. L., & Russell, D. W. (1997). Endothelial PAS domain protein 1 (EPAS1), a transcription factor selectively expressed in endothelial cells. *Genes & Development*, *11*(1), 72–82. https://doi.org/10.1101/gad.11.1.72

Timmers, H. J. L. M., Gimenez-Roqueplo, A.-P., Mannelli, M., & Pacak, K. (2009). Clinical aspects of SDHx-related pheochromocytoma and paraganglioma. *Endocrine-Related Cancer*, *16*(2), 391–400. https://doi.org/10.1677/ERC-08-0284

Timón-Gómez, A., Scharr, A. L., Wong, N. Y., Ni, E., Roy, A., Liu, M., Chau, J., Lampert, J. L., Hireed, H., Kim, N. S., Jan, M., Gupta, A. R., Day, R. W., Gardner, J. M., Wilson, R. J., Barrientos, A., & Chang, A. J. (2022). Tissue-specific mitochondrial HIGD1C promotes oxygen sensitivity in carotid body chemoreceptors. *eLife*, *11*. https://doi.org/10.7554/eLife.78915

Tischler, A. S., & Favier, J. (2022). Progress and challenges in experimental models for pheochromocytoma and paraganglioma. *Endocrine-Related Cancer*, *30*(5). https://doi.org/10.1530/ERC-22-0405

Toledo, R. A., Qin, Y., Srikantan, S., Morales, N. P., Li, Q., Deng, Y., Kim, S.-W., Pereira, M. A. A., Toledo, S. P. A., Su, X., Aguiar, R. C. T., & Dahia, P. L. M. (2013). In vivo and in vitro oncogenic effects of HIF2A mutations in pheochromocytomas and paragangliomas. *Endocrine-Related Cancer*, *20*(3), 349–359. https://doi.org/10.1530/ERC-13-0101

Trapp, S., Isabel Aller, M., Wisden, W., & Gourine, A. v. (2008). A Role for TASK-1 (KCNK3) Channels in the Chemosensory Control of Breathing. *The Journal of Neuroscience*, *28*(35), 8844–8850. https://doi.org/10.1523/JNEUROSCI.1810-08.2008

Turner, J. M., Mitchell, M. D., & Kumar, S. S. (2020). The physiology of intrapartum fetal compromise at term. *American Journal of Obstetrics and Gynecology*, *222*(1), 17–26. https://doi.org/10.1016/j.ajog.2019.07.032

Ureña, J., Fernández-Chacón, R., Benot, A. R., Alvarez de Toledo, G. A., & López-Barneo, J. (1994). Hypoxia induces voltage-dependent Ca2+ entry and quantal dopamine secretion in carotid body glomus cells. *Proceedings of the National Academy of Sciences*, *91*(21), 10208–10211. https://doi.org/10.1073/pnas.91.21.10208

Vaidya, A., Flores, S. K., Cheng, Z.-M., Nicolas, M., Deng, Y., Opotowsky, A. R., Lourenço, D. M., Barletta, J. A., Rana, H. Q., Pereira, M. A., Toledo, R. A., & Dahia, P. L. M. (2018). *EPAS1* Mutations and Paragangliomas in Cyanotic Congenital Heart Disease. *New England Journal of Medicine*, *378*(13), 1259–1261. https://doi.org/10.1056/NEJMc1716652

van Nederveen, F. H., Gaal, J., Favier, J., Korpershoek, E., Oldenburg, R. A., de Bruyn, E. M., Sleddens, H. F., Derkx, P., Rivière, J., Dannenberg, H., Petri, B.-J., Komminoth, P., Pacak, K., Hop, W. C., Pollard, P. J., Mannelli, M., Bayley, J.-P., Perren, A., Niemann, S., … Dinjens, W. N. (2009). An immunohistochemical procedure to detect patients with paraganglioma and phaeochromocytoma with germline SDHB, SDHC, or SDHD gene mutations: a retrospective and prospective analysis. *The Lancet Oncology*, *10*(8), 764–771. https://doi.org/10.1016/S1470-2045(09)70164-0

Verhofstad, A. A. J., H□kfelt, T., Goldstein, M., Steinbusch, H. W. M., & Joosten, H. W. J. (1979). Appearance of tyrosine hydroxylase, aromatic amino-acid decarboxylase, dopamine ?-hydroxylase and phenylethanolamine N-methyltransferase during the ontogenesis of the adrenal medulla. *Cell and Tissue Research*, *200*(1). https://doi.org/10.1007/BF00236882

Vizek, M., Pickett, C. K., & Weil, J. v. (1987). Increased carotid body hypoxic sensitivity during acclimatization to hypobaric hypoxia. *Journal of Applied Physiology*, *63*(6), 2403–2410. https://doi.org/10.1152/jappl.1987.63.6.2403

Vortmeyer, A. O., Huang, S. C., Pack, S. D., Koch, C. A., Lubensky, I. A., Oldfield, E. H., & Zhuang, Z. (2002). Somatic point mutation of the wild-type allele detected in tumors of patients with VHL germline deletion. *Oncogene*, *21*(8), 1167–1170. https://doi.org/10.1038/sj.onc.1205121

Wang, G. L., Jiang, B. H., Rue, E. A., & Semenza, G. L. (1995). Hypoxia-inducible factor 1 is a basic-helix-loop-helix-PAS heterodimer regulated by cellular O2 tension. *Proceedings of the National Academy of Sciences*, *92*(12), 5510–5514. https://doi.org/10.1073/pnas.92.12.5510

Wang, G. L., & Semenza, G. L. (1993). General involvement of hypoxia-inducible factor 1 in transcriptional response to hypoxia. *Proceedings of the National Academy of Sciences*, *90*(9), 4304–4308. https://doi.org/10.1073/pnas.90.9.4304

Wang, G. L., & Semenza, G. L. (1995). Purification and Characterization of Hypoxia-inducible Factor 1. *Journal of Biological Chemistry*, *270*(3), 1230–1237. https://doi.org/10.1074/jbc.270.3.1230

Wang, Z.-Z., Stensaas, L. J., Dinger, B., & Fidone, S. J. (1991). Co-existence of tyrosine hydroxylase and dopamine β-hydroxylase immunoreactivity in glomus cells of the cat carotid body. *Journal of the Autonomic Nervous System*, *32*(3), 259–264. https://doi.org/10.1016/0165-1838(91)90120-R

Weir, E. K., López-Barneo, J., Buckler, K. J., & Archer, S. L. (2005). Acute Oxygen-Sensing Mechanisms. *New England Journal of Medicine*, *353*(19), 2042–2055. https://doi.org/10.1056/NEJMra050002

Welander, J., Andreasson, A., Brauckhoff, M., Bäckdahl, M., Larsson, C., Gimm, O., & Söderkvist, P. (2014). Frequent EPAS1/HIF2α exons 9 and 12 mutations in non-familial pheochromocytoma. *Endocrine-Related Cancer*, *21*(3), 495–504. https://doi.org/10.1530/ERC-13-0384

Welander, J., Andreasson, A., Juhlin, C. C., Wiseman, R. W., Bäckdahl, M., Höög, A., Larsson, C., Gimm, O., & Söderkvist, P. (2014). Rare Germline Mutations Identified by Targeted Next-Generation Sequencing of Susceptibility Genes in Pheochromocytoma and Paraganglioma. *The Journal of Clinical Endocrinology & Metabolism*, *99*(7), E1352–E1360. https://doi.org/10.1210/jc.2013-4375

Wenger, R. H. (2002). Cellular adaptation to hypoxia: O_2 -sensing protein hydroxylases, hypoxia-inducible transcription factors, and O_2 -regulated gene expression. *The FASEB Journal*, *16*(10), 1151–1162. https://doi.org/10.1096/fj.01-0944rev

West, G. B., Shepherd, D. M., Hunter, R. B., & Macgregor, A. R. (1953). The function of the organs of Zuckerkandl. *Clinical Science*, *12*(4), 317–325.

Wiesener, M. S., Jürgensen, J. S., Rosenberger, C., Scholze, C., Hörstrup, J. H., Warnecke, C., Mandriota, S., Bechmann, I., Frei, U. A., Pugh, C. W., Ratcliffe, P. J., Bachmann, S., Maxwell, P. H., & Eckardt, K. (2003). Widespread, hypoxia-inducible expression of HIF-2α in distinct cell populations of different organs. *The FASEB Journal*, *17*(2), 271–273. https://doi.org/10.1096/fj.02-0445fje

Wilkins, S. E., Abboud, M. I., Hancock, R. L., & Schofield, C. J. (2016). Targeting Protein–Protein Interactions in the HIF System. *ChemMedChem*, *11*(8), 773–786. https://doi.org/10.1002/cmdc.201600012

Wilson, D. F., Mokashi, A., Chugh, D., Vinogradov, S., Osanai, S., & Lahiri, S. (1994). The primary oxygen sensor of the cat carotid body is cytochrome a_3 of the mitochondrial respiratory chain. *FEBS Letters*, *351*(3), 370–374. https://doi.org/10.1016/0014-5793(94)00887-6

Wu, D. J.-X., Lobo, A., McKenney, J., & Sangoi, A. R. (2026). Diagnostic sensitivity and specificity of INSM1 in pheochromocytomas versus adrenal cortical lesions. *American Journal of Clinical Pathology*, *165*(5). https://doi.org/10.1093/ajcp/aqag034

Wyatt, C. N., & Buckler, K. J. (2004). The effect of mitochondrial inhibitors on membrane currents in isolated neonatal rat carotid body type I cells. *The Journal of Physiology*, *556*(1), 175–191. https://doi.org/10.1113/jphysiol.2003.058131

Wyatt, C. N., & Peers, C. (1995). Ca(2+)-activated K+ channels in isolated type I cells of the neonatal rat carotid body. *The Journal of Physiology*, *483*(3), 559–565. https://doi.org/10.1113/jphysiol.1995.sp020606

Xiao, M., Yang, H., Xu, W., Ma, S., Lin, H., Zhu, H., Liu, L., Liu, Y., Yang, C., Xu, Y., Zhao, S., Ye, D., Xiong, Y., & Guan, K.-L. (2012). Inhibition of α-KG-dependent histone and DNA demethylases by fumarate and succinate that are accumulated in mutations of FH and SDH tumor suppressors. *Genes & Development*, *26*(12), 1326–1338. https://doi.org/10.1101/gad.191056.112

Yamamoto, Y., König, P., Henrich, M., Dedio, J., & Kummer, W. (2006). Hypoxia induces production of nitric oxide and reactive oxygen species in glomus cells of rat carotid body. *Cell and Tissue Research*, *325*(1), 3–11. https://doi.org/10.1007/s00441-006-0178-4

Yang, C., Matro, J. C., Huntoon, K. M., Ye, D. Y., Huynh, T. T., Fliedner, S. M. J., Breza, J., Zhuang, Z., & Pacak, K. (2012). Missense mutations in the human SDHB gene increase protein degradation without altering intrinsic enzymatic function. *The FASEB Journal*, *26*(11), 4506–4516. https://doi.org/10.1096/fj.12-210146

Yang, C., Zhuang, Z., Fliedner, S. M. J., Shankavaram, U., Sun, M. G., Bullova, P., Zhu, R., Elkahloun, A. G., Kourlas, P. J., Merino, M., Kebebew, E., & Pacak, K. (2015). Germ-line PHD1 and PHD2 mutations detected in patients with pheochromocytoma/paraganglioma-polycythemia. *Journal of Molecular Medicine (Berlin, Germany)*, *93*(1), 93–104. https://doi.org/10.1007/s00109-014-1205-7

Zhou, T., Chien, M., Kaleem, S., & Matsunami, H. (2016). Single cell transcriptome analysis of mouse carotid body glomus cells. *The Journal of Physiology*, *594*(15), 4225–4251. https://doi.org/10.1113/JP271936

Zhuang, J., Shang, Q., Rastinejad, F., & Wu, D. (2024). Decoding Allosteric Control in Hypoxia-Inducible Factors. *Journal of Molecular Biology*, *436*(3), 168352. https://doi.org/10.1016/j.jmb.2023.168352

Zhuang, Z., Yang, C., Lorenzo, F., Merino, M., Fojo, T., Kebebew, E., Popovic, V., Stratakis, C. A., Prchal, J. T., & Pacak, K. (2012). Somatic HIF2A gain-of-function mutations in paraganglioma with polycythemia. *The New England Journal of Medicine*, *367*(10), 922–930. https://doi.org/10.1056/NEJMoa1205119

Zoccal, D. B., Vieira, B. N., Mendes, L. R., Evangelista, A. B., & Leirão, I. P. (2024). Hypoxia sensing in the body: An update on the peripheral and central mechanisms. *Experimental Physiology*, *109*(4), 461–469. https://doi.org/10.1113/EP091206

Zuckerkandl, E. (1901). Über Nebenorgane des Sympathacus im Retroperitonealraum des Menschen. *Verhandlungen Der Anatomischen Gesellschaft*, *15*, 97–107.